

PLANKTONIC FORAMINIFERA BIOSTRATIGRAPHY AND MICROFACIES  
ANALYSIS OF THE CENOMANIAN-CAMPANIAN SUCCESSION  
IN THE HAYMANA-POLATLI BASIN (ANKARA, TURKEY)

A THESIS SUBMITTED TO  
THE GRADUATE SCHOOL OF NATURAL AND APPLIED SCIENCES  
OF  
MIDDLE EAST TECHNICAL UNIVERSITY

BY  
NİSAN SARIASLAN

IN PARTIAL FULFILLMENT OF THE REQUIREMENTS  
FOR  
THE DEGREE OF MASTER OF SCIENCE  
IN  
GEOLOGICAL ENGINEERING

SEPTEMBER 2017



Approval of the thesis:

**PLANKTONIC FORAMINIFERA BIOSTRATIGRAPHY AND MICROFACIES  
ANALYSIS OF THE CENOMANIAN - CAMPANIAN SUCCESSION IN THE  
HAYMANA - POLATLI BASIN (ANKARA, TURKEY)**

submitted by **NİSAN SARIASLAN** in partial fulfillment of the requirements for the degree of **Master of Science in Geological Engineering Department, Middle East Technical University** by,

Prof. Dr. Gülbin Dural Ünver

Dean, Graduate School of **Natural and Applied Sciences**

Prof. Dr. Erdin Bozkurt

Head of Department, **Geological Engineering**

Prof. Dr. Sevinç Altınır

Supervisor, **Geological Engineering Dept., METU**

**Examining Committee Members:**

Prof. Dr. İsmail Ömer Yılmaz

Geological Engineering Dept., Middle East Technical University

Prof. Dr. Sevinç Altınır

Geological Engineering Dept., Middle East Technical University

Prof. Dr. Cemal Tunoğlu

Geological Engineering Dept., Hacettepe University

Assoc. Prof. Dr. Bilal Sarı

Geological Engineering Dept., Dokuz Eylül University

Assoc. Prof. Dr. Kaan Sayıt

Geological Engineering Dept., Middle East Technical University

**Date:** 01.08.2017

**I hereby declare that all information in this document has been obtained and presented in accordance with academic rules and ethical conduct. I also declare that, as required by these rules and conduct, I have fully cited and referenced all material and results that are not original to this work.**

Name, Last Name: Nisan SARIASLAN

Signature:

## **ABSTRACT**

### **PLANKTONIC FORAMINIFERAL BIOSTRATIGRAPHY AND MICROFACIES ANALYSIS OF THE CENOMANIAN-CAMPANIAN SUCCESSION IN THE HAYMANA-POLATLI BASIN (ANKARA, TURKEY)**

Sariaslan, Nisan

M.Sc., Department of Geological Engineering

Supervisor: Prof. Dr. Sevinç Özkan Altıner

September 2017, 276 pages

In order to establish the planktonic foraminiferal biostratigraphy of the Cenomanian-Campanian deposits in the Haymana-Polatlı Basin, a stratigraphic section of 93.5 meters was measured and 75 samples were collected. The stratigraphic section starts with limestones containing late Cenomanian rotaliporid and dicarinellid species and continues with early-middle Turonian aged clayey limestones with sporadic shale beds. These units are overlain by red colored Santonian limestones and shales containing abundant globotruncanids. The stratigraphic section ends with monotonous grey colored silty shales of the Campanian, whose silt content increases more towards the upper part.

At the end of detailed taxonomic studies performed on both the washed material and thin sections of the samples, the distributions of planktonic foraminifera throughout the stratigraphic section were determined. Based on these findings, a biostratigraphic framework including 9 biozones and 2 subzones was established. In ascending order, the *Rotalipora cushmani* Zone - *Dicarinella algeriana* Subzone, *Whiteinella archaeocretacea* Zone, *Helvetoglobotruncana helvetica* Zone, *Dicarinella asymetrica* Zone - *Globotruncanita elevata*-*Dicarinella asymetrica* concurrent range Subzone, *Globotruncanita elevata* Zone, *Globotruncana ventricosa* Zone, *Globotruncanella* spp. Zone, *Globotruncana aegyptiaca* Zone and *Gansserina gansseri* Zone were identified.

Moreover, the evolution of depositional environment reflected by the changing microfacies types through the stratigraphic section was revealed. The microfacies identified from bottom to top were Planktonic Foraminiferal Packstone, Radiolarian Packstone, Packstone with Planktonic Foraminifera and Radiolaria, Radiolaria-bearing Spiculite Packstone, Planktonic Foraminiferal Wackestone, Wackestone with Planktonic Foraminifera and Radiolaria, Silty Wackestone-Mudstone with Planktonic Foraminifera and Wackestone-Mudstone.

The inability to determine the zones representing the late Turonian-Coniacian as well as the observation of an unconformity between the pre-Santonian and Santonian deposits were interpreted as the existence of a hiatus covering this time period.

Keywords: Biostratigraphy, Cenomanian-Campanian, Haymana-Polatlı Basin, planktonic foraminifera, microfacies analysis

## ÖZ

### HAYMANA-POLATLI HAVZASI'NDA (ANKARA, TÜRKİYE) SENOMANİYEN-KAMPANİYEN İSTİFİNİN PLANKTONİK FORAMİNİFER BİYOSTRATİGRAFİSİ VE MİKROFASİYES ANALİZİ

Sarıaslan, Nisan

Yüksek Lisans, Jeoloji Mühendisliği Bölümü

Tez Yöneticisi: Prof. Dr. Sevinç Özkan Altıner

Eylül 2017, 276 sayfa

Haymana-Polatlı Havzası'nda çökelen Senomaniyen-Kampaniyen yaşlı istifin planktonik foraminifer biyostratigrafisinin belirlenmesi amacıyla 93.5 metre kalınlığında bir stratigrafik kesit ölçülmüş ve 75 adet örnek toplanmıştır. İstif, geç Senomaniyen rotaliporid ve dicarinellid formlarını içeren kireçtaşları ve erken-orta Turoniyen yaşlı, yer yer şeyl tabakaları içeren killi kireçtaşları ile başlamaktadır. Bu birimler, bol globotruncanidli, kızıl renkli Santoniyen kireçtaşı ve şeylleri ile üzerlenmektedir. İstif, silt yoğunluğu üste doğru gittikçe artan, büyük çoğunluğu gri renkli siltli şeyllerden oluşan monoton Kampaniyen çökelleri ile son bulmaktadır.

Örneklerin hem yıkamalarında hem de ince-kesitlerinde yapılan ayrıntılı taksonomik çalışmalar sonucunda planktonik foraminiferlerin stratigrafik kesit boyunca göstermiş oldukları dağılımlar belirlenmiş, bu bulgulara dayanarak da 9 zon ve 2 altzondan oluşan bir biyostratigrafik çatı ortaya konmuştur. En altta *Rotalipora cushmani* Zonu-*Dicarinella algeriana* Altzonu, üste doğru *Whiteinella archaeocretacea* Zonu, *Helvetoglobotruncana helvetica* Zonu, *Dicarinella asymetrica* Zonu - *Globotruncanita elevata*-*Dicarinella asymetrica* kesişim Altzonu, *Globotruncanita elevata* Zonu, *Globotruncana ventricosa* Zonu, *Globotruncanella* spp. Zonu, *Globotruncana aegyptiaca* Zonu ve *Gansserina gansseri* Zonu tanımlanmıştır.

Ayrıca, kesit boyunca değişen mikrofasiyes tipleri de çökelim ortamındaki değişimleri saptamak amacıyla belirlenmiştir. Kesitte aşağıdan yukarıya belirlenen mikrofasiyesler Planktonik Foraminiferli İstiftaşı, Radyolaryalı İstiftaşı, Planktonik Foraminifer ve Radyolaryalı İstiftaşı, Radyolaryalı Spiküllü istiftaşı, Planktonik Foraminiferli vaketaşı, Planktonik Foraminifer ve Radyolaryalı vaketaşı, Siltli Planktonik Foraminiferli Vaketaşı-Çamurtaşı ve Vaketaşı-Çamurtaşı'dır.

Geç Turoniyen-Koniasiyen'i temsil eden zonların belirlenememesi ve Santoniyen öncesi ile Santoniyen istifleri arasında bir diskordansın gözlemlenmesi ise bu zaman dilimini kapsayan bir boşluğun varlığını düşündürmektedir.

Anahtar Kelimeler: Biyostratigrafi, Haymana-Polatlı Havzası, planktonik foraminifera Senomaniyen-Kampaniyen, mikrofasiyes analizi



*To my beloved family...*

## ACKNOWLEDGEMENTS

My deepest gratitude goes to Prof. Dr. Sevinç Özkan Altınır for her sincere and patient guidance throughout the research and writing of my thesis. I appreciate with all my heart that she has been a wonderful companion and guide in this challenging journey of my life.

I am grateful to Prof. Dr. Demir Altınır for his critical comments and guidance both in the field and the writing of my thesis.

I am also indebted to Prof. Dr. İsmail Ömer Yılmaz for the insightful recommendations and sincere help that I received whenever I applied to him during my study.

I thank Mr. Orhan Karaman for preparing the thin sections.

I would also like to thank Mr. Serkan Yılmaz for his photography work on my fossils.

I am deeply grateful to all my dear friends for supporting and helping me at each stage of this study; their presence made all the hardship bearable.

I would finally like to express my heartfelt gratefulness to my beloved parents (Zeynep and Necati), brother (Can) and cat (Mika). Their love is what makes anything possible for me to do.

## TABLE OF CONTENTS

ABSTRACT.....	v
ÖZ.....	vii
ACKNOWLEDGEMENTS.....	x
TABLE OF CONTENTS.....	xi
LIST OF TABLES.....	xiv
LIST OF FIGURES.....	xv

### CHAPTERS

1. INTRODUCTION .....	1
1.1. Purpose and Scope .....	1
1.2. Geographic Setting.....	3
1.3. Methods of Study.....	4
1.4. Previous Works .....	9
1.4.1. General Geology of the Central Anatolia and the Haymana Region .....	9
1.4.2. Planktonic Foraminifera Biostratigraphy .....	16
1.5. Regional Geology .....	21
2. STRATIGRAPHY .....	31
2.1. Lithostratigraphy.....	31
2.2. Biostratigraphy.....	39
2.2.1. Rotalipora cushmani Zone .....	45
2.2.2. Whiteinella archaeocretacea Zone .....	46
2.2.3. Helvetoglobotruncana helvetica Zone.....	47
2.2.4. Dicarinella asymetrica Zone .....	48

2.2.5.	Globotruncanita elevata Zone.....	49
2.2.6.	Globotruncana ventricosa Zone.....	50
2.2.7.	Globotruncanella spp. Zone.....	50
2.2.8.	Globotruncana aegyptiaca Zone .....	51
2.2.9.	Gansserina gansseri Zone .....	52
3.	MICROFACIES ANALYSIS .....	55
3.1.	Types of Microfacies and Depositional Environments .....	55
3.2.	Interpretation of the Microfacies Analysis Results .....	73
4.	STAGE BOUNDARIES .....	79
4.1.	Cenomanian-Turonian Boundary and the Oceanic Anoxic Event 2 .....	79
4.2.	On the absence of the Coniacian stage .....	81
4.3.	Santonian-Campanian Boundary.....	82
5.	SYSTEMATIC PALEONTOLOGY.....	85
6.	DISCUSSIONS AND CONCLUSIONS .....	163
	REFERENCES.....	167
	APPENDIX.....	201
	PLATE 1 .....	201
	PLATE 2 .....	204
	PLATE 3 .....	206
	PLATE 4 .....	208
	PLATE 5 .....	210
	PLATE 6 .....	213
	PLATE 7 .....	216
	PLATE 8 .....	219
	PLATE 9 .....	221
	PLATE 10 .....	223
	PLATE 11 .....	226
	PLATE 12 .....	229
	PLATE 13 .....	231
	PLATE 14 .....	233
	PLATE 15 .....	236
	PLATE 16 .....	238

PLATE 17 .....	242
PLATE 18 .....	244
PLATE 19 .....	246
PLATE 20 .....	249
PLATE 21 .....	251
PLATE 22 .....	254
PLATE 23 .....	257
PLATE 24 .....	260
PLATE 25 .....	263
PLATE 26 .....	266
PLATE 27 .....	269
PLATE 28 .....	271
PLATE 29 .....	274

## LIST OF TABLES

Table 1. Summary of the sample washing methods tried during the study for the best result. .....	8
Table 2. Microfacies types, corresponding depositional environments .....	61
Table 3. Microfacies Analysis Results .....	74

## LIST OF FIGURES

Figure 1. Geographic setting of the study area and the location of the measured section. A. Location of the study area in the Ankara regional setting. B. Access to the measured stratigraphic section from the Eskişehir Road. ....	3
Figure 2. Photographs of the measured section showing the southwestern portion of the outcrop (A and B) and the northeastern portion of the outcrop (C and D). ....	5
Figure 3. Simplified geological map of the Ankara region (modified from Okay and Altıner, 2017). ....	23
Figure 4. Close-up view of the geological map of the Ankara region around Alcı area (modified from Okay and Altıner, 2017). ....	24
Figure 5. Cretaceous stratigraphic sections from Haymana, Central Sakarya Basin and the Ankara region (taken from Okay and Altıner, 2016). ....	25
Figure 6. Generalized columnar section of the study area where MS denotes “measured section” (modified from Ünalán et al, 1976 and Okay and Altıner et al., 2016). ....	29
Figure 7. Photographs from the field, A. Limits and geological formations of the measured stratigraphic section, B. Start level of the stratigraphic section, C. Another view of the measured stratigraphic section, D. A view of the southern portion of the measured section, E. A close-up view of the southern portion of the measured stratigraphic section. ....	32
Figure 8. Lithostratigraphy of the measured section with the planktonic foraminiferal biozones determined in this study (shorter version). ....	34
Figure 9. Lithostratigraphy of the measured section with the planktonic foraminiferal biozones determined in this study. ....	35
Figure 10. Range chart of the planktonic foraminifera species identified in this study. ....	40
Figure 11. Biozonal comparison chart of the Cenomanian-Campanian planktonic foraminifera. ....	44
Figure 12. Dunham classification (1962). ....	56

Figure 13. The Standard Facies Zones on a Rimmed carbonate platform of the modified Wilson model (Flügel, 2004). .....56

Figure 14. Distribution of Standard Microfacies (SMF) types in the Facies Zones (FZ) of Wilson (1975) on a rimmed carbonate platform model (Flügel, 2004) (A: evaporitic, B: brackish). .....57

Figure 15. Generalized distribution of microfacies types (RMF) in different parts of a homoclinal carbonate ramp (Flügel, 2004). .....59

Figure 16. Photomicrographs of the planktonic foraminiferal packstone (MF I.I). (om: oxide minerals, p: pyrite, pf: planktonic foraminifera, q: quartz grains, r: radiolaria, si: silica replacement) Samples A. NS 1, B. NS 26, C. NS 30, D. NS 38 (Scale bar is 0.2 mm). .....63

Figure 17. Photomicrographs of radiolarian packstone (MFT I.II). (if: inoceramid fragment, om: oxide minerals, p: pyrite, q: quartz grains, r: radiolaria) Samples A. NS 6, B. NS 12, C. NS 17, D. NS 17 (Scale bar is 0.2 mm). .....64

Figure 18. Photomicrographs of packstone with planktonic foraminifera and radiolaria (MFT I.III). (om: oxide minerals, p: pyrite, pf: planktonic foraminifera, q: quartz grains, r: radiolaria, si: silica replacement) Samples A. NS 11, B. NS 11, C. NS 14, D. NS 22 (Scale bar is 0.2 mm). .....65

Figure 19. Photomicrographs of radiolaria-bearing Spiculite Packstone (MFT I.IV, Sample NS 18-1). (hbf: benthic foraminifera, hf: hyaline fragment, om: oxide minerals, p: pyrite, pf: planktonic foraminifera, q: quartz grains, r: radiolaria, sp: sponge spicule). Arrows show the direction of current flow (Scale bar is 0.2 mm). .....67

Figure 20. Photomicrographs of planktonic foraminiferal wackestone (MFT II.I). (om: oxide minerals, p: pyrite, pf: planktonic foraminifera, q: quartz grains, r: radiolaria) Samples A. NS 40, B. NS 45, C. NS 42, D. NS 10, E. NS 43, F. NS 10 (Scale bar is 0.2 mm). .....68

Figure 21. Photomicrographs of wackestone with planktonic foraminifera and radiolaria (MFT II.II). (om: oxide minerals, pf: planktonic foraminifera, q: quartz grains, r: radiolaria) Samples A. NS 8. B. NS 10. C. NS 13. D. NS 2. (Scale bar is 0.2 mm). .....69



Figure 22. Photomicrographs of silty wackestone-mudstone with planktonic foraminifera (MFT III.I) (af: agglutinated benthic foraminifera, om: oxide minerals, p: pyrite, pf: planktonic foraminifera, q: quartz grains, r: radiolaria) Samples A. NS 51, B. NS 57, C. NS 60, D. NS 58, E. NS 62, F. NS 67 (Scale bar is 0.2 mm). .....71

Figure 23. Photomicrographs of wackestone-mudstone (MFT III.II). (om: oxide minerals, p: pyrite, pf: planktonic foraminifera, q: quartz grains, r: radiolaria) Samples A. NS 14. B. NS 15. C. NS 16 (Scale bar is 0.2 mm).....72

Figure 24. Microfacies Evolution Chart showing the changing depositional environments through time for two different models: on a rimmed-shelf and on a ramp platform. ....73



## CHAPTER 1

### 1. INTRODUCTION

#### 1.1. Purpose and Scope

The primary objective of this study is to establish a detailed biostratigraphic framework based on the planktonic foraminifera for the Upper Cretaceous (Cenomanian-Campanian) succession of the Haymana-Polatlı Basin, Turkey. Other objectives are to identify lithological changes throughout the succession and to establish the evolution of depositional environment by using microfacies data in order to be able to finally define stage boundaries contained in the stratigraphic section.

The Haymana region has always been a popular location for geologists to study the evolution of Cretaceous System in the Central Anatolia. Belonging to the Central Pontides, the Haymana region constitutes an important source of information to understand the evolution of the Pontides, subduction of the Tethyan Ocean floor and opening of the Black Sea (Okay and Altıner, 2016, 2017; Yılmaz et al., 2010). In this sense, biostratigraphic studies represent a crucial tool to decipher the history of paleoevents took place in the region.

In the Ankara region, the lower part of the Upper Cretaceous has not been studied in detail in terms of biostratigraphy; studies regarding the Cretaceous of the Haymana Basin rather focused on the K/P boundary and its vicinity (see Subsection 1.4.1). Therefore, this study aimed to especially focus on the biostratigraphy of the the Lower-Upper Cretaceous (Cenomanian-Campanian) of the Haymana-Polatlı Basin succession. A stratigraphic succession regarding this part of the Cretaceous system outcropping near the Alagöz village, Ankara, was chosen in the aim for providing a complementary analysis to the one

performed by Afridi (2014) discussing the stratigraphical, sedimentological, geochemical and cyclostratigraphical aspects of the Upper Santonian-Campanian part of the same succession. To this end, planktonic foraminifera has been preferred for conducting the biostratigraphic analysis of this study and they have been identified both in washed specimens and in thin section of samples in the section. The planktonic foraminifera represent a very useful biostratigraphic tool for correlating strata in the Cretaceous stratigraphic system, given their widespread and abundant occurrence (BouDagher-Fadel, 2012), especially in the Tethyan region (Premoli-Silva et al., 1999; Premoli-Silva and Sliter, 1999; Petrizzo, 2003; Coccioni et al., 2015).

Given the broad age interval contained in the studied succession, the measured 93.5 m thick stratigraphic section was sampled at relatively larger intervals (~1.2 m) where these were kept smaller in the lower part of the section (Cenomanian-Santonian) due to its being not studied in detail previously.

In brief, the aim of this study is to provide a guiding biostratigraphic framework for the broad age interval (Cenomanian-Campanian) of which the stratigraphic section is composed. Moreover, obtained microfacies data was utilized to detect any changes took place in the depositional environment.

## 1.2. Geographic Setting

The location of the study area is approximately 40 km southwest of Ankara, in the Alagöz village, Polatlı (Figure 1). It is situated on the topographic map of Ankara – J28-b2 of 1/25.000 scale. GPS recordings give the coordinates of the start point as  $39^{\circ}45'23''\text{N}$  -  $32^{\circ}29'26''\text{E}$  and end point as  $39^{\circ}45'22''\text{N}$  -  $32^{\circ}29'19''\text{N}$ . The measured section is easily accessible from the Eskişehir road.

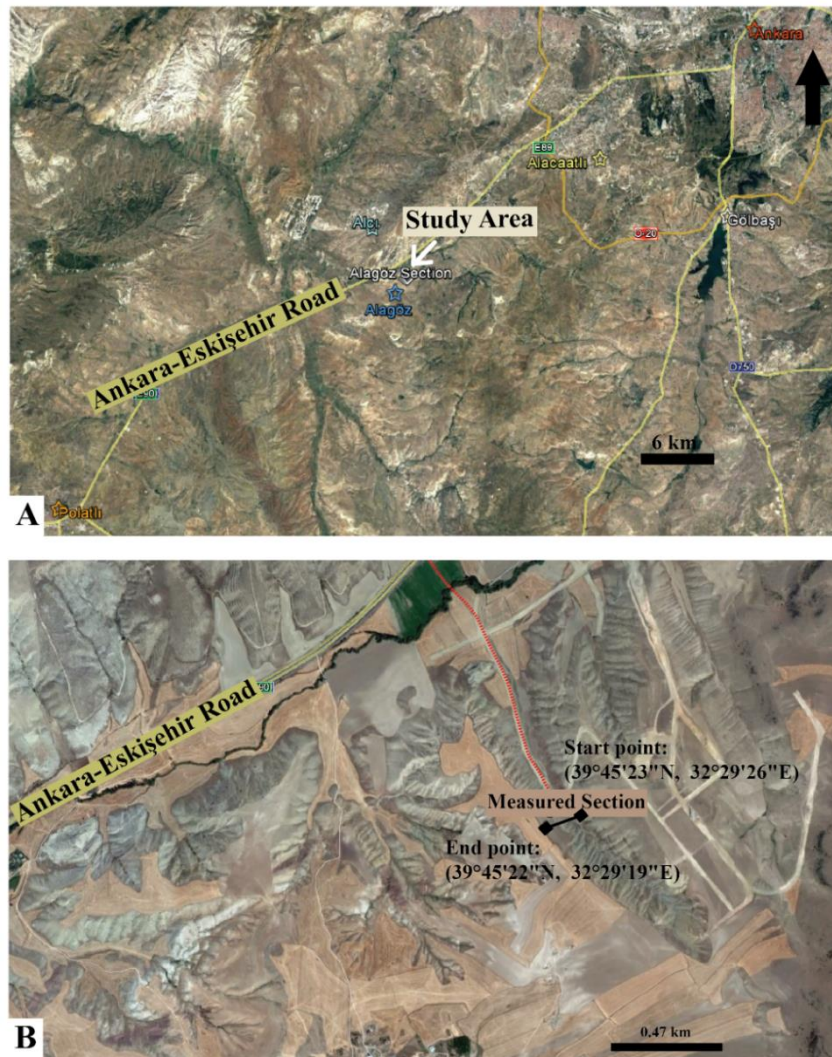


Figure 1. Geographic setting of the study area and the location of the measured section. A. Location of the study area in the Ankara regional setting. B. Access to the measured stratigraphic section from the Eskişehir Road.

### **1.3. Methods of Study**

First of all, a comprehensive literature survey focusing on the Late Cretaceous time interval was done. This included the biostratigraphy and evolution of microfossil assemblages of the study area as well as other study areas with the same age. Then, the field trips and laboratory studies were performed.

In total, there have been four field trips to the Alagöz village in the Haymana Basin. In the first one, the best outcrop for measuring the geological section was selected after the lithological units were identified. 46 samples at variable intervals of 10 cm to 150 cm were collected (Fig. 2, A and B). Remaining 29 samples were collected at the continuation of sequence up to middle part of the previously identified Campanian-Maastrichtian aged Haymana Formation (Fig. 2, C and D). Fewer samples were collected, because this part of the measured section comprised comparatively a much more monotonous succession, although the two sides were more or less of the same thickness. The measured section had 93.5 m of thickness.

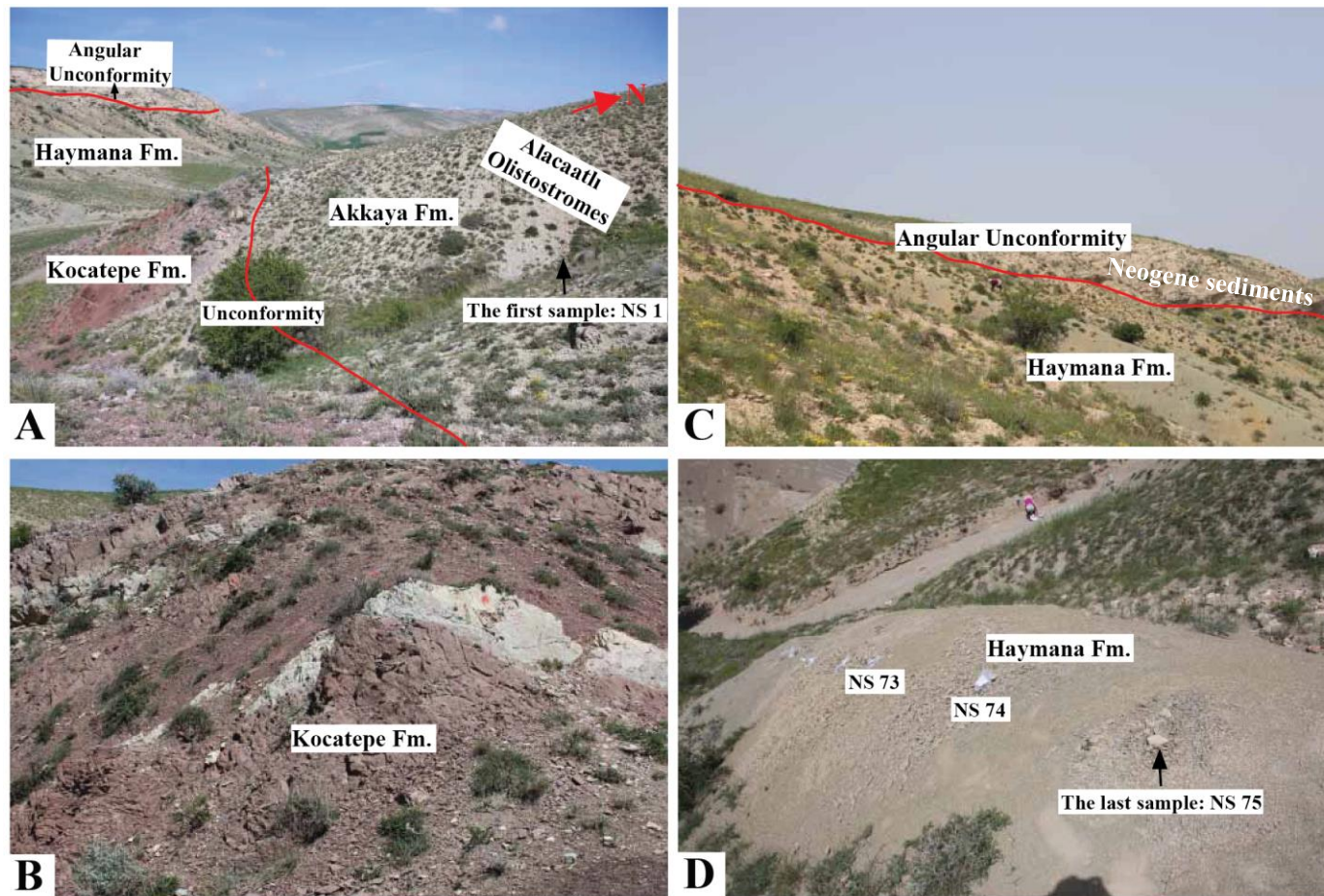


Figure 2. Photographs of the measured section showing the southwestern portion of the outcrop (A and B) and the northeastern portion of the outcrop (C and D).

Laboratory studies were much more time-consuming than the field studies. Nearly two months were spent on conducting trial sessions for determining which combination of crushing and washing method gives the best outcome. In addition to the traditional methods having been applied for years to extract planktonic foraminifera from calcareous rocks, some newer methods have also been utilized. Classical mechanical or chemical methods range from simple washing with tap water to soaking in H<sub>2</sub>O<sub>2</sub> at a desired concentration and then rinsing with water (Sohn, 1961; Knitter, 1979; Abramovich et al., 1998; Li and Keller, 1998; Arenillas et al., 2000; Petrizzo, 2000; Green, 2001; Abramovich and Keller, 2002; Petrizzo, 2002). These methods work best for the soft sediments. Among these there are also various freeze-thaw methods which in principal mimic the nature itself (Hanna and Church, 1928; Pojeta and Balanc, 1989). Except for the primary freeze-thaw method with simple water, there are Glauber's salt method, dry ice and liquid nitrogen freeze-thaw methods. In Glauber's salt method (Herrig, 1966; Surlyk, 1972; Schmid, 1974; Wissing and Herrig, 1999; Green, 2001), ordinary water is replaced by a saturated solution of sodium sulfate [Na<sub>2</sub>SO<sub>4</sub>×10H<sub>2</sub>O]. Crystallization of sodium sulfate in the pore system disintegrates the rock in a similar way as in the classic freeze-thaw method. The latest version of freeze-thaw procedures employs the use of liquid nitrogen (LN<sub>2</sub>) (Remin et al., 2011). Considering the extremely low boiling temperature of nitrogen which is -195.79 °C, the most dramatic freeze-thaw effect can be provided by LN<sub>2</sub> compared to regular water, sodium sulfate solution or dry ice. In this method, liquid nitrogen is poured onto the sample which is crushed to a desired size. When all the sample gets frosted, boiling water is added up to where it covers the whole sample. This procedure is repeated for multiple times until a satisfactory result of disintegration is attained, it was 15 in this case. More powerful extraction procedures include soaking the sample in acetic acid at a desired concentration with chloroform added where the volume of chloroform in milliliters is the same number as the weight of sample in grams (e.g. 100 ml of chloroform for 100 g of sample) (Özkan-Altiner and Özcan, 1999). For the hardest, compact calcareous rocks, the use of pure acetic acid is suggested (Bourdon, 1957) which was later described as the "hot acetolysis" method (Bourdon, 1962). Use of H<sub>2</sub>O<sub>2</sub> and



dilute  $\text{CH}_3\text{COOH}$  is also published as another method for disintegrating stubborn rocks (Costa de Moura et al., 1999).

In general, the collected samples were hard. In the first month, a special selection of 6 representative samples of different hardness level (soft, medium-hard, hard) were crushed to about  $5 \text{ mm}^3$  pieces. The aim was to extract as many intact planktonic foraminifera as possible from the samples. The other criterion was that the planktonic foraminifera specimens have the maximum level of test surface cleanliness in terms of not having sedimentary particles or any kind of crystallization on the test. Then, the methods described previously were applied to the samples. In the first trial, cleanest planktonic foraminifera specimens were obtained through the  $\text{LN}_2$  method compared to others. However, a possible bias was suspected to be caused by the constant size of particles in this first round of trial upon observing the embedded-look of the planktonic foraminifera in sediments of the acetic acid wash results. Moreover, reading about the benefits of powdering the hard and compact Upper Cretaceous and Paleocene samples (Costa de Moura et al., 1999), encouraged to perform a second round of trial with the same selected samples in powder size this time. The second round gave different results than the first and the acetic acid treatment yielded the cleanest specimens. Thus, acetic acid treatment was chosen to be the most effective washing method in this study. An important detail here is rubbing the sediments as rinsing with clean water. Rubbing should be applied softly enough not to harm the fossils and hard enough to get rid of the excessive loose sediments. The trial washes are summarized in Table 1 where the best method is indicated by the orange mark.

Table 1. Summary of the sample washing methods tried during the study for the best result.

Method Round no.	H2O2 (50%) (for 1, 2, 4, 8, 16, 24, 48, 72 hours)	Acetic acid + Chloroform (for 1, 2, 4, 6 hours)		H2O2 (50%) + Acetic acid (30%) (for 1 hour)	LN2 (15 freeze-thaw cycles)
		Acetic acid (50%)	Acetic acid (30%)		
1st round	✓	✓	✓	✗	✓
2nd round	✓	✗	✓	✓	✓

In addition to the primary cleaning with acetic acid treatment, a secondary fine cleaning was applied to the specimens which were still obscured by sediments. This additional cleaning included the application of soft soap, dishwashing soap and ultrasound. The 62.5 µm sized sieve was used. The best results were received by the ultrasound cleaning.

After these treatments, planktonic foraminifera specimens remained on the 125 µm sized sieve were picked under binocular microscope. Other major groups identified were radiolaria and much fewer ostracoda; these were not collected.

Thin sections were also prepared from each of the 75 samples for microfacies and paleontological analysis. They were examined and photographed under polarized microscope to give supplementary data to the main biostratigraphic data obtained from the washing results. Finally, scanning electron microscope (SEM) photographs of the well-preserved specimens were taken to provide more precise data on the morphology of tests.

## **1.4. Previous Works**

### **1.4.1. General Geology of the Central Anatolia and the Haymana Region**

The first formal investigation into the geology of Turkey was carried out by Chaput who was temporarily in charge of the Department of Geography at the Institute of Geography in Istanbul. He focused on the geology of Turkey between 1936 and 1939 (see Akyol, 1944). Regarding the Haymana Basin, he studied the Triassic-Eocene successions including radiolarites, shales, limestones and flysch deposits and established the basin's first detailed geological and biostratigraphical framework. He detected the tectonic deformation after discovering the occurrence of Upper Cretaceous-Eocene succession together with randomly distributed flysch deposits and concluded that these occurred in the Tertiary Period (Chaput, 1932, 1935a, 1935b, 1936).

In the late 1940's and early 1950's, based on Chaput's pioneering works, the geology of Turkey was studied in more detail. Also, Blumenthal documented some general structural observations in the Central Anatolia which now are classics in the literature (Blumenthal 1941a, 1941b, 1942). Lokman and Lahn (1946) studied the stratigraphy and tectonics of the Haymana Region. They established the lithological and fossil succession from the Senonian up to the Miocene. Thus, it was established that the marine facies ended by the end of Middle Eocene which was followed by freshwater and terrestrial deposits belonging to the Miocene. Lahn (1949) and Egeran and Lahn (1951) defined and discussed the structural evolution, lithological and fossil assemblages of the Central and Northern Anatolia, including the Haymana Basin. Several units in the Haymana succession belonging to various Upper Cretaceous and Lower Paleogene stages were defined by them.

Through the 1950's, Erol (1961) wrote an extensive compilation of all available geological data related to the the orogenic phases of the Ankara Region from various sources and by interpreting these in the light of his own observations and thoughts, he gave a brief summary on this subject. He classified the orogenic phases as pre-Alpine,

Alpine and Epeirogenic and described his interpretations with the referenced data belonging to the geological time intervals pre-Viséan to Permian, Kimmeridgian to Oligocene and Miocene to Pleistocene, respectively.

In the beginning of 1960's, petroleum geologists Reckamp and Özbey (1960) and Schmidt (1960) focused on the stratigraphy of the Haymana Basin and provided important data which improved the knowledge on the stratigraphy of the region. Dağer et al. (1963) measured five stratigraphic sections in the Haymana region and described their lithology with the identifiable micro- and macrofauna in detail. In this study, they defined and described Palaeozoic sequences, Carboniferous-Middle Permian, Jurassic, Cretaceous, Tertiary sequences and Pliocene lake successions. Especially in the Cretaceous deposits, many planktonic foraminifera were identified. Erk (1966, 1967) reported on the Late Paleozoic stratigraphy of the Ankara region.

Having reached a satisfactory level of understanding of the Haymana region's geology, researchers started to concentrate on the more specific aspects of the region in the 1970's. Norman and Rad (1971) and Rad (1971) studied the vertical variations in grain size parameters and the heavy mineral abundance of Eocene-aged Harhor Formation in the Çayraz Area, Haymana. From this, they speculated on the climatological and tectonic history of the area.

Petroleum geologist Arıkan (1975) described the structural evolution and detailed sedimentary succession of the Tuz Gölü and Haymana basins. At the end of his paper, he described the geological history of the region containing these two basins and evaluated this in terms of petroleum geological aspects such as surface hydrocarbon indicators, source rocks, reservoir rocks, cap rocks and trap structures.

One of the greatest contributors to the Anatolian stratigraphy and biostratigraphy, Sirel (1975) described the upper Jurassic-Eocene lithostratigraphy and biostratigraphy around the Haymana region. He established the biozones and microfossils characterizing them with corresponding ages of the units. His paleontological identifications included multiple groups of microfossils such as algae, foraminifera, ostracoda and gastropoda. He also

mentioned six new alveolinid species in this study, which were to be described in another study of his (Sirel, 1976).

Ünalın et al. (1976), conducted a very detailed study on the upper Cretaceous-lower Paleogene deposits in the Haymana Basin. The most notable points in this study were defining the formations and their contacts in the region and interpreting its palaeoenvironmental evolution. Erk (1976) studied the monotonous late Paleozoic succession in the Central Anatolia, with flysch formation at bottom and calcareous series on the top. The bottom flysch had been named as “Kulm type flysch” previously (Erk, 1966) and since it had a lack of fossils, sedimentological zonation was applied to this succession instead of biozonation. In the same year, Gökçen (1976) studied the sedimentology of the succession in the southwestern Haymana Basin. Later by the same author, oil-saturated sandstones of the region were also studied in terms of their sedimentological properties (Şenalp and Gökçen, 1978).

First biostratigraphic studies involving planktonic foraminifera and calcareous nannoplanktons in the Haymana Basin were conducted by Toker in the second half of the 1970’s and early 1980’s (Toker, 1975, 1977, 1979, 1980, 1981). In these, she focused on the biozonations of upper Cretaceous (upper Campanian) to middle Eocene formations in the Haymana Basin with planktonic foraminifera and calcareous nannoplanktons.

Meriç and Görür (1981) corrected the age of Çaldağ Limestone in the Haymana Basin by fossil evidence as Thanetian rather than Montian.

Çetin et al. (1986) provided important sedimentological and petrological data from previously poorly known sequences on the northern flank of the Haymana anticline. They identified the provenance of clastic rocks in the region as being located in the north-northwest of Haymana region. Transportation of sediments is thought to occur from north to south mostly by turbiditic currents. The possibility regarding the former existence of a Danian aged lagoon is also brought up. The authors’ interpretation suggested that there was bathyal-abyssal environment in the south to northwest whereas there was neritic environment in the east of the region. Finally, it is suggested that the upper Cretaceous-

lower Paleogene sediments of the Haymana Basin were deposited in subduction zone and fore-arc complex facies between the Kırşehir microplate and the Tethys oceanic plate.

Koçyiğit et al. (1988), discussed the tectonostratigraphical characteristics, nature and type of forearc basin remnants in the active margin of the Northern Neo-Tethys. For that, various geological features and boundary relationships of forearc basin deposits at different domains were studied in detail. The upper limit of the subduction complex development was given as late Santonian to early Campanian in age, but its emplacement age ranged between late Maastrichtian to late Pliocene.

Ocakoğlu and Çiner (1995) studied the basin fill geometries of the Paleocene-lower Eocene units of the Orhaniye-Güvenç region (northwestern Ankara) which hosted a well observable Mesozoic-lower Cenozoic succession. The authors defined the stratigraphy and detailed sedimentology of the geological sections and then attempted to establish the Paleocene-Eocene paleogeography of the region.

Rojay and Süzen (1997) aimed to document the Cretaceous tectonostratigraphy of the southwest Ankara region with their stratigraphic findings and to bring some clarification to the Cretaceous collisional history of the northern branch of Neotethys in Central Anatolia. According to their results, the Cretaceous-Paleogene basins developed on a dynamic accretionary ophiolitic melange prism since the Cenomanian and Cenomanian-Turonian arc-trench; and Maastrichtian-Paleocene fore-arc basins were shifted away from the trench towards magmatic arc, farther north.

Throughout late 1990's and early 2000's, Özkan-Altınar and Özcan published a series of important palaeontological studies involving planktonic foraminifera, large benthic foraminifera and calcareous nannofossils: Özcan and Özkan-Altınar (1997), Özkan-Altınar and Özcan (1997), Özcan and Özkan-Altınar (1999), Özkan-Altınar and Özcan (1999), Özcan and Özkan-Altınar (2001), Özcan et al. (2001) and Özcan (2002). Özcan and Özkan-Altınar (1997) examined the Santonian/Campanian-Eocene shallow water benthic foraminifera of deep-water turbiditic units. They documented the biometric aspects as evolutionary parameters such as embryo-size and number of epi-embryonic

chambers of the genera *Orbitoides* and *Lepidorbitoides*. Two years later (Özcan and Özkan-Altın, 1999), they published their results for testing the early ontogenic features recognized as evolutionary parameters in the previous study in several flysch successions of Anatolia. Özcan and Özkan-Altın (1999) established the main evolutionary trends in the two genera which enabled them to correlate these features with time. They distinguished the true phylogenetic stages with the false ones. At the end, they also proposed a correlation scheme of phylogenetic development in *Lepidorbitoides* and *Orbitoides* with the planktonic foraminiferal zones. This correlation scheme was reported in detail the same year in another paper (Özkan-Altın and Özcan, 1999). In this study, the Upper Cretaceous (Santonian-Maastrichtian) planktonic foraminifera biostratigraphy was established from samples collected from five different locations and the different phylogenetic development stages of *Orbitoides* and *Lepidorbitoides* populations and other larger benthonic foraminifera were calibrated with the planktonic foraminiferal zonation established in the same successions. This study is very important in terms that it added a valuable dimension to the Upper Cretaceous biostratigraphy of the Haymana Basin. Özcan (2002) examined the diverse assemblages of *Discocyclina*, *Orbitoclypeus*, *Nemkovella* and partly *Asterocyclina*, which characterize the lower-upper and late Cuisian shallow benthic zones in the Cuisian-early Lutetian aged Çayraz Formation, the Haymana-Polatlı Basin. Orthophragminids were identified for the first time in Anatolia in this study.

Rojay et al. (2001) sampled the tectonically detached blocks of pillow basalts in the Cretaceous ophiolitic melange from southern Ankara in the aim of defining the missing parts in the evolution of Central Anatolian melange. In between the lobes of pillow basalts, there were also trapped and accumulated pelagic calcareous sediments. Their results collectively supported the presence of a seamount in Dereköy (Haymana region) of the Central Anatolian terrain during the Callovian-Hauterivian interval. An alkaline ocean-island basalt setting of Rhaetian age is interpreted for the Dereköy (Haymana) pillow basalts.

Some of the important studies done in recent years regarding the Haymana Basin can be summarized as follows: Hoşgör and Okan (2010) studied the late Paleocene gastropods of

the Haymana-Polatlı Basin. This study deals with the taxonomy and stratigraphy of the gastropoda group and also proposing a new trochoidean species from the early Thanetian in the Haymana-Polatlı Basin. İslamoğlu et al. (2011) described caenogastropods collected in the Macunköy section from the upper part of the Kırkkavak Formation, the Haymana-Polatlı Basin. The result of this study marks the oldest occurrence of angariid gastropoda in the globe and this occurrence was supported by the foraminiferal and red-algae assemblages in the locality. Nairn et al., (2013) discussed and described in detail the tectonostratigraphic evolution of the upper Cretaceous-Cenozoic central Anatolian basins which are the Kırkkale, Çankırı, Tuz Gölü and Haymana basins. Together with their new stratigraphic and palaeontological data, they tested different hypotheses regarding the collisional history leading to the formation of these basins. Their evidence was consistent with a two-phase, progressive and diachronous continental collision.

Esmeray (2008), Esmeray-Senlet et al. (2015) delineated the K/Pg boundary in the Haymana Basin using planktonic foraminiferal biostratigraphy, microfacies analysis, and sequence stratigraphy. The paleoenvironments, systems tracts and planktonic foraminifera biozones were determined for the pre- and post-boundary successions. Thus, the catastrophic and abrupt occurrence of the K/Pg boundary in the Haymana Basin was detected. Amirov (2008) established the planktonic foraminifera biostratigraphy of the Upper Cretaceous-Paleogene marine succession, sequence stratigraphy and sedimentary cyclicity in the Haymana Basin. Most recently, Okay and Altıner (2016) recognized three unconformity-bounded pelagic carbonate sequences of Berriasian, Albian-Cenomanian and Turonian-Santonian stages. They also recognized that each depositional sequence was preceded by a period of tilting and submarine erosion during the Berriasian, early Albian and late Cenomanian, corresponding to phases of local extension in the active continental margin. They established the deposition of thick siliciclastic turbidites starting in the late Campanian and continuing into the Paleocene. It is noted that unlike most forearc basins, the Haymana region was a site of deep marine carbonate deposition until the Campanian. This resulted from the fact that the Pontide arc was extensional and the volcanic detritus was trapped in the intra-arc basins and did not reach the forearc or the trench. The opening



of the Black Sea as a backarc basin in the Turonian–Santonian also supports the extensional nature of the arc.

Finally, important studies regarding the CORB's in Turkey were published throughout the 2000's and 2010's. Yılmaz et al. (2004) studied the black shale interval in the Lower Aptian deposits, Nallıhan area of northwestern Turkey and established the OAE1a. Hu et al. (2005) studied CORB's in the Tethys from a number of different localities including the Eastern Pontides, Turkey. They attributed the changes in dissolved oxygen in the deep ocean to the changes in the location and formation of deep water and changes in ocean circulation. Yılmaz (2008) investigated the Aptian-Santonian red beds and black shales in northwestern Turkey in the frame of global anoxic and oxic events. He also applied sequence stratigraphic and cyclostratigraphic approaches. In this study, black shale levels corresponding to OAE1a and OAE1c were established. Formation of oceanic red beds in different locations including central Turkey, was investigated together with other climatic and oceanographic changes accompanying it. These were explained as the inevitable results of oceanic anoxic events by Wang et al. (2011). Hu et al. (2012) studied the stratigraphic transition from the early Aptian oceanic anoxic event 1a (OAE1a) to the oceanic red bed 1 (ORB1) along the pelagic Yenicesihlar section in the Mudurnu region of central Turkey. They estimated the transition as being approximately 1.3 Ma, and the  $\delta^{18}\text{O}$  values as showing an increase towards the ORB1, when the climate became cooler. Yılmaz et al. (2010) established the OAE2 in the Sakarya Zone, northwestern Turkey by studying three different stratigraphic sections in terms of their sedimentology, cyclostratigraphy and geochemistry. Yılmaz et al. (2012) established the first record of the late Hauterivian platform drowning of the Bilecik platform, Sakarya Zone, and associated this event with an Oceanic Anoxic Event. Afridi (2014) studied the Upper Santonian-Campanian successions from the Haymana basin and the Mudurnu-Göynük basin, where the first one is represented by a stratigraphic section equivalent to the section of this thesis study. He established the detailed sedimentology and lithofacies of the rocks to interpret the depositional environment. Moreover, he used the results of geochemical analyses to evaluate the levels of nutrient supply and primary productivity, sedimentary

influx to the basin, sea level change trend, type of source rock and oxygen level in the basin. Finally, he established a high resolution cyclostratigraphic framework for the succession.

#### **1.4.2. Planktonic Foraminifera Biostratigraphy**

Cushman first introduced the genus *Globotruncana* in which all trochospiral and keeled (single or double) Cretaceous planktonic foraminifera were included. Grigelis (1958) described *Globigerina oxfordiana* from the Upper Jurassic of Lithuania. Fuchs (1967, 1971, 1973, 1975, 1977) described Triassic and Jurassic planktonic foraminifera and discussed their origin and phylogeny in a series of papers. He argued that the earliest planktonic foraminifera were to be found in the Triassic, whereas these specimens are now thought to be highly recrystallized benthic taxa. In their book, “The Early Evolutionary History of Planktonic Foraminifera”, BouDagher-Fadel *et al.* (1997) described the earliest fossil planktonic foraminifera of the Jurassic and the Early Cretaceous which were, of course, recognized by their tests. According to them, the earliest planktonic foraminifera genus is the M. Jurassic *Conoglobigerina*. They also speculated on the *Praegubkinella* (European Toarcian) being the possible ancestors of the “real” planktonic foraminifera. According to the authors, the widespread development of anoxic/dysaerobic environments in the earliest Toarcian (coupled with a major extinction event) might have been the environmental stimulus to the evolutionary development of the planktonic foraminifera from the genus *Praegubkinella* which was the first meroplanktonic (pref. mero- = partially) taxon. Unfortunately, the Triassic-Jurassic planktonic foraminifera are still not clearly understood. However, their Cretaceous descendants increased their scientific popularity since they were first described, because they are much more abundant, diverse and distributed than their ancestors and therefore, constitute an important tool to understand the Cretaceous world. This made planktonic foraminifera the most studied microfossil group among the others. For that reason, there are an excessive number of studies done using planktonic foraminifera; here, only the ones regarding Cenomanian-Campanian planktonic foraminifera of various Tethyan-related sections are given.

Honigstein et al. (1987) and Almogi-Labin et al. (1991) established the planktonic foraminiferal biostratigraphy of Santonian-Campanian boundary and the interval late Coniacian-early Maastrichtian in Israel. They identified five biozones, namely, *D. asymetrica*, *G. elevata*, *G. rosetta*, *G. calcarata* and *G. falsostuarti*.

Chungkham and Jafar (1998) studied the scattered exotic blocks of pelagic limestone in the ophiolitic melange belt of Nagaland-Manipur, India. The authors presented an integrated calcareous nannoplankton and planktonic foraminiferal biostratigraphy comprising latest Santonian/earliest Campanian to late Maastrichtian timeslice. They identified the biozones *D. asymetrica*, *G. elevata*, *G. ventricosa*, *R. calcarata*, *G. havanensis*, *G. aegyptiaca*, *G. gansseri* and *A. mayaroensis* variably in five sections enabling their correlation.

Petrizzo (2000) made a review on the taxonomy and time ranges of upper Turonian-lower Campanian planktonic foraminifera from southern mid-high latitudes. She aimed to provide a reliable bio-chronostratigraphic scale that is useful for mid-high latitudes of the southern oceans by comparing her data with both the low-latitude standard zonation and the planktonic foraminiferal zonal scheme for the circum-Antarctic region.

Arz and Molina (2001) studied the Campanian-Maastrichtian transition at Tercis, Landes/France. The quite diverse planktonic foraminifera assemblage across the boundary yielded six biozones, five of which are included in the Campanian. The authors proposed a new C/M boundary at Tercis section. This boundary was known in the literature to be located in a higher level than the *Radotruncana calcarata* biozone, however in this study it is coincident with the first appearance of *Trinitella scotti* in the *Gansserina gansseri* biozone (latest Campanian). They also correlated the *R. calcarata* zone, which could not be established in the study due to the absence of the nominal taxon in the samples, to the *Heterohelix glabrans* zone.

Petrizzo (2003) compared the occurrence of planktonic foraminiferal bioevents at low, middle, and high latitudes (Petrizzo, 2001; 2002) in another publication where she reviewed the Late Cretaceous planktonic foraminiferal distribution recorded at several

drill sites (DSDP and ODP) in the South Atlantic and south Indian Ocean and from sediment outcrops in the Tethyan region (Gubbio and El Kef).

Chacon et al. (2004) performed the first detailed biostratigraphic analysis of the uppermost Santonian - uppermost Maastrichtian hemipelagic carbonate successions of southeastern Spain. The authors also compared their section with Tercis (France) and Kalaat Senan (Tunisia) stratigraphic sections. Seven biozones of planktic foraminifera were recognized for the time interval studied. These comprised the uppermost part of the *Dicarinella asymetrica* Zone, and the *Globotruncanita elevata*, *Globotruncana ventricosa*, *Globotruncanita calcarata*, *Globotruncana falsostuarti*, *Gansserina gansseri* and *Abathomphalus mayaroensis* zones.

Lamolda et al. (2007) published an instructive report including the planktonic foraminiferal bioevents occurred between the Coniacian-Santonian at Olazagutia, Navarra province, Spain. It was also emphasized that the first occurrence of “pill-box-like” morphotypes of *G. linneiana* can be used as a good proxy for the Coniacian/Santonian boundary.

Li et al. (2007) clarified the age and established the biostratigraphy of the Saiqu melange in southern Tibet. The assemblage was considered to be Campanian-early Maastrichtian in age based on planktonic foraminifera species found. Finally, the red member of the Saiqu melange was correlated with the Upper Cretaceous Red Beds (CORB) and this unit was interpreted to have possibly deposited in response to a global oxygenation event as its equivalents did.

Sarı (2006; 2009) identified planktonic foraminifera biozones from numerous stratigraphic sections of Upper Cretaceous hemipelagic and pelagic sequences of the northern Bey Dağları Autochthon (western Taurides) using thin section of samples.

Cetean et al. (2011) studied an upper Santonian to upper Campanian hemipelagic succession from the southern part of the Romanian Eastern Carpathians and established an integrated biostratigraphy based on planktonic foraminifera and calcareous

nannofossils, which they compared with the agglutinated foraminiferal biozonation used for the Carpathians. They were not able to identify planktonic foraminiferal biozones due to the absence of marker species, however they could identify some important bioevents such as the LO of *Globotruncanita elevata* and the FO of *Globotruncanella havanensis* in the *Radotruncana calcarata* biozone.

Ardestani et al. (2012) did a detailed planktonic foraminiferal biostratigraphic study of the Abderaz Formation of the East Kopet Dagh Basin, northeastern Iran. They recognized five successive foraminiferal zones from the lower Turonian to the lowermost Campanian. They also published (Ardestani et al., 2013) their paleoceanographic and paleobiogeographic interpretations regarding the same location.

In a detailed study, Bey et al. (2012) presented the biostratigraphy, lithology and tectonic history of the Ain Medheker (Northeast Tunisia) section interpreting it as representing an early Campanian to early Maastrichtian moderately deep carbonate shelf to distal ramp position.

Wagreich et al. (2012) studied an almost complete Santonian-lower Maastrichtian succession recorded in pelagic to hemipelagic deposits at the Postalm section, Austria, at the NW margin of the Tethys. The authors addressed the biostratigraphy, as well as the astronomical calibration of the *R. calcarata* Zone in the mid-Campanian at Postalm and emphasized the chronostratigraphical importance of the *R. calcarata* in the Tethyan Realm.

Falzone et al. (2013) established the depth preferences of numerous Santonian-Campanian planktonic foraminifera species based on species-specific stable isotope data ( $\delta^{13}\text{C}$  and  $\delta^{18}\text{O}$ ) obtained from very well preserved “pristine” specimens from the Santonian-Campanian sequences in southeastern Tanzania. Combining their geochemical and paleontological data they also inferred the oceanic structure for the Santonian-Campanian interval of the three high-latitude localities they studied: Tanzania, Shatsky Rise and the Exmouth Plateau.

Elamri and Zaghib-Turki (2014) established the Santonian-Campanian transition in the Kalaat Senan area, Tunisia. The authors proposed to use the LO of *Dicarinella asymetrica* as the index marker of S/C boundary, whereas several species of marginotruncanids were found to have crossed this boundary suffering a gradual extinction. The authors also speculated on the paleoceanographic conditions that have set the ground for the major turnover across S/C boundary, where marginotruncanids and dicarinellids were replaced by the genera *Globotruncanita* and *Globotruncana*.

Rawand et al. (2015) analysed the evolutionary patterns already established for the Turonian-Maastrichtian interval in an Arabian context and they studied the early Turonian to early Maastrichtian planktonic foraminiferal assemblages from two localities in the northeastern Iraq. They made a quantitative analysis of the planktonic foraminifera species and, at the end, established a precise planktonic foraminiferal biozonation and also identified fluctuations in diversity and abundance of major morphotypes as a response to environmental change.

Falzone et al. (2016) presented the first biostratigraphic, taxonomic and quantitative analysis of Cenomanian/Turonian planktonic foraminiferal assemblages from the Vocontian Basin, southeastern France, entirely studied in washed residues. An apparently earlier extinction of the genus *Rotalipora* is attributed to the presence of a condensed stratigraphic interval of about 3-m thick in the section. Moreover, the authors documented for the first time the occurrence of double-keeled specimens with raised umbilical sutures (i.e., *Marginotruncana caronae*) in the uppermost Cenomanian, which proved that primitive marginotruncanids co-occurred with rotaliporids and evolved before the onset of the OAE2, whilst species diversification began immediately after the OAE2 in the earliest Turonian. Lastly, three new species were described: *Pseudoclavhedbergella chevaliensis*, *Praeglobotruncana pseudoalgeriana* and *Praeglobotruncana clotensis*.

Wolfgring et al. (2016a) established a well-resolved assessment of foraminiferal communities in the Austrian Alps during the *Radotruncana calcarata* TRZ. They discussed the bioevents that can be observed in the Penninic Realm and concluded that

many of them require further investigations, except for *R. calcarata*, whose evolution is speculated to have occurred within an opening and closing adaptive zone within changing water masses of the late Cretaceous.

Wolfgring and Wagreich (2016b) presented a quantitative study on the planktonic foraminiferal assemblages in the *R. calcarata* TRZ at Postalm section. In their high-resolution examination, they assessed the composition of typical Tethyan pelagic assemblages and dealt with subtle changes in north-western planktonic foraminiferal communities just before major faunal turnover-events (Premoli Silva et al., 1999a).

Wolfgring et al. (2017) studied the Santonian-Campanian boundary interval in the northwestern Turkey in terms of planktonic foraminiferal and nannofossil biostratigraphy, magnetic polarity and magnetic susceptibility. At the end, three of the most cited marker events in the Santonian-Campanian transition in the Tethyan realm were identified. These are the base of magnetochron C33r, the HO of *Dicarinella asymmetrica* and the LO of the nannofossil *Broinsonia parca parca*.

### **1.5. Regional Geology**

Tectonic evolution of Pontides constitute a crucial part in understanding the geology of the Ankara region, which is located in the west of İzmir-Ankara Suture Zone in the Pontide tectonic unit (Figure 3). Central part of the Pontides has a more complete presence of Cretaceous stratigraphic units compared to western and eastern parts. In general, the Pontides display two distinctive and laterally traceable marker horizons throughout, which are the Upper Jurassic-Lower Cretaceous carbonates and the Campanian-Maastrichtian siliciclastics. The stratigraphic units between these two horizons are not well developed and occur in a laterally varying fashion (Okay and Altın, 2016).

The Haymana region, which is located in the west of Ankara, represents a good opportunity to understand the Cretaceous geology of the Ankara vicinity and the Central Pontides. The Haymana region is dominated by upper Campanian-Middle Eocene siliciclastic sequence over 5000 m in thickness and this constitutes the Haymana Basin.

Older sequences are found in the core of anticlines in this region, largest of which is close to the Haymana town (Okay and Altiner, 2016). The Haymana Basin is the only Central Anatolian basin in the Pontide region (Görür et al., 1998). It is a fore-arc basin above the northward-dipping Tethyan oceanic lithosphere (Görür et al., 1984; 1998; Koçyiğit, 1991; Nairn et al., 2013).

The oldest stratigraphic unit in the Ankara region is Karakaya Complex which is of Late Triassic age (Fig.3). The Karakaya Complex is composed of heavily crushed, scissored and locally slightly metamorphosed sandstone and shale; Carboniferous, Permian and Triassic limestone blocks of varying size are present in the clastics of this unit. In some places, Bayırköy Formation composed of terrestrial-shallow marine conglomerate, sandstone and shale of Early Jurassic age and local levels of ammonitico rosso facies type red nodular limestone occurs on top of the Karakaya Complex. The Bayırköy Formation is followed by marine limestones of Late Jurassic-Early Cretaceous age (Fig. 3).



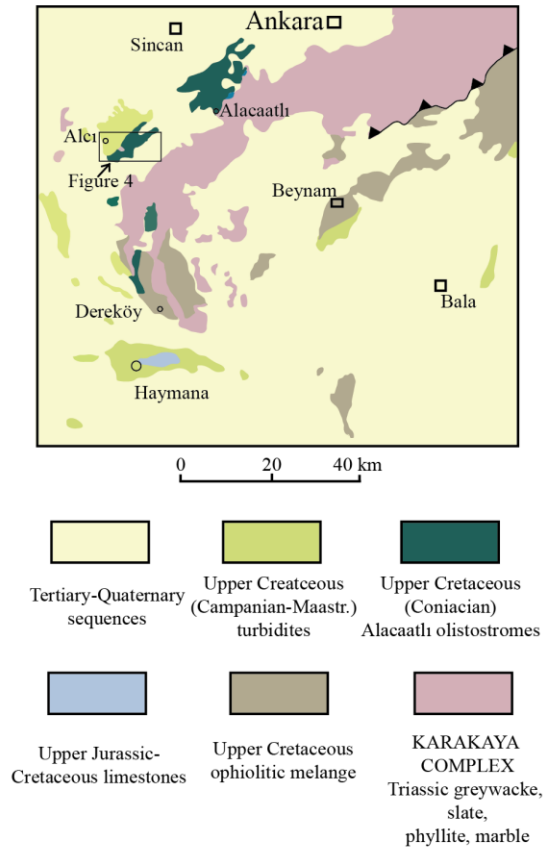


Figure 3. Simplified geological map of the Ankara region (modified from Okay and Altiner, 2017).

This type of shallow marine limestones (Bilecik Group) outcrops in the core of Haymana anticline. Three deep marine limestone-breccia successions of Berriasian, Albian-Cenomanian and Turonian-Santonian age occur on the Bilecik Group limestones with an unconformity in between (Fig. 4). Upper Jurassic-Cretaceous limestone succession is observed as carbonate blocks in the Alacaatlı olistostromes in zones near the İzmir-Ankara Suture Zone (Okay and Altiner, 2016) (Fig.3).

The stratigraphic units of the Haymana region (Figure 5) is described based on Okay and Altiner (2016), as follows:

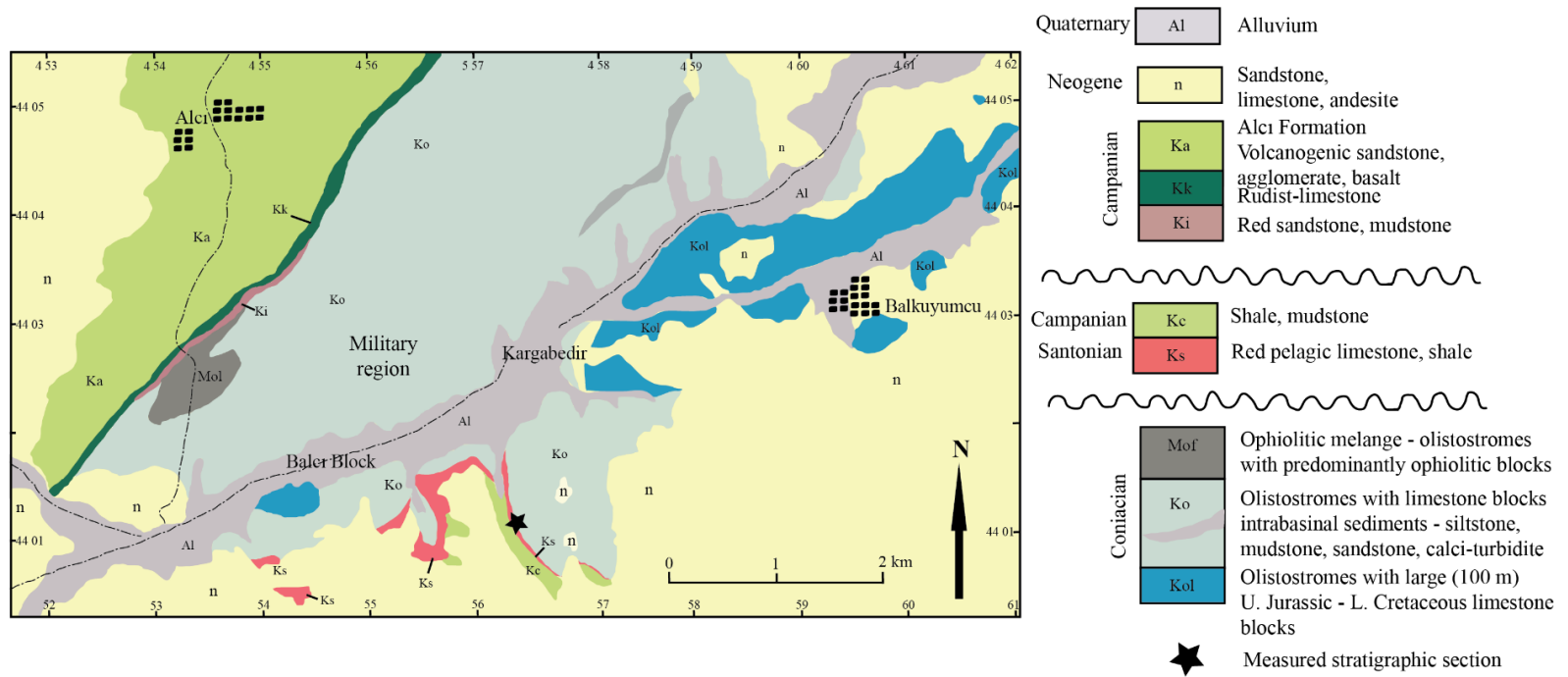


Figure 4. Close-up view of the geological map of the Ankara region around Alçı area (modified from Okay and Altner, 2017).

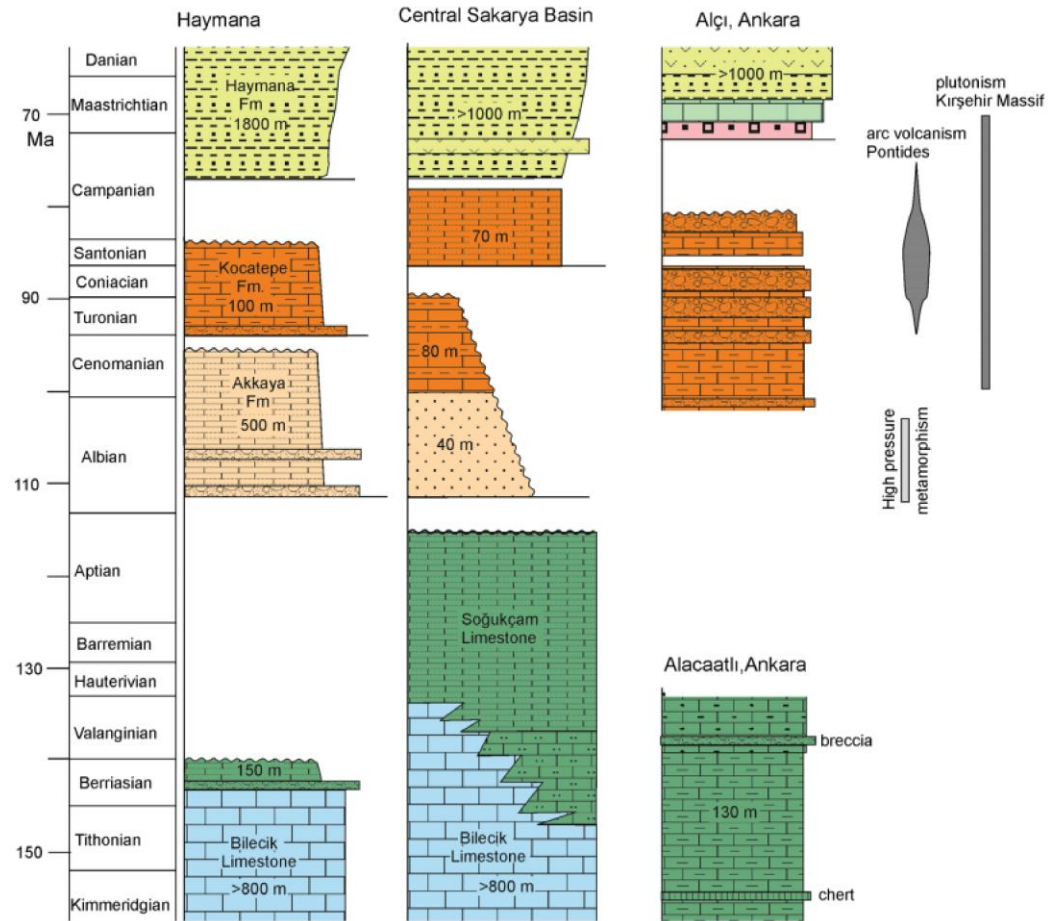


Figure 5. Cretaceous stratigraphic sections from Haymana, Central Sakarya Basin and the Ankara region (taken from Okay and Altner, 2016).

During the late Jurassic-early Cretaceous, shallow marine limestones, whose collective name is the Bilecik Limestone, were deposited in the Haymana Basin. This unit had previously been divided into two different formations called as the Taşçıbayırı Formation (Callovian-Kimmeridgian) and the Günören Limestone (Kimmeridgian-Hauterivian) in the Western Pontides, thereby raising the previously named Bilecik Limestone into the group rank (Altiner et al., 1991).

In the Early Cretaceous, formation of pelagic limestones and breccias called the Soğukçam Limestone follow the Bilecik Limestone in the Haymana region. This rarely-exposed sequence is described as having been preserved only in a small area east of the town of Haymana, starting with a thin breccia horizon consisting of angular to subrounded clasts of the Bilecik Limestone, on which it lies. In the Central Sakarya Basin, the basal age of the Soğukçam Limestone is time-transgressive and ranges from late Tithonian in the east to Hauterivian in the west; its upper age is late Aptian (Altiner, 1991; Altiner and Özkan, 1991).

The previously-unknown interval of Albian to Cenomanian age is described as glauconite-bearing marly limestone and radiolaria-bearing pelagic limestone with lesser amounts of breccia, calciturbidite and sandstone in the Haymana region. This unit which is composed mainly of Albian deposits and unconformably overlies the underlying Bilecik Limestone and Soğukçam Limestone is called as the Akkaya Formation by Okay and Altiner (2016). In its upper parts, pelagic limestones are intercalated with thin- to medium-bedded fine-grained sandstones with carbonate and quartz grains. This part contains a Cenomanian foraminiferal fauna.

During the late Cretaceous, deposition of a pelagic limestone and shale sequence named as the Kocatepe Formation, occurs in the Haymana region (Yüksel, 1970). The lower part of this pelagic sequence is made up of beige radiolarian micrites of lower middle Turonian age. These are overlain by red pelagic micrites of Santonian age with thin red shale intervals whose frequency increases up-section. The Coniacian stage is observed as pelagic limestones containing a Coniacian (uppermost Turonian-lowermost Santonian)

foraminiferal fauna. A condensed carbonate deposition from early Turonian to late Santonian is also detected by Okay and Altiner (2016) based on the palaeontological data obtained from several sections. This period was characterized by intense submarine volcanism in the outer Pontides, whose only evidence in the Haymana region is rare altered volcanic ash clasts in the limestone beds, which make up less than 2 % of the rock.

The latest Cretaceous witnessed the deposition of thin- to medium-bedded sandstone and shale of the Haymana Formation of Campanian-Maastrichtian age (Yüksel, 1970; Ünalın et al. 1976). The Haymana Formation starts with mudstones and shales with thin sandstone and siltstone beds, representing distal turbidites and basin deposits. This formation gives a broad Campanian age based on planktonic foraminifera and transported benthic foraminifera (Toker 1979; Özkan Altiner and Özcan, 1999). The contact between the Santonian limestone of the Kocatepe Formation and the Campanian-Maastrichtian turbidites has been identified as conformable (e.g., Özcan and Özkan-Altiner 1997; Özkan-Altiner and Özcan, 1999; Huseynov 2007).

With the initiation of the Galatean arc activity in the Maastrichtian, the Haymana-Polatlı Basin started to shallow at its arcward side while its trenchward side was still under deep-marine conditions. This shallowing is reflected in the coarsening-upward sequence character of the units (Haymana Formation) in west-northwest part of the Haymana Basin (Koçyiğit, 1991).

Continued shallowing in the Paleocene resulted in the widespread and rapid fluvial to lacustrine sedimentation (Kartal, Alcı, and Uzunçarşılı formations) in the arcward periphery of the Haymana-Polatlı Basin, and olistolith occurrence derived from the reefal buildups in the deep-marine sediments (Yeşilyurt and Kırkkavak formations) in the southeastern part of the Haymana Basin (Koçyiğit, 1991) (Figure 6).

The previously emerged parts of the Haymana-Polatlı Basin periphery were covered by a short-term shallow and transgressing sea in the early to middle Eocene which is attributed to local subsidence along the margin of the forearc basin due to the variation in the isostatic balance caused by the increasing load of basin-filling sediments together

with the growing and rising accretionary wedge (Koçyiğit, 1991). This event resulted in the deposition of a widespread *Nummulites*-bearing sandy limestone (Akpınar Limestone) and clastics (Beldede and Çayraz formations) (Figure 6).

Retreat of the sea occurred during the Late Eocene and Early Oligocene resulting in becoming of the complete Ankara region a part of the land. This progressing convergence between the Sakarya continent and the Menderes-Tauride block caused the formation of a tectonical stacking up of both the forearc sediments and their basement rocks in an imbricate thrust zone. These were finally thrust onto Upper Eocene-Lower Oligocene fluvial to lacustrine deposits accumulated in the coastal plains and large lakes (Figure 6). Afterwards, the Ankara region continued to experience the effects of the convergent events until the emergence of a strike-slip neotectonic regime during early Quaternary time (Koçyiğit and Doğan, 2016).

In this geological framework, the stratigraphic section studied in this thesis project belongs to the lower to upper parts of the Upper Cretaceous of the Haymana-Polatlı Basin comprising the Akkaya, Kocatepe and Haymana formations (Figure 6).

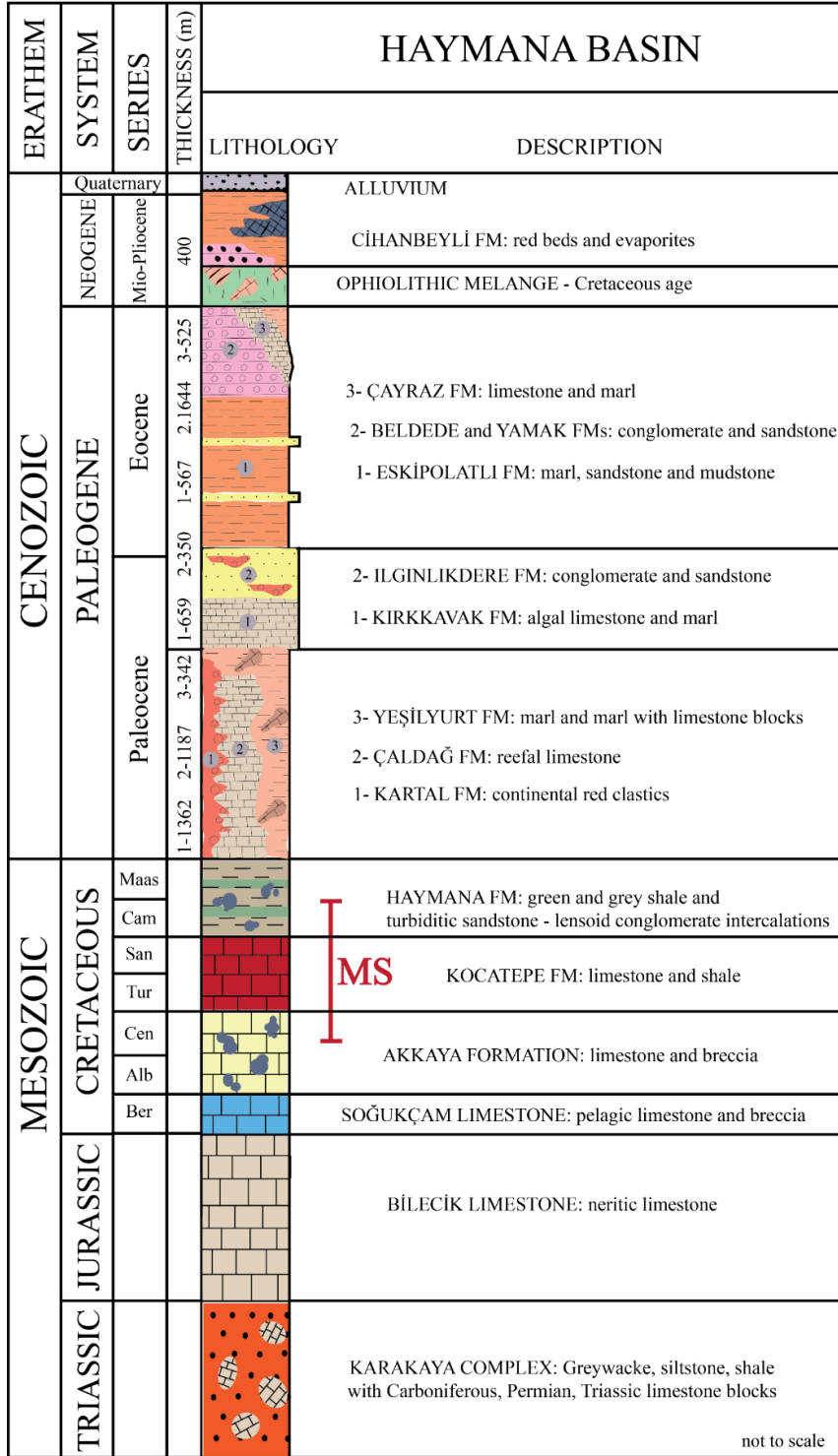


Figure 6. Generalized columnar section of the study area where MS denotes “measured section” (modified from Ünalın et al, 1976 and Okay and Altınır et al., 2016).





## CHAPTER 2

### 2. STRATIGRAPHY

#### 2.1. Lithostratigraphy

The stratigraphic section of this study was measured in the Alagöz village that is located in 40 km north of Haymana district, Ankara, Turkey. The exact coordinates of the section are 39°45'23"N - 32°29'26"E and 39°45'22"N - 32°29'19"E, respectively for the start and end points. 75 samples were collected from the section which was measured to be 93.5 m in total. Sampling interval was increased as going towards southern and monotonous parts of the section. This section comprises the Upper Cretaceous carbonate formations of the Haymana region which from older to younger are the Akkaya Formation (Albian-Cenomanian), the Kocatepe Formation (Turonian-Santonian) and the Haymana Formation (Campanian-Maastrichtian) (Figures 7 and 8).

The previously unknown Albian to Cenomanian sequence in the Haymana region has recently been recognized by Okay and Altınır (2016) and called as the Akkaya Formation. This formation was well known in the northern Turkey, most commonly in Boyabat, Sinop (Gedik et al., 1981; Korkmaz et al., 1991) and should not be confused with the Akkaya Formation in the southwestern Turkey (Kaya et al., 2001). The first 13 samples of the stratigraphic section were taken from the Akkaya Formation and these correspond to the first 8.7 m of the section. The Akkaya Formation is composed of breccia deposits which were the product of submarine debris flows (Figure 7. A-C). It mostly comprises very hard limestones and clayey limestones in the northern part; whereas the lithology becomes relatively softer and more shaly towards the south. Color of the formation also changes

from pale colors as green, gray and light brown to darker colors as dark gray and brown from the north to the south of the section (Figure 8).

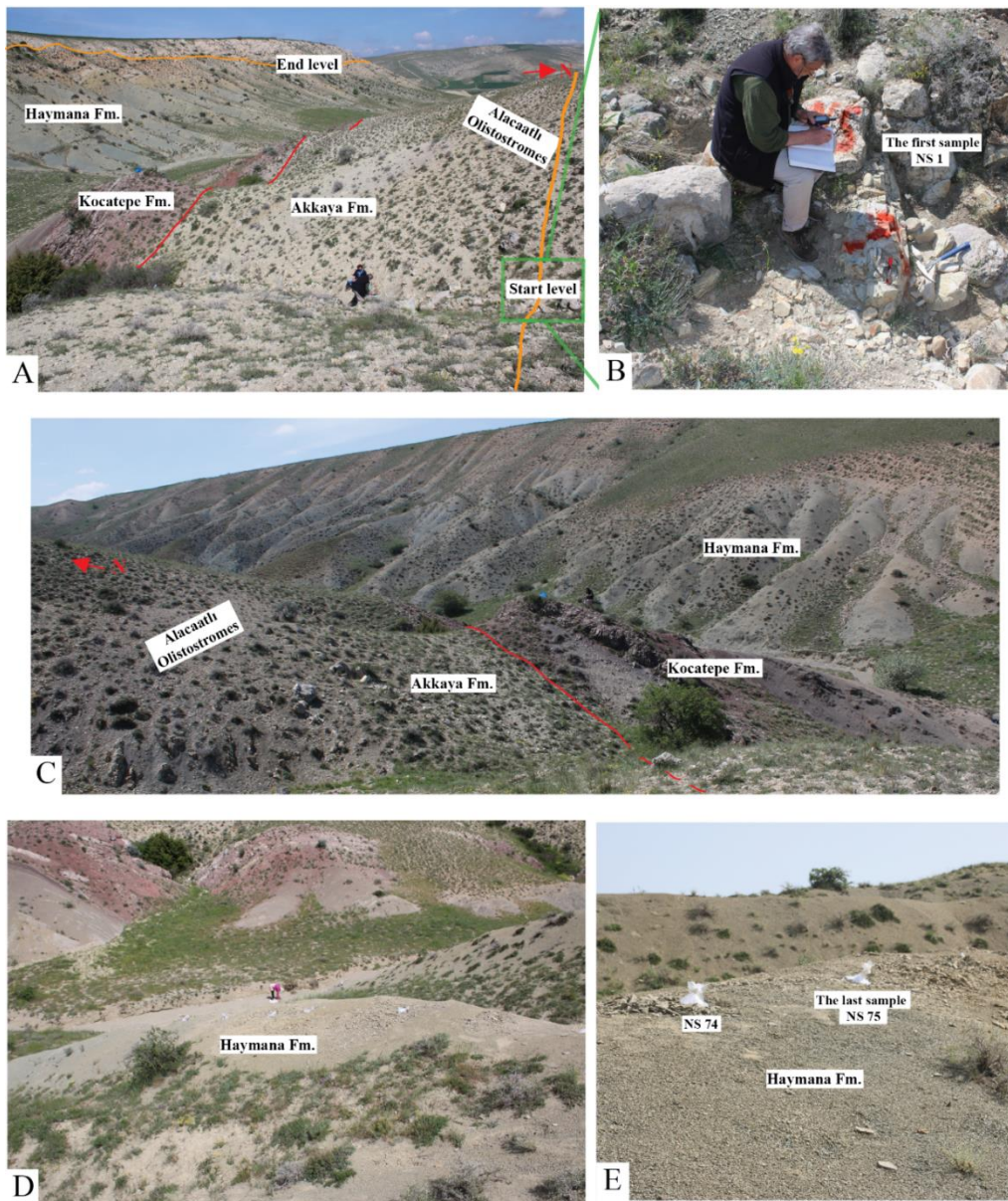


Figure 7. Photographs from the field, A. Limits and geological formations of the measured stratigraphic section, B. Start level of the stratigraphic section, C. Another view of the measured stratigraphic section, D. A view of the southern portion of the measured section, E. A close-up view of the southern portion of the measured stratigraphic section.

A pelagic Upper Cretaceous sequence of mainly limestone and shale of nearly 15 m in thickness, called the Kocatepe Formation (Yüksel, 1970) (Figure 7. A and C), unconformably overlies the Akkaya formation. Lithology becomes dominated more by shales compared to limestones towards the southern part. In addition to the unconformity marking the transition between the two formations, the Kocatepe Formation is also striking with its bright red color on top of the pale colored Akkaya Formation. 25 samples were collected from the Kocatepe Formation.

The Kocatepe formation is followed by medium-bedded silty shale and shale of the conformably overlying Haymana Formation (Figure 7. A, C, D, E.) It starts with a brief interval of red to pink silty shale, then becomes mainly greenish gray in the northeastern and bluish gray in the southwestern parts with intervening brown to yellowish brown levels of mostly silty shale (Figure 8, 9). The Haymana Formation occupies the largest portion of the measured stratigraphic section with 70 m. 37 samples were collected from this unit with relatively larger intervals compared to the northeastern part of the section. Amount of silt in the lithology increases noticeably towards the southwest, which indicates that the Haymana Formation represents distal turbidites and basin deposits on top of the red pelagic limestones of the underlying the Kocatepe Formation.



Figure 8. Lithostratigraphy of the measured section with the planktonic foraminiferal biozones determined in this study (shorter version).

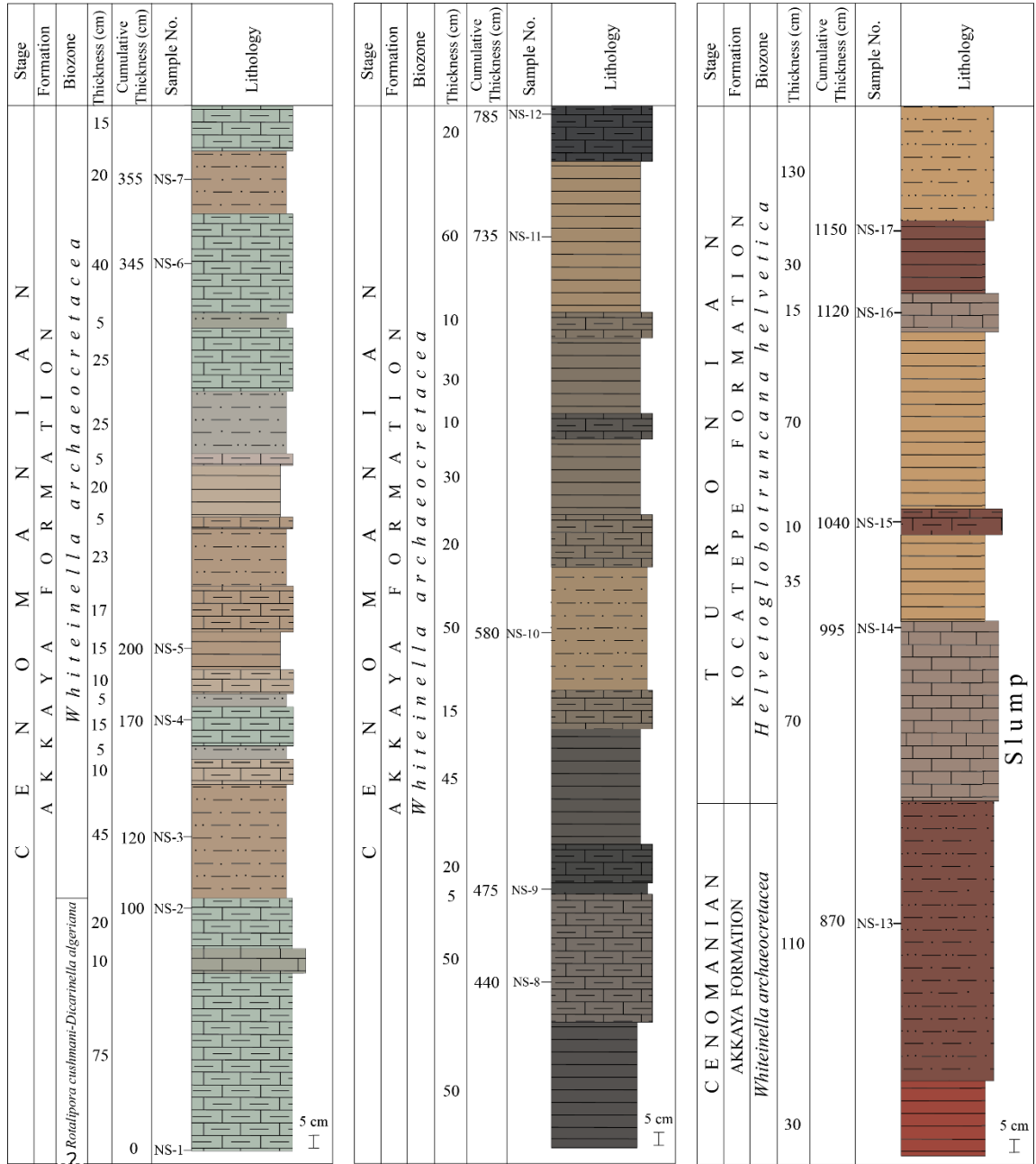


Figure 9. Lithostratigraphy of the measured section with the planktonic foraminiferal biozones determined in this study.

Stage	Formation	Biozone	Thickness (m)	Cumulative Thickness (m)	Sample No.	Lithology
T U R O N I A N	K O C A T E P E F O R M A T I O N	<i>Helvetoglobotruncana helvetica</i>	25	15.7	NS-20	
			100	14.8	NS-19	
			5			
			40			
			10			
			20			
			5			
			30			
			5			
			30			
			10			
			30	12.8	NS-18	
			130			
			(continued)			

Stage	Formation	Biozone	Thickness (m)	Cumulative Thickness (m)	Sample No.	Lithology
S A N T O N I A N	K O C A T E P E F O R M A T I O N	<i>G. elevata - D. asymeritica</i>	15	19.5	NS-34	
			5			
			10			
			20			
			15	19.2	NS-33	
			5			
			19	19	NS-32	
			5			
			10			
			5			
			15	18.7	NS-31	
			5			
			10			
			30	18.4	NS-30	
			5			
			20	18.2	NS-29	
			5			
			18	18	NS-28	
			25			
			17.5	17.5	NS-27	
			35			
			17.2	17.2	NS-26	
			17	17	NS-25	
			120	16.7	NS-24	
			16.5	16.5	NS-23	
			16.2	16.2	NS-22	
			10	16	NS-21	

Stage	Formation	Biozone	Thickness (m)	Cumulative Thickness (m)	Sample No.	Lithology
S A N T O N I A N	K O C A T E P E F O R M A T I O N	<i>G. elevata - D. asymeritica</i>	140	22	NS-37	
			10	20.7	NS-36	
			130			
			19.5	19.5	NS-35	

Figure 9. Continued



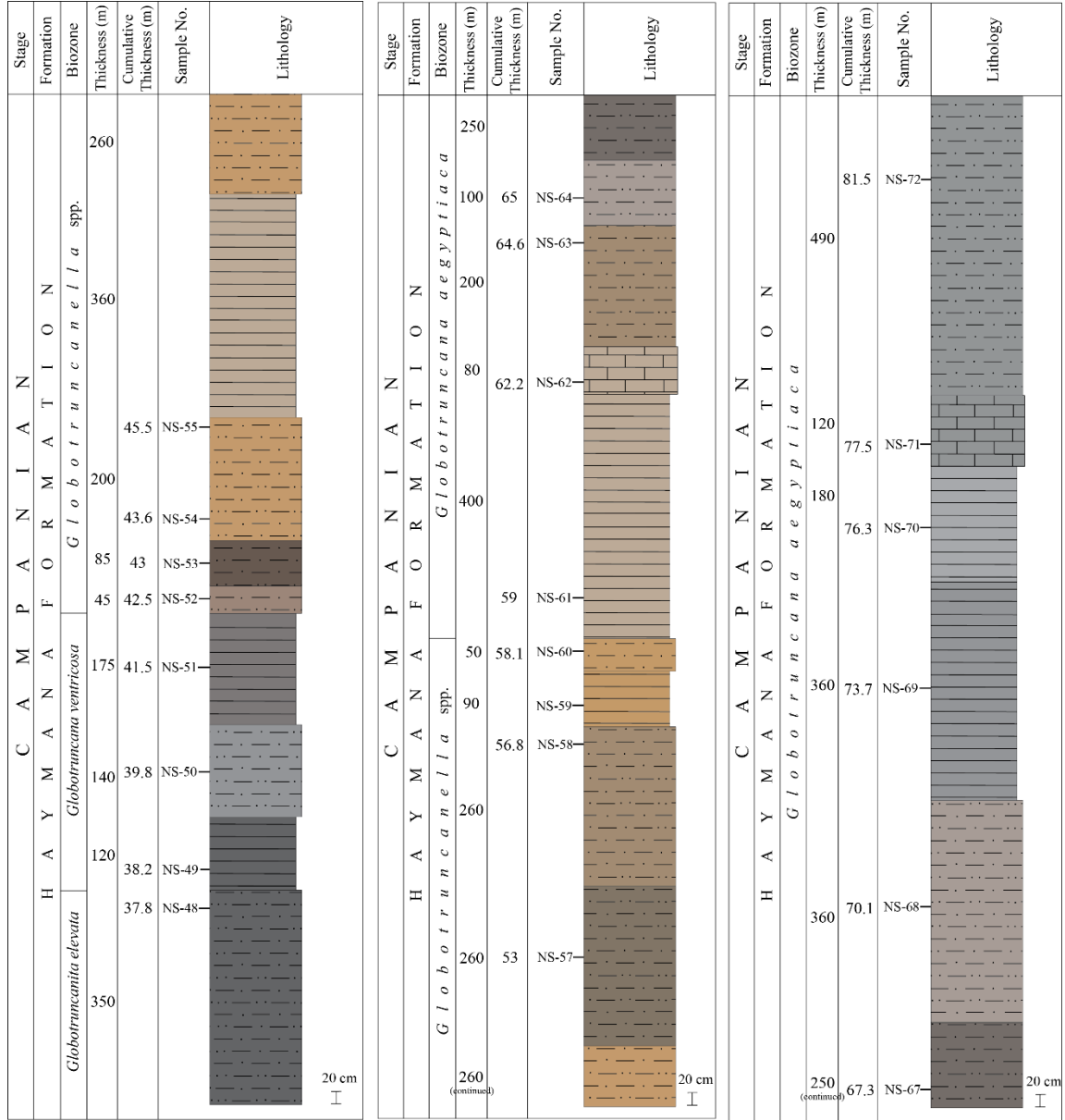


Figure 9. Continued



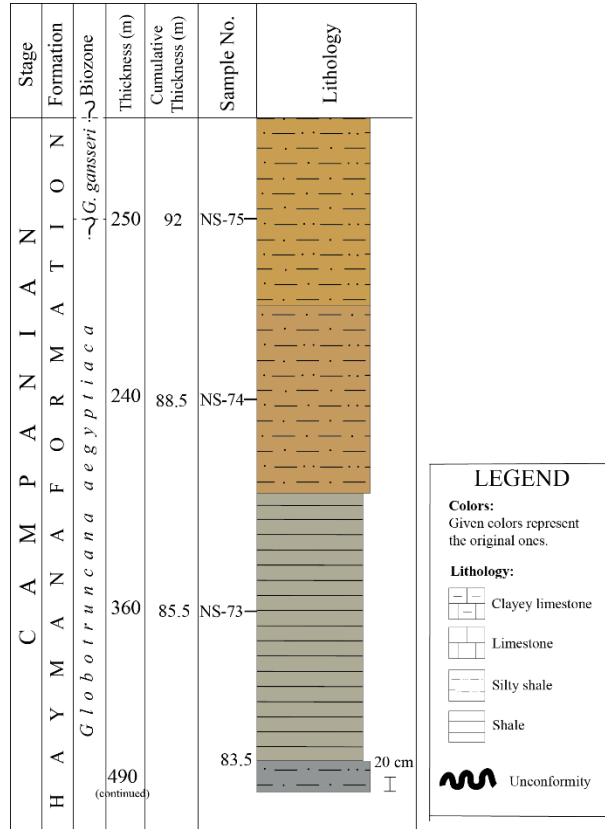


Figure 9. Continued

## 2.2. Biostratigraphy

The primary aim of this study was to establish a reliable and detailed biostratigraphic framework for the upper Cretaceous pelagic succession of the Haymana Basin. To this end, three formations in the Haymana Basin, the Akkaya, Kocatepe and Haymana Formation's, have been examined in terms of their planktonic foraminiferal content. A 93.5 meters thick sedimentary succession was measured and sampled. At the end, 80 planktonic foraminifera species belonging to 22 different genera are identified and their first and last occurrence levels are recorded (Figure 10). Then, the measured stratigraphic section is divided into ten biozones by using planktonic foraminiferal bioevents.

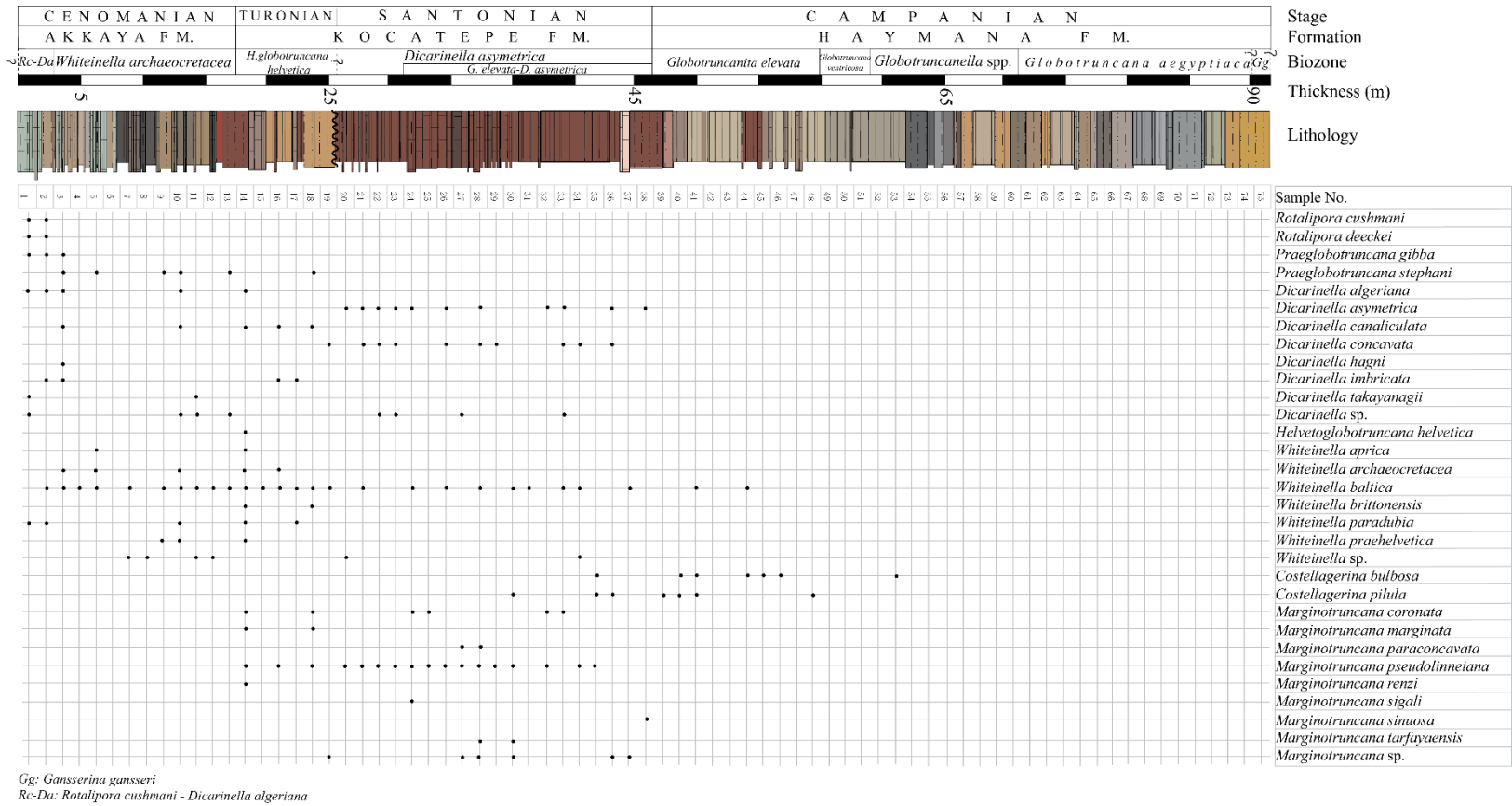


Figure 10. Range chart of the planktonic foraminifera species identified in this study.

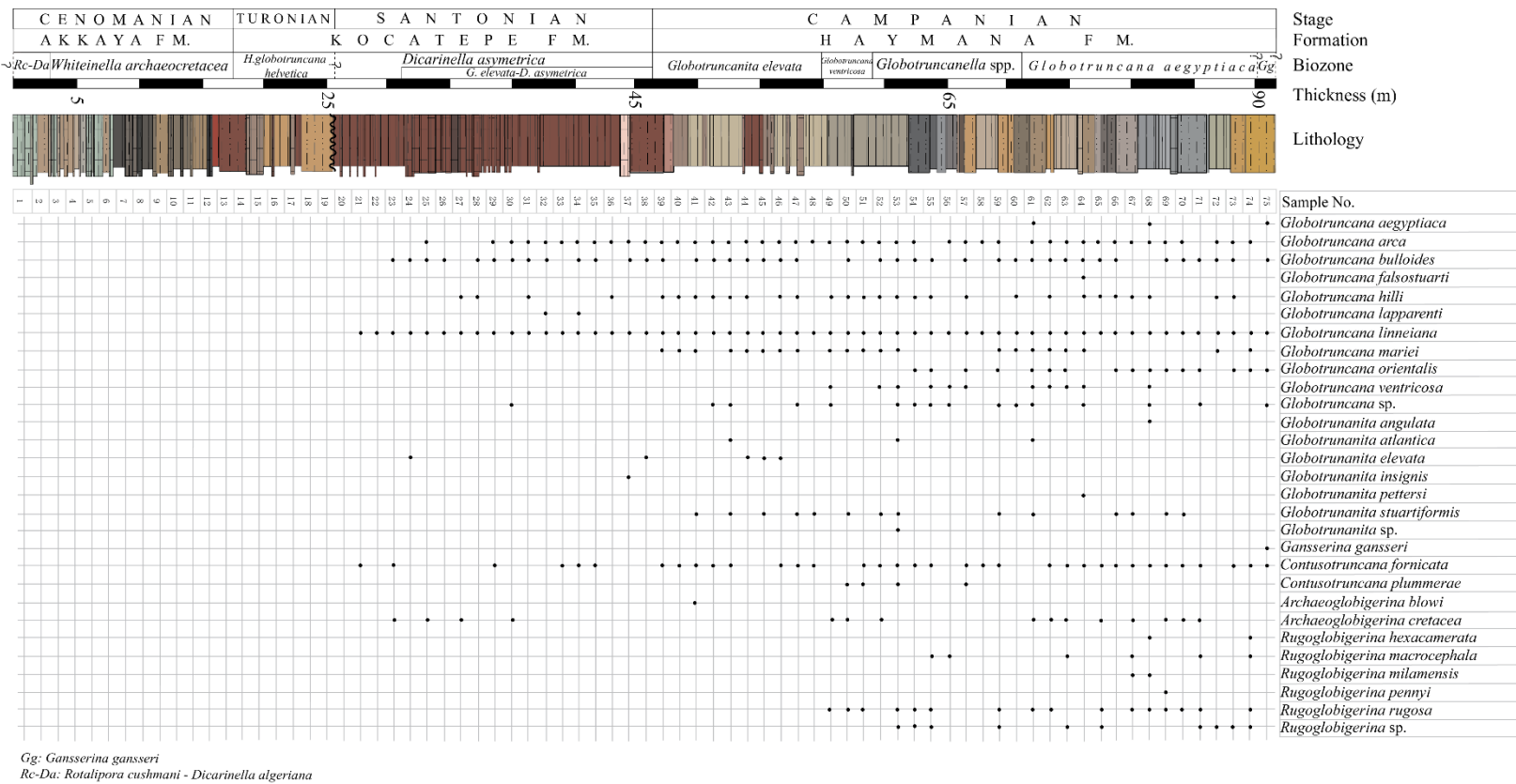
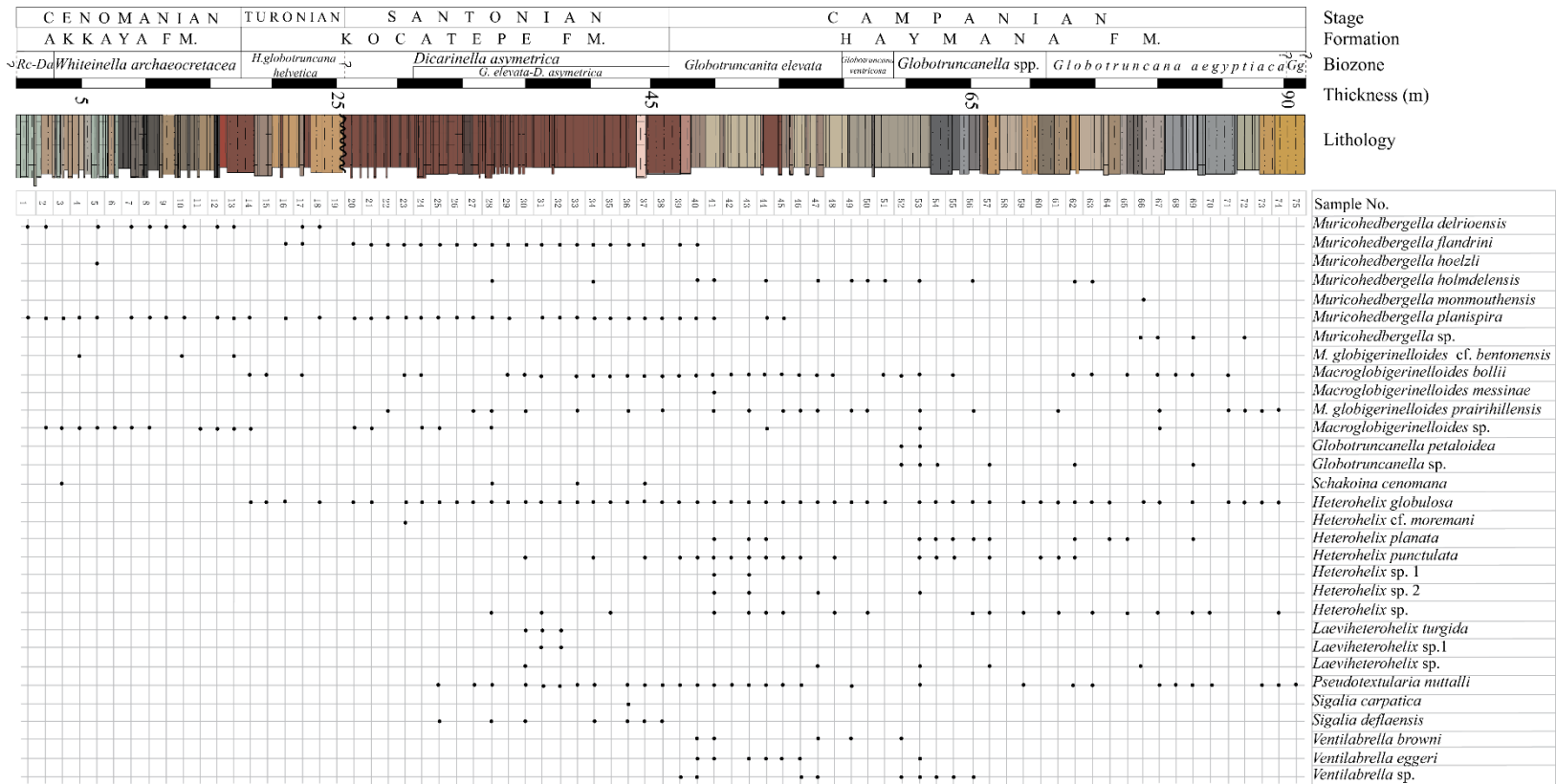


Figure 10. Continued.



Gg: *Gansserina gansseri*  
 Re-Da: *Rotalipora cushmani* - *Dicarinella algeriana*

Figure 10. Continued.

Based on the planktonic foraminiferal biostratigraphy, the boundaries between stages Cenomanian-Turonian and Santonian-Campanian are also established. The Cenomanian-Turonian boundary is placed at the lowest occurrence of the important species *Helvetoglobotruncana helvetica*. It is not coincident with a major lithology change; this boundary is represented by dark grey shale and clayey limestones below and light brown limestones above in the measured stratigraphic section. Late Turonian, Coniacian and probably earliest Santonian were absent in the measured stratigraphic section. This hiatus between early Turonian and early Santonian was observed to be coincident with a major lithological boundary between very hard greenish to grey limestones below and relatively softer red limestones and shales above. No stratigraphic discontinuity has been detected throughout the Santonian-Campanian successions which occupy the greatest portion in the measured stratigraphic section. Therefore, the boundary between these two stages could be studied in the most detail. The Santonian-Campanian boundary falls exactly at the transition where the red Santonian limestones leave their place to the light brown Campanian shales. As for the Campanian-Maastrichtian boundary, it is envisaged to be close to the end of the measured stratigraphic section as signaled by the first occurrence of *Globotruncanita pettersi* (NS-64), *Globotruncanita angulata* (NS-68) and *Gansserina gansseri* (NS-75).

The planktonic foraminiferal biozones and stage boundaries established in this study (Figure 11) are given in the following descriptions in detail.

Stage	Substages		Author (Year)	Location	Stratigraphy					Species	Remarks
	U	L			Santonian	Coniacian	Turonian	Cenomanian	Datum Markers		
Campanian	U	L	Glibotruncana iricarinata	Libya	Glibotruncanilla elevata	Glibotruncanilla elevata	Dicarinella concavata	M. sigali	H. helvetica	R. cushmani	Barr (1972)
	U	L	Glibotruncanilla elevata	Egyt	Dicarinella concavata	M. schneegansi	H. helvetica	Not studied			
									U	L	Glibotruncanilla elevata
	U	L	Glibotruncanilla elevata	Mediterranean	Dicarinella concavata	M. schneegansi	H. helvetica	Sigal (1977)			
									U	L	Glibotruncanilla elevata
	U	L	Glibotruncanilla elevata	Paris Basin	Dicarinella concavata	M. schneegansi	H. helvetica	Robaszynski & Caron (1995)			
									U	L	Glibotruncanilla elevata
	U	L	Glibotruncanilla elevata	S Bulgaria	Dicarinella concavata	M. sigali	H. helvetica	Dimitrova & Vokhlev (2007)			
									U	L	Glibotruncanilla elevata
	U	L	Glibotruncanilla elevata	Generalized	Dicarinella concavata	M. sigali	H. helvetica	Robaszynski et al. (1984)			
									U	L	Glibotruncanilla elevata
	U	L	Glibotruncanilla elevata	Generalized	Dicarinella concavata	M. sigali	H. helvetica	Siler (1989)			
									U	L	Glibotruncanilla elevata
	U	L	Glibotruncanilla elevata	NE Iran	Dicarinella concavata	M. sigali	H. helvetica	Ardestani et al. (2012)			
U									L	Glibotruncanilla elevata	Turkey
	U	L	Glibotruncanilla elevata	E Iran	Dicarinella concavata	M. sigali	H. helvetica	Bairazadeh et al. (2007)			
U									L	Glibotruncanilla elevata	N Iraq
	U	L	Glibotruncanilla elevata	E Iran	Dicarinella concavata	M. sigali	H. helvetica	Ogg and Hinov (2012)			
U									L	Glibotruncanilla elevata	Central Turkey

Substages Datum Markers  
U: Upper HO: Highest occurrence  
M: Middle LO: Lowest occurrence  
L: Lower

Figure 11. Biozonal stratigraphic comparison chart of the Cenomanian-Campanian planktonic foraminifera.

### 2.2.1. *Rotalipora cushmani* Zone

**Definition:** Total range zone of *Rotalipora cushmani* (Borsetti, 1962). However, this part of the section corresponds to the uppermost part of the *Rotalipora cushmani* Zone in this study.

**Remarks:** Although this zone is officially defined as a total-range zone, the lower boundary of this zone is depicted with ambiguity. The first appearance of the nominal species could not be recorded since the first sample of the measured section is above this level. However, the presence of *Rotalipora cushmani* in the first two samples (NS-1 and NS-2) definitely shows that this part of the section is in the *Rotalipora cushmani* biozone. Moreover, coexistence of *Dicarinella algeriana*, *Whiteinella baltica*, *W. paradubia* and *R. cushmani* in these samples supports this interpretation. It is envisaged to cover the uppermost part of the *Rotalipora cushmani* Zone. It corresponds to middle to late portion of the Cenomanian in the measured section and its thickness is 1 meter.

Important planktonic foraminifera identified in this biozone are as follows: *Rotalipora cushmani*, *Rotalipora deecke*, *Praeglobotruncana gibba*, *Whiteinella paradubia* and *Dicarinella algeriana*.

**Stratigraphic distribution:** From sample NS-1 to sample NS-2

**Age:** Middle to Late Cenomanian

#### *Dicarinella algeriana* Subzone

**Definition:** Interval between the lowest occurrence of *Dicarinella algeriana* and extinction of the genus *Rotalipora*.

**Author:** PREMOLI-SILVA and VERGA, 2004

**Remarks:** This subzone covers only the first two samples (NS-1 and NS-2) of the section where the lowest occurrence of *Dicarinella algeriana* (NS-1) and highest occurrence of the rotaliporids (NS-2) are detected. However, the lower boundary of this zone is

delineated with uncertainty due to the highly possible lower first occurrence of *Dicarinella algeriana* that defines the base of this zone.

Notable planktonic foraminifera characterizing this biozone are as follows: *Rotalipora cushmani*, *Rotalipora deeckeii*, *Whiteinella gibba*, *Whiteinella paradubia* and *Dicarinella algeriana*.

**Stratigraphic distribution:** From sample NS-1 to sample NS-2

**Age:** Late Cenomanian

### 2.2.2. *Whiteinella archaeocretacea* Zone

**Definition:** Partial range zone between the highest occurrence of *Rotalipora cushmani* and the lowest occurrence of *Helvetoglobotruncana helvetica*.

**Author:** BOLLI, 1966

**Remarks:** *Whiteinella archaeocretacea* is a biozone covering almost 9 meters in the measured stratigraphic section. This zone is commonly characterized by a low-diversity assemblage related to the widespread deposition of organic rich sediments during the OAE2. Assemblages in this interval are known to include rare specimens of *Muricohedbergella*, *Whiteinella* and *Dicarinella* (Premoli-Silva and Verga, 2004). This situation is evident also in this study. The interval from sample NS-6 to sample NS-9 lacks whiteinellid and dicarinellid diversification. Although they occur rarely, *Whiteinella* and *Dicarinella* species start to diversify starting from sample NS-10.

The marker planktonic foraminifera of this biozone are as follows: *Macroglobigerinelloides bentonensis*, *Muricohedbergella planispira*, *Muricohedbergella delrioensis*, *Whiteinella baltica*, *Whiteinella aprica*, *Whiteinella archaeocretacea*, *Whiteinella prae-helvetica*, *Whiteinella paradubia*, *Dicarinella canaliculata* and *Heterohelix moremani*.

**Stratigraphic distribution:** From sample NS-3 to sample NS-13.



**Age:** Latest Cenomanian to earliest Turonian

### **2.2.3. *Helvetoglobotruncana helvetica* Zone**

**Definition:** Total range zone of *Helvetoglobotruncana helvetica*. However, due to not observing the last occurrence of the nominal species, this zone has been used as an assemblage zone of *Helvetoglobotruncana helvetica* in this study.

**Author:** SIGAL, 1955

**Remarks:** *Helvetoglobotruncana helvetica* Zone covers almost 7 meters in the Middle Turonian of the measured stratigraphic section. Presence of *H. helvetica* can be given as the hallmark of the Turonian stage. Although previous work suggested that *H. helvetica* is indicative of the mid-Turonian (Salaj, 1980, 1997; Wonders, 1980; Robaszynski et al., 1984; Caron, 1985; Sliter, 1989; Abdel-Kireem et al., 1996; Premoli Silva & Verga, 2004; Abawi & Mahmood, 2005), it is now considered to denote an interval in the early Turonian (Caron et al., 2006; Desmares et al., 2007; Gebhardt et al., 2010; Ogg and Hinnov, 2012; Huber and Petrizzo, 2014; Vahidinia et al., 2014).

This zone is actually defined as a total range zone by using the stratigraphic distribution of *Helvetoglobotruncana helvetica*. The problem with the definition of this zone arises from the fact that the nominal species is found in only one sample (NS-14). This level must be the lowest occurrence (LO) *H. helvetica* since it co-occurs with some other characteristic species as *W. praehelvetica* and *W. archaeocretacea* in sample NS-14. Although the highest occurrence of *H. helvetica* was not detected, the Turonian planktonic foraminiferal fauna suddenly disappears after sample NS-19. Moreover, the highest occurrence of *Praeglobotruncana stephani*, which is known to have its last appearance top in the Turonian stage, and the lowest occurrence of *Dicarinella concavata*, whose first appearance is known as the upper Turonian, also occur in the latest portion of this zone in samples NS-18 and NS-19, respectively. These indicate that the upper boundary of this zone is at least closely approximated in the studied section. Another important point indicated here is that the *Dicarinella concavata* zone may already be present starting from the sample NS-19. However, it is not defined here due to insufficient data and requires

further and more detailed examination of this interval. The upper boundary of this zone is delineated with the unconformity between samples NS-19 and NS-20.

The important planktonic foraminifera observed in this biozone are *Helvetoglobotruncana helvetica*, *Marginotruncana renzi*, *Marginotruncana coronata*, *Marginotruncana pseudolinneiana* and *Heterohelix globulosa*.

**Stratigraphic distribution:** From sample NS-14 to sample NS-19. Although the last occurrence of the nominal species *H. helvetica* was not observed in the section, this biozone is defined between samples NS-14 and NS-19 based on the presence of secondary characteristic species described above and the lowest occurrence of *Dicarinella asymetrica* in sample NS-20. The boundary between these two samples also correspond to an unconformity in the section.

**Age:** Early to middle Turonian

#### 2.2.4. *Dicarinella asymetrica* Zone

**Definition:** Total range zone of *Dicarinella asymetrica*

**Author:** POSTUMA, 1971

**Remarks:** *Dicarinella asymetrica* Zone whose lower boundary corresponds to an unconformity in the section starts with the first occurrence of the nominal species *Dicarinella asymetrica* in the first sample above the unconformity, NS-20. This important bioevent is followed by consequent first occurrences of some *Globotruncana* species as *G. linneiana* in sample NS-21 and *G. bulloides* in sample NS-23. It covers almost 7 meters of the measured stratigraphic section.

The marker planktonic foraminifera species characterizing this biozone are *Dicarinella asymetrica*, *Pseudotextularia nuttalli*, *Sigalia deflaensis*, *Sigalia carpatica*, *Laeviheterohelix turgida*, *Globotruncana linneiana*, *Globotruncana arca*, *Globotruncana bulloides* and *Globotruncana hilli*.

**Stratigraphic distribution:** From sample NS-20 to sample NS-38.

**Age:** Early Santonian to earliest Campanian

*Globotruncanita elevata*- *Dicarinella asymetrica* Concurrent Range Subzone

**Definition:** The interval between the lowest occurrence of *Globotruncanita elevata* and the highest occurrence of *Dicarinella asymetrica*.

**Author:** This is not a formal planktonic foraminiferal biozone, but is a concept used by many authors to reach higher resolution in the planktonic foraminiferal biostratigraphy at the S/C boundary (Masters, 1970, 1977; Van Hinte, 1976; Wonders, 1980; Dowsett, 1984).

**Remarks:** This important biozone is detected to occupy an approximately 6 m interval at the S/C transition of the stratigraphic section. Marginotruncanids gradually disappear towards the top of this zone. The genera *Dicarinella* and *Marginotruncana* completely become extinct at the end. So, the last occurrence of marginotruncanids and *D. asymetrica* are detected in this interval. *Muricohedbergella flandrini* exhibits a very consistent occurrence pattern throughout the previous and this biozone. Contrary to the general opinion (Premoli Silva and Verga, 2004; Babazadeh et al., 2007; Wagreich et al., 2016), *Muricohedbergella flandrini* continues to exist further above the *Globotruncanita elevata*-*Dicarinella asymetrica* concurrent range Subzone up to the sample NS-40 in this study; this situation may suggest an extension of the range zone of *M. flandrini*.

**Stratigraphic distribution:** From sample NS-24 to sample NS-38.

**Age:** Late Santonian or earliest Campanian (Robaszynski et al., 1984; Wagreich, 1992)

**2.2.5. *Globotruncanita elevata* Zone**

**Definition:** Partial range zone between the highest occurrence of all *Dicarinella* species to the lowest occurrence of *Globotruncana ventricosa*.

**Author:** ROBASZYNSKI and CARON, 1995

**Remarks:** *Globotruncanita elevata* Zone is the second Campanian biozone and it is nearly 15 meters in thickness in the stratigraphic section. Important bioevents in this biozone include the first occurrence of the rare *Globotruncanita atlantica*. This zone comprises the further diversification of the genera *Globotruncana*, *Ventilabrella* and *Heterohelix* as well as frequent occurrences of multiple *Costellagerina* species.

*Globotruncanita stuartiformis*, *Globotruncanita atlantica*, *Ventilabrella browni* and *Ventilabrella eggeri* firstly appeared in this biozone.

**Stratigraphic distribution:** From sample NS-39 to sample NS-48.

**Age:** Early Campanian

#### **2.2.6. *Globotruncana ventricosa* Zone**

**Definition:** Interval between the lowest occurrence of *Globotruncana ventricosa* to the lowest occurrence of *Globotruncanella* spp. (substituted for *Radotruncana calcarata*).

**Author:** ROBASZYNSKI and CARON, 1995

**Remarks:** *Globotruncana ventricosa* Zone extends along the middle part for 3.5 meters of the recorded Campanian in the measured section. First occurrence of *Contusotruncana plummerae* and Genus *Rugoglobigerina* in this biozone is noteworthy.

Important lowest occurrences in this biozone belong to *Globotruncana ventricosa*, *Contusotruncana plummerae* and *Rugoglobigerina rugosa*.

**Stratigraphic distribution:** From sample NS-49 to sample NS-51.

**Age:** Middle Campanian

#### **2.2.7. *Globotruncanella* spp. Zone**

**Definition:** Interval zone from the lowest occurrence of *Globotruncanella* spp. (substituted for the highest occurrence of *Radotruncana calcarata*) to the lowest occurrence of *Globotruncana aegyptiaca*.

**Author:** CARON, 1978

**Remarks:** *Globotruncanella* spp. Zone covers 16 meters in the upper part of the stratigraphic section. This zone is originally named as *Globotruncanella havanensis* Zone, however the nominal species is not found in this study. Therefore, an equivalent bioevent, the diversification of the genus *Globotruncanella*, is used to define this biozone here.

Important bioevents include the lowest occurrence and diversification of the genus *Globotruncanella* including the first appearance of *Globotruncanella petaloidea* and the maximum diversification of the genus *Heterohelix* in sample NS-54.

**Stratigraphic distribution:** From the sample NS-52 to the sample NS-60.

**Age:** Late Campanian

#### **2.2.8. *Globotruncana aegyptiaca* Zone**

**Definition:** Interval between the lowest occurrence of *Globotruncana aegyptiaca* to the lowest occurrence of *Gansserina gansseri*.

**Author:** CARON, 1985

**Remarks:** *Globotruncana aegyptiaca* zone is the latest biozone completely identified and it covers 33 meters in the measured section. A very important bioevent observed in this zone is the diversification and increasing abundance of the genus *Rugoglobigerina*. Toward the upper part of this zone, they have been observed to fill the niches emptied by disappearing muricohedbergellids and macroglobigerinelloids quite noticeably. This is known as a signal for the transition from *Globotruncana aegyptiaca* zone to *Gansserina gansseri* zone (Premoli Silva and Verga, 2004).

Other important bioevents are the first occurrences of genus *Rugotruncana*, *Globotruncanita angulata*, *Globotruncanita pettersi* and *Muricohedbergella monmouthensis*. The maximum abundance and diversification of globotruncanids is observed in this biozone, coincident with the global abundance data presented by Premoli Silva and Sliter (1999; see Figs 9 and 10).

The marker planktonic foraminifera of this biozone are *Globotruncanita angulata*, *Globotruncanita pettersi*, *Rugoglobigerina macrocephala*, *Rugoglobigerina pennyi* and *Rugoglobigerina hexacamerata*.

**Stratigraphic distribution:** From the sample NS-61 to the sample NS-74.

**Age:** Late Campanian to latest Campanian/the beginning of Maastrichtian

### 2.2.9. *Gansserina gansseri* Zone

**Definition:** Interval between the lowest occurrence of *Gansserina gansseri* to the lowest occurrence of *Contusotruncana contusa* and *Racemiguembelina fruticosa*.

**Author:** CARON, 1985

#### **Remarks:**

*Gansserina gansseri* zone begins in the last sample of this study. Its upper boundary was not identified and thus delineated with uncertainty; it should continue higher into the marls of the Haymana Formation. Its lower boundary was also delineated with uncertainty due to lowest occurrences of *Globotruncanita angulata* and *Globotruncanita pettersi* in samples NS-68 and NS-64, respectively.

*Gansserina gansseri* appears for the first time in this zone. Although in the previous decades *Gansserina gansseri* was thought to have its first occurrence in the Maastrichtian (Barr, 1972; Premoli Silva and Bolli, 1973; Caron, 1985; Sliter, 1989; Li and Keller, 1998; Li et al., 1999), today it is widely accepted to be contained in the latest Campanian (Premoli Silva and Sliter, 1994, 1999; Robaszynski, 1998; Özkan-Altiner and Özcan, 1999; Robaszynski et al., 2000; Chacon et al., 2004; Premoli Silva and Verga, 2004; Sari, 2006, 2009; Ogg and Hinnov, 2012; Beiranvand and Ghasemi-Nejad, 2013). Therefore, it is a highly reliable bioevent to determine the latest Campanian. It is crucial for this study in terms of approximating the Campanian-Maastrichtian boundary that the first occurrence of *G. gansseri* could be observed in the latest sample NS-75 together with the lowest

occurrences of *Globotruncanita angulata* and *Globotruncanita pettersi* in samples NS-68 and NS-64, respectively.

**Stratigraphic distribution:** Sample NS-75.

**Age:** Latest Campanian to early Maastrichtian





## CHAPTER 3

### 3. MICROFACIES ANALYSIS

#### 3.1. Types of Microfacies and Depositional Environments

First definitions of “microfacies” were originally coined by Brown (1943) and again independently by Cuvillier (1952) shortly as “petrographic and paleontological criteria studied in thin-sections”. Today, microfacies is regarded as the total of all sedimentological and paleontological data which can be described and classified from thin sections, peels, polished slabs or rock samples (Flügel, 2004).

Microfacies analyses can yield a vast amount of information about carbonate rocks, including their depositional and diagenetic history, the biological controls on carbonate sedimentation and the fossil content of these rocks, the relationships between diagenetic processes, porosity and dolomitization. These, in turn, provide the necessary knowledge for evaluating sequence stratigraphic frameworks and depositional models, differentiating paleoclimate changes, tracing platform-basin relationships, evaluating reservoir rocks and limestone resources (Flügel, 2004).

In this study, the samples have been examined in terms of their paleontological and sedimentological content in order to interpret the depositional history of the area and then to combine this result with the other findings of this study. A number of criteria have been evaluated for the samples to this end; these are listed in the Microfacies Analysis Table given. Then, the samples have been named using the data obtained from their microfacies analysis and the usual Dunham Classification (Figure 12) (Dunham, 1962).

**Carbonates**

**Dunham (1962)**

Groundmass:		Fine carbonate matrix		+ spar	sparry cement	Bioconstruction
<b>Matrix-supported</b>		<b>Grain-supported</b>				
Grains: < 10%		Grains: > 10%				BOUNDSTONE
MUDSTONE	WACKESTONE	PACKSTONE		GRAINSTONE		




Figure 12. Dunham classification (1962).

The data obtained from microfacies analysis is transformed into the kind of practical knowledge described previously by use of facies models. Application of these models to the raw microfacies data gives one the insight into the depositional conditions and history of a carbonate rock. The most frequently used facies models are those hypothesizing on platforms and ramps (Flügel, 2004). One of the most useful facies models belong to Wilson (1975), in which he used idealized facies belts defined along an abstract transect from open-marine deep basins across a slope, a pronounced platform marginal rim (characterized by reefs or/and a zone with sand shoals), and an inner platform to the coast (Figure 13).

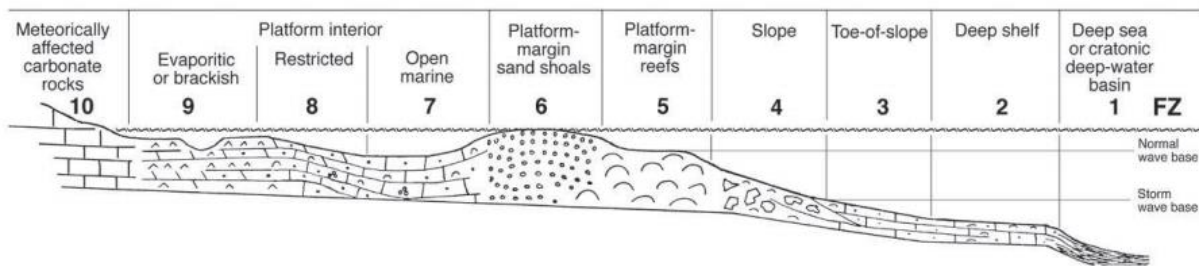


Figure 13. The Standard Facies Zones on a Rimmed carbonate platform of the modified Wilson model (Flügel, 2004).

Based on the recognition of consistently recurrent patterns of carbonate facies in the Phanerozoic stratigraphic record and the environmental interpretation of these patterns by

using characteristics of Holocene sedimentation patterns, Flügel (2004) modified the Wilson model and established the “Standard Facies Zones” exhibiting specific “Standard Microfacies Types (SMF)” (Figure 14).

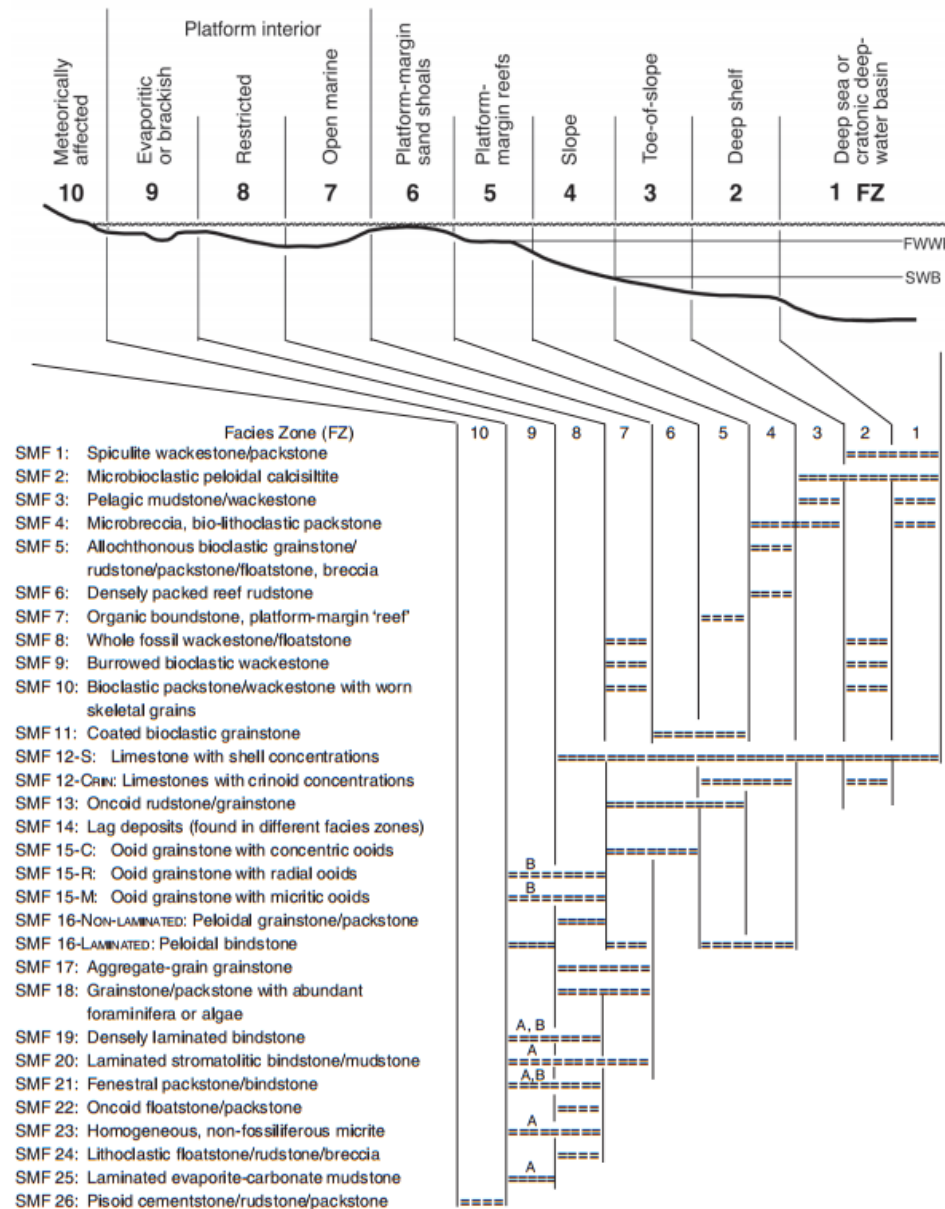


Figure 14. Distribution of Standard Microfacies (SMF) types in the Facies Zones (FZ) of Wilson (1975) on a rimmed carbonate platform model (Flügel, 2004) (A: evaporitic, B: brackish).

However, these facies belt definitions are intended for tropical platforms and are not applicable to platforms in cool-water settings which often correspond better to non-rimmed platforms or ramps (Flügel, 2004). Consequently, Flügel (2004) defined another set of microfacies types called “Ramp Microfacies Types (RMF)” (Fig 15).

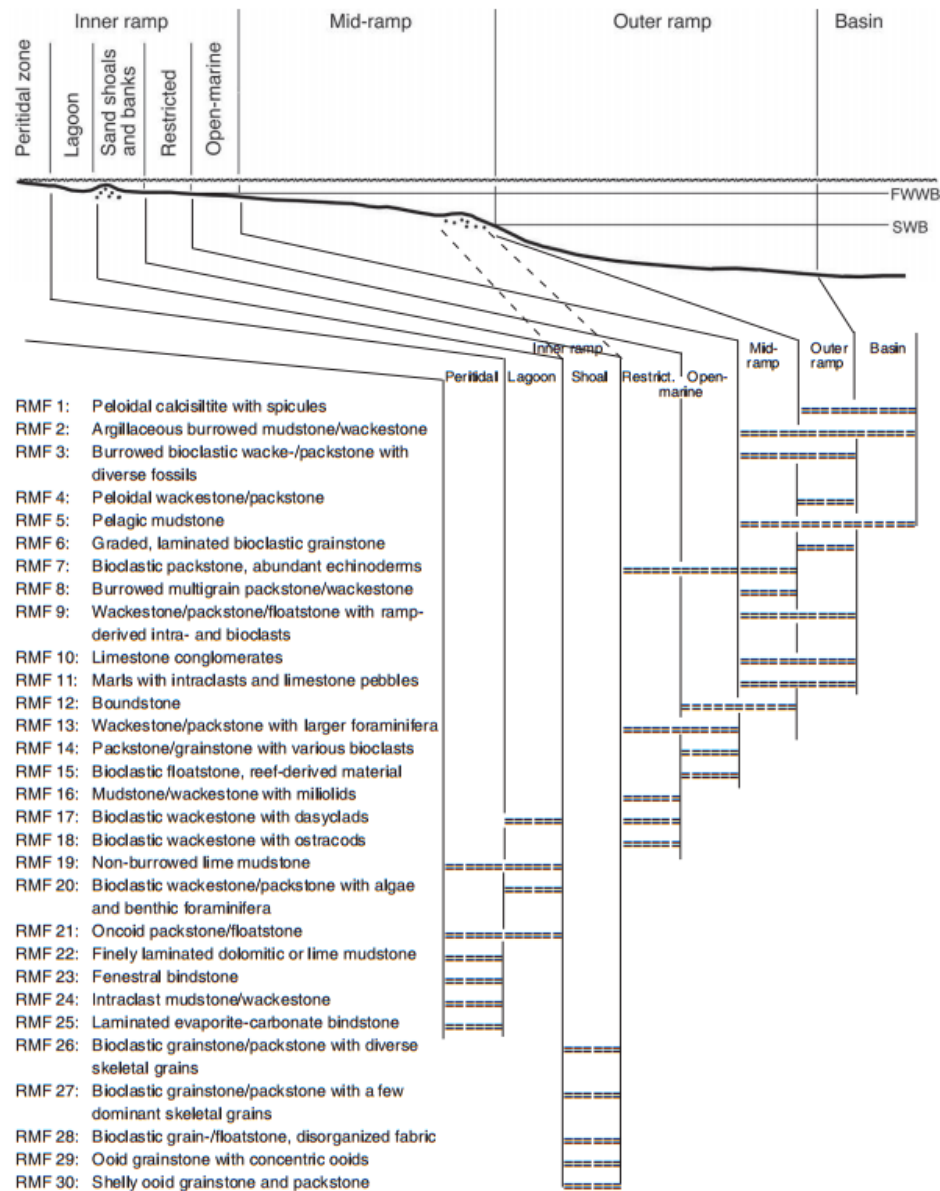


Figure 15. Generalized distribution of microfacies types (RMF) in different parts of a homoclinal carbonate ramp (Flügel, 2004).

As he notes, “Some of these Ramp Microfacies Types (RMF) correspond in their criteria to SMF Types of carbonate platforms, but other RMF Types do not. The RMF Types should not be regarded as obligatory categories comparable with the SMF Types. The

latter are better defined and are based on more case studies than the RMF Types, which only reflect a summary of the current state of the art.”

In this study, 77 thin sections representing 75 samples have been examined to identify their paleontological (planktonic foraminifera, radiolaria and ostracoda) and sedimentological content. They are named according to Dunham’s Classification (1962) and field observations. As a result, 10 different microfacies have been defined. The equivalents among “Standard Microfacies Types (SMF)” and “Ramp Microfacies Types (RMF)” are also given in order to be able to interpret the depositional history of the basin (Table 2).

These microfacies are namely, Planktonic Foraminiferal Packstone, Radiolarian Foraminiferal Packstone, Packstone with Planktonic Foraminifera and Radiolaria, Radiolaria-bearing Spiculite Packstone, Planktonic Foraminiferal Wackestone, Wackestone with Planktonic Foraminifera and Radiolaria, Silty Wackestone-Mudstone with Planktonic Foraminifera and Wackestone-Mudstone.

Table 2. Microfacies types, corresponding depositional environments

No	Microfacies Type	Description	Grain Types/ Fossils	Lithofacies Type	Depositional Environment	
<b>I. Packstone</b>	<b>I.I</b>	Planktonic Foraminiferal Packstone	Packstone with very abundant planktonic foraminifera and less abundant radiolaria	Planktonic foraminifera, radiolaria, oxide minerals, silica replaced fossils, pyrite and quartz grains, burrowings	SMF 2 & RMF 4	Deeper basin and/or open-marine shelf
	<b>I.II</b>	Radiolarian Packstone	Packstone with very abundant radiolaria	Radiolaria, pyrite and quartz grains, burrowings, ostracods, hyaline shell fragments	SMF 2 & RMF 4	Deep-shelf - toe-of-slope
	<b>I.III</b>	Packstone with Planktonic Foraminifera and Radiolaria	Packstone with even amounts of planktonic foraminifera and radiolaria	Quartz grains, burrowings, spicules, silica replaced fossils	SMF 2 & RMF 4	Deeper basin and/or open-marine shelf
	<b>I.IV</b>	Radiolaria-bearing Spiculite Packstone	Packstone with abundant monaxone megascleres and a less amount of radiolaria	Monaxone megascleres, radiolaria, ostracod, mollusc and hyaline fragments, pyrite and quartz grains, oxide minerals	SMF 1 & RMF 1	Basinal deep-water
<b>II. Wackestone</b>	<b>II.I</b>	Planktonic Foraminiferal Wackestone	Wackestone with relatively less planktonic foraminifera	Pyrite and quartz grains, burrowings, oxide minerals	SMF 1 & RMF 1	Basin and/or open-marine shelf
	<b>II.II</b>	Wackestone with Planktonic Foraminifera and Radiolaria	Wackestone with even amounts of planktonic foraminifera and radiolaria	Planktonic foraminifera, radiolaria, quartz grains	SMF 3 & RMF 5	Basin and/or open deep-shelf
<b>III. Wackestone - Mudstone</b>	<b>III.I</b>	Silty Wackestone - Mudstone with Planktonic Foraminifera	Wackestone - mudstone abundant pyrite and quartz grains	Planktonic, hyaline and agglutinated benthic foraminifera, oxide minerals, mollusc fragments, bryozoan, silica replacement, hyaline and clay mineral fragments	SMF 3 - FOR & RMF 5	Basin and/or open deep-shelf
	<b>III.II</b>	Wackestone - Mudstone	Wackestone - mudstone with few planktonic foraminifera and radiolaria	Planktonic foraminifera, radiolaria, silica replaced fossils	SMF 3 & RMF 5	Basin and/or open deep-shelf

## I. Packstone

### I.I. Planktonic Foraminiferal Packstone

This lithofacies is one of the most common lithofacies types defined in this study; it is seen in samples NS 1, NS 2, NS 18-2 and from NS 23 to NS 39 (Table 3). It is observed mostly in red but also occurs in different colors as greenish gray, reddish gray and light brown. It is characterized by the occurrence of very abundant planktonic foraminifera and consistent presence of radiolaria. Other common features observed are, varying degrees of oxidation related with the occurrence of oxide minerals, silica replacement in fossils, presence of pyrite and quartz minerals in variable amounts and burrowing structures (Figure 16).

This lithofacies is the equivalent of SMF 2 and RMF 4, these are “microbioclastic peloidal calcisiltite” and “peloidal wackestone and packstone”, respectively. This microfacies type is common in deeper basins and open-marine shelf.



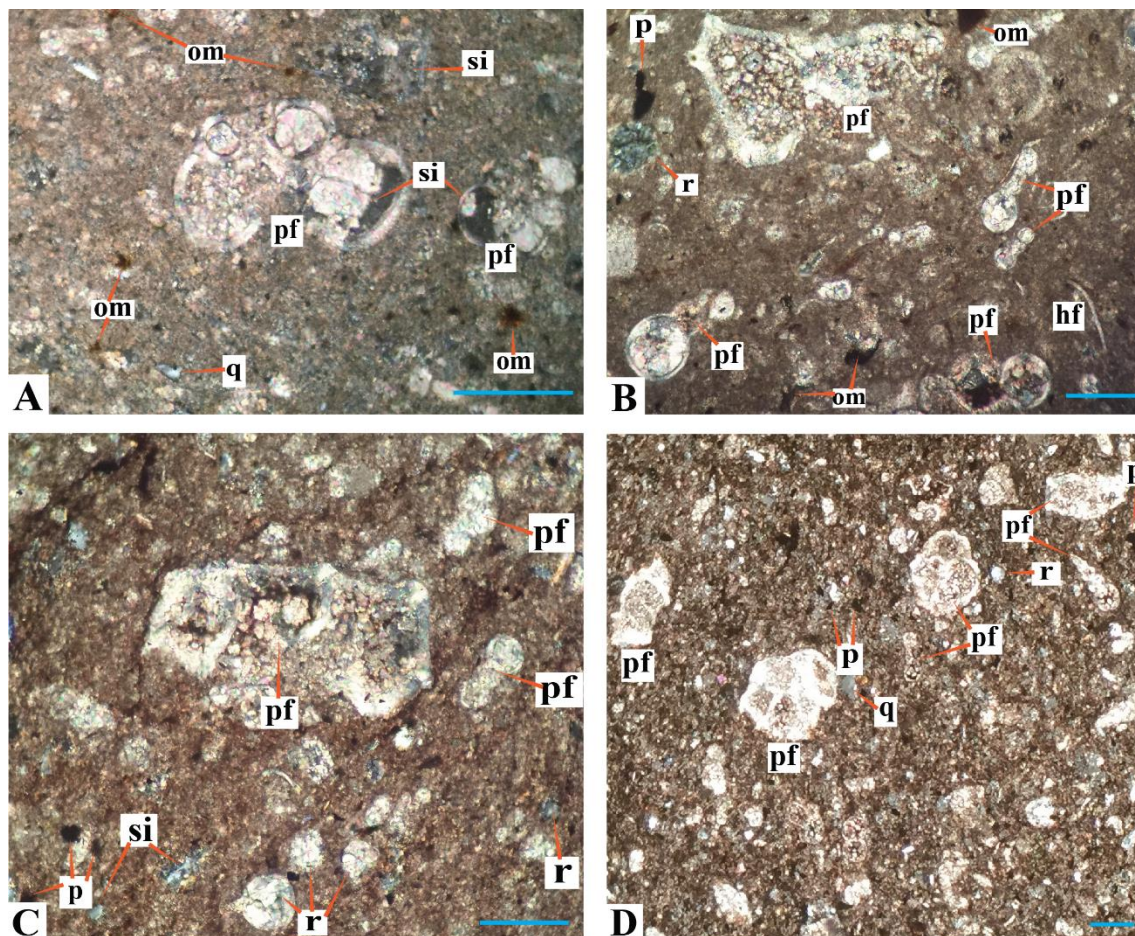


Figure 16. Photomicrographs of the planktonic foraminiferal packstone (MF I.I). (om: oxide minerals, p: pyrite, pf: planktonic foraminifera, q: quartz grains, r: radiolaria, si: silica replacement) Samples A. NS 1, B. NS 26, C. NS 30, D. NS 38 (Scale bar is 0.2 mm).

### I.II. Radiolarian Packstone

This lithofacies type differs from other packstone lithofacies in that it has a distinctively high amount of radiolaria. It is identified in samples NS 3, NS 4, NS 6, NS 12 and NS 17 (Figure 17). Other constituents accompanying radiolaria are detrital grains as quartz and pyrite, burrowing structures, ostracods, echinoderm spines and hyaline shell fragments. Radiolarian packstone occurs in different tones of gray in the geological section, namely greenish gray, dark gray and reddish gray (Table 3).

Radiolarian packstone lithofacies corresponds to SMF 2 and RMF 4 which are “microbioclastic peloidal calcisiltite” and “peloidal wackestone and packstone”, respectively. It is common in deeper basins and open-marine shelf environments.

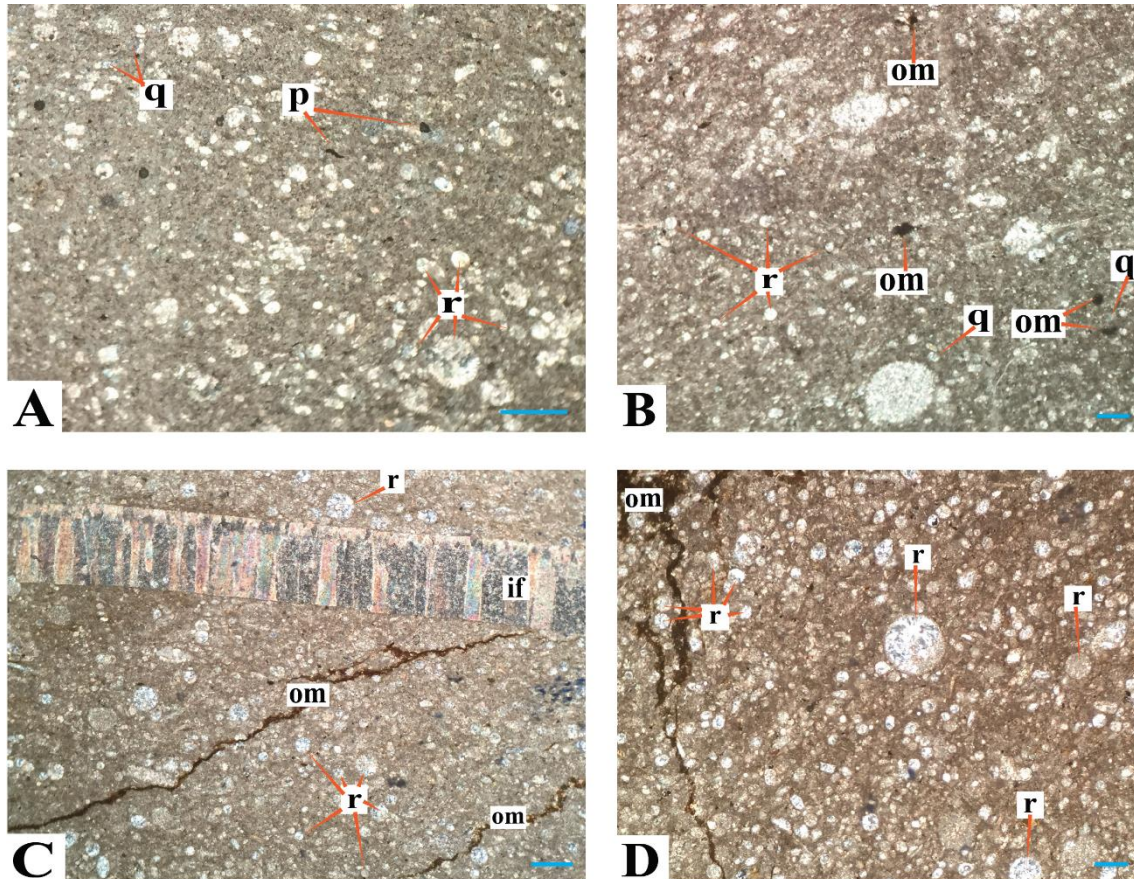


Figure 17. Photomicrographs of radiolarian packstone (MFT I.II). (if: inoceramid fragment, om: oxide minerals, p: pyrite, q: quartz grains, r: radiolaria) Samples A. NS 6, B. NS 12, C. NS 17, D. NS 17 (Scale bar is 0.2 mm).

### I.III. Packstone with Planktonic Foraminifera and Radiolaria

Packstone with planktonic foraminifera and radiolaria facies is represented by the even occurrence of planktonic foraminifera and radiolarian tests in the thin section (Figure 18). This microfacies is identified in samples NS 5, NS 11 and NS 22. Other findings are quartz grains, burrowings, spicules and silica replacement in fossils (Table 3). It is light brown in color but becomes red towards the middle part of the Santonian.

This lithofacies is another one that corresponds to SMF 2 and RMF 4, that are “microbioclastic peloidal calcisiltite” and “peloidal wackestone and packstone”, respectively. This microfacies is representative of a deep basin and/or open-marine shelf.

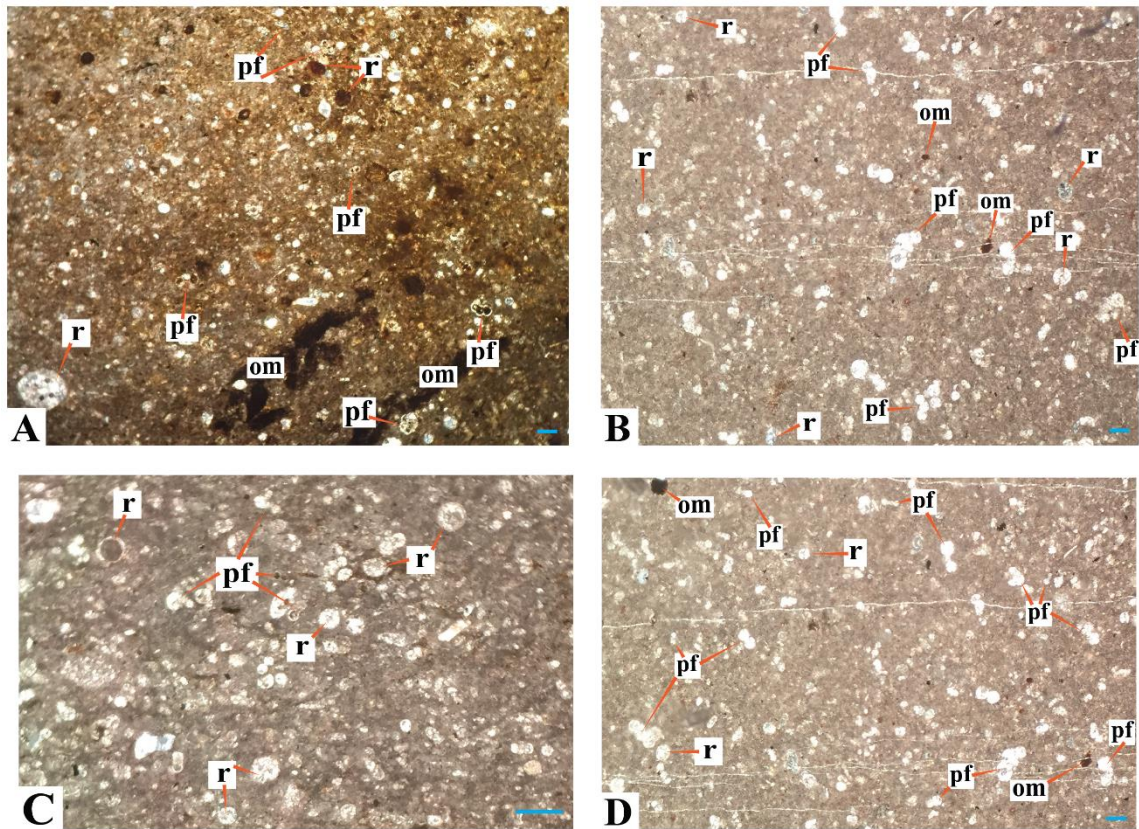


Figure 18. Photomicrographs of packstone with planktonic foraminifera and radiolaria (MFT I.III). (om: oxide minerals, p: pyrite, pf: planktonic foraminifera, q: quartz grains, r: radiolaria, si: silica replacement) Samples A. NS 11, B. NS 11, C. NS 14, D. NS 22 (Scale bar is 0.2 mm).

#### I.IV. Radiolaria-bearing Spiculite Packstone

Spiculite packstone lithofacies is observed once in the samples (NS 18-1) and is light brown in color. It is dominated by abundant monaxone megascleres (sponge spicules) and a less amount of radiolaria (Table 3). It is interpreted to represent a brief interval of possible deepening at the level it is observed (Figure 19), however the accumulation still occurs above the CCD as implied by the presence of ostracod, mollusc and hyaline

fragments. Occurrence of pyrite and quartz minerals and oxidation stains are also important. Possible causes for concentrations of spicules are given as in-place deposition of spicules derived from the disintegration of soft-bodied demosponges, or an accumulation of spicules of decaying soft sponges within organic mats (Flügel, 2004). Regarding the possible depositional environment of this lithofacies, fossil spiculites are known to be common in deep-marine settings, both in basinal and slope position and they are usually interpreted as deep or cold-water deposits. However, today it is known that many siliceous demosponges live in warm shallow waters, suggesting that ancient spiculites could have originated in shallow-marine shelf and near-coast environments, too (Flügel, 2004).

It can be said that this lithofacies is identical with SMF 1, “spiculite wackestone or packstone” which occurs often in dark colored limestones, and is commonly argillaceous and includes pelagic microfossils such as radiolaria. Abundant siliceous (or calcified) sponge spicules are often oriented in this microfacies type. This lithofacies is the result of a slow sedimentation in a basinal deep-water environment. Its RMF equivalent is RMF 1 which is “calcisiltite and mudstone with peloids, very fine skeletal debris, sponge spicules”.

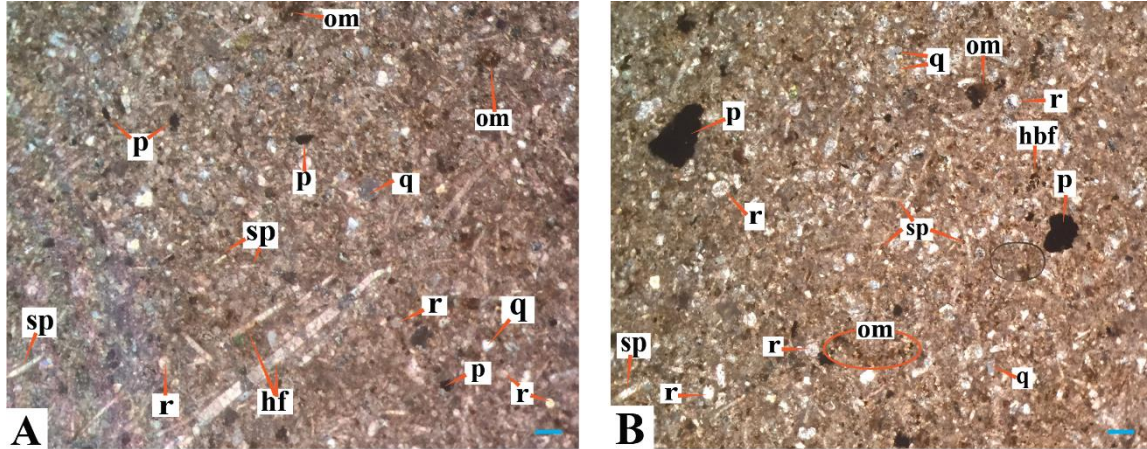


Figure 19. Photomicrographs of radiolaria-bearing Spiculite Packstone (MFT I.IV, Sample NS 18-1). (hbf: benthic foraminifera, hf: hyaline fragment, om: oxide minerals, p: pyrite, pf: planktonic foraminifera, q: quartz grains, r: radiolaria, sp: sponge spicule). Arrows show the direction of current flow (Scale bar is 0.2 mm).

## II. Wackestone

### II.I. Planktonic Foraminiferal Wackestone

This lithofacies is the most common wackestone lithofacies and is differentiated from the similar packstone microfacies by the fewer occurrence of planktonic foraminifera tests. It is observed in samples NS 21 and from NS 40 to NS 47 (Table 3). Other main constituents are highly to moderately abundant oxidation stains and quartz and pyrite grains (Figure 20). It occurs in dark grey and light brown colors in the geological section.

This lithofacies is almost identical with SMF 1 – Burrowed, which is different from SMF 1 in the dominance of sparsely distributed skeletal grains representing a mixture of benthic and planktonic elements. Burrowed bioclastic wackestone is abundant with fine pelagic and benthic biodebris. Its very small bioclasts, commonly shell debris, are scattered within a dense, strongly burrowed matrix. It corresponds to RMF 1 in the ramp carbonate microfacies classification scheme. It is found in basinal, open sea shelf and outer ramp carbonates.

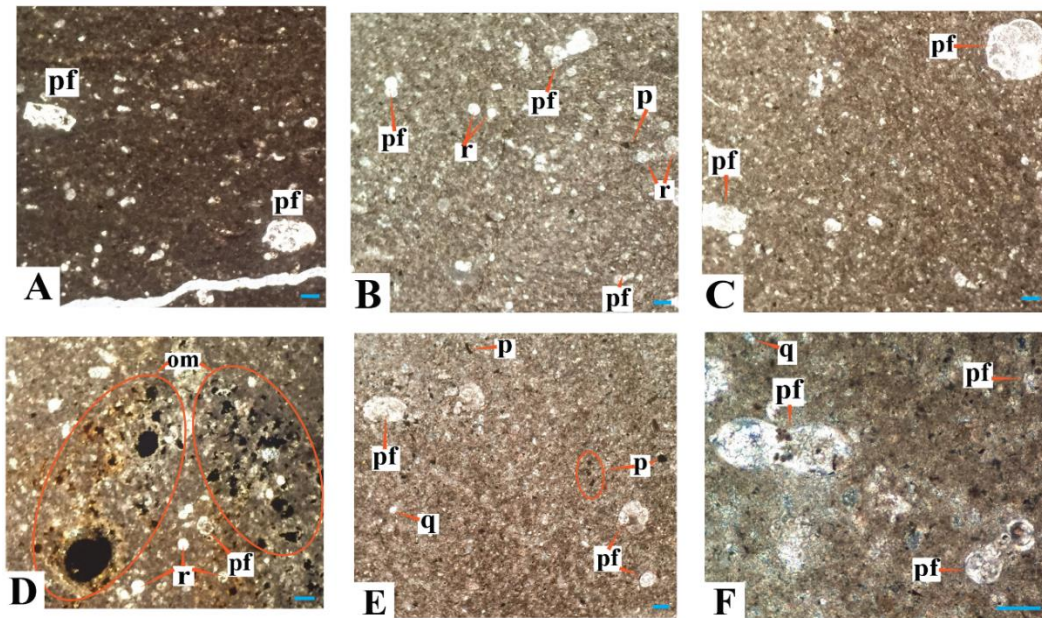


Figure 20. Photomicrographs of planktonic foraminiferal wackestone (MFT II.I). (om: oxide minerals, p: pyrite, pf: planktonic foraminifera, q: quartz grains, r: radiolaria) Samples A. NS 40, B. NS 45, C. NS 42, D. NS 10, E. NS 43, F. NS 10 (Scale bar is 0.2 mm).

## II.II. Wackestone with Planktonic Foraminifera and Radiolaria

This wackestone facies includes planktonic foraminifera and radiolaria in even amounts (Table 3). Few quartz grains are also observed (Figure 21). It occurs in samples NS 8, NS 9, NS 10, NS 13 and NS 19.

It corresponds to SMF 3, “pelagic lime mudstone and wackestone with planktonic microfossils”. Its RMF equivalent is RMF 5, “pelagic mudstone with planktonic microfossils and open-marine nektonic fossils”. This microfacies is found in basin and open deep shelf deposits.

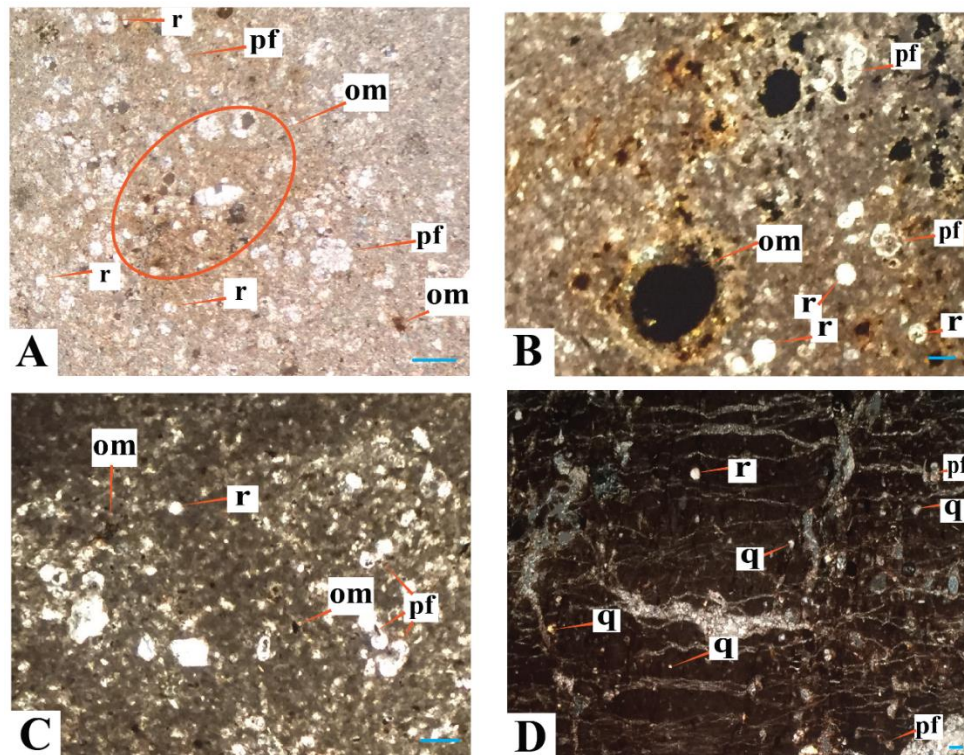


Figure 21. Photomicrographs of wackestone with planktonic foraminifera and radiolaria (MFT II.II). (om: oxide minerals, pf: planktonic foraminifera, q: quartz grains, r: radiolaria) Samples A. NS 8. B. NS 10. C. NS 13. D. NS 2. (Scale bar is 0.2 mm).

### III. Wackestone-Mudstone

#### III.I. Silty Wackestone-Mudstone with Planktonic Foraminifera

Silty Wackestone-Mudstone lithofacies is the most prevalent one among the lithofacies types identified in this study. It is once observed in the Lower Santonian, then occurs strictly in the Middle to Upper Campanian of the measured geological section in samples NS 20 and from NS 48 to NS 75 (Table 3). As its name implies, this lithofacies contains a very high amount of detrital grains as quartz and pyrite, even increasingly towards the Upper Campanian part. Other important characteristic is the presence of oxide minerals representing varying degrees of oxidation. Planktonic foraminifera, hyaline and agglutinated benthic foraminifera are observed abundantly in the Upper Campanian of the

measured geological section. Mollusc, bryozoan fragments, silicification, hyaline and clay fragments are rare in this lithofacies (Figure 22).

Silty wackestone-mudstone lithofacies corresponds to SMF 3-FOR (pelagic foraminifera), “pelagic lime mudstone and wackestone with planktonic microfossils” and RMF 5, “pelagic mudstone with planktonic microfossils and open-marine nektonic fossils”. This microfacies is found in basin and open deep shelf depositional environments.



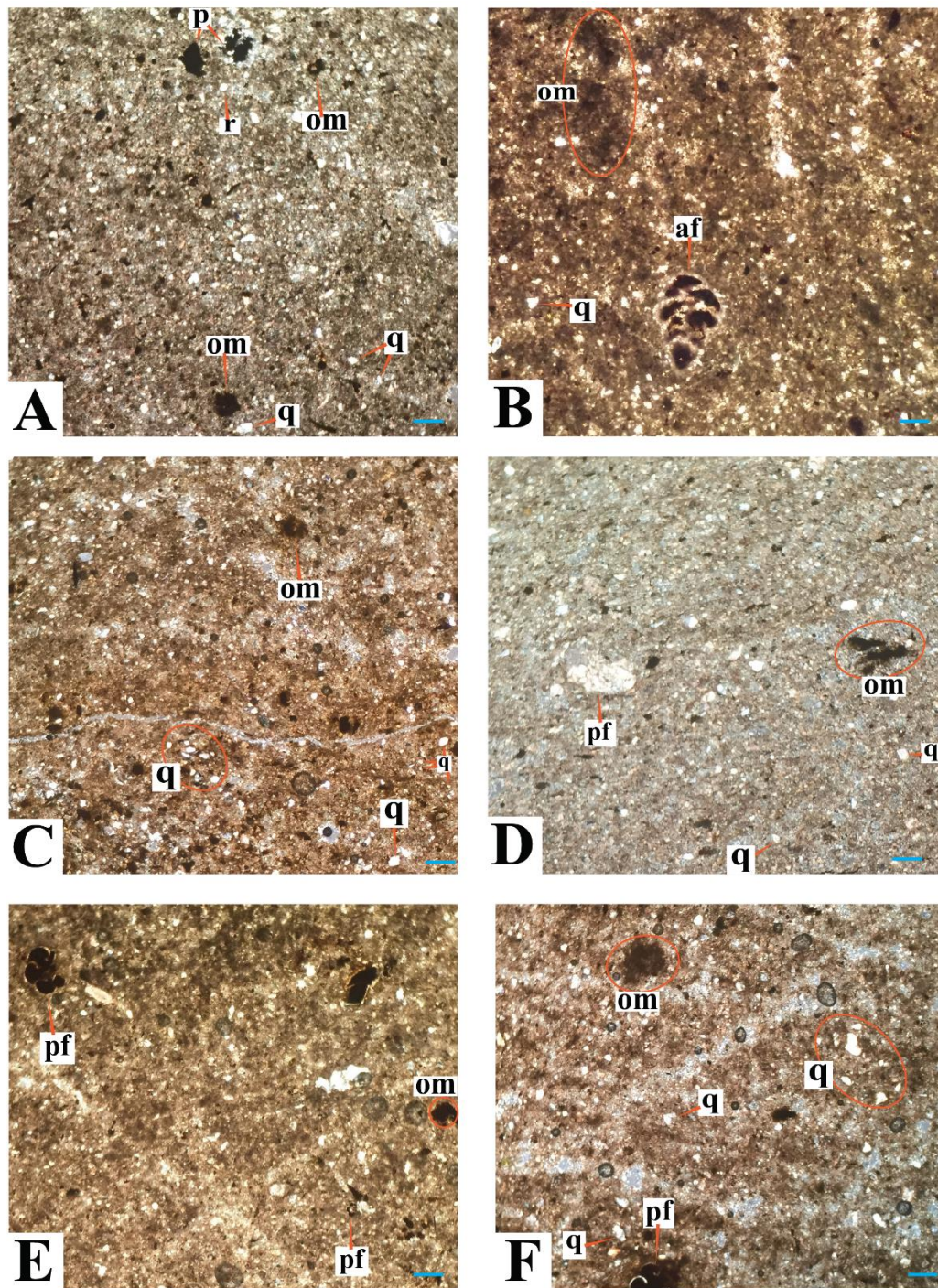


Figure 22. Photomicrographs of silty wackestone-mudstone with planktonic foraminifera (MFT III.I) (af: agglutinated benthic foraminifera, om: oxide minerals, p: pyrite, pf: planktonic foraminifera, q: quartz grains, r: radiolaria) Samples A. NS 51, B. NS 57, C. NS 60, D. NS 58, E. NS 62, F. NS 67 (Scale bar is 0.2 mm).

### III.II. Wackestone-Mudstone

Wackestone-Mudstone lithofacies represents an episodic interval where the dicarinellid-dense upper Turonian is interrupted by a short break where the microfacies includes fewer occurrence of planktonic foraminifera and radiolaria (in samples NS 14, NS 15 and NS 16) (Table 3). Silicification of fossils is observed (Fig 23).

The correspondent SMF type to this lithofacies is SMF 3, “pelagic lime mudstone and wackestone with planktonic microfossils” and RMF 5, “pelagic mudstone with planktonic microfossils and open-marine nektonic fossils”. This lithofacies type is found in basin and open deep shelf environments.

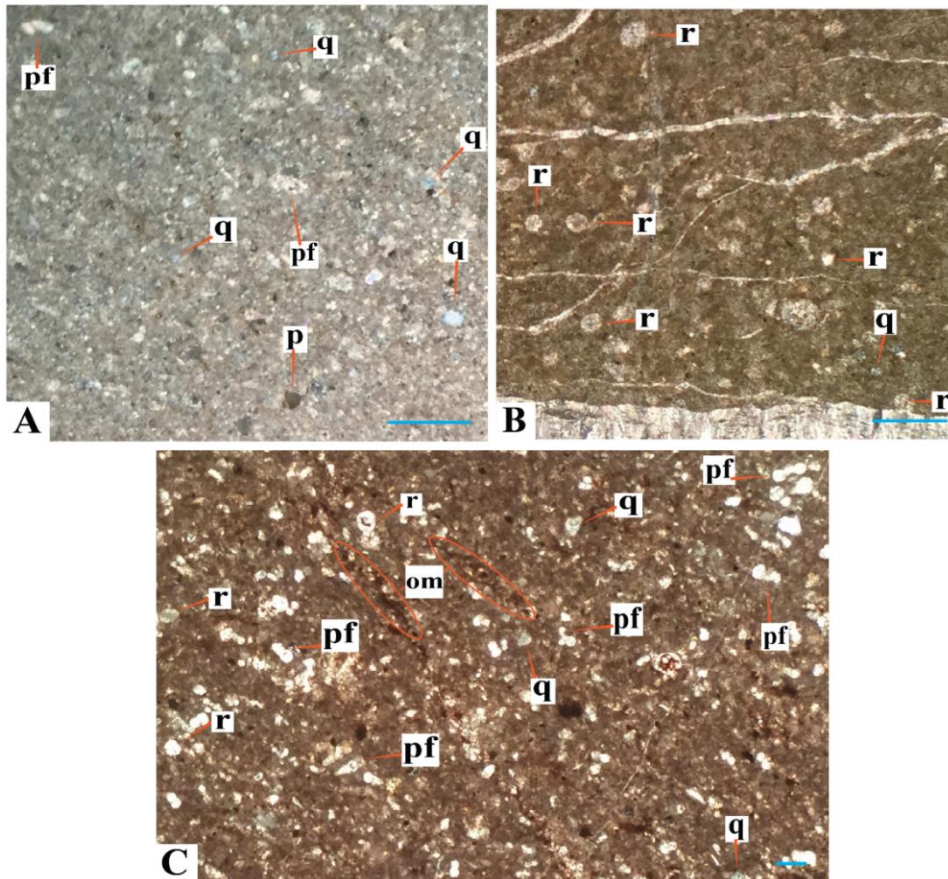


Figure 23. Photomicrographs of wackestone-mudstone (MFT III.II). (om: oxide minerals, p: pyrite, pf: planktonic foraminifera, q: quartz grains, r: radiolaria) Samples A. NS 14. B. NS 15. C. NS 16 (Scale bar is 0.2 mm).

### 3.2. Interpretation of the Microfacies Analysis Results

The results of the microfacies analysis described in the previous part shows no remarkable facies change in the measured stratigraphic section (Table 3 and Figure 24). Although there are sea-level increases recorded globally (e. g., Haq et al., 1987; Skelton, 2003) and locally (e. g., Rojay and Altner, 1998; Yılmaz et al., 2010) at the stage boundaries detected in this study, the results of this study do not reflect major changes in the sea-level.

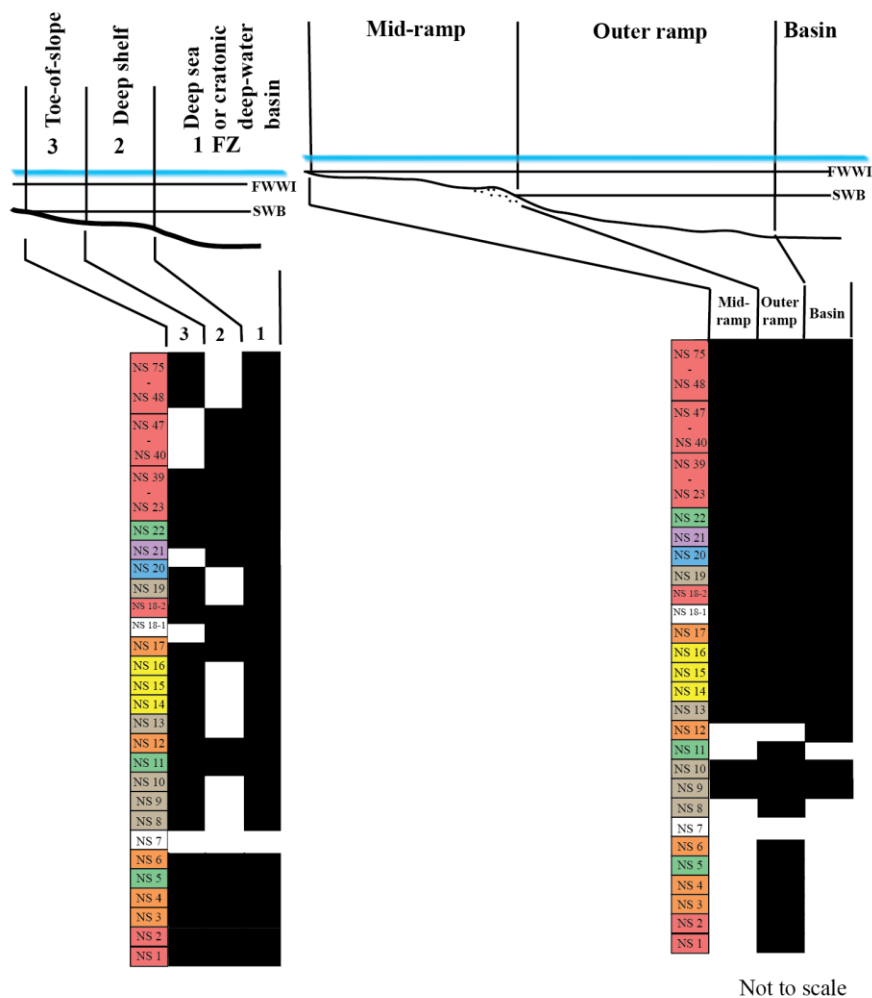


Figure 24. Microfacies Evolution Chart showing the changing depositional environments through time for two different models: on a rimmed-shelf and on a ramp platform.

Table 3. Microfacies Analysis Results

AGE	MICROFACIES TYPE	SAMPLE NO.	Lithology	Color	Planktonic Foraminifera	Radiolaria	Quartz grains	Pyrite grains	Burrowings	Oxidation/ Iron oxide minerals	Ostracoda	Hyaline benthic foraminifera	Agglutinated benthic foraminifera	Mollusc fragments	Echinodermata	Bryzoa	Silica replacement	Hyaline fragments	Spicules	Clay content
SANTONIAN	I.I	NS 36	lst	r	**	*	**	*	*	*										
	I.I	NS 35	m	r	**	*	*	*	*	*										
	I.I	NS 34	lst	r	**	*	*	*	*	*										
	I.I	NS 33	lst	r	**	*	*	*	*	*										
	I.I	NS 32	lst	r	**	*			*	*								*		
	I.I	NS 31	lst	r	**	*			*	*								*		
	I.I	NS 30	cl	r	**	*			*	*								*		
	I.I	NS 29	lst	r	**	*			*	*								*		
	I.I	NS 28	cl	r	**	*			*	*								*		
	I.I	NS 27	lst	rg	**	*			*	*								*		
	I.I	NS 26	lst	r	**	*			*	*								*		
	I.I	NS 25	lst	r	**	*			*	*								*		
	I.I	NS 24	lst	lb	**	*			*	*								*		
	I.I	NS 23	lst	r	**	**	*													*
TURONIAN	I.III	NS 22	lst	r	**	**	*										*			
	II.I	NS 21	cl	r	**	**	*										*			
	III.I	NS 20	cl	r	**	**	*										*		*	
	II.II	NS 19	ss	r	**	**	*													
CENOMANIAN	I.I	NS 18-2	ss	lb	**	**				*										
	I.IV	NS 18-1	ss	lb		**	*	*	*	*	*			*	*			*	*	
	I.II	NS 17	sh	rg	*	**		*	*	*	*			*	*			*	*	
	III.II	NS 16	lst	lb	*	**		*										*	*	
	III.II	NS 15	cl	lb	*	**												*		
	III.II	NS 14	lst	lb	**	**			*									*	*	
	II.II	NS 13	sh	dg	**	**				*										
	I.II	NS 12	cl	dg	*	**			*		*							*		
	I.III	NS 11	sh	lb	*	**	*		*	*	*	*							*	
	II.II	NS 10	cl	lb	*	**	*	*		*		*								
	II.II	NS 9	ss	g	*	**	*	*		*		*		*				*		
	II.II	NS 8	cl	lg	*	**	*	*		*								*	*	
	Undefined	NS 7	ss																	
	I.II	NS 6	cl	lb	*	**	*		*						*			*		
I.III	NS 5	sh	lb	*	**	*	*		*									*		
I.II	NS 4	cl	gg	*	**	*	*		*	?							*			
I.II	NS 3	ss	lb	*	**	*	*		*											
I.I	NS 2	cl	gg	*	**															
I.I	NS 1	cl	gg	*	**	*		*	*	*										

**LEGEND**

- I.I: Planktonic Foraminiferal Packstone
  - I.II: Radiolarian Packstone
  - I.III: Packstone with Planktonic Foraminifera and Radiolaria
  - I.IV: Radiolaria-bearing Spiculite Packstone
  - II.I: Planktonic Foraminiferal Wackestone
  - II.II: Wackestone with Planktonic Foraminifera and Radiolaria
  - III.I: Silty Wackestone-Mudstone with Planktonic Foraminifera
  - III.II: Wackestone-Mudstone
- lst: limestone
  - ss: silty shale
  - sh: shale
  - cl: clayey limestone
  - \* Low abundance
  - \*\* Medium Abundance
- gg: greenish grey
  - lb: light brown
  - sh: shale
  - lg: light grey
  - g: grey
  - dg: dark grey
  - r: red
  - rg: reddish grey

Table 3. Continued.

AGE	MICROFACIES TYPE	SAMPLE NO.	Lithology	Color	Planktonic Foraminifera	Radiolaria	Quartz grains	Pyrite grains	Burrowings	Oxidation/ Iron oxide minerals	Ostracoda	Hyaline benthic foraminifera	Agglutinated benthic foraminifera	Mollusc fragments	Echinodermata	Bryzoa	Silica replacement	Hyaline fragments	Spicules	Clay content	
C A M P A N I A N	III.I	NS 75	ss	lb	**		**	**		**											
	III.I	NS 74	ss	lb	**		**	**		**			*								
	III.I	NS 73	ss	lb	**		**	**		**											
	III.I	NS 72	ss	lb	**		**	**	*	**			*								
	III.I	NS 71	ss	lb	**		**	**		**											
	III.I	NS 70	ss	lb	**		**	**	*	**			*								
	III.I	NS 69	ss	lb	**		**	**		**		*	*								
	III.I	NS 68	ss	lb	**		**	**		**		*	*								
	III.I	NS 67	ss	lb	**		**	**		**		*	*	*							
	III.I	NS 66	ss	lb	**		**	**		**		*	*								
	III.I	NS 65	ss	lb	**		**	**	*	**		*	*								
	III.I	NS 64	ss	lb	**		**	**		**											
	III.I	NS 63	ss	lb	**		**	**		**											
	III.I	NS 62	ss	lb	**		**	**		**											
	III.I	NS 61	ss	lb	**		**	**		**		*						*			*
	III.I	NS 60	ss	lb	**		**	**		**					*				*		
	III.I	NS 59	ss	lb	**		**	**		**											
	III.I	NS 58	ss	lb	**		**	**		**											
	III.I	NS 57	ss	lb	**		**	**		**											
	III.I	NS 56	ss	lb	**		**	**		**											
	III.I	NS 55	ss	lb	**		**	**		**											
	III.I	NS 54	ss	lb	**		**	**		**											
	III.I	NS 53	ss	lb	**		**	**		**											
	III.I	NS 52	ss	lb	**		**	**		**		*									
	III.I	NS 51	ss	gg	**		**	**		**											
	III.I	NS 50	ss	lb	**		**	**		**											
	III.I	NS 49	ss	gg	*		**	**		**											
	III.I	NS 48	ss	gg	*		**	**		**											
	II.I	NS 47	lst	g	**		**	**		**		*						*	*		
	II.I	NS 46	sh	lb	**		**	**		**		*						*	*		
	II.I	NS 45	lst	lb	**		**	**		**											
	II.I	NS 44	lst	lb	**		**	**		**											
	II.I	NS 43	sh	lb	**		**	**		**											
II.I	NS 42	sh	lb	**		**	**		**												
II.I	NS 41	sh	lb	**	*	**	**		**					*					*		
II.I	NS 40	sh	lb	**	*	**	**		**												
I.I	NS 39	sh	r	**	*	**	**	*	**												
I.I	NS 38	lst	lb	**	*	**	**	*	**												
I.I	NS 37	sh	r	**	*	**	**	*	**												

**LEGEND**

- I.I: Planktonic Foraminiferal Packstone
  - I.II: Radiolarian Packstone
  - I.III: Packstone with Planktonic Foraminifera and Radiolaria
  - I.IV: Radiolaria-bearing Spiculite Packstone
  - II.I: Planktonic Foraminiferal Wackestone
  - II.II: Wackestone with Planktonic Foraminifera and Radiolaria
  - III.I: Silty Wackestone-Mudstone with Planktonic Foraminifera
  - III.II: Wackestone-Mudstone
- lst: limestone  
 ss: silty shale  
 sh: shale  
 cl: clayey limestone  
 \* Low abundance  
 \*\* Medium Abundance
- gg: greenish grey  
 lb: light brown  
 lg: light grey  
 g: grey  
 dg: dark grey  
 r: red  
 rg: reddish grey

Although the sea-level changes observed from the results are not dramatic, the Cenomanian-Turonian boundary anoxia which is known as the OAE2 and followed by the Upper Cretaceous oceanic red beds (CORBs) is observed to a considerable degree in the samples investigated; observations regarding this are explained in this part. Moreover, the eustatic sea-level highstand occurred during the S/C boundary (Miller et al. 2005; Jarvis et al., 2006; Wagreich and Neuhuber, 2005; Wagreich et al., 2010) is also detected as a consistent change in the microfacies just after the proposed S/C boundary in this study.

OAE2 at the C/T boundary represents the most severe global climatic perturbation in the Cretaceous Period marked by globally distributed organic-carbon deposition (Owens et al., 2017). This boundary indicates a kind of interplay between paleoproductivity, climate induced (Milankovitch bands) small-scale sea-level changes superimposed on larger-scale, volcanism and tectonic movements (Yılmaz et al., 2010).

Due to the large sampling interval of this study (~1.2 m), small-scale sea-level changes could not be observed; however, dark-colored radiolarite lithologies characterizing the pre-C/T boundary successions are clearly present (Table 3). As seen in (Table 3), the interval leading to the C/T boundary comprises radiolaria packstone and wackestone with planktonic foraminifera and radiolaria microfacies of colors ranging between brown and grey tones, with dark grey color occurring at the boundary. Rock colours often bear a genetic significance attesting to redox conditions during deposition and/or early diagenesis. For example, black and green radiolarites, common at the base of Tethyan sections, are indicative of at least dysoxic conditions and the original presence of organic matter (Baumgartner, 2013). This part of the stratigraphic section is followed by post-anoxia wackestones with opportunist planktonic foraminifera (Figure III.II. Wackestone-Mudstone). This is interpreted as the result of a eutrophication process by proliferation of opportunist plankton with the diminishing anoxia. This event is very clearly reflected in the sample interval [NS-12 – NS-16]. In samples NS-12 and NS-13, oceanic anoxia makes its peak with dark-grey-colored radiolaria rich microfacies. It is followed by samples NS-14, NS-15 and NS-16 which solely contain the simplest opportunist planktonic foraminifera morphotypes, such as genera *Macroglobigerinelloides*, *Muricohedbergella*

and *Heterohelix*, together with abundant radiolarians. These results are satisfactorily compatible with the literature. The C/T boundary drowning is reported from all over the globe including the locality itself (e. g., Wang et al., 2005; Yılmaz et al., 2010; Coccioni et al., 2012; Omana et al., 2012, Afridi, 2014; Okay and Altuner, 2016). The sea-level-rise and eutrophication enables the development of opportunist species (Omana et al., 2012) and the decline of other fossil groups during the OAE is attributed to the expansion of anoxic and euxinic conditions that were unfavorable and even toxic to life (Leckie et al., 2002; Snow et al., 2005). Moreover, the radiolarians are also evidence of highly eutrophic conditions (Coccioni and Luciani, 2004).

The intervals corresponding to the OAE2 and post-OAE2 are followed by the upper Cretaceous Oceanic Red Beds (CORBs) which are observed covering almost the exact Santonian stage defined in this study with very abundant keeled planktonic foraminifera (Table 3). This is also completely compatible with the already known red bed occurrence in the highly oxygenated Santonian deep-sea environment and Santonian-early Campanian diversity peak of planktonic foraminifera (Premoli-Silva et al, 1999; Wapreisch, 1995; Wang et al., 2005; Hu et al., 2005; Yılmaz, 2008; Yılmaz et al., 2010; Tüysüz et al, 2016).





## CHAPTER 4

### 4. STAGE BOUNDARIES

Two stage boundaries have been identified in this study based on planktonic foraminiferal biostratigraphy. These boundaries are delineated between stages Cenomanian-Turonian and Santonian-Campanian. These identifications have been supported with microfacies data when available, such as in the Cenomanian-Turonian boundary. The Coniacian stage is not recognized to be present in the measured stratigraphic section together with the Uppermost Turonian and Lower Santonian. The discussions regarding these boundaries are given as follows.

#### 4.1. Cenomanian-Turonian Boundary and the Oceanic Anoxic Event 2

The base of Turonian stage is placed at the lowest occurrence of the ammonite *Watinoceras devonense* near the expression of the OAE 2 at Pueblo (Colorado), where its GSSP is located, and almost coincides with the HO of calcareous nannofossil *Microstaurus chiastius* (Kennedy et al. 2005). In planktonic foraminiferal biostratigraphic framework, this boundary is placed within the *W. archaeocretacea* Partial Range Zone (Premoli-Silva et al., 1999; Omana et al., 2012; Kopaeich and Vishnevskaya, 2016; Reolid et al., 2016).

Cenomanian-Turonian (C/T) Boundary interval witnessed major biotic and oceanographic changes (e. g., Kopaeich and Vishnevskaya, 2016; Falzoni et al., 2016), including reductions in paleontological diversity of both benthic and planktic foraminifera, calcareous nannoplankton, ostracods, radiolarians, aragonitic rudist bivalves and ammonoids from marine sediments located around the world. These changes also include major perturbations in oceanic conditions such as a sea-level rise of nearly 300 m relative

to present and an increased water temperature at middle bathyal depths up to 20°. The Oceanic Anoxic Event (OAE 2) occurred during this warming peak with the burial of large amounts of organic matter in outer shelf and deep ocean environments (Omana et al., 2012).

In Central Anatolia, this interval is also characterized by a shale succession with a color ranging between dark grey and black. Occurrence of distinct black shales within the *R. cushmani* zone is observed in the Mudurnu area of the Sakarya Continent and this event has been found coeval with the black shale interval (OAE 2) which has been reported from several locations worldwide. Furthermore, this black shale interval is followed by white pelagic carbonates with the beginning of Turonian, which is next overlain by red-purple marls/mudstones. These red-purple units have abundant planktonic foraminifera and iron minerals indicating oxidizing conditions under which the sedimentation took place (Yılmaz, 2008; Yılmaz et al., 2010).

The Cenomanian-Turonian boundary is delineated between samples NS-13 and NS-14 in this study. The microfacies analysis shows that the color of lithology changes between green and grey tones up to this level, where dark grey color occurs in samples NS-12 and NS-13 in the part closest to the boundary; these become light brown immediately starting from NS-14. These dark grey samples are identified as radiolarian packstone (shale) and planktonic foraminifera wackestone (clayey limestone) facies, respectively. They include sparse planktonic foraminifera and abundant radiolaria. Additionally, burrowing structures and few hyaline fragments are observed in sample NS-12; although these constituents disappear, oxidation/iron oxide minerals are present in sample NS-13. Moreover, a striking disappearance of planktonic foraminifera species takes place in samples NS-12 and NS-13, including the disappearance of *M. bentonensis* in sample NS-13 (Premoli-Silva et al., 1999). The only species present in these two samples are *M. delrioensis*, *M. planispira*, *Macroglobigerinelloides* sp. and *W. baltica*. Except for a *Dicarinella* sp. occurring only in NS-13. The species present in these samples clearly lack complex k-taxa; they are simple and opportunist r-strategists (Petrizzo, 2002). These data are in complete accordance with previous findings which show that only the less

specialized groups such as the younger dicarinelids and whiteinellids, with higher tolerance, together with the opportunistic hedbergellids and heterohelicids, survived this boundary and resumed after the acme of the perturbation ceased. The last but not the least important of these bioevents is the lowest occurrence of *Helvetoglobotruncana helvetica* in sample NS-14, which marks the beginning of *H. helvetica* biozone in the lower to middle Turonian (Premoli-Silva et al., 1999; Kopaevich and Vishnevskaya, 2016; Falzoni et al., 2016; Reolid et al., 2016). Although the boundary is put in the *W. archaeocretacea* zone and *H. helvetica* zone follows this towards the middle Turonian in most of the recent studies (Figure 11), the datum between samples NS-13 and NS-14 corresponds also to the boundary between these two biozones here. This situation can be resulting from the large sampling interval in this study (~ 1.2 m).

#### **4.2. On the absence of the Coniacian stage**

In the measured stratigraphic section of this study, Turonian deposits are unconformably overlain by middle Santonian succession. This sudden transition missing the Coniacian stage is explained by Okay and Altınır's (2017) recent study on the geological history of the Alcı and Bağlum regions in the Haymana, Ankara region.

It is known that both the Akkaya Formation and Bilecik Limestone is unconformably overlain by red pelagic Kocatepe Formation in the Ankara region (Yüksel, 1970). Okay and Altınır (2016) describe a section measured at the Küçükyayla Ridge, 8 km northeast of Haymana where the limestone breccia of the Bilecik Limestone is overlain with a pelagic sequence composed of beige and red pelagic limestones. In this section, beige pelagic limestones represent the lower middle Turonian age, whereas red pelagic limestones give a characteristic Santonian age planktonic foraminiferal fauna. The same situation is also recorded in the Çalıçukuru village about 2 km east of Haymana where the Bilecik Limestone is overlain by Turonian-lower Santonian fauna. It is noted that a condensed carbonate deposition is indicated by planktonic foraminiferal data from early Turonian to late Santonian for a period of 10 million years. This period is known to have gone through intense submarine volcanism in the outer Pontides (Okay and Altınır, 2016).

Okay and Altıner (2017) discuss the olistostromes occurring in the zones near the İzmir-Ankara Suture. In these, Upper Jurassic-Cretaceous limestone succession cannot be observed, but it instead occurs as carbonate blocks with differing size in the Alacaatlı Olistostromes which outcrop near Alcı, Ankara (Figures 3, 4).

In the Alcı region, the Alacaatlı olistostromes are unconformably overlain by red micritic limestones and shales. By using planktonic foraminiferal data, this red unit is identified to be middle to upper Santonian and overlain conformably by Campanian succession (Okay and Altıner, 2017).

Oldest blocks identified in the Alacaatlı olistostromes are of late Turonian age, and they are unconformably overlain by middle-late Santonian pelagic limestones. This indicates that the Alacaatlı olistostromes were formed during the Coniacian. The limestone blocks in the Alacaatlı olistostromes have varying ages, namely as Callovian-Oxfordian, Tithonian-Berriasian, Valanginian-Aptian, Albian, Cenomanian and Turonian. These blocks can be correlated in terms of lithology and age with the autochthonous Jurassic-Cretaceous succession observed in the Middle Sakarya Basin or in the Haymana Anticline. Almost all the limestone blocks are of pelagic quality. These show that the Jurassic-Cretaceous succession of the Sakarya Zone were transferred to debris flows in the Coniacian as the subduction was taking place in the Pontides. This tectonic episode is envisaged to occur due to the collision of an aseismic ridge with the Pontides and the consequent rising of the outer parts of the forearc basin. The eroded material was transferred as debris flows into the local depression formed in front of the bulging carbonates with the collision. This episode of olistostrome formation and recycling occurring until the colliding end, was followed by normal forearc deposition back again in the Santonian (Okay and Altıner, 2017).

### **4.3. Santonian-Campanian Boundary**

Since the naming of the Campanian Stage by Coquan in 1857, the definition of its base has been debated (Wagreich et al., 2010; Kita et al., 2017). There is currently no ratified biostratigraphic marker or Global Boundary Stratotype Section and Point (GSSP) for the

base of the Campanian Stage (Ogg and Hinnov, 2012; Coccioni, 2015). Various fossil groups are used in the identification of Santonian-Campanian (S/C) boundary. Main boundary events defining the S/C transition are the extinction of the crinoid *Marsupites testudinarius*, the appearance of the ammonite *Placenticeras bidorsatum* and that of the belemnite *Goniot euthis granulata quadrata*. These bioevents may also coincide with secondary marker bioevents of the S/C boundary which are the appearance of the planktonic foraminifera *Globotruncanites elevata*, the disappearance of the planktonic foraminifera *Dicarinella asymetrica* together with all other dicarinellids or presence of the concurrent range interval of *G. elevata* and *D. asymetrica* (e.g., Gale et al., 1995; Premoli Silva and Verga, 2004; Gale et al., 2008; Wagreich et al., 2010; Vahidinia et al., 2014; Jaff et al., 2015). Other secondary bioevents include the disappearance of the planktonic foraminifera *Sigalia carpatica*, which is widespread in the Mediterranean region of the Tethys (Premoli Silva and Verga, 2004; Kita et al., 2017) and that of the genus *Marginotruncana* (e. g., Premoli Silva and Verga, 2004; Gale et al., 2008; Vahidinia et al., 2014; Jaff et al., 2015), with *Marginotruncana sinuosa* recorded as having disappeared slightly above the boundary (Gale et al., 2008). Finally, the disappearance of *Muricohedbergella flandrini* also accepted to predate the S/C boundary (e. g., Petrizzo, 2000; Premoli Silva and Verga, 2004; Gale et al., 2008).

Several authors defined the beginning of the Campanian as the first appearance datum of *G. elevata* (Wagreich, 1992), whereas others at the extinction level of *D. asymetrica* or *D. asymetrica* and *D. concavata* together (e.g. Caron, 1985; Premoli Silva and Sliter, 1994). However, Gale et al. (1995, 2008) placed the global S/C boundary as the FO of *Marsupites testudinarius*, within the short *G. elevata*-*D. asymetrica* concurrent range zone. In their Boreal-Tethyan correlation of the S/C boundary, Wagreich et al. (2010) also show that there is correlation between the *M. testudinarius* zone with parts of the *G. elevata*-*D. asymetrica* concurrent range zone and thus place the base of the Campanian after the FO of *G. elevata* but before the LO of *D. asymetrica*.

In this study, the S/C boundary is delineated between samples NS-38 and NS-39 in terms of detailed planktonic foraminiferal bioevents. The bioevents observed are the

disappearance of genera *Marginotruncana* and *Sigalia* in sample NS-38, *Dicarinella* in sample NS-36 and the species *Muricohedbergella flandrini* in sample NS-40. Moreover, the overlapping range zones of *D. asymetrica* and *G. elevata* fall between samples NS-24 and NS-38. This interval also represents the transition from the well-known red limestone lithofacies representing the oxygenated Santonian oceans to the light brown Campanian shales. These findings suggest that the S/C boundary can be delineated in the sample NS-38 which is in the concurrent range zone of *G. elevata* and *D. asymetrica* and represent the highest occurrence datum of the genera *Marginotruncana* and *Sigalia*. The genus *Dicarinella* is already extinct in sample NS-38 and the species *M. flandrini* lastly observed in sample NS-40.

## CHAPTER 5

### 5. SYSTEMATIC PALEONTOLOGY

The primary concern of this study was to establish a detailed planktonic foraminiferal biozonation of the measured stratigraphic section. The reason why the taxonomic work is especially important in this study is that more detailed the taxonomic analysis is done, the higher resolution in the biostratigraphic framework can be obtained. From this point of view, utmost importance has been given to determine the diverse and extensive planktonic foraminifera obtained from both washed samples and thin sections of the studied samples.

The taxonomic study has been carried out based on the observations of the shape, number and arrangement of the chambers, properties of sutures and presence or absence of keel/keels, mode of coiling, wall texture properties, peripheral outline, positions of primary and secondary apertures, apertural and surface ornamentations. The harder samples of the section were exposed to the acid treatment for a longer time compared to softer samples, in order to be able to extract planktonic foraminifera. This caused dissolution in the test walls to some degree. However, this situation did not hamper the classification process.

Main sources for the identification of planktonic foraminifera species are Robaszynski *et al.* (1984), Loeblich and Tappan (1988), Nederbragt (1991) and Premoli-Silva and Verga (2004). The online databases CHRONOS, TaxonConcept and mikrotax have also been used. The stratigraphic distribution for each species is given based on the range charts of Premoli-Silva and Verga (2004), unless otherwise stated.

In addition to giving brief descriptions highlighting important morphological features of the species one by one, commentary to identify the planktonic foraminifera are also given

in this chapter to provide a roughly outlined guideline that has been used to identify the planktonic foraminifera in this study.

**Phylum Protozoa**

**Order Foraminiferida EICHWALD, 1830**

**Suborder Globigerinina DELAGE and HEROURARD, 1896**

**Superfamily Globotruncanacea BROTZEN, 1942**

**Family Globotruncanidae BROTZEN, 1942**

**Genus *Dicarinella* PORTHAULT 1970**

Type species: *Dicarinella canaliculata* REUSS, 1854

***Dicarinella algeriana* CARON, 1966**

Pl. 3, fig. 1-2; Pl. 23, fig. 1-4

*Dicarinella algeriana* KELLER and PARDO, 2004, p. 99, pl. 3, figs. 8 – 11.

*Dicarinella algeriana* KALANAT *et al.*, 2015, pl. 2, figs. 13 – 15.

*Praeglobotruncana algeriana* FALZONI *et al.*, 2016, p. 88, fig. 12 – 7-10.

**Diagnostic features:**

Spiroconvex, underdeveloped double keel that becomes less prominent in the last chamber of the final whorl, 4.5-6 chambers in the last whorl, finely pustulose wall texture.

**Remarks:**

At the first glance, this species stands out with its moderate to high spiroconvexity. Its underdeveloped keels (especially towards the end of the last whorl) is the other important criterion in its identification.



**Stratigraphic distribution:**

From *Rotalipora cushmani* zone, *Dicarinella algeriana* subzone (middle to upper Cenomanian) to *Dicarinella concavata* zone (Coniacian)

**Occurrence:**

NS-1 – NS-14

***Dicarinella asymetrica* SIGAL, 1952**

Pl. 4, fig. 1; Pl. 23, fig. 8-10

*Dicarinella asymetrica* LAMOLDA *et al.*, 2007, p. 24, fig. 5 – M.

*Dicarinella asymetrica* ARDESTANI *et al.*, 2012. p. 26, fig. 5 - 1.

*Dicarinella asymetrica* EGGER *et al.*, 2013, p. 104, fig. 8 – 1-3.

*Dicarinella asymetrica* LAMOLDA *et al.*, 2014. fig. 11 – G.

**Diagnostic features:**

Planoconvex/umbilico-convex which is sometimes accompanied by a slightly concave spiral side, closely-spaced double keel, 5-6.5 chambers in the final whorl, petaloid chambers on the spiral side, a well-developed periumbilical ridge

**Remarks:**

*Dicarinella asymetrica* is almost impossible to confuse with other contemporary species because of its unique appearance as given in the diagnostic features. The most similar species to *D. asymetrica* can be *D. concavata* both stratigraphic-range-wise and morphology-wise. However, they can confidently be distinguished by the presence of a periumbilical ridge in *D. asymetrica*.

**Stratigraphic distribution:**

From *Dicarinella concavata* zone (uppermost Coniacian) to *Dicarinella asymetrica* zone (uppermost Santonian to lowermost Campanian)

**Occurrence:**

NS-20 – NS-38

***Dicarinella canaliculata* REUSS, 1854**

Pl. 4, fig. 3-7; Pl. 23, fig. 5-7

*Dicarinella canaliculata* PETRIZZO, 2000, p. 502, fig. 15 – 3.

*Dicarinella canaliculata* FALZONI et al., 2016, p. 75, fig. 5 – 2.

**Diagnostic features:**

Flat spiral and umbilical sides, wide double keel, crescentic-petaloid spiral chambers, wedge-shaped umbilical chambers, 5.5-7 chambers in the last whorl, smooth texture

**Remarks:**

*Dicarinella canaliculata* occurs in high numbers in the lower part of the measured section. It is distinctive among other double keeled species by its flat spiral and umbilical sides and widely separated double keel. Slightly spiroconvex specimens of *D. canaliculata* are also present and these specimens display a jagged appearance in the edge view with the inclined flat chamber surfaces aligned one after the other due to the spiroconvexity, this creates a characteristic look.

**Stratigraphic distribution:**

From *Dicarinella algeriana* subzone (middle to late Cenomanian) to *Dicarinella concavata* zone (late Coniacian)

**Occurrence:**

NS-3 –NS-18

***Dicarinella concavata* BROTZEN, 1934**

Pl. 4, fig. 2; Pl. 23, fig. 11-13

*Dicarinella concavata* LAMOLDA *et al.*, 2007, p. 25, fig. 6 – E.

*Dicarinella concavata* EGGER *et al.*, 2013, p. 104, fig. 8 – 4-6.

*Dicarinella concavata* KALANAT *et al.*, 2015, pl. 2, figs. 1 – 3.

**Diagnostic features:**

Planoconvexity/umbilicoconvexity which sometimes results in a slightly concave spiral side, closely-spaced double keel, petaloid chambers on the spiral side, 5 – 7 chambers in the final whorl

**Remarks:**

*Dicarinella concavata* is observed frequently in the middle part of the measured section. It is most similar to *D. asymetrica* and they are distinguished by the absence of the periumbilical ridge present in *D. asymetrica*.

**Stratigraphic distribution:**

From *Dicarinella concavata* (late Turonian) to *Dicarinella asymetrica* zone (early Campanian)

**Occurrence:**

NS-19 – NS-36

*Dicarinella hagni* SCHEIBNEROVA, 1962

Pl. 4, fig. 8

*Dicarinella hagni* FALZONI et al., 2016, fig. 4 – 9.

*Dicarinella hagni* HUBER et al., 2017, pl. 3 – 1-8.

**Diagnostic features:**

Biconvex, double keel, petaloid chambers on the spiral side, 5 – 6 chambers in the last whorl

**Remarks:**

*Dicarinella hagni* occurs in the lower part of the measured section. This species differs from *D. imbricata* in having a less convex spiral side. It is distinguished from other dicarinellids as *D. canaliculata* and *D. takayanagii* in being more convex and a much more closely spaced double keel.

**Stratigraphic distribution:**

From *Whiteinella archaeocretacea* zone (uppermost Cenomanian - lowermost Turonian) to *M. sigali-D. primitiva* zone (uppermost Turonian)

**Occurrence:**

NS-3

***Dicarinella imbricata* MORNOD, 1950**

Pl. 3, fig. 7-9

*Dicarinella imbricata* KELLER and PARDO, 2004, p. 99, pl. 3, figs. 9, 10.

*Dicarinella imbricata* KALANAT et al., 2015, pl. 1, figs. 10 – 12.

*Dicarinella imbricata* AZADBAKHT et al., 2016, p. 133, pl. 1 – e.

*Dicarinella imbricata* FALZONI et al., 2016, p. 75, fig. 5 – 1.

**Diagnostic features:**

Spiroconvex, double keel which border an imperforate peripheral band, subtriangular chambers on the umbilical side, 5 – 6 chambers in the last whorl.

**Remarks:**

*Dicarinella imbricata* occurs in the lower part of the measured section. This species resembles *D. hagni*, however it has fewer chambers in the last whorl and a concavo-convex appearance in the side view.

**Stratigraphic distribution:**

From *Dicarinella algeriana* subzone (middle to late Cenomanian) to *Dicarinella concavata* zone (early Coniacian)

**Occurrence:**

NS-2 – NS-17

***Dicarinella takayanagii* HASEGAWA, 1999**

Pl. 3, fig. 3-6

*Dicarinella takayanagii* HASEGAWA, 1999, p. 187, fig. 8, fig. 3 – A-C.

*Dicarinella takayanagii* FALZONI et al., 2016, p. 84, fig. 10 – 5-8.

**Diagnostic features:**

Unequally biconvex, low trochospiral, weakly developed double keel with a wide peripheral band, wedge shaped and flat chambers in the final whorl on the spiral side, few number of chambers in the last whorl (4.5-5) enlarging rapidly in size, laterally elongated last chamber

**Remarks:**

*Dicarinella takayanagii* is distinguished from other members of the genus *Dicarinella* mainly with its rapidly enlarging chambers with wedge-shaped chambers in the last whorl. Its diagnostically elongated last chamber also differentiates it from other dicarinellids.

**Stratigraphic distribution:**

*Whiteinella archaeocretacea* zone (uppermost Cenomanian - lowermost Turonian)  
(Hasegawa, 1999; Falzoni et al., 2016)

**Occurrence:**

NS-11

**Genus *Marginotruncana* HOFKER, 1956**

Type species: *Rosalina marginata* REUSS, 1845

***Marginotruncana coronata* BOLLI, 1945**

Pl. 13, fig. 2-3; Pl. 27, 4-6

*Marginotruncana coronata* LAMOLDA et al., 2007, p. 25, fig. 6 – I.

*Marginotruncana coronata* EGGER et al., 2013, p. 105, fig. 9 – 6-8.

**Diagnostic features:**

Compressed test (evident especially on the last chamber), closely to very closely spaced double keels, perfectly petaloid shaped chambers on the spiral side, 7 chambers in the last whorl.

**Remarks:**

This species is abundant in the lower to middle part of the measured section. *Marginotruncana coronata* is quite similar to *M. pseudolinneiana* in terms of having a compressed large test, numerous chambers and double keels. However, they are clearly different in details. *M. coronata* has petaloid-shaped chambers contrary to *M. pseudolinneiana*'s crescentic and elongated chambers in the last whorl. *M. coronata* has a much closely spaced double keels and also has a higher trochospiral coiling than *M. pseudolinneiana*.

**Stratigraphic distribution:**

From *Helvetoglobotruncana helvetica* zone (early to middle Turonian) to *Globotruncanita elevata* zone (early Campanian)

**Occurrence:**

NS-14 –NS-33

***Marginotruncana marginata* REUSS, 1845**

Pl. 27, fig. 7-9

*Marginotruncana pseudomarginata*, NEAGU, 2012, fig. 7, 4A-C.

*Marginotruncana marginata* ELAMRI and ZAGHBIB-TURKI, 2014, fig. 9 – 8-10.

**Diagnostic features:**

Biconvex test, closely spaced double keels bordering a narrow peripheral band, inflated chambers on the spiral side, depressed sutures on both sides, deep and wide umbilicus.

**Remarks:**

*Marginotruncana marginata* is abundant in the lower part of the section. It is distinguished from other marginotruncanids by its inflated chambers at first. *M. marginata* may also have its closely-spaced double keel facing toward umbilical side, this can aid in its identification additional to its chamber shape.

**Stratigraphic distribution:**

From *Helvetoglobotruncana helvetica* zone (early to middle Turonian) to *Dicarinella asymetrica* zone (early Campanian)

**Occurrence:**

NS-14 – NS-18



***Marginotruncana paraconcavata* PORTHAULT, 1970**

Pl. 13, fig. 6-8

*Marginotruncana paraconcavata* LAMOLDA *et al.*, 2007, p. 25, fig. 6 – N.

*Marginotruncana paraconcavata* DUBICKA *et al.*, 2014, p. 47, fig. 4 – E.

**Diagnostic features:**

Planoconvex test, closely spaced double keels bordering an imperforate peripheral band, flat to concave surfaced petaloid-shaped spiral chambers elongated in the direction of coiling, 4-6 chambers in the last whorl slowly increasing in size.

**Remarks:**

*Marginotruncana paraconcavata* catches the eye with its planoconvex test at first. It is unlike all other marginotruncanids, however can be very similar to the contemporaneous species *D. concavata*. But, they can be confidently distinguished by their umbilical chamber shape and size. *M. paraconcavata* has trapezoidal chambers exhibiting v-shaped sutures (if observable, not in this study) in the umbilical side. Moreover, the planoconvexity is not as pronounced in *M. paraconcavata* as it is in *D. concavata*.

**Stratigraphic distribution:**

From *Dicarinella concavata* zone (early Coniacian) to *Dicarinella asymetrica* zone (early Campanian)

**Occurrence:**

NS-27 – NS-28

***Marginotruncana pseudolinneiana* PESSAGNO, 1967**

Pl. 13, fig. 1; Pl. 27, 1-3

*Marginotruncana pseudolinneiana* LAMOLDA et al., 2007, p. 25, fig. 6 – J.

*Marginotruncana pseudolinneiana* ARDESTANI et al., 2012. p. 24, fig. 3 - 3.

*Marginotruncana pseudolinneiana* EGGER et al., 2013, p. 105, fig. 9 – 2-5.

**Diagnostic features:**

Perfectly flat on both sides (some specimens may exhibit slight spiroconvexity or spiroconcavity), widely spaced double keels, crescent shaped chambers on the spiral side, subrectangular shaped chambers on the umbilical side, 7-8 slowly enlarging chambers in the last whorl bordered by U-shaped raised sutures.

**Remarks:**

*Marginotruncana pseudolinneiana* is the most abundant marginotruncanid in the measured section. *M. pseudolinneiana* is very similar to *G. linneiana* as also indicated by their names. However, this morphological resemblance does not imply an ancestor-descendant relationship. *M. pseudolinneiana* has an extraumbilical-umbilical primary aperture, as *G. linneiana* has an umbilical one. In the edge view, *M. pseudolinneiana* is clearly thinner and longer than *G. linneiana* which has a chunky look and resembles a box. *D. canaliculata* is another resembling species, they can be distinguished by *M. pseudolinneiana*'s horse-shoe shaped umbilical and crescentic, rather than petaloid, spiral chambers. *M. pseudolinneiana* is also much more slender-looking in the edge view and it has a higher number of chambers in the last whorl. Finally, not to confuse *M. pseudolinneiana* with *M. coronata*, it would be enough to notice the wider-spaced double keel and crescentic chambers on the spiral side of *M. pseudolinneiana*.

**Stratigraphic distribution:**

From *Helvetoglobotruncana helvetica* zone (early to middle Turonian) to *Globotruncanita elevata* zone (early Campanian)

**Occurrence:**

NS-14 – NS-35

*Marginotruncana renzi* GANDOLFI, 1942

Pl. 27, fig. 5

*Marginotruncana renzi* PREMOLI SILVA and VERGA, 2004, Pl. 28, 3-9; Pl. 90, 3-4.,

**Diagnostic features:**

Slightly trochospiral and equally biconvex test, double keel, shallow and wide umbilicus.

**Remarks:**

*Marginotruncana renzi* is once identified in thin section in the lower part of the section. It co-occurs with abundant *Marginotruncana coronata* specimens where the two can look quite similar to each other. *M. renzi* is distinguished from *M. coronata* by its slightly umbilicus-facing double keel, resulting from not being as compressed as *M. coronata* tests are. Furthermore, *M. renzi* is distinguished from another contemporaneous species, *M. marginata* by its non-inflated chambers.

**Stratigraphic distribution:**

From *Helvetoglobotruncana helvetica* zone (early to middle Turonian) to *Dicarinella asymetrica* zone (early Santonian)

**Occurrence:** NS-14

***Marginotruncna sigali* REICHEL, 1950**

Pl. 27, fig. 10

*Marginotruncana sigali* PREMOLI SILVA and VERGA, 2004, Pl. 29, 1-9; Pl. 91, 3-4.

**Diagnostic features:**

Moderately high trochospiral and equally biconvex test, single keel.

**Remarks:**

*Marginotruncana sigali* is also once identified in a thin section sample in the lower part of the section. It is characteristic for its bilateral symmetry across its single keel in the peripheral view.

**Stratigraphic distribution:**

From *Helvetoglobotruncana helvetica* zone (early to middle Turonian) to *Dicarinella asymetrica* zone (early Santonian)

**Occurrence:** NS-24

***Marginotruncana sinuosa* PORTHAULT, 1970**

Pl. 13, fig. 5

*Marginotruncana sinuosa* LAMOLDA et al., 2007, p. 25, fig. 6 – M.

*Marginotruncana sinuosa* EGGER et al., 2013, p. 105, fig. 9 – 9-11.

**Diagnostic features:**

Moderately to highly trochospiral test with a sinuous edge view, double keel, strongly elongated crescentic chambers on the spiral side, chambers are elongated in the direction of coiling on both sides, curved oblique and raised sutures on the spiral side, V-shaped raised sutures on the umbilical side, 5-6 chambers in the last whorl.

**Remarks:**

*Marginotruncana sinuosa* is distinguished from similar marginotruncanids, such as *M. sigali*, *M. undulata* and *M. tarfayaensis*, by its quite strongly elongated chambers and clearly separate double keels. Another species it resembles the most is *C. fornicata* which occurs together with *M. sinuosa* from Turonian up to the end-Santonian. Actually, it is thought that *M. sinuosa* could be the ancestor of *C. fornicata* (Robaszynski et al., 1979; Caron, 1985). When it comes to distinguish these two, *M. sinuosa* does not have chambers as elongated and undulated as those of *C. fornicata* and *C. fornicata* mostly occurs in a much higher trochospiral. Finally, *M. sinuosa* is known to have prominently globular chambers in the early whorls (Robaszynski et al., 1979; Caron, 1985), but unfortunately this detail could not be observed here due to problematic preservation. *M. sinuosa* is found just below the proposed Santonian-Campanian boundary in the measured section.

**Stratigraphic distribution:**

From *Helvetoglobotruncana helvetica* zone (early to middle Turonian) to *Dicarinella asymetrica* zone (early Campanian)

**Occurrence:**

NS-38

***Marginotruncana tarfayaensis* LEHMANN, 1963**

Pl. 13, fig. 4

*Marginotruncana tarfayaensis* LAMOLDA et al., 2007, p. 25, fig. 6 – L.

*Marginotruncana tarfayaensis* WALASZCZYK et al., 2012, p. 585, fig. 5 - 5.

**Diagnostic features:**

Slightly trochospiral and inequally biconvex large test, very closely spaced double keels, petaloid chambers on the spiral side, reniform chambers on the umbilical side, compressed chambers especially towards the edges, 6-7 chambers on the spiral side.

**Remarks:**

*Marginotruncana tarfayaensis* is observed in the middle part of the measured section. It can be similar to *M. coronata* and *M. pseudolinneiana*, but it has much more closely spaced keels and noticeably compressed chambers. It is distinguished from *M. sinuosa* by its non-elongated chambers and closely spaced double keel.

**Stratigraphic distribution:**

From *Marginotruncana sigali* – *Dicarinella primitiva* zone (late Turonian) to *Dicarinella asymetrica* zone (early Campanian)

**Occurrence:**

NS-28 – NS-30

**Subfamily Globotruncaninae BROTZEN, 1942****Genus *Globotruncana* CUSHMAN, 1927**

Type species: *Pulvinulina arca* CUSHMAN, 1926

***Globotruncana aegyptiaca* NAKKADY, 1950**

Pl. 5, fig. 13, 18

*Globotruncana aegyptiaca* JAFF *et al.*, 2015. p. 128, pl. 3, figs. 1, 2.

*Globotruncana aegyptiaca* SARI *et al.*, 2016. p. 101, fig. 10, D.

**Diagnostic features:**

Planoconvex, double keels bordering an imperforate peripheral band of variable thickness, umbilical keel never placed at the maximum width of the last chamber, petaloid chambers on both sides, inflated spiral chambers (in some cases), few number (3-5) of rapidly enlarging chambers.

**Remarks:**

The *Globotruncana aegyptiaca* morphotype identified in this study is the one with quite inflated chambers. *G. aegyptiaca* is similar to *G. rosetta*. They are distinguished by *G. aegyptiaca*'s characteristic widely spaced double keels and *G. rosetta*'s weakly developed umbilical keel. *G. ventricosa* shares the just mentioned double keel structure with *G. aegyptiaca*, however it also has a much higher number of chambers in its last whorl. The chambers of *G. ventricosa* are also never inflated.

**Stratigraphic distribution:**

From *Globotruncana aegyptiaca* zone (late Campanian) to *Abathomphalus mayaroensis* zone (late Maastrichtian)

**Occurrence:**

NS-61 – NS-75

***Globotruncana arca* CUSHMAN, 1926**

Pl. 6, fig. 7-18; Pl. 24, fig. 6-9

*Globotruncana arca*, GEORGESCU, 2006, p. 112, fig. 7 – 3-6.

*Globotruncana arca* ARDESTANI *et al.*, 2012. p. 27, fig. 6 - 1.

*Globotruncana arca* SARI *et al.*, 2016. p. 101, fig. 10, E.

**Diagnostic features:**

Biconvex, double keels, petaloid shaped chambers on the spiral side, 6-7 chambers slowly increasing in size in the final whorl.

**Remarks:**

*Globotruncana arca* is another globotruncanid present in almost all samples covering the middle-upper parts of the measured section. It resembles *G. mariei*, but *G. arca* has a

higher number of chambers and a slower rate of chamber size increase. *G. arca* is also rather spiroconvex, especially compared to biconvex *G. mariei*. *C. fornicata* is also similar to *G. arca*, however the latter has chambers that are fewer in number and more elongated in shape. *G. arca* also has petaloid chambers on the umbilical side, unlike *C. fornicata*'s reniform umbilical chambers. It is distinguished from *G. orientalis* by its more distantly spaced double keel and more curved sutures on the spiral side.

**Stratigraphic distribution:**

From *Dicarinella asymetrica* zone (Santonian) to *Abathomphalus mayaroensis* zone (late Maastrichtian)

**Occurrence:**

NS-25 – NS-74

***Globo truncana bulloides* VOGLER, 1941**

Pl. 7, fig. 10-12; Pl. 24, fig. 1-3

*Globo truncana bulloides* PETRIZZO *et al.*, 2011. p. 396, fig. 5 – 4, 8.

*Globo truncana bulloides* ARDESTANI *et al.*, 2012. p. 25, fig. 4 – 2.

*Globo truncana bulloides*, ELAMRI and ZAGHBIB-TURKI, 2014, p. 196, fig. 9 – 11, 12.

*Globo truncana bulloides* SARI *et al.*, 2016. p. 101, fig. 10, F.

**Diagnostic features:**

Planiform to slightly convex on both sides, double keels separated by a wide imperforate peripheral band, perfectly petaloid shaped chambers on the spiral side, 5-6 chambers in the final whorl.



**Remarks:**

*Globotruncana bulloides* occurs abundantly in the measured section. Moreover, it exhibits a considerable variation in its morphological properties. Therefore, it has required extra attention to establish the morphological limits of this species. *G. bulloides* is observed having chambers both with a flat and inflated surface. This resulted in planiform and biconvex morphotypes, respectively. Morphologically closest species to *G. bulloides* is *G. linneiana*. However, they can be differentiated by comparing the two in the edge view. The one having the closer double keel and inflated chambers/biconvexity would be *G. bulloides*. Moreover, *G. bulloides* has a characteristic layout of its chambers in the final whorl; they do not overlap as they do in *G. linneiana*, they are rather separately formed.

**Stratigraphic distribution:**

From *Dicarinella asymetrica* zone (Santonian) to *Abathomphalus mayaroensis* zone (middle Maastrichtian)

**Occurrence:**

NS-23 – NS-75

***Globotruncana falsostuarti* SIGAL, 1952**

Pl. 5, fig. 12

*Globotruncana falsostuarti* CHACON *et al.*, 2004. p. 589, fig. 3 – G.

*Globotruncana falsostuarti* PREMOLI-SILVA and VERGA *et al.*, 2004. p. 107, pl. 37, fig. 1, 2; p. 241, pl. 11, fig. 13-15; p. 242, pl. 12, fig. 1-6.

*Globotruncana falsostuarti* DARVISHZAD *et al.*, 2007. p. 141, pl. 1, fig. 12.

*Globotruncana falsostuarti* ROBASZYNSKI and MZOUGHY, 2010. pl. 2, fig. 2.

**Diagnostic features:**

Equal to unequal biconvexity, closely spaced double keels, petaloid shaped chambers on the spiral side, straight or slightly curved sutures on the spiral side joining the suture around the previous coil at acute to right angles (towards the end of last chamber), numerous chambers (7-8) in the last whorl very slowly increasing in size.

**Remarks:**

*Globotruncana falsostuarti* is observed in only one sample in the uppermost part of the measured section. This species is distinguished from *G. arca* by its sutures on the spiral side, higher number of chambers in the last whorl and most importantly its double keel getting closer in the middle of each chamber. It is differentiated from *G. orientalis*, again, with how its double keel gets closer in the middle of chambers and also by not having merging keels in the last chamber and not having a planiform spiral side. Finally, *G. esnehensis* and *G. dupeblei* are also very similar to this species. However, they both have a single keel unlike double keels of *G. falsostuarti*.

**Stratigraphic distribution:**

From *Globotruncana ventricosa* zone (middle Campanian) to *Abathomphalus mayaroensis* zone (late Maastrichtian)

**Occurrence:**

NS-64

***Globotruncana hilli* PESSAGNO, 1967**

Pl. 7, fig. 1-9; Pl. 24, fig. 4, 5

*Globotruncana hilli* PETRIZZO, 2000, p. 503, fig. 18 – 3.

*Globotruncana hilli* SARI *et al.*, 2016, p. 101, fig. 10, G.

**Diagnostic features:**

Planiform on both sides, double keel separated by an imperforate peripheral band, petaloid chambers on the spiral side, 4.5-5.5 chambers moderately increasing in size in the final whorl, noticeably smaller test size compared to other globotruncanids.

**Remarks:**

*Globotruncana hilli* is another very abundant and frequently occurring species in the measured section. It is immediately identified with its relatively small test, box-like appearance in the edge view, prominent beaded spiral and umbilical sutures and a widely spaced double keel. Roughly speaking, *G. hilli* looks like a smaller version of *G. linneiana*. Therefore, their size and number of chambers in the last whorl must be compared to eliminate this problem. Finally, *G. hilli* may have inflated chambers on the spiral side and its texture can range between smooth and finely pustulose. *G. hilli* has more distantly spaced keels, a greater rate of chamber size increase and a noticeably smaller test size compared to *G. bulloides*.

**Stratigraphic distribution:**

From *Dicarinella asymetrica* zone (Santonian) to *Abathomphalus mayaroensis* zone (late Maastrichtian)

**Occurrence:**

NS-39 – NS-73

***Globo truncana insignis* GANDOLFI, 1955**

Pl. 24, fig. 13-14

*Globo truncana insignis* JANSEN and KROON, 1987, pl. 2, fig. 1, 2.

*Globo truncana insignis* FALZONI and PETRIZZO, 2011, fig. 4 – 10, 11; fig. 5 – 3, 4.

**Diagnostic features:**

Prominently planoconvex test, single keel, acute periphery.

**Remarks:**

The species is distinguished from *G. gansseri* by the acute peripheral angle and narrow umbilicus.

**Stratigraphic distribution:**

From *Globo truncana ventricosa* zone (middle Campanian) to *Abathomphalus mayaroensis* zone (late Maastrichtian)

**Occurrence:**

NS-37

***Globo truncana lapparenti* PESSAGNO, 1967**

Pl. 24, fig. 10-12

*Globo truncana lapparenti* PREMOLI SILVA and VERGA, 2004, Pl. 13, 1-5; Pl. 38, 3-4, Pl. 39, 1.

**Diagnostic features:**

Trochospiral and equally biconvex test, double keel.

**Remarks:**

Being diagnosed only in thin section samples, *Globotruncana lapparenti* is differentiated from *Globotruncana linneiana* by its trochospiral and biconvexity. It has a lower trochospiral than *Globotruncana arca*; has non-inflated chambers compared to *Globotruncana bulloides*.

**Stratigraphic distribution:**

From *Dicarinella concavata* zone (Coniacian) to *Gansserina gansseri* zone (middle Maastrichtian)

**Occurrence:**

NS-32 – NS-34

***Globotruncana linneiana***

Pl. 6, fig. 1-6; Pl. 25, fig. 1-14

*Globotruncana linneiana* PETRIZZO *et al.*, 2011. p. 389, fig. 2 – 9; p. 394, fig. 3 – 3.

*Globotruncana linneiana* ARDESTANI *et al.*, 2012. p. 25, fig. 4 – 1; fig. 5 – 4.

*Globotruncana linneiana*, ELAMRI and ZAGHBIB-TURKI, 2014, p. 195, fig. 8 – 13-15.

*Globotruncana linneiana* LAMOLDA *et al.*, 2014. fig. 11 – D-E.

*Globotruncana linneiana* SARI *et al.*, 2016. p. 101, fig. 10, H.

**Diagnostic features:**

Planiform on both sides, a well-developed double keel separated by a wide imperforate peripheral band, crescentic to petaloid shaped chambers on the spiral side, 5-7 chambers in the last whorl.

**Remarks:**

*Globotruncana linneiana* is a very abundant and numerically the most frequently occurring species in the measured section. It has a plain morphology with no convexity or significant ornamentation on either side of the test; it can have a finely pustulose texture, though. It resembles a box in the edge view just like *G. hilli*. However it differs from *G. hilli* in having a larger test, more chambers and flat surfaced chambers on the spiral side.

**Stratigraphic distribution:**

From *Dicarinella asymerica* zone (Santonian) to *Abathomphalus mayaroensis* zone (middle Maastrichtian)

**Occurrence:**

NS-14 – NS-75

***Globotruncana mariei* BANNER and BLOW, 1960**

Pl. 5, fig. 4-8

*Globotruncana mariei* GEORGESCU, 2006, p. 112, fig. 7 – 8.

*Globotruncana mariei* FAROUK, 2014, p. 243, fig. 6 – 10-12.

**Diagnostic features:**

Equally biconvex test, double keel, petaloid chambers on the spiral side, 4.5-5.5 chambers in the last whorl.

**Remarks:**

*Globotruncana mariei* is observed frequently between the middle-upper parts of the measured section. It has slightly elongated petaloid shaped chambers on the spiral side and a biconvex test. The most similar species to *G. mariei* is *G. arca*, especially when the latter has less than six chambers. To distinguish these two, the rate of chamber size increase in the last whorl and the degree of convexity on the spiral side should be checked.

The specimen with the rapidly enlarging chambers and the lower spiroconvexity would be *G. mariei*, in addition to that *G. arca* mostly has equal to or more than 6 chambers in the last whorl. Other similar species are *G. orientalis* and *G. rosetta*. *G. mariei* has much fewer chambers than *G. orientalis* in the last whorl and also its double keel is always present as two separate keels unlike *G. orientalis* and *G. rosetta*.

**Stratigraphic distribution:**

From *Globo truncanita elevata* zone (early Campanian) to *Abathomphalus mayaroensis* zone (middle Maastrichtian)

**Occurrence:**

NS-14 – NS-74

***Globo truncana orientalis* EL NAGGAR, 1966**

Pl. 5, fig. 1-3

*Globo truncana orientalis* FALZONI *et al.*, 2013, p. 17, fig. 2 – 6.

*Globo truncana orientalis*, ELAMRI and ZAGHBIB-TURKI, 2014, p. 195, fig. 8 – 13-15.

*Globo truncana orientalis* SARI *et al.*, 2016. p. 101, fig. 10, J.

**Diagnostic features:**

Equal to unequal biconvexity, closely spaced double keel with the umbilical one less developed and disappearing/merging with the other one at the last chamber, straight to slightly curved spiral sutures, 5-7 petaloid spiral chambers increasing very slowly in size.

**Remarks:**

*Globo truncana orientalis* is a common species in the measured section. It is distinguished from *G. arca* by its closely spaced double keel (becoming a single keel in the last chamber)

and straighter sutures on the spiral side. It differs from *G. falsostuarti* in that the latter has a narrower keel band in the middle of its chambers.

**Stratigraphic distribution:**

From *Globotruncanita elevata* zone (early Campanian) to *Abathomphalus mayaroensis* zone (middle Maastrichtian)

**Occurrence:**

NS-54 – NS-75

***Globotruncana ventricosa* WHITE, 1928**

Pl. 5, fig. 9-11; Pl. 24, fig. 15

*Globotruncana ventricosa* PETRIZZO, 2000, p. 503, fig. 17 – 1.

*Globotruncana ventricosa* PETRIZZO *et al.*, 2011. p. 389, fig. 2 – 1-5, 10-14.

*Globotruncanita ventricosa* SARI *et al.*, 2016. p. 103, fig. 12, L.

**Diagnostic features:**

Prominently planoconvex test, a moderately spaced double keel bordering an imperforate peripheral band, petaloid shaped chambers on the spiral side, umbilical keel never placed at the maximum width of the last chamber, high number (5 – 9) of rapidly enlarging chambers in the last whorl.

**Remarks:**

*Globotruncana ventricosa* occurs at a moderate frequency in the upper part of the measured section. It is a quite important form, thus its correct identification is crucial in this study. *G. ventricosa* can look very similar to *G. linneiana* at first sight. Although they both have planiform spiral sides, unlike *G. linneiana*, *G. ventricosa* has a very convex umbilical side. This species may also resemble *G. aegyptiaca* in some cases. They are distinguished by *G. ventricosa*'s characteristic loss of umbilical keel at the last chamber.



It also has a much higher number of chambers in its last whorl and its chambers are never inflated.

**Stratigraphic distribution:**

From *Globo truncana ventricosa* zone (middle Campanian) to *Contusotruncana contusa-Racemiguembelina fructicosa* zone (middle Maastrichtian)

**Occurrence:**

NS-49 – NS-68

**Genus *Globo truncanita* REISS, 1957**

Type species: *Rosalina stuarti de lapparent*, 1918

***Globo truncanita angulata* TILEV, 1951**

Pl. 8, fig. 6

*Globo truncanita angulata* ROBASZYNSKI and MZOUGHY, 2010. pl. 5, fig. 1.

*Globo truncanita angulata* ORABI and ZAHRAN, 2013. p. 81, pl. 2 – 1, 2.

*Globo truncanita angulata* SARI *et al.*, 2016. p. 103, fig. 12, B.

**Diagnostic features:**

Strong planoconvexity/umbilicoconvexity, straight spiral sutures joining the peripheral suture at acute angles in the beginning of the last whorl and at almost right angles towards the end of it, trapezoidal shaped chambers on the spiral side, 5-6 chambers in the last whorl.

**Remarks:**

*Globo truncanita angulata* is observed in the washed specimen as only one specimen, but this still made an important contribution to develop the biostratigraphic framework of the measured section. This species is similar to *G. gansseri*. They can be accurately

differentiated by *G. angulata*'s straight sutures on the spiral side. Another single-keeled form *G. angulata* is similar with is *G. pettersi*. However, after close examination one can easily notice how *G. pettersi* has curved sutures and fewer chambers compared to *G. angulata*. Moreover, *G. angulata* is almost hemi-spherical whereas *G. pettersi* has a more conical shape in the side view.

**Stratigraphic distribution:**

From *Globotruncana aegyptiaca* zone (late Campanian) to *Abathomphalus mayaroensis* zone (late Maastrichtian)

**Occurrence:**

NS-69 – NS-71

***Globotruncanita atlantica* CARON, 1972**

Pl. 8, fig. 1, 2

*Globotruncanita atlantica* CHEN *et al.*, 2011, fig. 3 – 10.

*Globotruncanita cf. atlantica* CHEN *et al.*, 2011, fig. 3 – 19.

*Globotruncanita atlantica* PETRIZZO *et al.*, 2011. p. 395, fig. 4 – 3-10.

**Diagnostic features:**

Strongly spiroconvex, single keel, strongly elongated crescentic to triangular shaped chambers on the spiral side, 6 – 7 chambers in the last whorl.

**Remarks:**

*Globotruncanita atlantica* marks the middle to upper part of the Campanian. So, detecting its interval of occurrence is quite important and it is found just in coherence with this assumption in the measured section. This species looks like an inverted bowl in the spiral view. Another form with this look is *G. conica*, however it has straight sutures as opposed

to the curved sutures of *G. atlantica* in the spiral view; therefore they are impossible to confuse with each other.

**Stratigraphic distribution:**

From *Globotruncanita elevata* zone (early Campanian) to *Globotruncana ventricosa* zone (middle Campanian)

**Occurrence:**

NS-43 – NS-61

***Globotruncanita elevata* BROTZEN, 1934**

Pl. 23, fig. 14-15

*Globotruncana elevata* LONGORIA and VONFELDT, 1991, p. 225, pl. 3, figs. 1 – 10; p. 235, pl. 8, figs. 1 – 6; p. 237, pl. 10, figs.13; p. 241, pl. 11, figs. 5, 9, 12, 17.

*Globotruncana elevata* PETRIZZO, 2000, p. 503, fig. 18 – 6.

*Globotruncanita elevata* FALZONI et al., 2013, p. 17, fig. 2 – 9.

*Globotruncanita elevata* SARI et al., 2016. p. 103, fig. 12, C.

**Diagnostic features:**

Umbilicoconvex with a slightly elevated middle part of the spiral side, crescentic chambers on the spiral side, deep and large umbilicus, numerous chambers (5-9) in the last whorl.

**Remarks:**

*Globotruncanita elevata* could only be identified in thin section in this study. Its hallmark feature is the raised middle part of its spiral side, as the name implies. This feature together with the observation of a single keel are found enough to identify this species and distinguish it from others.

**Stratigraphic distribution:**

From *Dicarinella asymetrica* zone (Santonian) to *Globo truncana ventricosa* zone (middle Campanian)

**Occurrence:**

NS-38 – NS-46

***Globo truncana pettersi* Gandolfi, 1955**

Pl. 8, fig. 7

*Globo truncana pettersi* ROBASZYNSKI and MZOUGH, 2010. pl. 5, fig. 2.

*Globo truncana pettersi* SARI *et al.*, 2016. p. 103, fig. 12, F.

**Diagnostic features:**

Umbilicoconvex and conical shape in the side view, smaller test compared to tests of congener species, trapezoidal shaped chambers with curved sutures on the spiral side, 4-5 chambers in the last whorl.

**Remarks:**

*Globo truncana pettersi* is observed as only one in the measured section, but this has been enough to define its morphological properties. Its rapidly enlarging trapezoidal shaped chambers on the spiral side and single keel characterize *G. pettersi*. It lacks *G. angulata*'s characteristic straight spiral sutures. Finally, to differentiate *G. pettersi* from *G. gansseri*, they must be examined in the edge view. *G. pettersi* has a last chamber with a straight outline, whereas *G. gansseri* has a last chamber with a clearly curved outline observed in the side view. Furthermore, *G. pettersi* has curved sutures and fewer chambers compared to *G. angulata*. In the side view, *G. angulata* is almost hemi-spherical whereas *G. pettersi* has a more conical shape as a result of its acute peripheral angle.

**Stratigraphic distribution:**

From *Gansserina gansseri* zone (Santonian) to *Abathomphalus mayaroensis* zone (late Maastrichtian)

**Occurrence:**

NS-64

***Globotruncanita stuartiformis* DALBIEZ, 1955**

Pl. 8, fig. 3-5

*Globotruncana stuartiformis* LONGORIA and VONFELDT, 1991, p. 231, pl. 6, figs. 1 – 12; p. 237, pl. 9, figs. 1 – 3; p. 237, pl. 10, figs: 2, 5, 8, 11, 14, 16; p. 241, pl. 11, figs. 8, 13, 14.

*Globotruncana stuartiformis* PETRIZZO, 2000, p. 503, fig. 18 – 4.

*Globotruncanita stuartiformis*, GEORGESCU, 2006, p. 107, fig. 4 – 14-15.

*Globotruncanita stuartiformis* ROBASZYNSKI and MZOUGHJI, 2010. pl. 3, fig. 3.

*Globotruncanita stuartiformis* FALZONI et al., 2013, p. 17, fig. 2 – 5.

*Globotruncanita stuartiformis* SARI et al., 2016. p. 103, fig. 12, G.

**Diagnostic features:**

Low trochospiral coiling with an equal to unequal biconvexity, single keel, triangular to sub-triangular shaped chambers on the spiral side with steeply sloping sutures towards the periphery in the last ones, 5 – 7 chambers in the last whorl.

**Remarks:**

*Globotruncanita stuartiformis* is the most frequently observed *Globotruncanita* species in the measured section. It is differentiated from other *Globotruncanita* forms very simply by its spiral chamber shape and lateral profile.

**Stratigraphic distribution:**

From *Dicarinella asymetrica* zone (Santonian) to *Abathomphalus mayaroensis* zone (late Maastrichtian)

**Occurrence:**

NS-41 – NS-70

**Genus *Contusotruncana* KORCHAGIN, 1982**

Type species: *Pulvinulina arca contusa* CUSHMAN, 1926

***Contusotruncana fornicata* PLUMMER 1931**

Pl. 2, fig. 1-5

*Contusotruncana fornicata* LAMOLDA et al., 2007, p. 25, fig. 6 – A.

*Contusotruncana fornicata* FALZONI et al., 2013, p. 17, fig. 2 – 1.

*Contusotruncana fornicata* SARI et al., 2016. p. 101, fig. 10, A.

**Diagnostic features:**

Spiroconvex, circular to lobate outline of the test, well-developed double keel, very strongly elongated crescentic shaped chambers on the spiral side, few chambers in the last whorl (most of the time 4, but may also be 5).

**Remarks:**

*Contusotruncana fornicata* is a very abundant species in general. It is recorded continuously from almost bottom to top in the measured section. Spiroconvexity of this species is quite variable, all degrees have been observed in this study. The hallmark of *C. fornicata* is its narrow and strongly elongated chambers in the direction of coiling. It has a potentially problematic resemblance to *M. sinuosa*, where the two can be differentiated

in that *M. sinuosa* does not have chambers as elongated and undulated as *C. fornicata*'s and *C. fornicata* mostly occurs in a much higher trochospiral.

**Stratigraphic distribution:**

*Dicarinella concavata* zone (early Coniacian) to *Abathomphalus mayaroensis* zone (middle Maastrichtian)

**Occurrence:**

NS-21 – NS-75

***Contusotruncana plummerae* GANDOLFI, 1955**

Pl. 2, fig. 6

*Contusotruncana plummerae* PETRIZZO *et al.*, 2011. p. 396, fig. 5 – 1-3, 5-7.

*Contusotruncana plummerae* JAFF *et al.*, 2015. p. 128, pl. 3, figs. 13, 14.

**Diagnostic features:**

Slightly to highly spiroconvex, circular to lobate outline of the test, well-developed double keel, crescentic shaped chambers on the spiral side, distorted horse-shoe shaped chambers on the umbilical side, 4 – 5 chambers in the last whorl.

**Remarks:**

Although not as abundant as *C. fornicata*, *Contusotruncana plummerae* is also an abundant and extensively-occurring species in the measured section. In the author's opinion, it is like an inflated and distorted version of *C. fornicata*. Therefore, it is distinguished from *C. fornicata* firstly by its inflated chambers, on both sides. Moreover, its umbilical sutures do not display the broad V-shape which is present in *C. fornicata*, they are rather depressed except for the edge of last chamber. The space between the keels of *C. plummerae* is also broader than the one between the keels of *C. fornicata*.

**Stratigraphic distribution:**

From *Globotruncana ventricosa* zone (middle Campanian) to *Contusotruncana contusa-Racemiguembelina fructicosa* zone (middle Maastrichtian)

**Occurrence:**

NS-50 – NS-57

**Genus *Gansserina* CARON et al., 1984**

Type Species: *Globotruncana gansseri* BOLLI, 1951

***Gansserina gansseri* BOLLI, 1951**

Pl. 8, fig. 8

*Gansserina gansseri* CHACON et al., 2004, fig. 4 – G, H.

*Gansserina gansseri* COCCIONI and PREMOLI-SILVA, 2015, pl. 1, figs. 9a-c.

*Gansserina gansseri* JAFF et al., 2015. p. 128, pl. 3, figs. 5, 6.

**Diagnostic features:**

Strongly planoconvex, sub-triangular shaped chambers on the spiral side, finely to heavily pustulose test, 4.5-5.5 chambers with curved sutures in the last whorl.

**Remarks:**

Only one *Gansserina gansseri* specimen is found uppermost part of the measured section. This has been a very nice ending to the biostratigraphic zonation, since it signals the lowermost part of *G. gansserina* biozone marking the Latest Campanian. It is quite similar to *G. pettersi* and *G. angulata* at first sight. However, it can be distinguished from both by the curved outline of its last chambers in the edge view. Moreover, *G. gansseri* has mostly a larger test and a higher number of chambers than *G. pettersi*; it has curved spiral sutures compared to *G. angulata*.



**Stratigraphic distribution:**

*Globotruncana aegyptiaca* zone (latest Campanian) to *Abathomphalus mayaroensis* zone (middle Maastrichtian)

**Occurrence:**

NS-75

**Genus *Rugotruncana* BRONNIMANN and BROWN**

Type species: *Rugotruncana tilevi* BRONNIMANN and BROWN, 1956, junior synonym of *Globigerina circumnodifer* FINLAY, 1940

***Rugotruncana circumnodifer* FINLAY, 1940**

Pl. 20, fig. 4-7

*Rugotruncana subcircumnodifer* GEORGESCU, 2005, p. 93, fig. 3 – 7-9.

*Rugotruncana subcircumnodifer*, GEORGESCU, 2006, p. 107, fig. 4 – 9-12.

*Rugotruncana circumnodifer* GEORGESCU and HUBER, 2007. p. 155, pl. 1, figs. 1 – 4; pl. 3, figs. 1 – 5.

*Rugotruncana circumnodifer* KALANAT *et al.*, 2015, pl. 3, figs. 19 - 21.

**Diagnostic features:**

Low to medium high spire, double keel with an imperforate peripheral band, meridional costallae which may disappear towards the last chambers, 4.5-5.5 chambers in the final whorl, large aperture.

**Remarks:**

*Rugotruncana* is accepted as a monotypic genus due to the poor understanding of the species and its high morphological variability (Georgescu and Huber, 2007). Therefore, it is accepted as a monotypic genus in also this study. *Rugotruncana circumnodifer* is very

simply a double-keeled rugoglobigerinid or archaeoglobigerinid, depending on the characteristics of its wall texture. Its texture ranges between scatteredly pustulose and meridionally costellate, this is the case in this measured section, too.

**Stratigraphic distribution:**

*Globotruncana ventricosa* zone (middle Campanian) to *Abathomphalus mayaroensis* zone (middle Maastrichtian)

**Occurrence:**

NS-62 – NS-72

**Genus *Praeglobotruncana* BERMUDEZ, 1952**

Type species: *Globorotalia delrioensis* PLUMMER, 1931

***Praeglobotruncana gibba* KLAUS, 1960**

Pl. 15, fig. 7-9; Pl. 28, fig. 5-9

*Praeglobotruncana gibba* PERYT, 1983, pl. 32, figs. 1, 2, 4, 5.

*Praeglobotruncana gibba* PETRIZZO, 2000, pl. 3, fig. 9, 5a-c.

*Praeglobotruncana gibba* DUBICKA and MACHALSKI, 2016, fig. 6, i1, i2.

**Diagnostic features:**

High trochospiral spiroconvex test, single keel, petaloid chambers on spiral side, 5-6.5 chambers in the final whorl, deep and narrow umbilicus.

**Remarks:**

*Praeglobotruncana gibba* has the highest trochospire among praeglobotruncanids. It is observed in the lowermost part of the measured stratigraphic section.

**Stratigraphic distribution:**

From *Rotalipora cushmani* zone (late Cenomanian) to *Helvetoglobotruncana helvetica* zone (Turonian)

**Occurrence:**

NS-62 – NS-72

***Praeglobotruncana stephani* GANDOLFI, 1942**

Pl. 15, fig. 1-6; Pl. 28, fig. 10-15

*Praeglobotruncana stephani* PETRIZZO, 2000, p. 499, fig. 9 – 4.

*Praeglobotruncana stephani* NISHI *et al.*, 2003, p. 878, fig. 10 – 5.

*Praeglobotruncana stephani* KELLER and PARDÓ, 2004, p. 98, pl. 2, figs. 12-14, 15, 16.

*Praeglobotruncana stephani* FALZONI *et al.*, 2016, p. 74, fig. 4 – 4.

**Diagnostic features:**

Highly spiroconvex/concavoconvex, single keel, petaloid shaped chambers on the spiral side with raised and beaded sutures, triangular to subtriangular shaped chambers on the umbilical side with depressed sutures, 4-6 chambers in the last whorl

**Remarks:**

*Praeglobotruncana stephani* occurs far more frequently than its congener *P. gibba* in the measured section. *P. stephani* has a lower spire than *P. gibba*.

**Stratigraphic distribution:**

*Rotalipora subticinensis* subzone (late Albian) to *Helvetoglobotruncana helvetica* zone (early Turonian)

**Occurrence:**

NS-3 – NS-13

**Subfamily GLOBOTRUNCANELLINAE MASLAKOVA, 1964**

**Genus *Globotruncanella* REISS, 1957**

Type species: *Globotruncana citae* BOLLI, 1951 (= *Globotruncana havanensis* VOORWIJK, 1937 = *Globorotalia pschadae* KELLER, 1946)

***Globotruncanella petaloidea* GANDOLFI, 1955**

Pl. 20, fig. 1-3

*Globotruncanella petaloidea* PREMOLI-SILVA and VERGA, 2004, p. 114, p. 44, figs. 1, 2.

*Globotruncanella petaloidea* OBAIDALLA, 2005, p. 215, pl. 1, fig. 5.

*Globotruncanella petaloidea* JAFF *et al.*, 2015. p. 130, pl. 4, figs. 1, 2.

**Diagnostic features:**

Spiroconvex and compressed test, petaloid shaped chambers on the spiral side, depressed sutures on both sides, 4 chambers in the last whorl, finely pustulose wall texture

**Remarks:**

*Globotruncanella petaloidea* is observed in one sample in the measured stratigraphic section. It is a distinct form with its compressed test and few number of chambers in the last whorl. Among other globotruncanellids, *G. petaloidea* is distinguished by its rapidly enlarging 4 (always) chambers in the last whorl, unlike *G. havanensis* which has 4.5 to 5 more or less constantly sized chambers in the last whorl. It is not as spiroconvex as *G. pschadae* as well as not having as compressed chambers as the latter does.

**Stratigraphic distribution:**

*Radotruncana calcarata* zone (late Campanian) to *Abathomphalus mayaroensis* zone (late Maastrichtian)

**Occurrence:**

NS-52 – NS-53

**Subfamily ROTALIPORINAE Sigal, 1958**

**Genus *Rotalipora* Brotzen, 1942**

Type species: *Rotalipora turonica* Brotzen, 1942

***Rotalipora cushmani* MORROW, 1934**

Pl. 28, fig. 3-4

*Rotalipora cushmani* DIMITROVA and VALCHEV, 2007, pl.1, fig. 1.

*Rotalipora cushmani* COCCIONI et al., 2016, pl.1, fig. 1-16.

**Diagnostic features:**

Trochoid test, convex spiral side with inflated chambers, scalloped periphery, sutures deeply grooved.

**Remarks:**

*Rotalipora cushmani* is observed in the first sample in thin section of the measured stratigraphic section. It has a characteristic form with its inflated chambers and wide and shallow umbilicus.

**Stratigraphic distribution:**

*Rotalipora globotruncanoides* zone (early Cenomanian) to *Whiteinella archaeocretacea* zone (latest Cenomanian-earliest Turonian)

**Occurrence:**

NS-1

***Rotalipora deecke* FRANCKE, 1925**

Pl. 28, fig. 1-2

*Rotalipora deecke* KOPAEVICH and VISHNEVSKAYA., 2016, fig.8, j-l.

*Rotalipora deecke* FALZONI et al., 2016, fig.4, 2A-C.

**Diagnostic features:**

Low trochospiral test with a flat spiral side, single keel, high rate of chamber size increase, peri-umbilical ridge, deep and narrow umbilicus.

**Remarks:**

*Rotalipora deecke* is the other rotaliporid found in the first first sample in thin section of the measured stratigraphic section. Its distinctive morphological features are the raised middle part of the test due to being low trochospiral, flat spiral chamber surface and a deep but narrow umbilicus.

**Stratigraphic distribution:**

*Rotalipora greenhornensis* subzone (middle Cenomanian) to *Dicarinella algeriana* subzone (late Cenomanian)

**Occurrence:**

NS-1

**Family RUGOLOBIGERINIDAE SUBBOTINA, 1959**

**Genus *Rugoglobigerina* BRONNIMANN, 1952**

Type species: *Globigerina rugosa* PLUMMER, 1927

***Rugoglobigerina hexacamerata* BRONNIMANN, 1952**

Pl. 16, fig. 22

*Rugoglobigerina hexacamerata* ARZ and MOLINA, 2001, p. 346, pl. 1, figs. 9-11.

*Rugoglobigerina hexacamerata* FALZONI *et al.*, 2014. p. 91, fig. 2, 2; p. 92, fig. 3 – 5, 6.

*Rugoglobigerina cf. hexacamerata* FALZONI *et al.*, 2014. p. 93, fig. 4 – 5, 6; p. 94, fig. 5 – 2.

**Diagnostic features:**

Spiroconvex, six chambers increasing very slowly in size in the last whorl, meridionally costellate and coarsely rugose wall texture.

**Remarks:**

This species is observed as only one specimen in the uppermost part of the measured section. *Rugoglobigerina hexacamerata* draws the attention with its rugoglobigerinid texture, at first. After making sure that this specimen is a *Rugoglobigerina* species, it can be distinguished from other rugoglobigerinid species by its numerous chambers (5.5 – 6.5, but ideally 6) with a very low rate of size increase and, again, a very low trochospiral coil. If observable, its large aperture covered with tegilla can also aid in its identification.

**Stratigraphic distribution:** *Radotruncana calcarata* zone (late Campanian) to *Abathomphalus mayaroensis* zone (late Maastrichtian)

**Occurrence:**

NS-68 - NS-74

***Rugoglobigerina macrocephala* BRONNIMANN, 1952**

Pl. 16, fig. 16-18

*Rugoglobigerina macrocephala* GEORGESCU, 2005, p. 93, fig. 3 – 1, 2.

*Rugoglobigerina macrocephala* SARI *et al.*, 2016. p. 103, fig. 12, J.

**Diagnostic features:**

Very large last chamber covering almost the half of the test diameter, 3 – 3.5 chambers increasing very rapidly in size in the last whorl, meridionally costallate and coarsely rugose wall texture.

**Remarks:**

*Rugoglobigerina macrocephala* occurs at a moderate frequency in the upper portion of the measured section. *R. macrocephala* differs from other rugoglobigerinids by its few number of chambers in the last whorl and distinctly large last chamber.

**Stratigraphic distribution:**

*Globotruncana aegyptiaca* zone (late Campanian) to *Abathomphalus mayaroensis* zone (late Maastrichtian)

**Occurrence:**

NS-55 - NS-74

***Rugoglobigerina milamensis* SMITH and PESSAGNO, 1973**

Pl. 16, fig. 20-21

*Rugoglobigerina milamensis* FALZONI *et al.*, 2014. p. 92, fig. 3 – 9, 10.

*Rugoglobigerina cf. milamensis* FALZONI *et al.*, 2014. p. 93, fig. 4 – 9, 10.

*Rugoglobigerina milamensis* SARI *et al.*, 2016. p. 103, fig. 12, K.



**Diagnostic features:**

Five chambers (may be six) moderately increasing in size in the last whorl coiled in a high trochospiral, meridionally costellate and coarsely rugose wall texture.

**Remarks:**

*R. milamensis* is identified in the uppermost part of the measured section. The greatest difference between *R. milamensis* and other rugoglobigerinids is its strong spiroconvexity. A high trochospiral coil coupled with rugoglobigerinid wall texture are the main criteria in identifying this species. It can be, in some cases, said to resemble *R. pennyi* among the rugoglobigerinids, however its fewer number of chambers and noticeably higher trochospire would eliminate any possible confusion.

**Stratigraphic distribution:**

*Globotruncana aegyptiaca* zone (late Campanian) to *Abathomphalus mayaroensis* zone (late Maastrichtian)

**Occurrence:**

NS-67 – NS-68

***Rugoglobigerina pennyi* BRONNIMANN, 1952**

Pl. 16, fig. 19; Pl. 22, fig. 14

*Rugoglobigerina pennyi* GEORGESCU, 2005, p. 93, fig. 3 – 4-6.

*Rugoglobigerina pennyi* FALZONI et al., 2013, p. 17, fig. 2 – 7.

*Rugoglobigerina pennyi* FALZONI et al., 2014. p. 92, fig. 3 – 9.

*Rugoglobigerina cf. pennyi* FALZONI et al., 2014. p. 93, fig. 4 – 7, 8, 9; p. 94, fig. 5 – 3, 4.

**Diagnostic features:**

Presence of six chambers (may be seven) very slowly or not increasing in size in the last whorl coiled in a moderate trochospiral, meridionally costellate and coarsely rugose wall texture.

**Remarks:**

Only one specimen is identified as *Rugoglobigerina pennyi* in the measured section. *R. pennyi* resemble *R. milamensis* in the high number of chambers in its last whorl, but *R. pennyi* has an obviously lower trochospire than the latter. Another rugoglobigerinid *R. pennyi* occurring together with and resembling it is *R. hexacamerata*. However, in this case *R. hexacamerata*'s almost planispiral coil would differentiate these two.

**Stratigraphic distribution:**

*Globotruncana aegyptiaca* zone (late Campanian) to *Abathomphalus mayaroensis* zone (late Maastrichtian)

**Occurrence:**

NS-69

***Rugoglobigerina rugosa* PLUMMER, 1926**

Pl. 16, fig. 1-15; Pl. 22, fig. 13

*Rugoglobigerina rugosa* PETRIZZO, 2000, p. 501, fig. 14 – 5.

*Rugoglobigerina rugosa* GEORGESCU, 2005, p. 93, fig. 3 – 3, 4.

*Rugoglobigerina rugosa* FALZONI *et al.*, 2014. p. 91, fig. 2, 1; p. 92, fig. 3 – 2, 3, 4; p. 101, fig. 11 – 5.

*Rugoglobigerina cf. rugosa* FALZONI *et al.*, 2014. p. 93, fig. 4 – 1-4; p. 94, fig. 5 – 1, 5, 6.

*Rugoglobigerina rugosa* SARI *et al.*, 2016. p. 103, fig. 12, L.

**Diagnostic features:**

Presence of 4-5 chambers rapidly increasing in size in the last whorl coiled in a moderate to high trochospiral, meridionally costellate and coarsely rugose wall texture.

**Remarks:**

*Rugoglobigerina rugosa* has the highest occurrence number among the Genus *Rugoglobigerina* in the measured section. It is distinguished from other rugoglobigerinids described previously, by the combination of its few number of chambers and low to high trochospire. Moreover, it occurs much before all the other *Rugoglobigerina* species in the stratigraphic record and thus, its identification can be problematic as it occurs with costellagerinids. As also described in detail in the *Costellagerina* species descriptions, *R. rugosa* can be quite similar to *C. pilula* and *C. bulbosa*. They can be distinguished only based on the intensity and continuity of rugosities and costellae and features of the primary aperture. When observable, primary aperture is another criteria in distinguishing these two genera; it is interiomarginal-umbilical in the costellagerinids, whereas it is umbilical in rugoglobigerinid species.

**Stratigraphic distribution:**

*Globotruncanita elevata* zone (early Campanian) to *Abathomphalus mayaroensis* zone (late Maastrichtian)

**Occurrence:**

NS-49 - NS-74

**Subfamily Archaeoglobigerinae subfam. nov. SALAJ, 1987**

**Genus *Archaeoglobigerina* PESSAGNO, 1967**

***Archaeoglobigerina blowi* PESSAGNO, 1967**

Pl. 22, fig. 1

*Archaeoglobigerina blowi* NISHI *et al.*, 2003, p. 879, fig. 11 – 13.

*Archaeoglobigerina blowi* GEORGESCU, 2005, p. 92, fig. 2 – 1-3.

*Archaeoglobigerina blowi* GEORGESCU, 2006, p. 114, fig. 8 – 8-10.

*Archaeoglobigerina blowi* FALZONI *et al.*, 2014. p. 101, fig. 11 – 7, 8.

**Diagnostic features:**

Chambers with a high rate of size increase, imperforate peripheral band, moderately to slightly muricate wall texture.

**Remarks:**

*Archaeoglobigerina blowi* is observed in one specimen in the mid-section. In the thin section view, it has a thicker and more muricate wall compared to muricohedbergellids. However, when compared to genera *Whiteinella* and *Rugoglobigerina*, *A. blowi* has a thinner and less coarse test wall. Moreover, *A. blowi* displays its imperforate peripheral band in an equatorial section and this is the main criterion in its identification.

**Stratigraphic distribution:**

From *Marginotruncana sigali-Dicarinella primitiva* zone (late Turonian) to *Abathomphalus mayaroensis* zone (late Maastrichtian)

**Occurrence:**

NS-41

*Archaeoglobigerina cretacea*

Pl. 14, fig. 5

*Archaeoglobigerina cretacea* PETRIZZO, 2000, p. 501, fig. 14 – 2.

*Archaeoglobigerina cretacea* GEORGESCU, 2005, p. 92, fig. 2 – 4-6.

*Archaeoglobigerina cretacea* GEORGESCU, 2006, p. 114, fig. 8 – 14-16.

*Archaeoglobigerina cretacea* ARDESTANI *et al.*, 2012. p. 25, fig. 4 - 4.

**Diagnostic features:**

An almost circular test outline with a very low rate of chamber size increase, presence of a double keel, moderately to densely muricate wall texture.

**Remarks:**

*Archaeoglobigerina cretacea* occurs frequently in the measured section. It is distinctly different than *A. blowi* in terms of its wall texture, number of chambers in the last whorl, general test outline, rate of chamber size increase and most importantly with its possession of a double keel instead of an imperforate peripheral band as *A. blowi* has. It is much more densely muricate than *A. blowi* which can even have a smooth texture. It always has globular and very slowly enlarging chambers contrary to *A. blowi*'s, they are not as inflated as *A. blowi*'s, though. It also has 5-6 chambers, whereas *A. blowi* has 4-5 chambers

**Stratigraphic distribution:**

From *Marginotruncana sigali-Dicarinella primitiva* zone (late Turonian) to *Abathomphalus mayaroensis* zone (late Maastrichtian)

**Occurrence:**

NS-23 – NS-71

**Superfamily Planomalinoidea BOLLI *et al.*, 1957****Family Schakoinidae POKORNY, 1958****Genus *Schakoina* THALMANN, 1932*****Schackoina cenomana* SCHACKO, 1897**

Pl. 28, fig. 16

*Schakoina cenomana* PETRIZZO, 2000, p. 501, fig. 13 – 5.

*Schakoina cenomana* EGGER *et al.*, 2013, p. 107, fig. 11 – 13.

*Schakoina cenomana* FALZONI *et al.*, 2016, p. 75, fig. 5 – 10.

**Diagnostic features:**

Slightly compressed funnel-shaped chambers in the last whorl, presence of mostly 4 chambers in the last whorl.

**Remarks:**

Although *Schakoina cenomana* is known to occur throughout a long geological time span (late Albian-Maastrichtian), it is encountered only a couple of times in the lower part of the measured section. It is immediately recognized by the shape and few number of chambers in the last whorl. The chambers are known to range in the degree which they are elongated vertically, however here, they were short and of the standard funnel shape.

**Stratigraphic distribution:**

From *Rotalipora appenninica* zone (late Albian) to *Abathomphalus mayaroensis* zone (late Maastrichtian)

**Occurrence:**

NS-3 – NS-28

**Family Globigerinelloididae LONGORIA, 1974**

**Subfamily Globigerinelloidinae LONGORIA, 1974**

**Genus *Globigerinelloides* CUSHMAN & TEN DAM, 1948**

Type species: *Globigerinelloides algeriana* CUSHMAN & TEN DAM, 1948

***Macroglobigerinelloides bentonensis* MORROW, 1934**

Pl. 21, fig. 1

*Globigerinelloides bentonensis* KELLER AND PARDO, 2004, p. 101, pl. 5, figs. 15 - 18.

*Macroglobigerinelloides bollii* LAMOLDA et al., 2007, p. 23, fig. 4 – C.

**Diagnostic features:**

7-9 chambers in the last whorl with a rapid increase in chamber size (sometimes creating an anomalously large last chamber), smooth wall texture.

**Remarks:**

In the measured section, *Macroglobigerinelloides bentonensis* occurs rarely. It is identified when a globigerinid form was found with a combination of smooth wall texture together with an abnormally shaped large last chamber.

**Stratigraphic distribution:**

From *Ticinella primula* zone (late Maastrichtian) to *Whiteinella archaeocretacea* (latest Cenomanian-earliest Turonian)

**Occurrence:**

NS-4 – NS-13

***Macroglobigerinelloides bollii* PESSAGNO, 1967**

Pl. 21, fig. 3-9; Pl. 22, fig. 15-19

*Macroglobigerinelloides bollii* PETRIZZO, 2000, p. 499, fig. 10 – 1.

*Macroglobigerinelloides bollii* LAMOLDA *et al.*, 2007, p. 23, fig. 4 – A.

*Macroglobigerinelloides bollii* EGGER *et al.*, 2013, p. 107, fig. 11 – 6-10.

**Diagnostic features:**

6-7 chambers in the last whorl, slowly increasing chamber size, smooth wall texture.

**Remarks:**

*Macroglobigerinelloides bollii* is one of the most frequently occurring species in the measured section. It literally occurs through the whole middle to upper portion of the measured section. It is differentiated from other contemporaneous macroglobigerinelloids by its simple and well-defined morphological features. These are its pustule-free smooth texture, numerous globular chambers and low to moderate rate of chamber size increase.



**Stratigraphic distribution:**

From *Marginotruncana sigali* – *Dicarinella primitiva* zone (late Turonian) to *Gansserina gansseri* zone (latest Campanian-early Maastrichtian)

**Occurrence:**

NS-14 – NS-71

*Macroglobigerinelloides messinae* BRONNIMANN, 1952

Pl. 21, fig. 2

*Macroglobigerinelloides messinae* PREMOLI SILVA and VERGA, 2004, Pl. 85, 4-6.

**Diagnostic features:**

Small and compressed test, 4.5-5.5 chambers in the last whorl.

**Remarks:**

*Macroglobigerinelloides messinae* is distinguished from other macroglobigerinellids as *M. bolli*, *M. prairihillensis* and *M. bentonensis* by its fewer chambers and compressed test which makes it appear in hourglass shape in the lateral view.

**Stratigraphic distribution:**

From *Dicarinella asymetrica* zone (Santonian) to *Abathomphalus mayaroensis* zone (upper Maastrichtian)

**Occurrence:**

NS-41

***Macroglobigerinelloides prairihillensis* PESSAGNO, 1967**

Pl. 21, fig. 10-12; Pl. 22, fig. 20-21

*Macroglobigerinelloides prairihillensis* PETRIZZO, 2000, p. 499, fig. 10 – 7.

*Macroglobigerinelloides prairihillensis* JAFF *et al.*, 2015. p. 130, pl. 4, figs. 9, 10.

**Diagnostic features:**

High rate of chamber size increase coupled with a laterally elongated large last chamber, 6-7 chambers in the last whorl, finely to normally muricate wall texture

**Remarks:**

*Macroglobigerinelloides prairihillensis* is a common species throughout the middle to upper portion of the measured section. In the samples, *M. prairihillensis* was always standing out with its distinctively large and laterally elongated last chamber and differentiated from other globigerinelloides by this trait.

**Stratigraphic distribution:**

From *Dicarinella asymetrica* zone (Santonian) to *Contusotruncana contusa-Racemiguembelina fructicosa* zone (middle Maastrichtian)

**Occurrence:**

NS-22 – NS-74

**Superfamily Rotaliporacea SIGAL, 1958**

**Family Hedbergellidae LOEBLICH & TAPPAN, 1961**

**Subfamily Helvetoglobo truncaninae LAMOLDA, 1976**

**Genus *Helvetoglobo truncana* CARON et al., 1984**

Type Species: *Helvetoglobo truncana helvetica* BOLLI, 1951

***Helvetoglobo truncana helvetica* BOLLI, 1951**

Pl. 9, fig. 1-2; Pl. 29, fig. 9-12

*Helvetoglobo truncana helvetica* PETRIZZO, 2000, fig. 12 – 5a-c.

*Helvetoglobo truncana helvetica* HUBER and PETRIZZO, 2014, fig. 4 – 1; fig. 11.

**Diagnostic features:**

Low trochospiral planoconvex test, single keel, petaloid and flattened chambers on spiral side, raised and beaded sutures on spiral side, adumbilically offset last chamber, deep and wide umbilical-extraumbilical aperture, 5-8 chambers in the last whorl.

**Remarks:**

*Helvetoglobo truncana helvetica* is differentiated from the similar *H. prae helvetica* by its well-developed pustulose keel, raised inner-whorl chambers relative to the final whorl chambers, petaloid and flattened spiral chambers with raised and curved sutures and finally by a last chamber that is offset towards the umbilical side.

**Stratigraphic distribution:**

From *Helvetoglobo truncana helvetica* zone (Turonian) to *Helvetoglobo truncana helvetica* zone (Turonian)

**Occurrence:**

NS-14

**Genus *Muricohedbergella* HUBER & LECKIE, 2011**

Type species: *Muricohedbergella delrioensis* CARSEY, 1926

***Muricohedbergella delrioensis* CARSEY, 1926**

Pl. 19, fig. 14-15; Pl. 22, 8-10

*Muricohedbergella delrioensis* KELLER AND PARDO, 2004, p. 101, pl. 5, figs. 5 - 9.

*Muricohedbergella delrioensis* EGGER *et al.*, 2013, p. 106, fig. 10 – 8, 9, 13.

*Muricohedbergella delrioensis* DIONNE *et al.*, 2016. p. 130, fig. 4, 6 - 8.

**Diagnostic features:**

Having fewer (5 - 6) and larger chambers in the last whorl compared to other species with globular chambers in this genus, often slightly offset last chamber towards the umbilical side.

**Remarks:**

This species stands out among the other contemporary muricohedbergellids with its fewer and inflated globular chambers. Moreover, its last chamber can often be observed as located towards the dorsal side. It occurs not very commonly in the measured section, but when it occurs it is present in the lower part of the section.

**Stratigraphic distribution:**

From *Muricohedbergella planispira* zone (early Albian) to *Dicarinella concavata* zone (latest Coniacian)

**Occurrence:**

NS-1 – NS-18

***Muricohedbergella flandrini* PORTHAULT, 1970**

Pl. 20, fig. 8-10; Pl. 21 fig. 6-7

*Muricohedbergella flandrini* ARDESTANI *et al.*, 2012. p. 26, fig. 5 - 3.

*Muricohedbergella flandrini* EGGER *et al.*, 2013, p. 106, fig. 10 – 10-12.

*Muricohedbergella flandrini* KALANAT *et al.*, 2015, pl. 3, figs. 19 - 21.

**Diagnostic features:**

Strongly compressed oval shape and few number (4.5-5) of chambers in the last whorl, very narrow umbilicus.

**Remarks:**

*Muricohedbergella flandrini* is a very abundant form in the lower part of the measured section. It is easily discernable with its characteristic chamber shape and remarkably compressed look in the side view. It ranges between small and large in size above the 125 µm sieve washed sample.

**Stratigraphic distribution:**

From *Helvetoglobotruncana helvetica* zone (early to middle Turonian) to *Dicarinella asymetrica* zone (Santonian)

**Occurrence:**

NS-16 – NS-40

***Muricohedbergella holmdelensis* OLSSON, 1964**

Pl. 14, fig. 11-15, Pl. 22, fig. 11-12

*Muricohedbergella holmdelensis* PETRIZZO, 2000, p. 498, fig. 8 – 3.

*Muricohedbergella holmdelensis* BOUDAGHER-FADEL, 2012, p. 105, fig. 14 – 16.

**Diagnostic features:**

Planoconvex with tapering form of the last chamber in the edge view.

**Remarks:**

This species occurs starting from the lower part up to the end of the measured section. It is characterized by its high rate of chamber size increase, sometimes yielding a distinctively large last chamber, and moderate number (5-6) of chambers in the last whorl. However, it is only distinguished by its edge view which displays a marked planoconvexity and tapering shape of the last chamber.

**Stratigraphic distribution:**

From *Dicarinella concavata* (latest Turonian-Coniacian) to *Guembelitria cretacea* (earliest Danian) (Arz and Arenillas, 2016)

**Occurrence:**

NS-28 – NS-74

***Muricohedbergella hoelzli* OLSSON, 1964**

Pl. 14, fig. 1-4

*Muricohedbergella hoelzli* PETRIZZO, 2000, p. 498, fig. 8 – 4.

*Muricohedbergella hoelzli* BOUDAGHER-FADEL, 2012, p. 105, fig. 19 – 21.

**Diagnostic features:**

Spiroconvex, globular chambers with moderately depressed sutures, with a low rate of size increase, 5-7 chambers in the last whorl, moderately muricate test

**Remarks:**

This rarely occurring species can be distinguished from *M. flandrini* by its smaller chambers and having more chambers in the last whorl. Its chambers are also petaloid in shape on both sides, contrary to *M. flandrini*'s oval/spatulate-shaped chambers. It is distinguished from *W. aprica* by its less depressed sutures and umbilical/extra-umbilical aperture.

**Stratigraphic distribution:**

From *Whiteinella archaeocretacea* (latest Cenomanian) to *Marginotruncana sigali-Dicarinella primitiva* (latest Turonian)

**Occurrence:**

NS-5

*Muricohedbergella monmouthensis* OLSSON, 1960

Pl. 22, fig. 2

*Muricohedbergella monmouthensis* PREMOLI SILVA and VERGA, 2004, Pl. 97, 1-4;  
Pl. 30, 9-10.

**Diagnostic features:**

Trochospiral and inequally biconvex test, globular chambers with strongly depressed sutures, high rate of chamber size increase, finely pustulose wall texture.

**Remarks:**

*M. monmouthensis* is observed once in the upper part of the section. The specimen is distinguished from planispira/nearly-planispiral muricohedbergellids as *M. planispira* and *M. holmdelensis* by its trochospiral. It differs from *M. flandrini* in having perfectly globular chambers. Moreover, *M. monmouthensis* has a more finely pustulose wall texture compared to whiteinellids.

**Stratigraphic distribution:**

From *Globotruncana ventricosa* (middle Campanian) to *Abathomphalus mayaroensis* (upper Maastrichtian)

**Occurrence:**

NS-66



***Muricohedbergella planispira* TAPPAN, 1940**

Pl. 14, fig. 6-10; Pl. 22, fig. 3-4

*Muricohedbergella planispira* KELLER AND PARDO, 2004, p. 102, pl. 6, figs. 1 - 5.

*Muricohedbergella planispira* EGGER et al., 2013, p. 107, fig. 11 – 1, 2.

*Muricohedbergella planispira* DIONNE et al., 2016, p. 130, fig. 4, 9 - 10.

*Muricohedbergella planispira* FALZONI et al., 2016, p. 88, fig. 12 – 6.

**Diagnostic features:**

Perfectly planispiral 5-7 chambers in the last whorl with almost the same size.

**Remarks:**

*Muricohedbergella planispira* is a very common form up to the middle part of the measured section. Although it displays a range of differentiation of total size and rate of chamber size increase, it still can be easily identified among the other muricohedbergellids with being perfectly planispiral, its having generally more chambers and not showing a high (mostly none) rate of chamber size increase.

**Stratigraphic distribution:**

From *Muricohedbergella planispira* zone (early Albian) to *Globotruncanita elevata* zone (early Campanian)

**Occurrence:**

NS-1 – NS-45

**Genus *Whiteinella* PESSAGNO, 1967**

Type species: *Whiteinella archaeocretacea*

***Whiteinella aprica* LOEBLICH and TAPPAN, 1961**

Pl. 29; fig. 3

*Whiteinella aprica* KELLER AND PARDO, 2004, p. 100, pl. 4, figs. 5, 6, 9.

*Whiteinella aprica* DIONNE *et al.*, 2016. p. 131, fig. 5, 1 - 3.

**Diagnostic features:**

Planoconvex, inflated globular chambers on both sides with a low rate of size increase and strongly depressed sutures, 5.5-6 chambers in the last whorl, coarsely hispid wall texture.

**Remarks:**

*Whiteinella aprica* specimens are identified in the lower part of the measured section. It is distinguished from muricohedbergellids by its strongly depressed sutures, globular chambers, characteristic whitenellid wall texture and umbilical aperture.

**Stratigraphic distribution:**

From *Dicarinella algeriana* subzone (middle to late Cenomanian) to *Dicarinella concavata* zone (latest Turonian)

**Occurrence:**

NS-5 – NS-14

***Whiteinella archaeocretacea* PESSAGNO, 1967**

Pl. 29, fig. 4, 5

*Whiteinella archaeocretacea* KELLER AND PARDO, 2004, p. 100, pl. 4, figs. 1, 2.

*Whiteinella archaeocretacea* LAMOLDA et al., 2007, p. 24, fig. 5 – L.

*Whiteinella archaeocretacea* KALANAT et al., 2015, pl. 3, figs. 10 - 12.

*Whiteinella archaeocretacea* FALZONI et al., 2014. p. 101, fig. 11 – 6.

**Diagnostic features:**

Low spire, strongly depressed sutures on both sides, 5-6 chambers in the last whorl with a compressed last chamber, large umbilical/extraumbilical aperture.

**Remarks:**

*Whiteinella archaeocretacea* is observed rarely in the middle portion of the measured section. It differs from *W. aprica* in having more compressed chambers in general and mostly a smaller number of chambers in the last whorl. On the other hand, this species is distinguished from *W. inornata* by having not as compressed chambers as the latter and more chambers in the last whorl.

**Stratigraphic distribution:**

From *Whiteinella archaeocretacea* zone (latest Cenomanian) to *Dicarinella concavata* zone (latest Turonian)

**Occurrence:**

NS-2 – NS-16

***Whiteinella baltica* DOUGLAS and RANKIN, 1969**

Pl. 19, fig. 1-11; Pl. 29, fig. 1-2

*Whiteinella baltica* KELLER AND PARDO, 2004, p. 99, pl. 3, figs. 12 – 14, 14, 16.

*Whiteinella baltica* EGGER et al., 2013, p. 106, fig. 10 – 1-3.

*Whiteinella baltica* KALANAT et al., 2015, pl. 1, figs. 13 - 15.

**Diagnostic features:**

Equally biconvex trochospiral test with a characteristic quadrate test outline, four chambers in the last whorl.

**Remarks:**

*Whiteinella baltica* is one of the most abundant species in the measured section, it occurs from the lower to middle parts of the measured section. The moderately muricate or pustulose wall texture coupled with four perfectly globular chambers with a high rate of size increase coiled in a low trochospire summarizes the morphology of *W. baltica*. Furthermore, it has a large interiomarginal, umbilical-extraumbilical aperture and, if observable, this aperture is covered with a large porticus. It is easily distinguished from other whitenellids with these characteristic properties.

**Stratigraphic distribution:**

From *Rotalipora greenhornensis* subzone (middle Cenomanian) to *Dicarinella asymetrica* (Santonian)

**Occurrence:**

NS-2 – NS-53

***Whiteinella brittonensis* TAPPAN, 1961**

Pl. 19, fig. 12-13

**Diagnostic features:**

Moderately high trochospiral spiroconvex test, muricate wall texture, 5-6 chambers in the last whorl.

**Remarks:**

*Whiteinella brittonensis* is distinguished from other whiteinellids by its higher trochospiral (except for *Whiteinella paradubia*). It also has more chambers than *W. baltica*.

**Stratigraphic distribution:**

From *Dicarinella algeriana* subzone (late Cenomanian) to *Dicarinella concavata* (Coniacian)

**Occurrence:**

NS-14 – NS-38

***Whiteinella paradubia* SIGAL, 1952**

Pl. 29, fig. 6-8

**Diagnostic features:**

High trochospiral spiroconvex test, moderately pustulose wall texture, 6 chambers in the last whorl, wide and shallow aperture.

**Remarks:**

*Whiteinella paradubia* is frequently observed in the lowermost part of the measured stratigraphic section. It is distinguished from other whiteinellids by its distinctively high trochospire.

**Stratigraphic distribution:**

From *Dicarinella algeriana* subzone (late Cenomanian) to *Dicarinella concavata* (Coniacian)

**Occurrence:**

NS-1 – NS-17

***Whiteinella praehelvetica* TRUJILLO, 1960**

Pl. 9, fig. 3-6; Pl. 29, fig. 13-14

*Whiteinella praehelvetica* PETRIZZO, 2000, fig. 12 – 4a-c.

*Helvetoglobotruncana praehelvetica* HUBER and PETRIZZO, 2014, fig. 4 – 2, 3; fig. 10.

*Helvetoglobotruncana praehelvetica* VAHIDINIA et al., 2014, pl. 3, fig. 9.

*Helvetoglobotruncana praehelvetica* FALZONI et al., 2016, fig. 5, 11A-C.

**Diagnostic features:**

Low to middle conically trochospiral spiroconvex test, petaloid and inflated chambers on spiral side, depressed sutures on both sides, deep and wide interiomarginal aperture, 5-6 chambers in the last whorl, moderately pustulose wall texture.

**Remarks:**

*H. praehelvetica* occurs before *H. helvetica* in the measured geological section. It can be said to be a more primitive version of the latter in that it lacks a keel and a non-umbilical aperture unlike globotruncanids additional to its having a lumpy texture.

**Stratigraphic distribution:**

From *Rotalipora cushmani* zone (late Cenomanian) to *Helvetoglobotruncana helvetica* zone (Turonian)

**Occurrence:**

NS-14

**Genus *Costellagerina* EL-NAKHAL, and CIFELLI, 1983**

Type species: *Rugoglobigerina bulbosa* Belford, 1960

***Costellagerina bulbosa* PETTERS, EL-NAKHAL, and CIFELLI, 1983**

Pl. 1, fig. 5-17

*Costellagerina bulbosa* PETRIZZO, 2000, p. 501, fig. 14 – 3.

*Costellagerina bulbosa* ARDESTANI *et al.*, 2012. p. 24, fig. 3 - 2.

*Costellagerina bulbosa* FALZONI *et al.*, 2014. p. 101, fig. 11 – 2, 4.

**Diagnostic features:**

Globular shaped 4-5 chambers in the last whorl, aligned and fused single pustules into short ridges forming thin and discontinuous costae.

**Remarks:**

In some cases, *Costellagerina bulbosa* can resemble *R. rugosa* very much. This is the major problem in the identification of this species, where these occur together especially in the middle part of the measured section. This problem arises due to the high variability of the meridional ornamentation, the umbilical structure, and the presence of an imperforate peripheral band which can be observed in rugoglobigerinids. This issue can be overcome by firstly examining the wall texture of the specimen in detail. In *Costellagerina*, the meridional ornamentation is formed by the alignment of single pustules plus few pustules fused into short ridges so that costae are thin and discontinuous (Petrizzo and Premoli-Silva, 2000). Secondly, if the aperture is well-preserved and not infilled, then the presence of portici and tegilla should be checked. *Costellagerina* species possess only portici. Although the problematic discrimination between the genera

*Rugoglobigerina* and *Costellagerina* is further revealed by the fact that the extinction level of the *Costellagerina* species has not been precisely established (Petruzzo and Premoli Silva, 2000; Premoli Silva and Verga, 2004), with a somewhat rough generalization, the pre-Middle Campanian meridionally costellate hedbergellids are most of the time *Costellagerina*.

**Stratigraphic distribution:**

From *Dicarinella asymetrica* (Santonian) to *Globotruncanita elevata* (early Campanian)

**Occurrence:**

NS-35 – NS-53

***Costellagerina pilula* BELFORD, 1960**

Pl. 1, fig. 1-4

*Costellagerina pilula* LAMOLDA *et al.*, 2007, p. 24, fig. 5 – I, J.

*Costellagerina pilula* ARDESTANI *et al.*, 2012. p. 24, fig. 3 - 1.

*Costellagerina pilula* FALZONI *et al.*, 2014. p. 101, fig. 11 – 1, 3.

*Costellagerina pilula* LAMOLDA *et al.*, 2014. fig. 11 – H.

**Diagnostic features:**

Aligned and fused single pustules into short ridges forming thin and discontinuous costae, globular shaped chambers, moderate number (5-6) of chambers in the last whorl.

**Remarks:**

*Costellagerina pilula* stands out with its texture at first. But again, its occurrence together with rugoglobigerinids and *C. bulbosa* can pose serious identification problems. As stated just previously, the difference between *C. pilula* and rugoglobigerinids lie in its having a porticus instead of tegillum and a different arrangement (discontinuous and short) and



thickness (thinner) of the meridional costae. More specifically, based on the observation of the morphological variability of *C. pilula* during the Santonian and of *R. rugosa* in the upper Campanian-Maastrichtian, the chamber growth rate can be used as a criterion (Falzoni et al., 2014). This rate is slower in *C. pilula*. This observation is consistent with test dissections illustrated by Huber (1994) showing that early growth rate in the topotypes of *C. pilula* is slower than in topotypes of *R. rugosa* and, thus they are likely not phylogenetically related. Moreover, the inner whorl in *C. pilula* is raised on spiral view, whereas it tends to be more depressed in *R. rugosa*. When it comes to discriminate between two costellagerinid species *C. bulbosa* and *C. pilula*, a difference in the number of chambers is evident at first. *C. pilula* has more numerous chambers as well as having a clearly noticeable lower rate of chamber size increase. Moreover, these two species are not known to produce intermediate morphotypes (Petruzzo, 2000), whose presence can be very problematic. Thus they are reported to have sufficient differences for being kept as two separate forms even if they exhibit the same stratigraphic range (Petruzzo and Premoli-Silva, 2000).

**Stratigraphic distribution:**

From *Dicarinella asymetrica* (Santonian) to *Globotruncanita elevata* (early Campanian)

**Occurrence:**

NS-30 – NS-53

**Superfamily HETEROHELICACEA CUSHMAN, 1927**

**Family HETEROHELICIDAE CUSHMAN, 1927**

**Subfamily HETEROHELICINAE CUSHMAN, 1927**

**Genus *Heterohelix* EHRENBERG, 1843**

Type species: *Textularia americana* EHRENBERG, 1843

***Heterohelix globulosa* EHRENBERG, 1840**

Pl. 11, fig. 1-6; Pl. 26, fig. 1-11

*Heterohelix striata* ARDESTANI *et al.*, 2012. p. 27, fig. 6 - 3.

*Heterohelix striata* JAFF *et al.*, 2015. p. 132, pl. 5, fig. 10.

*Heterohelix globulosa* JAFF *et al.*, 2015. p. 132, pl. 5, figs. 6, 7.

*Heterohelix globulosa* DIONNE *et al.*, 2016. p. 130, fig. 4, 1 - 3.

**Diagnostic features:**

Depressed and slightly curved sutures, globular shaped moderately enlarging 11-15 chambers, fine costae.

**Remarks:**

*Heterohelix globulosa* is one of the mostly occurring species in the measured section. It has a quite simple morphology making its identification very easy. Its rate of chamber size increase may range between moderate to high and test size also ranges between 100-200 microns. But it is always cone shaped, has globular chambers and finely striated all over the test.

**Stratigraphic distribution:**

From *Helvetoglobotruncana helvetica* (early to middle Turonian) to *Abathomphalus mayaroensis* (latest Maastrichtian)

**Occurrence:**

NS-14 – NS-74

***Heterohelix planata* CUSHMAN, 1938**

Pl. 10, fig. 1-5

*Heterohelix planata* PETRIZZO, 2000, p. 500, fig. 11 – 5.

*Heterohelix planata*, GEORGESCU, 2006, p. 107, fig. 4 – 4, 5.

*Heterohelix planata* EGGER *et al.*, 2013, p. 109, fig. 13 – 7-15.

**Diagnostic features:**

Rapidly flaring subtriangular shaped compressed test with subrectangular – reniform chambers, depressed triangular areas in the adult part, straight and depressed sutures slightly oblique to the growth axis, possible presence or absence of an incipient planispiral coil in the juvenile stage, fine costae.

**Remarks:**

*Heterohelix planata* is identified in the upper part of the measured section. It occurs mostly as a large test which has well-developed reniform chambers in the adult stage. Its another characteristic feature is the depressed area in the latest parts of the adult portion along the median suture. Finally, if observable, the semi-developed planispirally coiled part at the bottom of the test can be a very important clue in the identification of this species. If the test is not well preserved, than the roundness at the juvenile stage of the test, instead of a pointed end, would signal the planispiral coiling at the beginning.

**Stratigraphic distribution:**

From *Dicarinella asymetrica* (late Santonian) to *Abathomphalus mayaroensis* (latest Maastrichtian)

**Occurrence:**

NS-41 – NS-69

***Heterohelix punctulata* CUSHMAN, 1938**

Pl. 10, fig. 6-8

*Heterohelix punctulata* NEDERBRAGT, 1991, p. 349, pl. 3, fig. 6.

*Heterohelix punctulata* ABRAMOVICH *et al.*, 2003, p. 6, pl. 1, fig. 9; p. 8, pl. 2, fig. 5.

*Heterohelix punctulata* PREMOLI-SILVA and VERGA, 2004, p. 143, pl. 73, figs. 1-5; p. 253, pl. 23, fig. 5.

**Diagnostic features:**

Broad rounded and long test, very rapid flaring of chambers in the initial part of the test, subparalleling globular chamber growth in the remaining part, fine costae.

**Remarks:**

*Heterohelix punctulata* occurs frequently from the middle to uppermost part of the measured section. Its long and rectangular-shaped (except for the initial part) test resulting from subparalleling globular chamber growth quickly draws attention and gives *H. punctulata* a unique appearance.

**Stratigraphic distribution:**

From *Dicarinella asymetrica* (late Santonian) to *Abathomphalus mayaroensis* (latest Maastrichtian)

**Occurrence:**

NS-30 – NS-75

***Heterohelix* sp. 1**

Pl. 10, fig. 9-10

**Diagnostic features:**

Moderately flaring compressed test, initially globular chambers becoming more reniform shaped in the remaining part, low rate of chamber size increase, depressed sutures, fine costae.

**Remarks:**

*Heterohelix* sp. 1 is present in the middle part of the measured section. It is different than *H. planata* in having broader and fewer chambers. It is not as rectangular-shaped as *Pseudotextularia nuttalli* is both in lateral and side views. It is also distinguished by genus *Sigalia* by its non-petaloid reniform-shaped chambers.

**Stratigraphic distribution:**

*Globotruncanita elevata* (lower Campanian)

**Occurrence:**

NS-41

***Heterohelix* sp. 2**

Pl. 10, fig. 11-14

**Diagnostic features:**

Triangular-shaped test, initially globular chambers becoming more reniform shaped in the remaining part, high rate of chamber size increase, depressed sutures, fine costae.

**Remarks:**

*Heterohelix* sp. 2 is present in the middle part of the measured section. It is different than *H. planata* which has a compressed test, in having a thick one. It also has a larger flare than other contemporaneous heterohelics.

**Stratigraphic distribution:**

From *Globo truncanita elevata* (lower Campanian) to *Globo truncanella* spp. (middle to upper Campanian)

**Occurrence:**

NS-41 – NS-53

**Genus *Laeviheterohelix* NEDERBRAGT, 1991**

Type species: *Gumbelina pulchra* BROTZEN, 1936

***Laeviheterohelix turgida*, NEDERBRAGT, 1991**

Pl. 12, fig. 1-4; Pl. 26, fig. 12

*Laeviheterohelix turgida*, GEORGESCU, 2006, p. 107, fig. 4 – 21.

**Diagnostic features:**

Subglobular juvenile chambers becoming more reniform in the adult stage, inflated chambers, strongly depressed sutures (deepest near the median suture), pinched edges, pore mounds on the test wall, thick flanges at the aperture.

**Remarks:**

*Laeviheterohelix turgida* is observed from middle to upper parts in the measured section. As all other, *Laeviheterohelix* specimens are not well preserved and thus, the texture cannot be confidently used as a criterion for their identification. Fortunately, *L. turgida* has characteristic strongly inflated reniform chambers with depressions between them as

well as pinched edges and thick flanges (the last two are not always observable though). These make its identification possible among other congener species.

**Stratigraphic distribution:**

From *Dicarinella asymetrica* (early Santonian) to *Globotruncanita elevata* (early Campanian)

**Occurrence:**

NS-14 – NS-45

***Laeviheterohelix* sp. 1**

Pl. 12, fig. 5-8; Pl. 26, fig. 13

**Diagnostic features:**

Overlapping reniform chambers, moderately depressed sutures, pore mounds, smooth texture, flanges may be present at the aperture.

**Remarks:**

*Laeviheterohelix* sp. 1 is observed in the middle part of the section. It is differentiated from other laeviheterohelicids by its distinctively more robust test.

**Stratigraphic distribution:**

*G. elevata-D. asymetrica* (middle to late Santonian)

**Occurrence:**

NS-31 – NS-32

**Genus *Ventilabrella* CUSHMAN, 1928**

Type species: *Ventilabrella eggeri* CUSHMAN, 1928

***Ventilabrella browni* MARTIN, 1972**

Pl. 18, figs. 1-4

*Ventilabrella browni* BOUDAGHER-FADEL, 2012, p. 110, pl. 4.19 – 31.

**Diagnostic features:**

High proliferation, flabelliform compressed test, a numerous chambered test with 6-8 subglobular chambers in the biserial portion and up to 10 subglobular to pyriform chambers in the multiserial portion, thick to fine costae from lower to upper part of the test.

**Remarks:**

*Ventilabrella browni* occurs in the middle portion of the measured section. It is the *Ventilabrella* species having the highest number of chambers in among all *Ventilabrella* specimens. It is noticeably thinner/more compressed than the thick *Ventilabrella* species *V. eggeri* and *V. austinana*.

**Stratigraphic distribution:**

From *Globotruncana ventricosa* (middle Campanian) to *Abathomphalus mayaroensis* (latest Maastrichtian)

**Occurrence:**

NS-40 – NS-52



***Ventilabrella eggeri* CUSHMAN, 1928**

Pl. 18, figs. 5-7

*Ventilabrella eggeri* PETRIZZO, 2000, p. 500, fig. 11 – 10.

*Ventilabrella eggeri*, GEORGESCU, 2006, p. 109, fig. 5 – 1-6.

*Ventilabrella browni* BOUDAGHER-FADEL, 2012, p. 110, pl. 4.19 – 9-11.

*Ventilabrella eggeri*, ELAMRI and ZAGHBIB-TURKI, 2014, p. 195, fig. 8 – 8.

**Diagnostic features:**

Moderate proliferation, globular chambers, thick costae.

**Remarks:**

*Ventilabrella eggeri* is the most frequently occurring *Ventilabrella* species in the measured section. It stands out among its congeners with its thickly costate texture at first. It is neither as proliferating and compressed as *V. browni*, nor has as globular chambers and fine costae as *V. austinana* does.

**Stratigraphic distribution:**

From *Dicarinella concavata* (latest Coniacian) to *Globotruncana ventricosa* (middle Campanian)

**Occurrence:**

NS-40 – NS-53

**Genus *Pseudotextularia* RZEHAK, 1891**

Type species: *Cuneolina elegans* RZEHAK, 1891

***Pseudotextularia nuttalli* VOORWIJK, 1937**

Pl. 11, fig. 7-11

*Pseudotextularia nuttalli* LAMOLDA et al., 2007. p. 28, figs 4N1-2, O1-2.

*Pseudotextularia nuttalli* EGGER et al., 2013, p. 108, fig. 12 – 5-7.

**Diagnostic features:**

Low flaring angle of the test, wide and elongate chambers in the edge view, fine costae.

**Remarks:**

Being one of the most common planktonic foraminifera species in the measured section, *Pseudotextularia nuttalli* occurs from the recorded lower portion up to the end of measured section. The lateral elongation of the chambers can reach extreme levels in some specimens, so this species is primarily identified by its appearance in the edge view. Moreover, it is differentiated from the very similar *P. elegans* by its much finer costae.

**Stratigraphic distribution:**

From *Dicarinella concavata* (middle Coniacian) to *Abathomphalus mayaroensis* (latest Maastrichtian)

**Occurrence:**

NS-14 – NS-75

**Genus *Sigalia* REISS, 1957**

Type species: *Guembelina deflaensis* SIGAL, 1952

***Sigalia carpatica* SALAJ and SAMUEL, 1963**

Pl. 17, fig. 5

*Sigalia carpatica* LAMOLDA et al., 2007, p. 23, fig. 4 – P, S.

*Sigalia carpatica* EGGER et al., 2013, p. 108, fig. 12 – 1, 2.

*Sigalia carpatica* FALZONI et al., 2013, p. 17, fig. 2 – 2.

*Sigalia carpatica* LAMOLDA et al., 2014, fig. 11 – A, C.

**Diagnostic features:**

Biserial test, petaloid chambers, raised and beaded sutures, smooth wall texture in between sutures.

**Remarks:**

*Sigalia carpatica* is observed in the middle part of the measured section. It is differentiated from the sister species *S. deflansis* by having a smooth texture between its raised and beaded sutures.

**Stratigraphic distribution:**

From *Dicarinella concavata* (middle Coniacian) to *Dicarinella asymetrica* (early Santonian)

**Occurrence:**

NS-36

***Sigalia deflaensis* SIGAL, 1952**

Pl. 17, fig. 1-4

*Sigalia deflaensis* LAMOLDA *et al.*, 2007, p. 23, fig. 4 – Q, R.

*Sigalia deflaensis* EGGER *et al.*, 2013, p. 107, fig. 11 – 15; p. 108, fig. 12 – 15, 16.

**Diagnostic features:**

Biserial test, petaloid chambers, depressed sutures, costate wall texture.

**Remarks:**

*Sigalia deflaensis* occurs abundantly in the middle part of the measured section. This species differs from *V. eggeri* in its rounded shoulders on the last two chambers with raised sutures along the earlier chambers. Finally, it is differentiated from *S. carpatica* by having a costate wall texture.

**Stratigraphic distribution:**

From *Dicarinella concavata* (middle Coniacian) to *Dicarinella asymetrica* (late Santonian)

**Occurrence:**

NS-25 – NS-38

## CHAPTER 6

### 6. DISSCUSSIONS AND CONCLUSIONS

Near the Alagöz Village, Polatlı (Ankara, Turkey), a 93.5 m thick lower Upper Cretaceous stratigraphic section composed of limestones and shales was measured and 75 samples were collected. This section comprised Cenomanian of the Akkaya Formation, Turonian and Santonian of the Kocatepe Formation and Campanian of the Haymana Formation. The primary aim of this thesis study has been to establish a reliable biostratigraphic framework for this extensive interval in the Haymana-Polatlı Basin, which was not studied in detail previously in terms of biostratigraphy.

To this end, washed samples and thin sections of the samples were examined at first. As a result, 80 planktonic foraminifera species belonging to 23 different genera and 6 different families have been identified and their first and last occurrences have been established. These species were assigned to families *Globotruncanidae*, *Globigerinelloidae*, *Rugoglobigerinidae*, *Schakoinidae*, *Hedbergellidae* and *Heterohelix*; to genera *Helvetoglobotruncana*, *Rotalipora*, *Praeglobotruncana*, *Dicarinella*, *Costellagerina*, *Whiteinella*, *Macroglobigerinelloides*, *Muricohedbergella*, *Marginotruncana*, *Archaeoglobigerina*, *Schakoina*, *Contusotruncana*, *Globotruncana*, *Globotruncanita*, *Globotruncanella*, *Rugoglobigerina*, *Rugotruncana*, *Heterohelix*, *Laeviheterohelix*, *Pseudotextularia*, *Sigalia*, *Ventilabrella* and *Gansserina*. Accordingly, 9 biozones and 2 subzones have been defined in the Cenomanian, Turonian, Santonian and Campanian stages. These biozones are *Rotalipora cushmani* (Middle to Upper Cenomanian)-*Dicarinella algeriana* (Upper Cenomanian), *Whiteinella archaeocretacea* (Upper Cenomanian-Lower Turonian), *Helvetoglobotruncana helvetica* (Turonian),

*Dicarinella asymetrica* (Santonian) - *Globotruncanita elevata*- *Dicarinella asymetrica* (Middle to Upper Santonian), *Globotruncanita elevata* (Lower Campanian), *Globotruncana ventricosa* (Middle Campanian), *Globotruncanella* spp. (Upper Campanian), *Globotruncana aegyptiaca* (Upper Campanian) and *Gansserina gansseri* (Uppermost Campanian).

In the second phase of this study, a sedimentological investigation was conducted on the samples to gain insight on the depositional history of the measured section. Although this analysis cannot directly indicate any stage boundary, it was useful in determining especially the Cenomanian-Turonian transition with the occurrence of black shales at this level. This analysis yielded 8 microfacies types which namely were Planktonic Foraminiferal Packstone, Radiolarian Packstone, Packstone with Planktonic Foraminifera and Radiolaria, Radiolaria-bearing Spiculite Packstone, Planktonic Foraminiferal Wackestone, Wackestone with Planktonic Foraminifera and Radiolaria, Silty Wackestone-Mudstone with Planktonic Foraminifera and Wackestone-Mudstone. These microfacies types were described and interpreted across time; no significant change in the depositional environment was detected. It was hypothesized to change between toe-of-slope, deep shelf and deep basin on a rimmed carbonate platform model, whereas it ranged between mid-ramp, outer-ramp and basin on a homoclinal carbonate ramp model.

Combining the results of biostratigraphical and sedimentological analyses, two stage boundaries in the Upper Cretaceous were explicitly defined in this study. These are the Cenomanian-Turonian (C/T) boundary and the Santonian-Campanian (S/C) boundary.

The Cenomanian-Turonian boundary is placed at the lowest occurrence of the marker species *Helvetoglobotruncana helvetica*. There is no major lithology change at this proposed boundary; dark grey shale and clayey limestones below and light brown limestones above the boundary are found in the measured stratigraphic section. The characteristic fossil-barren black/dark grey shales at the Cenomanian-Turonian boundary corresponding to the Oceanic Anoxic Event 2 (OAE2) was also clearly observed in the results of both washed samples and thin section of the samples. In sample NS-13 on top

of which the C/T Boundary is delineated, the lithology is dark grey and contains only the opportunist species *Muricohedbergella delrioensis*, *Macrolobigerinelloides planispira*, *Macrolobigerinelloides sp.* and *Whiteinella baltica* and abundant radiolaria. First occurrence of *Helvetoglobotruncana helvetica* in sample NS-14 is a global proof for the already occurred onset of the stage Turonian.

Planktonic foraminiferal data regarding latest Turonian, Coniacian and earliest Santonian were not found in the measured stratigraphic section. This absence between early Turonian and early Santonian was observed to be coincident with a major lithological boundary between very hard greenish to grey limestones below and relatively softer red limestones and shales above. This finding has been found totally compatible with the Okay and Altiner's studies (2016, 2017) regarding the geology of the study area. These suggest that olistostromal units of pre-Santonian age in the Ankara region are unconformably overlain by red Middle to Upper Santonian pelagic limestones. In this sense, the results of this study also support the interpretation that the Jurassic-Cretaceous succession of the Sakarya Zone were transferred to debris flows in the Coniacian as the subduction was taking place in the Pontides and this episode of olistostrome formation and recycling occurring until the colliding end, was followed by normal forearc deposition back again in the Santonian.

A stratigraphic discontinuity has not been detected throughout the Santonian-Campanian succession which correspond to the thickest portion in the section. Therefore, the boundary between these two stages could be studied in the most detail. The main bioevents marking this boundary are the appearance of the planktonic foraminifera *Globotruncanita elevata*, the disappearance of the planktonic foraminifera *Dicarinella asymetrica* together with the genera *Dicarinella*, *Marginotruncana*, *Sigalia*, the species *Muricohedbergella flandrini* and/or presence of concurrent range zone of *G. elevata* and *D. asymetrica*, all of which were detected in this study (see Subsection 4.3 for details). The extinction of *Muricohedbergella flandrini* slightly after the proposed boundary (at NS-38) after its almost complete occurrence between NS-16 – NS-40, is thought to perhaps suggest a longer stratigraphic range for this species. Lithologically, the S/C boundary falls exactly

at the transition where the red Santonian limestones are followed by the light brown Campanian shales. The transition has been observed to be conformable.

The last boundary between Campanian-Maastrichtian was not clearly observed, however it has been envisaged to be close to the end of the measured stratigraphic section as signaled by the first occurrences of *Globotruncanita pettersi* (NS-64), *Globotruncanita angulata* (NS-68) and *Gansserina gansseri* (NS-75).



## REFERENCES

- Abawi, T., S., Mahmood, S., A., 2005. Biostratigraphy of the Kometan and Gulneri Formations (Upper Cretaceous) in Jambur Well No.46, Northern Iraq. *Iraqi Jour. Earth Sci.*, Vol. 5, No. 1, pp. 1-8
- Abdel Kireem, M., R., Schrank, E., Samir, A., M., Ibrahim, M., I., A., 1996. Palaeoecology, palaeogeography and palaeoclimatology of the northern Western Desert, Egypt. *Journal of African Earth Sciences* 22 (1), pp. 93-112
- Abramovich, S., Almogi-Labin, A., Benjamini, C., 1998. Decline of the Maastrichtian pelagic ecosystem based on planktic foraminifera assemblage change: implications for the terminal Cretaceous faunal crisis. *Geology*, 26, pp. 63-66
- Abramovich, S., Keller, G., 2002. High stress late Maastrichtian paleoenvironment: inference from planktonic foraminifera in Tunisia. *Palaeogeography, Palaeoclimatology, Palaeoecology*, vol. 178, pp. 145-164.
- Afridi, Z., B., 2014. Stratigraphical, Sedimentological, Geochemical and Cyclostratigraphical Analyses of Upper Cretaceous (Upper Santonian-Campanian) Pelagic Successions of Haymana and Mudurnu-Göynük Basins of the Sakarya Continent, Turkey. MSc thesis. METU, Department of Geological Engineering.
- Akyol, İ., H., 1944. Ölümünün Yıldönümü Münasebetiyle: Müderris Faik Sabri Duran ve Profesör Ernest Chaput, *Türk Coğrafya Dergisi*, Vol. V-VI, Ankara, pp. 143-152
- Almogi-Labin, A., Esht, Y., Flexer, A., Honigstein, A., Moshkovitz, S., Rosenfeld, A., 1991. Detailed biostratigraphy of the Santonian-Campanian boundary interval in Northern Israel. *Journal of Micropalaeontology* 10 (1), pp. 39-50
- Altner, D., 1991. Microfossil biostratigraphy (mainly foraminifers) of the Jurassic-Lower Cretaceous carbonate successions in north-western Anatolia (Turkey). *Geologica Romana*, 27, pp. 167-213.

Altiner, D., Koçyiğit, A., Farinacci, A., Nicosia, U., Conti, M., A., 1991. Jurassic–Lower Cretaceous stratigraphy and paleogeographic evolution of the southern part of north-western Anatolia. *Geologica Romana*, 28, pp. 13-80

Altiner, D., Özkan, S., 1991. Calpionellid zonation in Northwestern Anatolia (Turkey) and calibration of the stratigraphic ranges of some benthic foraminifera the Jurassic-Cretaceous boundary. *Geologica Romana*, 28, pp. 215-235.

Amirov, E., 2008. Planktonic foraminiferal biostratigraphy, sequence stratigraphy and foraminiferal response to sedimentary cyclicity in the Upper Cretaceous-Paleocene of the Haymana Basin (Central Anatolia, Turkey).

Ardestani, M. S., Vahidinia, M., Sadeghi, A., Arz, J. A., Dochev, D., 2012. Integrated biostratigraphy of the Upper Cretaceous Abderaz Formation of the East Kopet Dagħ Basin (NE Iran). *Geologica Balcanica* 40 (1–3), pp. 21–37.

Ardestani, M. S., Vahidinia, M., Sadeghi, A., 2013. Paleooceanography and Paleobiogeography Patterns of the Turonian-Campanian Foraminifers from the Abderaz Formation, North Eastern Iran. *Open Journal of Geology*, Vol. 3 No. 1, 2013, pp. 19-27.

Arenillas, I., Arz, J. A., Molina, E., Dupuis, C., 2000. The Cretaceous/Paleogene (K/P) boundary at Ain Settara, Tunisia: sudden catastrophic mass extinction in planktic foraminifera, *Journal of Foraminiferal Research*, 30, pp. 202-218

Arıkan, Y., 1975. Tuzgölü havzasının jeolojisi ve petrol imkanları. *MTA Bülteni*, 85, pp. 17-38.

Arz, J. A. and Molina, E., 2001. Planktic foraminiferal quantitative analysis across the Campanian/Maastrichtian Boundary at Tercis (Landes, France). *Developments in Palaeontology and Stratigraphy*, Vol. 19, pp. 338–348

- Aydemir, A., 2011. An integrated geophysical investigation of Haymana Basin and hydrocarbon prospective Kirkkavak Formation in central Anatolia, Turkey. *Petroleum Geoscience* (February 2011) 17 (1): 91-100
- Aydemir, A., Ateş, A., 2006. Structural interpretation of the Tuzgölü and Haymana basins, Central Anatolia, Turkey, using seismic, gravity and aeromagnetic data. *Earth Planets Space*, 58, 951-961
- Azadbakht, S., Majidifard, M., R., Mohtat, T., 2016. Biostratigraphy and lithostratigraphy Upper Cretaceous sediments (Ilam Formation) in southwest Iran. *JCRS S* (1), 2016: 128-134.
- Babazadeh, S., A., Robaszynski, F., Courme, M., D., 2007. New biostratigraphic data from Cretaceous planktic foraminifera in Sahlabad province, eastern Iran. *Geobios*, 40, pp. 445-454.
- Bak, K., 1995. Trace fossils and ichnofabrics in the Upper Cretaceous red deep-water marly deposits of the Pieniny Klippen Belt, Polish Carpathians. *Annales Societatis Geologorum Poloniae* 64, 81-97.
- Bak, K., 1998. Planktonic foraminiferal biostratigraphy, Upper Cretaceous red pelagic deposits, Pieniny Klippen Belt, Carpathians. *Studia Geologica Polonica* 111, pp. 7–92.
- Bak, K., 2000a. Biostratigraphy of deep-water agglutinated foraminifera in Scaglia Rossa-type deposits of the Pieniny Klippen Belt, Carpathians, Poland. In: Hart, M.B., Kaminski, M.A., Smart, C.W. (Eds.), *Proceedings of the Fifth International Workshop on Agglutinated Foraminifera*. Grzybowski Foundation, Special Publication 7, pp. 15–41.
- Bak, M., 2000b. Radiolaria from the upper Cenomanian–lower Turonian deposits of the Silesian Unit (Polish Flysch Carpathians). *Geologica Carpathica* 51, pp. 309-324.
- Barr, F., T., 1972. Cretaceous biostratigraphy and planktonic foraminifera of Libya. *Micropaleontology* 18, pp. 1–46

Beiranvand, B., Ghasemi-Nejad, E., 2013. High resolution planktonic foraminiferal biostratigraphy of the Gurpi Formation, K/Pg boundary of the Izeh Zone, SW Iran. *Rev. bras. paleontol.* 16(1), pp. 5-26

Bey, S., Kuss, J., Premoli-Silva, I., Negra, M. H., Gardin, S., 2012. Fault-controlled stratigraphy of the Late Cretaceous Abiod Formation at Ain Medheker (Northeast Tunisia). *Cretaceous Research* 34, pp. 10-25.

Bingöl, E., Akyürek, B., Korkmazer, B., 1975. Biga yarımadasının jeolojisi ve Karakaya Formasyonunun bazı özellikleri (The geology of the Biga Peninsula and some features of the Karakaya Formation). *Cumhuriyetin 50. Yılı Yerbilimleri Kongresi Tebliğleri, Maden Tetkik ve Arama Enstitüsü (MTA) Publications*, pp. 70–77 (in Turkish with English abstract)

Birkenmajer, K., 1977. Jurassic and Cretaceous lithostratigraphic units of the Pieniny Klippen Belt, Carpathians, Poland. *Studia Geologica Polonica* 45, pp. 1-159.

Bjerrum, C., J., 2006. Sea-level Change and Shelf-Ocean Exchange in Relation to Ocean Anoxic Events. Abstract from American Geophysical Union, Fall Meeting 2006, abstract #PP31D-07

Blumenthal, M., 1941a. Eskipazar Transversal Dağları Jeolojisi ve Maden Suyu Menbaları (Çankırı Vilayeti). (Geologie des montahnes de la transversale d'Eskipazar et al., leurs sources minerales) *MTA Mecmuası*, 3/24, pp. 320-352.

Blumenthal, M., 1941b. Eskipazar Transversal Dağları Jeolojisi ve Maden Suyu Menbaları II. Part (Çankırı Vilayeti). (Geologie des montahnes de la transversale d'Eskipazar et al., leurs sources minerales) *MTA Mecmuası*, 4/25, pp. 550-593.

Blumenthal, M., 1942. Ankara şimalbatısındaki Bağlum ve Yakacık dolayları jeolojisi. *MTA report archive no. 447*, Ankara.

BouDagher-Fadel, M. K., Banner, F. T., Whittaker, J. E., 1997. *The Early Evolutionary History of Planktonic Foraminifera*. Springer-Science+Business Media, B.V.

- BouDagher-Fadel, M. K., 2012. The biological and molecular characteristics of living planktonic foraminifera. *Developments in Palaeontology & Stratigraphy*, 22. 289 p.
- Bourdon, M., 1957. Utilisation de l'acide acétique dans la désagrégation des roches dures. *Revue de l'Institut Français du Pétrole*, 12, pp. 14-15
- Bourdon, M., 1962. Méthode de dégagement des microfossiles par acétylolyse à chaud. *Comptes Rendus sommaires de la Société Géologie France*. pp. 267–268.
- Brown J.S. 1943. Suggested use of the word microfossils. *Economic Geology*, 38, p. 325.
- Butt, A., 1981. Depositional environments of the Upper Cretaceous rocks in the northern part of the Eastern Alps. *Cushman Foundation for Foraminiferal Research, Special Publication 20*, pp. 1-81.
- Caron, M. 1985. Cretaceous planktic foraminifera. - [In:] Bolli, H.M; Saunders, J.B. & Perch-Nielsen, K. [eds.] *Plankton stratigraphy*: pp. 17–86, Cambridge (Cambridge University Press)
- Caron, M., Dall' Agnolo, S., Accarie, H., Barrera, E., Kauffman, E., G., Amedro, F., Robaszynski, F., 2006. High-resolution stratigraphy of the Cenomanian-Turonian boundary interval at Pueblo (USA) and Wadi Bahloul (Tunisia): stable isotope and bio-events correlation. *Geobios*, 39, pp. 171-200
- Carter, D. J., Hart, M. B., 1977. Aspects of mid-Cretaceous stratigraphical paleontology. *Bull. Br. Mus. nat. Hist (Geol.)* 29, pp.1-135.
- Cengiz Çinku, M., Hisarlı, Z., M., Yılmaz, Y., Ülker B., Kaya N., Öksüm, E., 2016. The tectonic history of the Niğde-Kırşehir Massif and the Taurides since the Late Mesozoic: Paleomagnetic evidence for two-phase orogenic curvature in Central Anatolia, vol. 35, pp. 772-811
- Cetean, C. G., Balç, R., Kaminski, M. A., Filipescu, S., 2011. Integrated biostratigraphy and palaeoenvironments of an upper Santonian e upper Campanian succession from the southern part of the Eastern Carpathians, Romania. *Cretaceous Research* 32, pp. 575-590.

Çetin, H., Demirel, İ. H., Gökçen, S. L., 1986. Haymana'nın (SW Ankara) doğusu ve batısındaki Üst Kretase-Alt Tersiyer istifinin sedimantolojik ve sedimanter petrolojik incelemesi. TJK Bülteni, 29/2, pp. 21-33.

Chacon, B., Martin-Chivelet, J., Grafe, K. U., 2004. Latest Santonian to latest Maastrichtian planktic foraminifera and biostratigraphy of the hemipelagic successions of the Prebetic Zone (Murcia and Alicante provinces, south-east Spain). *Cretaceous Research* 25, pp. 585-601.

Chaput, E., 1932. Observations géologiques en Asie Mineure: Le Crétacé supérieur dans l'Anatolie Centrale. C. R. A. S., 194, pp. 1960-1961.

Chaput, E., 1935a. L'Eocene du plateau de Galatie (Anatolie Centrale). C. R. A. S., 200, pp. 767-768.

Chaput, E., 1935b. Les plissements Tertiaire de l'Anatolie Centrale. C. R. A. S., 201, pp. 1404-1405.

Chaput, E., 1936. Voyages d'études géologiques et géomorphologiques en Turquie. Mém. Inst. Français D'Archéo. İstanbul, II, p. 312.

Chen X., Wang C., Li Xianghui and Hu Xiurnian, 2005, Characteristics and correlation of Upper Cretaceous oceanic red beds in Alps-Carpathian area. *Earth Science Frontiers*, 2005, 12 (2): pp. 61-68 (in Chinese with English abstract).

Chen X., Wang C., Kuhnt, W., Holbourn, A., Huang, Y., Ma, C., 2011. Lithofacies, microfacies and depositional environments of Upper Cretaceous Oceanic red beds (Chuangde Formation) in southern Tibet. Volume 235, Issues 1–2, 15 March 2011, Pages 100-110

Chungkham, P., Jafar, S. A., 1998. Late Cretaceous (Santonian - Maastrichtian) integrated Coccolith- Globotruncanid biostratigraphy of pelagic limestones from the accretionary prism of Manipur, northeastern India. *Micropaleontology*, vol. 44, no. 1, pp. 69-83.

Coccioni, R., 2005. Planktonic foraminifers across the Bonarelli Event (OAE2, latest Cenomanian): the Italian record. *Palaeogeography, Palaeoclimatology, Palaeoecology* 224, pp. 167-185.

Coccioni, R., Marsili, A., 2006. Cretaceous oceanic anoxic events and radially elongated chambered planktonic foraminifera: paleoecological and paleoceanographic implications. *Palaeogeography, Palaeoclimatology, Palaeoecology*, 235, pp. 66-92.

Coccioni, R., Premoli Silva, I., 2015. Revised Upper Albian–Maastrichtian planktonic foraminiferal biostratigraphy and magnetostratigraphy of the classical Tethyan Gubbio section (Italy). *Newsletters on Stratigraphy*, Vol. 48/1 (2015), 47–90.

Coccioni, R., Sabatino, N., Frontalini, F., Gardin, S., Sideri, M., Sprovieri, M., 2015.

The neglected history of Oceanic Anoxic Event 1b: insights and new data from the Poggio le Guaine section (Umbria – Marche Basin). *Stratigraphy* 11, pp. 245 –282.

Coccioni, R., Sideri, M., Frontalini, F., Montanari, A., 2016. The *Rotalipora cushmani* extinction at Gubbio (Italy): Planktonic foraminiferal testimonial of the onset of the Caribbean large igneous province emplacement? *The Geological Society of America Special Paper* 524.

Costa de Moura, J., De Maoraes Rios-Netto, A., Wanderley, M., D., Pereira De Sousa, F., 1999. Using acids to extract calcareous microfossils from carbonate rocks. *Micropaleontology*, 45, pp. 429-436

Coşkun, B., Özdemir, A., and Işık, V., 1990, HaymanaMandira-Dereköy arasındaki sahanin petrol imkanlari: *Turk. Assoc. Petrol. Geol. Bull.*, v. 2, p. 135-143.

Cuvillier, J., 1952. Le notion de microfacies et ses applications. *Microfacies of carbonate rocks: analysis, interpretation and application*, Springer-Verlag Berlin Heidelberg 803.

Dağer, Z., Öztümer, E., Sirel, E., Yazlak, Ö., (1963). Ankara civarında birkaç stratigrafik kesit. T.J.K. Bült., VIII, 1/2, pp. 84-95, Ankara

Darvishzad, B., Ghasemi-Nejad, E., Ghourchaei, S., Keller, G., 2007. Planktonic Foraminiferal Biostratigraphy and Faunal Turnover across the Cretaceous-Tertiary Boundary in Southwestern Iran. *Journal of Sciences, Islamic Republic of Iran* 18(2): 139-149.

Desmares, D., Grosheny, D., Beaudoin, B., Gardin, S., Gauthier-Lafaye, F., 2007. High resolution stratigraphic record constrained by volcanic ashes layers at the Cenomanian–Turonian boundary in the Western Interior Basin, USA. *Cretac. Res.* 28, 561-582

Dizer, A., Meriç, E., 1981. Kuzeybatı Anadolu'da Üst Kretase-Paleosen Biyostratigrafisi. *MTA Bülteni*, 95-96, 149-163.

Dimitrova, E., Valchev, B., 2007. Attempt for Upper Cretaceous planktic foraminiferal zonation of the Srednogoriã and Eastern Balkan Zones (Bulgaria). *Geologica Balcanica* 6, 1-2, pp. 55-63.

Dowsett, H., J., 1984, Documentation of the foraminiferal Santonian-Campanian boundary in the northeastern Gulf of Mexico: *Journal of Foraminiferal Research*, v. 14, no. 2, p. 129-133.

Dubicka, Z., Peryt, D., Szuskiewicz, M. 2014. Foraminiferal evidence for paleogeographic and paleoenvironmental changes across the Coniacian–Santonian boundary in western Ukraine. *Palaeogeography, Palaeoclimatology, Palaeoecology*, 401, 43-56.

Dubicka, Z., Machalski, M., 2016. Foraminiferal record in a condensed marine succession: a case study from the Albian and Cenomanian (mid-Cretaceous) of Annopol, Poland. *Geological Magazine*, Cambridge University Press.



- Dunham, R. J., 1962. Classification of carbonate rocks according to depositional texture. In: Ham, W. E. (ed.), Classification of carbonate rocks: American Association of Petroleum Geologists Memoir, p. 108-121.
- Egeran, N., Lahn, E., 1951. Kuzey ve Orta Anadolu'nun tektonik durumu hakkında not. MTA Bülteni, 41, pp. 23-28.
- Egger, H., Mohamed, O., Rögl, F., 2013. Austrian Journal of Earth Sciences. 2013, Vol. 106 Issue 2, p89-114. 26p.
- Elamri, Z., Zaghib-Turki, D., 2014. Santonian-Campanian biostratigraphy of the Kalaat Senan area (West-Central Tunisia). Turkish J Earth Sci (2014) 23: pp. 184-203.
- Erba, E., 2004. Calcerous nannofossils and Mesozoic oceanic anoxic events. Marine Micropaleontology 52, pp. 85-106.
- Erbacher, J., Thurow, J., 1996. Influence of oceanic anoxic events on the evolution of mid-Cretaceous radiolarian in the North-Atlantic and western Tethys. Marine Micropaleontology 30 pp. 139-158.
- Erbacher, J., Thurow, J., Littke, R., 1996. Evolution patterns of radiolaria and organic matter variations: A new approach to identify sea-level changes in mid-Cretaceous pelagic environments. Geology June 1996 v. 24 no. 6 pp. 499-502.
- Eren, M., Kadir, S., 1999. Colour origin of upper cretaceous pelagic red sediments within the Eastern Pontides, northeast Turkey. Int Journ Earth Sciences 88: pp. 593-595.
- Erk, A., S., 1966. Ankara yöresinin genç Paleozoyik stratigrafisi. TÜBİTAK. V. Bilimsel Kongresi Bülteni.
- Erk, A., S., 1967. Ankara yöresinin genç Paleozoyik stratigrafisi. TÜBİTAK. Araştırma Raporu.
- Erk, A.S., 1976, Ankara civarında genç Paleozoyik'in Kulm Fliş Formasyonu: Maden Tetkik ve Arama Enst. Derg, 88, pp. 73-93.

Erol, O., 1961. Ankara bölgesinin tektonik gelişmesi. Bull. Geol. Soc. of Turkey. VII/I, pp. 57-85.

Falzone, F., Petrizzo, M. R., MacLeod, K. G., Huber, B. T., 2013. Santonian–Campanian planktonic foraminifera from Tanzania, Shatsky Rise and Exmouth Plateau: Species depth ecology and paleoceanographic inferences. *Marine Micropaleontology* 103, pp. 15–29.

Falzone, F., Petrizzo, M.R., Huber, B.T., MacLeod, K.G., 2014, Insights into the meridional ornamentation of the planktonic foraminiferal genus *Rugoglobigerina* (Late Cretaceous) and implications for taxonomy: *Cretaceous Research*, v.47, p. 87–104, doi: 10.1016/j.cretres.2013.11.001.

Falzone, F., Petrizzo, M. R., Jenkyns, H. C., Gale, A. S., Tsikos, H., 2016. Planktonic foraminiferal biostratigraphy and assemblage composition across the Cenomanian/Turonian boundary interval at Clot Chevalier (Vocontian Basin, SE France). *Cretaceous Research* 59, pp. 69-97.

Farouk S., 2014. Maastrichtian carbon cycle changes and planktonic foraminiferal bioevents at Gebel Matulla, west-central Sinai, Egypt. *Cretaceous Research*, 50: 238–251.

Flügel, E. 2004. *Microfacies of Carbonate Rocks. Analysis, Interpretation and Application.* 976 pp.

Forquin, C., 1975, North-West Anatolia, Tectonic evolution of the south margin of the European continent during Tertiary time. *Bulletin of the Geological Society of France*, vol..17. p. 1058-1070. (In french).

Franke, W., Paul, J., 1980. Pelagic redbeds in the Devonian of Germany: deposition and diagenesis. *Sediment Geol* 25: pp. 231–256.

Fuchs, W., 1967. Über Ursprung und Phylogenie der Trias- "Globigerinen" und die Bedeutung dieses Formenkreises für das echte Plankton. Verhandlungen der Geologischen Bundesanstalt, 1967: pp.135-176.

Fuchs, W., 1971. Eine alpine Foraminiferenfauna des tieferen Mittel-Barremes aus den Drusbergschichten von Ranzenberg bei Hohenems in Vorarlberg. Abhandlungen der Geologischen Bundesanstalt, Wien.

Fuchs, W., 1973. Ein Beitrag zur Kenntnis der Jura- "Globigerinen" und verwandter Formen an Hand polnischer Materialien des Callovien und Oxfordien. Verhandlungen der Geologischen Bundesanstalt, 1973: pp. 445-487.

Fuchs, W., 1975. Zur Stammesgeschichte der Plankton-foraminiferen und verwandter Formen im Mesozoikum. Jahrbuch der Geologischen Bundesanstalt, 118: pp. 193-246.

Fuchs, W., 1977. A contribution to the phylogeny of the Mesozoic planktonic foraminifera. In Actes du VI<sup>e</sup> Colloque Africain de Micropaléontologie. Annales des Mines et de la Géologie, 28: pp. 71-74.

Gale A., S., Montgomery P., Kennedy W., J., Burnett J., A., McArthur J., M., 1995. Definition and global correlation of the Santonian-Campanian boundary. *Terra Nova* 7: 611–622.

Gale, A., S., Hancock, J., M., Kennedy W., J., Petrizzo, M., R., Lees, J., A., Walaszczyk, I., Wray, D., S., 2008. An integrated study (geochemistry, stable oxygen and carbon isotopes, nannofossils, planktonic foraminifera, inoceramid bivalves, ammonites and crinoids) of the Waxahachie Dam Spillway section, north Texas: a possible boundary stratotype for the base of the Campanian Stage. *Cretaceous Res* 29: 131–167

Gebhardt, H., Friedrich, O., Schenk, B., Fox, L., Hart, M., Wägrich, M., 2010. Paleooceanographic changes at the northern Tethyan margin during the Cenomanian-Turonian Oceanic Anoxic Event (OAE-2) *Marine Micropaleontology*. 2010; 77:25-45. doi: 10.1016/j.marmicro.2010.07.002

Gedik, A., Özbudak, N., İztan, H., Korkmaz, S., Ağırıdağ, D., S., 1981. Sinop Havzasının jeolojisi ve petrol olanakları ile ilgili ön sonuçlar. Türkiye Jeoloji Kurultayı, 35, Bil. Tek. Kurul. Bil. özetleri, pp. 35-36, Ankara.

Georgescu, M. D., 2005, On the systematics of rugoglobigerinids (planktonic Foraminifera, Late Cretaceous): *Studia Geologica Polonica*, v. 124, p. 87–97.

Georgescu, M., D., 2006. Santonian-Campanian planktonic foraminifera in the New Jersey coastal plain and their distribution related to the relative sea-level changes. *Canadian Journal of Earth Sciences*, 43, pp. 101-120.

Georgescu, M., D., Huber, B., T., 2007. Taxonomic revision of the late Campanian-Maastrichtian (Late Cretaceous) Planktonic Foraminiferal Genus *Rugotruncana* Brönnimann and Brown, 1956, and a new paleontological species concept for planktonic foraminifera. *Journal of Foraminiferal Research*, v. 37, no. 2, p. 150–159

Gökçen, S. L., 1976. Haymana güneyinin sedimentolojik incelemesi. I. Stratigrafik birimler ve tektonik. *Yerbilimleri*, 2, pp. 161-201.

Görür, N., Oktay, F. Y., Seymen, İ., and Şengör, A. M. C, 1984, Palaeotectonic evolution of the Tuzgölü basin complex, Central Turkey: Sedimentary record of a Neo-Tethyan closure, in Dixon, J. E., and Robertson, A. H. F., eds., *The geological evolution of the eastern Mediterranean*: *Geol. Soc. Lond. Spec. Publ. no. 17*, p. 467 – 482.

Görür, N., Tüysüz, O., Akyol, A., Sakınç, M., Yiğitbaş, E., Akkök, R., 1993. Cretaceous red pelagic carbonates of northern Turkey: their place in the opening history of Black Sea. *Eclogae Geologicae Helveticae* 36, pp. 819–838.

Görür, N., Tüysüz, O., Şengör, A. M. C., 1998. Tectonic Evolution of the Central Anatolian Basins, *International Geology Review*, 40:9, 831-850.

Green, O., R., 2001. *A Manual of Practical Laboratory and Field Techniques in Palaeobiology*. Kluwer Academic Publishers, Dordrecht

- Grigelis, A. A., 1958. *Globigerina oxfordia* sp.n. - an occurrence of *Globigerina* in the Upper Jurassic strata of Lithuania. . Nauchnye Doklady Vyssei Shkoly, Geologo-Geograficheskie Nauki Vol. 3 pp. 109-111.
- Gümbel, C.W., 1861. Geognostische Beschreibung des bayerischen Alpengebirges und seines Vorlandes. J. Perthes, Gotha. pp. 1-950.
- Hancock, J. M., 1976. The petrology of the Chalk. Proc. Geol. Ass. 86, pp. 499-535.
- Hancock, J. M., Kauffmann, E. G., 1979. The great transgressions of the Late Cretaceous. J. geol. Soc., Lond. 136, pp. 175-86.
- Hanna, C., D., Church, C., C., 1928. Freezing and thawing to disintegrate shales. Journal of Paleontology 2, p. 131
- Hart, M. B., Ball, K. C., 1986. Late Cretaceous anoxic events, sea-level changes and the evolution of the planktonic foraminifera. North Atlantic Palaeoceanography, Geological Society Special Publication No. 21, pp. 67-78.
- Hart, M., B., 1999. The evolution and biodiversity of Cretaceous planktonic foraminifera. Geobios, 32: 242–255. Hasegawa, T., 1999. Planktonic foraminifera and biochronology of the Cenomanian-Turonian (Cretaceous) sequence in the Oyubari area, Hokkaido, Japan. Paleontological Research Vol. 3 (1999) No. 3 P 173-192.
- Haq, B., Hardenbohl, J., and Vail, P. R., 1987, Chronology of fluctuating sea levels since the Triassic (250 million years ago to present). Science, v. 235, p. 1156–1167
- Herrig, E., 1966. Ostracoden aus der Weißen Schreiekreide (Unter-Maastricht) der Insel Rügen. Paläontologische Abhandlungen (A: Paläozoologie) 2, pp. 693-1024
- Hinte, J., E., Van, 1976. A Cretaceous time scale: American Association of Petroleum Geologists Bulletin, v. 60, p. 498-516.

Hoşgör, İ., Okan, Y., 2010. A New Species of Angariid Gastropod from the Early Thanetian of the Haymana-Polatlı Basin, Turkey. Turkish Journal of Earth Sciences (Turkish J. Earth Sci.), Vol. 20, 2011, pp. 243–253.

Honigstein, A., Almogi-Labin, A., Rosenfeld, A., 1987. Combined ostracod and planktonic foraminiferal biozonation of the Late Coniacian - Early Maastrichtian in Israel. J. micropalaeontol., 6 (2), pp. 41-60.

Hu, X., M., Jansa, L., Wang, C.S., Sarti, M., Bak, K., Wagneich, M., Michalik, J., Sotak, J., 2005. Upper Cretaceous oceanic red beds (CORBs) in the Tethys: occurrences, lithofacies, age, and environments. Cretaceous Research 26 (1), pp. 3-20.

Hu, X., Zhao, K., Yılmaz, İ., Ö., Li, Y., 2012. Stratigraphic transition and palaeoenvironmental changes from the Aptian oceanic anoxic event 1a (OAE1a) to the oceanic red bed 1 (ORB1) in the Yenicesihlar section, Central Turkey. Cretaceous Research, Vol. 38, pp. 40-51.

Huber, B., Petrizzo, M., R., 2014. Evolution and taxonomic study of the cretaceous planktic foraminiferal genus *Helvetoglobotruncana* reiss, 1957. The Journal of Foraminiferal Research 44 (1): pp. 40-57.

Huber, B., T., Petrizzo, M., R., Watkins, D., K., Haynes, S., J., MacLeod, K., G., 2017. Correlation of Turonian continental margin and deep-sea sequences in the subtropical Indian Ocean sediments by integrated planktonic foraminiferal and calcareous nannofossil Biostratigraphy. Newsletters on Stratigraphy, Vol. 50/2. pp. 141-185.

Hüseynov, A., 2007. Sedimentary cyclicity in the Upper Cretaceous successions of the Haymana Basin (Turkey): depositional sequences as response to relative sea-level changes. M.Sc. Thesis, Middle East Technical University, 120 p.

Islamoğlu, Y., Dominio, S., Kowalke, T., 2011. Early Eocene Caenogastropods (Mollusca, Gastropoda) from Haymana-Polatlı Basin, Central Anatolia (Turkey): taxonomy and palaeoecology. Geodiversitas 33 (2): pp. 303–330.

- Jaff, R. B. N., Wilkinson, I. P., Lee, S., Zalasiewicz, J., Lawa, F., Williams, M. 2015. Biostratigraphy and palaeoceanography of the early turonian–early Maastrichtian planktonic foraminifera of ne Iraq. *Journal of Micropalaeontology*, 34, 2015, 105–138
- Jansen, H., Kroon, D., 1987, Maastrichtian foraminifers from Site 605, Deep Sea Drilling Project Leg 93, Northwest Atlantic: in Van Hinte, J. E., Wise, S. W., Jr., et al., *Initial Reports DSDP*, v. 93, Washington, D. C. (U. S. Government Printing Office), p.555–575.
- Jackson, E.D., Schlanger, S.O., 1976. Regional Synthesis, Line Islands Chain, and Manihiki Plateau, Central Pacific Ocean, DSDP Leg 33. *Initial Reports of the Deep Sea Drilling Project*, v. 33, (U.S. Government Printing Office, Washington), pp. 915-927.
- Jarvis, I., Carson, G.A., Cooper, M.K.E., Hart, M.B., Leary, P.N., Tocher, B.A., Horne, D., Rosenfeld, A., 1988. Microfossil assemblages and the Cenomanian-Turonian (Late Cretaceous) oceanic anoxic event. *Cretaceous Research* 9, 3e103.
- Jarvis, I., Gale, A., S., Jenkyns H., Pearce, M., A., 2006. Secular variation in Late Cretaceous carbon isotopes: a new  $\delta^{13}\text{C}$  carbonate reference curve for the Cenomanian–Campanian (99.6–70.6 Ma). *Geol. Mag.*, 143, (5), pp. 561–608. doi:10.1017/S0016756806002421.
- Jenkyns, H.C., 1976. Sediments and sedimentary history of the Manihiki Plateau, South Pacific Ocean. *Initial Reports of the Deep Sea Drilling Project*, v. 33 (U.S. Government Printing Office, Washington), pp. 873-890.
- Jenkyns, H. C., 1980. Cretaceous anoxic events: From continents to oceans. *Journal of Geology Soc. London*, Vol. 137, 1980, pp. 171-188.
- Kalanat, B., Vahidinia, M., Vaziri-Moghaddam, H. et al. *Arab J Geosci* (2015) 8: 8373. doi: 10.1007/s12517-015-1779-6
- Kazancı, N. ve Gökten, E., 1988, Lithofacies features and tectonic environment of the continental Paleocene volcanoclastics in Ankara region: *METU Journal of Pure and applied Sciences*, 21,1-3, 271-282.

Keller, G. and Pardo, A., 2004. Biostratigraphy and Palaeoenvironments of the Cenomanian-Turonian stratotype section at Pueblo, Colorado. *Marine Micropaleontology* 51, pp. 95-128

Keller, G., Adatte, T., Berner, Z., Chellai, E.H., Stueben, D., 2008. Oceanic events and biotic effects of the Cenomanian-Turonian anoxic event, Tarfaya Basin, Morocco. *Cretaceous Research* 29, 976-994.

Ketin, I., 1969. Kuzey Anadolu Fayı Hakkında. *Bull. Miner. Res. Explor. Inst. Turk.* 76, 1-25.

Knitter, H., 1979. Eine verbesserte methode zur gewinnung von mikrofosilien aus harten, nicht schlammaren kalken. *Geol. Bl. Nor-Bayern*, 29, pp. 182-186

Koçyiğit, A., Özkan, S., Rojay, B., 1988. Examples of the forearc basin remnants at the active margin of northern Neo-Tethys: development and emplacement ages of the Anatolian Nappe, Turkey. *Middle East Technical University Journal of Pure and Applied Sciences*, 3, pp. 183-210.

Koçyiğit, A., 1991, An example of an accretionary forearc basin from Northern central Anatolia and its implications for the history of subduction of Neo-Tethys in Turkey: *Geol. Soc. of Amer. Bull.*, 103, 22-36.

Koçyiğit, A., Doğan, U., 2016. Strike-slip neotectonic regime and related structures in the Cappadocia region: a case study in the Salanda basin, Central Anatolia, Turkey. *Turkish Journal of Earth Sciences*, 25, pp. 393-417.

Kopaeovich, L., Vishnevskaya, V., 2016. Cenomanian–Campanian (Late Cretaceous) planktonic assemblages of the Crimea–Caucasus area: Palaeoceanography, palaeoclimate and sea level changes. *Palaeogeography, Palaeoclimatology, Palaeoecology* 441 (2016) 493–515.



Korbar, T., Montanari, A., Premec Fucek, V., Fucek, L., Coccioni, R., McDonald, Iain, Claeys, P., Schulz, T., Koeberl, C., 2015. Potential Cretaceous-Paleogene boundary tsunami deposit in the intra-Tethyan Adriatic carbonate platform section of Hvar (Croatia). *Geological Society of America Bulletin*, published online on 7 May 2015. doi:10.1130/B31084.1

Korkmaz, S., Gedik, A., Pelin, S., 1991. Türkiye'deki bazı tortul havzalara petrol potansiyeli açısından bir bakış. *Geological Engineering*, n. 39, pp. 5-14.

Lahn, E., 1949. Orta Anadolu'nun jeolojisi hakkında, *TJK Bülteni*, 1, 1.

Lamolda, M. A., Peryt, D., Ion, J., 2007. Planktonic foraminiferal bioevents in the Coniacian/Santonian boundary interval at Olazagutia, Navarra province, Spain. *Cretaceous Research* 28, pp. 18-29.

Lamolda M.A., Paul C.R.C., Peryt D., Pons J.M., 2014. The global boundary stratotype and section point (GSSP) for the base of the Santonian stage, 'Cantera de Margas', Olazagutia, northern Spain. *Episodes*, 37: 2 13.

Leckie, M., R., Bralower, T., J., Cashman, R., 2002. Oceanic anoxic events and plankton evolution: Biotic response to tectonic forcing during the Mid-Cretaceous. *Paleoceanography*, Vol. 17, No. 3, 10.1029/2001PA000623.

Lefebvre, C., Meijers, M., J., M., Kaymakçı, N., Peynircioğlu, A., Langereis, C., G., van Hinsbergen, D., J., J., 2013. Reconstructing the geometry of central Anatolia during the late Cretaceous: Large-scale Cenozoic rotations and deformation between the Pontides and Taurides. *Earth and Planetary Science Letters*, 366, pp. 83-98.

Lenniger, M., Pedersen, G. K., & Bjerrum, C. J., 2011. OAE2 in marine sections at high northern palaeolatitudes. Abstract from 21th Annual V.M. Goldschmidt Conference, Prague, Czech Republic.

Li, L., Keller, G., 1998. Maastrichtian climate, productivity and faunal turnovers in planktic foraminifera in South Atlantic DSDP Sites 525A and 21. *Marine Micropaleontology*, 33, 55-86.

Li L, Keller G, Stinnesbeck W., 1999. The Late Campanian and Maastrichtian in northwestern Tunisia: palaeoenvironmental inferences from lithology, macrofauna and benthic foraminifera. *Cretaceous Res* 20: 231-252.

Li, G., Wan, W., Jiang, G., Hu, X., Goudemand, N, Han, H., Chen, X., 2007. Late Cretaceous Foraminifera Faunas from the Saiqu “melange” in Southern Tibet. Vol. 81 NO. 6 pp. 917-924.

Loeblich Jr., A., R., Tappan, H., 1988. *Foraminiferal Genera and their Classification* [volume 1]. Van Nostrand Reinhold Company, New York, I, 1-970.

Lokman, K., Lahn, D., 1946. Haymana bölgesi jeolojisi. *MTA Bülteni*, 36, pp. 292-300.

Longoria, J., F., Vonfeldt, A. E., 1991. Taxonomy, phylogenetics and biochronology of single-keeled globotruncanids (genus *Globotruncanita* Reiss): *Micropaleontology*, v. 37, p. 197–243.

Masters, B., A., 1970. Stratigraphy and planktonic foraminifera of the Upper Cretaceous Selma Group, Alabama: Ph.D. dissertation, University of Illinois (Urbana-Champaign), 372 pp.

Masters, B., A., 1977. Mesozoic planktonic foraminifera, in Ramsay, A. T. S. ed., *Oceanic micropaleontology*, I: London, Academic Press, pp. 301-731.

Mathisen, M. E., and McPherson, J. G., 1991, Volcaniclastic deposits: Implications for hydrocarbon exploration: *Soc. Sediment. Geol. Spec. Publi.* v. 45, p. 27-36.

Meriç, E., Görür, N., 1981. Haymana-Polatlı havzasındaki Çaldağ kireçtaşının kireçtaşının yaş konağı. *MTA Bülteni*, 93/94, pp. 137-142.

Miller, K., G., Kominz, M., A., Browning, J., V., Wright, J., D., Mountain, G., S., Katz, M., E., Sugarman, P., J., Ramer, B., S., Christie-Blick, N., Andpekar, S., F., 2005. The Phanerozoic record of global sea-level change: *Science*, v. 310, pp. 1293–1298

Moberly, R., Larson, L., R., 1975. Mesozoic Magnetic Anomalies, Oceanic Plateaus, and Seamount Chains in the Northern Pacific Ocean. Hawaii Institute of Geophysics Contribution No. 676.

Nairn, S. P., Robertson, A. H. F., Ünlügenç, U., C., Taşlı, K., İnan, N., 2013. Tectonostratigraphic evolution of the Upper Cretaceous–Cenozoic central Anatolian basins: an integrated study of diachronous ocean basin closure and continental collision. *Geological Society London Special Publications* 372 (1): pp. 343-384.

Nederbragt, A., J., 1991. Late Cretaceous biostratigraphy and development of Heterohelicidae (planktic foraminifera). *Micropaleontology*, 37 (1991), pp. 329–372.

Nishi, H., Reishi, T., Hatsugai, T., Saito, T., Moriya, K., Ennyu, A., Sakai, T., 2003. Planktonic foraminiferal zonation in the Cretaceous Yezo Group, Central Hokkaido, Japan. *Journal of Asian Earth Sciences* 21, 867–886.

Norman, T., Rad, M. R., 1971. Çayraz (Haymana) civarının Horhor (Eosen) formasyonunda alttan üste doğru doku parametrelerinde ve ağır mineral bolluk derecelerinde değişimler. *TJK Bülteni*, 14/2, pp. 205-225.

Obaidalla, N., A., 2005. Complete Cretaceous/Paleogene (K/P) boundary section at Wadi Nukhul, southwestern Sinai, Egypt: inference from planktonic foraminiferal biostratigraphy. *Rev. Paleobiologic*, Geneve 24, 1, pp. 201-224.

Ocakoğlu, F., Çiner, A., 1995. Sedimentary evolution of the Orhaniye-Güvenç (NW Ankara) continental deposits during Paleocene-Early Eocene. *Türkiye Jeoloji Bülteni*, 38/2, pp. 41-53.

Ogg, J.G., Hinnov, L.A., 2012. The Cretaceous Period. In: Gradstein et al., *The Geologic Time Scale 2012*. Elsevier Publ. Co.

Okano, K., Sawada, K., Takashima, R., Nishi, H., Hisateke, O. Depositional Environments Revealed From Biomarkers in Sediments Deposited During the Mid-Cretaceous Oceanic Anoxic Events (OAEs) in the Vocontian Basin (SE France).

Okay, A.I., 2008; Geology of Turkey: A synopsis. *Anschnitt*, 21, 19-42.

Okay, A., Altıner, D., 2016. Carbonate sedimentation in an extensional active margin: Cretaceous history of the Haymana region, Pontides. *Int J Earth Sci (Geol Rundsch)* (2016). doi:10.1007/s00531-016-1313-4.

Okay, A., Altıner, D., 2017. Alacaatlı Olistostromları: Ankara’da Alcı ve Bağlum Bölgelerinin Jeolojisi (Alacaatlı Olistostromes: The Geology of Alcı and Bağlum Regions in Ankara). *Field Guide Book*.

Okay, A., I., 1989. Geology of the Menderes Massif and the Lycian Nappes south of Denizli, Western Taurides. *Bulletin of the Mineral Research and Exploration*, 109, 37-51.

Okay, A., I., Satır, M., Maluski, H., Siyako, M., Monie, P., Metzger, R., Akyüz, S., 1996. Paleo- and NeoTethyan events in northwest Turkey: geological and geochronological constraints. *Tectonics of Asia* (eds A. Yin and M. Harrison), pp. 420–41.

Okay, A.I., Siyako, M. & Bürkan, K.A., 1991, Geology and tectonic evolution of the Biga Peninsula. *Special Issue on Tectonics* (ed. J.F. Dewey), *Bulletin of the Technical University of Istanbul*, 44, 191-255.

Okay, A.I., Şengör, A.M.C. & Görür, N., 1994, Kinematic history of the opening of the Black Sea and its effect on the surrounding regions. *Geology*, 22, 267-270 .

Okay, A., I., Tüysüz, O., 1999. Tethyan sutures of northern Turkey. *Geological Society, London, Special Publications*, v. 156, pp. 475-515.

Orabi, O., Zahran, E., 2013. Paleotemperatures and paleodepths of the Upper Cretaceous rocks in El Qusaima, Northeastern Sinai, Egypt. *Journal of African Earth Sciences* 91. DOI: 10.1016/j.jafrearsci.2013.11.014.

Owens, J., D., Lyons, T., W., Hardisty, D., S., Lowery, C., M., Lu, Z., Lee, B., Jenkyns, H., C., 2017. Patterns of local and global redox variability during the Cenomanian–Turonian Boundary Event (Oceanic Anoxic Event 2) recorded in carbonates and shales from central Italy. *Sedimentology* 64 (1), pp. 168–185.

Özcan, E., 2002. Cuisian orthophragminid assemblages (*Discocyclina*, *Orbitoclypeus* and *Nemkovella*) from the Haymana-Polatlı Basin (Central Turkey): biometry and description of two new taxa. *Eclogae geol. Helv.*, 95, 75-97. Hokkaido University Collection of Scholarly and Academic Papers.

Özcan, E., Özkan-Altınır, S., 1997. Late Campanian-Maastrichtian evolution of orbitoid foraminifera in Haymana basin succession (Ankara, Central Turkey). *Revue de Paléobiologie*, 16/1, pp. 271-290.

Özcan, E., Özkan-Altınır, S. 1999. The genera *Lepidorbitoides* and *Orbitoides*: Evolution and stratigraphic significance in some Anatolian basins (Turkey). *Geological Journal*, 34/3, pp. 275-286.

Özcan, E., Özkan-Altınır, S., 2001. Description of an early ontogenetic evolutionary step in *Lepidorbitoides*: *Lepidorbitoides bisambergensis asymmetrica* subsp. n., Early Maastrichtian (Central Turkey). *Rivista Italiana di Paleontologia e Stratigrafia*, 107, pp. 137-144.

Özcan, E., Sirel, E., Özkan-Altınır, S., Çolakoğlu, S., 2001. Late Paleocene Orthophragminae (foraminifera) from the Haymana-Polatlı Basin, Central Turkey) and description of a new taxon, *Orbitoclypeus haymanaensis*. *Micropaleontology*, 47/4, pp. 339-357.

Özkan, S., Altınır, D., 1987. Maastrichtian planktonic foraminifera from the Germav Formation in Gercüş area (SE Anatolia, Turkey), with notes on the suprageneric classification of globotruncanids. *Revue de Paléobiologie*, 6/2, 261 – 277.

Özkan-Altıner, S., Özcan, E., 1997. Microfacies variations around Cretaceous-Tertiary boundary: an integrated zonation of calcareous nannofossil, planktonic foraminifera and benthonic foraminifera, Project no. TÜBİTAK-YDABÇAG-69.

Özkan-Altıner, S., Özcan, E., 1999. Upper Cretaceous planktonic foraminiferal biostratigraphy from NW Turkey: calibration of the stratigraphic ranges of larger benthonic foraminifera. *Geological Journal*, 34/3, pp. 287-301.

Özkaptan, M., Gulyuz, E., Kaymakci, N., Langereis, C. G., Ozacar, A. A., Lefebvre, C. 2014. Large Vertical Axis Rotations along Neotethyan Sutures in TURKEY. American Geophysical Union, Fall Meeting 2014, abstract #GP43A-3632.

Petrizzo, M., R., 2000. Upper Turonian–lower Campanian planktonic foraminifera from southern mid–high latitudes (Exmouth Plateau, NW Australia): biostratigraphy and taxonomic notes. *Cretaceous Research* (2000) 21, 479–505.

Petrizzo, M. R., 2001. Late Cretaceous planktonic foraminifera from Kerguelen Plateau (ODP Leg 183): new data to improve the Southern Ocean biozonation. *Cretaceous Research* (2001) 22, pp. 829-855.

Petrizzo, M. R., 2002. Palaeoceanographic and palaeoclimatic inferences from Late Cretaceous planktonic foraminiferal assemblages from the Exmouth Plateau (ODP Sites 762 and 763, eastern Indian Ocean). *Marine Micropaleontology* 45, pp. 117-150.

Petrizzo, M., R., 2003. Late Cretaceous Planktonic Foraminiferal Bioevents in the Tethys and in the Southern Ocean Record: An Overview. *Journal of Foraminiferal Research*, v. 33, no. 4, pp. 330-337.

Petrizzo, M., R., 2008. The impact of climate instability on marine ecosystems: planktonic foraminiferal biological response to the latest Albian Oceanic Anoxic Event 1d and to the Paleocene-Eocene Thermal Maximum. *Geophysical Research Abstracts*, Vol. 10, EGU2008-A-06859.

- Petrizzo, M.R., Falzoni, F., Premoli Silva, I., 2011. Identification of the base of the lower-to-middle Campanian *Globotruncana ventricosa* Zone: comments on reliability and global correlations. *Cretaceous Research* 32, 387-405
- Pourteau, A., Oberhänsli, R., Candan, O., Barrier, E., Vrielynck, B., 2016. Neotethyan closure history of western Anatolia: a geodynamic discussion. *Int. J. Earth Sci.* 105, pp. 203-224.
- Premoli Silva, I. and Bolli, H.M., 1973. Late Cretaceous to Eocene Planktonic Foraminifera and Stratigraphy of Leg 15 Sites in the Caribbean Sea. *Deep Sea Drilling Project Reports and Publication*, 15, pp. 499-547.
- Premoli Silva, I., 1977. Upper Cretaceous–Paleocene magnetic stratigraphy at Gubbio, Italy, II. Biostratigraphy. *Geological Society of America, Bulletin* 88, pp. 371–374.
- Premoli-Silva, I. and Sliter, W.V. (1994) Cretaceous planktonic foraminiferal biostratigraphy and evolutionary trends from the Bottaccione section. *Paleontographia Italica*, Gubbio.
- Premoli Silva, I., Erba, E., Salvin, G., Locatelli, C., Verga, D., 1999. Biotic changes in Cretaceous Oceanic Anoxic Events of the Tethys. *Journal of Foraminiferal Research*, v. 29, no. 4, pp. 352–370.
- Premoli Silva, I., Sliter, W. V., 1999. Cretaceous paleoceanography: Evidence from planktonic foraminiferal evolution, in Barrera, E., and Johnson, C. C., eds., *Evolution of the Cretaceous Ocean-Climate System: Boulder, Colorado*, Geological Society of America Special Paper 332.
- Premoli-Silva, I., Verga, D., 2004. Practical manual of Cretaceous Planktonic Foraminifera. *International School on Planktonic Foraminifera*, 3. Course: Cretaceous. Verga & Rettori eds. Universities of Perugia and Milan, Tipografia Pontefelcino, Perugia (Italy), 283 p.

Pojeta Jr., J., Balanc, M., 1989. Freezing and thawing of fossils, 223–226. In: Feldmann, R.M., Chapman, R.E., Hannibal, J.T. (Eds.), *Paleotechniques: The Paleontological Society, Special Publication*, 4, pp. 1-358.

Pourteau, A., Candan, O., Oberhänsli, R., 2010. High pressure metasediments in central Turkey: Constraints on the Neotethyan closure history. *Tectonics* 29, TC5004.

Reckamp, J., U., Özbey, S., 1960. Petroleum geology of Temelli and Kuştepe structures, Polatlı area. *Pet. İş. Gen. Md.*, Ankara.

Rad, M. R., 1971. Vertical variations in textural parameters and heavy mineral abundance of Harhor formation (Eocene) in the Çayraz (Haymana) area. MSc thesis. METU, Department of Geological Engineering.

Rawand, B., N., J., Wilkinson, I., P., Lee, S., Zalasiewicz, J., Lawa, F., Williams, M., 2015. Biostratigraphy and palaeoceanography of the early Turonian–early Maastrichtian planktonic foraminifera of NE Iraq. *Journal of Micropalaeontology*, 34, pp. 105-138.

Reolid, M., Sanches-Quinonez, C. A., Alegret, L., Molina, E., 2016. The biotic crisis across the Oceanic Anoxic Event 2: Palaeoenvironmental inferences based on foraminifera and geochemical proxies from the South Iberian Palaeomargin. *Cretaceous Research* 60, pp. 1-27.

Remin, Z., Dubicka, Z., Kozłowska, A., Kuchta, B., 2011. A new method of rock disintegration and foraminiferal extraction with the use of liquid nitrogen [LN<sub>2</sub>]. Do conventional methods lead to biased paleoecological and paleoenvironmental interpretations? *Marine Micropaleontology*, 86-87, pp. 11-14

Ricou, L., E., 1994. Tethys reconstructed: plates, continental fragments and their boundaries since 260 Ma from Central America to South-Eastern Asia. *Geodin. Acta* 7, pp. 169-218.



Robaszynski, F., Caron, M., 1979. Atlas of MidCretaceous planktonic foraminifera (Boreal Sea and Tethys). Cah. Micropal. CNRS, part 1, 1-185; part 2, pp. 1-181.

Robaszynski, F., Caron, M. (Coord.), and the European Working Group on Planktonic Foraminifera, 1979. Atlas de Foraminifères Planctoniques du Crétacé Moyen (Vols. 1 and 2). Cah. Micropaleontol.

Robaszynski, F., Mzoughi, M., 2010. The Abiod Formation at Ellès (Tunisia): tripartite lithology, biohorizons based on globotruncanids and ammonites, duration, location of Campanian-Maastrichtian boundary, correlation with Kalaat Senan and the Tercis (France) stratotype. Notebooks on Geology CG2010–A04.

Robaszynski, F., Caron, M. 1995. Foraminifères planctoniques du Crétacé : commentaire de la zonation Europe-Méditerranée. Bulletin de la Société Géologique de France 6, 681–692.

Robaszynski, F., 1998. Cretaceous planktonic foraminiferal biozonation in Exxon chart 2000.

Robaszynski, F., Caron, M., Gonzalez Donoso, J.M., Wonders, A.A.H., 1984. Atlas of Late Cretaceous Globotruncanids. Rev. Micropalont. 26, pp. 145-305.

Robaszynski F, Gonzalez Donoso JM, Linares D, Amedro F, Caron M, Dupuis C, Dhondt AV, Gartner S (2000). Le Crétacé Supérieur de la région de Kalaat Senan, Tunisie centrale. Lithobiostratigraphie intégrée zones d'ammonites, de Foraminifères planctonique et de nannofossiles du Turonien supérieur au Maastrichtien. B Cent Rech Expl 22: 359–490 (in French).

Robertson, A.H.F., Ünlügenç, U.C., İnan, N., Taslı, K. 2004. The Misis–Andırın complex: a Mid-Tertiary melange related to late-stage subduction of the Southern Neotethys in S Turkey. Journal of Asian Earth Sciences 22, 413–453.

Rojay, B., Süzen, L., 1997. Tectonostratigraphic evolution of the Cretaceous dynamic basins on accretionary ophiolitic melange prism, SW of Ankara region. TPJD Bülteni, 9/1, pp. 1-12.

Rojay, B., Altiner, D., 1998. Middle Jurassic–Lower Cretaceous biostratigraphy in the Central Pontides (Turkey): remarks on the paleogeography and tectonic evolution. *Rivista Italiana di Paleontologia e Stratigrafia* 104 (2), 167–180.

Rojay, B., Yalınız, K., Altiner, D., 2001. Age and origin of some pillow basalts from Ankara mélangé and their tectonic implications to the evolution of northern branch of Neotethys, Central Anatolia. *Turkish Journal of Earth Sciences*, 10, pp. 93-102.

Salaj, J. 1980. *Microbiostratigraphie du Crétacé et du Paléogène de la Tunisie Septentrionale et Orientale (Hypostratotypes Tunisiens)*. Institut Géologique de Dionýz Stúr, Bratislava, 238pp.

Salaj, J. 1997. Microbiostratigraphical (Foraminifera) division of the Turonian to Santonian in Tunisia (El Kef and Dj. Fguira Salah Area). *Geologica Carpathica*, 48: 171–178.

Sari, B. 2006. Upper Cretaceous planktonic foraminiferal biostratigraphy of the Bey Dağları autochthon in the Korkuteli area, western Taurides, Turkey. *Journal of Foraminiferal Research*, v. 36, no. 3, p. 241-261.

Sarı, B., 2009. Planktonic foraminiferal biostratigraphy of the Coniacian-Maastrichtian sequences of the Bey Dağları Autochthon, western Taurides, Turkey: thin-section zonation. *Cretaceous Research* 30, pp. 1103–1132.

Sarı, B., Yıldız, A., Korkmaz, T., Petrizzo, M., R., 2016. Planktonic foraminifera and calcareous nannofossils record in the upper Campanian-Maastrichtian pelagic deposits of the Malatya Basin in the Hekimhan area (NW Malatya, eastern Anatolia). *Cretaceous Research* 61, 91-107.

- Schlanger, S. O., Jenkyns, H. C., 1976. Cretaceous Oceanic Anoxic Events: Causes and Consequences. *Geologie en Mijnbouw*. Volume 55 (3-4), pp. 179-184.
- Schmid, F., 1974. Die präparativen Voraussetzungen für paläontologische Arbeiten an Fossilien aus der Schreibkreide. *Der Präparator* 20, pp. 9-22
- Schmidt, G., C., 1960. AR/MEM/365-266-367 sahalarının nihai terk raporu. *Pet. İş. Gen. Md.*, Ankara.
- Sigal, J. 1977. Essai de zonation du Cretace mediterraneen alaide des foraminiferes planctoniques. *Geologie Mediterraneenne* 4, 99–108.
- Sirel, E., 1975. Polatlı (GB Ankara) güneyinin stratigrafisi. *TJK Bülteni*, 18/2, pp. 181-192.
- Sirel, E., 1976. Description of six new species of the Alveolina found in the South of Polatlı (SW Ankara) region. *TJK Bülteni*, 19, pp. 19-22.
- Skelton, P., 2003. Fluctuating sea-level. In: Skelton, P. (ed.). *The Cretaceous World*. The Open University and Cambridge University Press. Milton Keynes and Cambridge, pp. 67-83.
- Sliter, W.V., 1989. Biostratigraphic zonation for Cretaceous planktonic foraminifers examined in thin section. *Journal of Foraminiferal Research* 19, 1-19.
- Stampfli, G., M., 1996. The Intra-Alpine terrain: A Paleotethyan remnant in the Alpine Variscides. *Eclogae geol. Helv.* 89 (1), pp. 13-42.
- Stampfli, G.M. 2000. Tethyan oceans. In: E. Bozkurt, J.A. Winchester and J.D.A. Piper (Eds.), *Tectonics and magmatism in Turkey and surrounding area*. Geological Society of London, Special Publication 173, pp. 163-185.
- Stampfli, G. M., Borel, G. D., 2002, A plate tectonic model for the Paleozoic and Mesozoic constrained by dynamic plate boundaries and restored synthetic oceanic isochrons: *Earth and Planetary Science Letters*, v. 196, pp. 17–33.

Stur, D., 1860. Bericht über die geologische Übersicht - Aufnahme d. Wassergebietes der Waag und Meutra. Jahrbuch der Geologischen Reichsanstalt, 11: pp. 17-149.

Sohn, I., G., 1961. Techniques for preparation and study of fossil ostracods. Q-64-Q70. In Moore, R., C. (ed.). Treatise of invertebrate paleontology. Part Q, Arthropoda 3. Geological Society of America, Boulder, and University of Kansas Press, Lawrence, 442 p.

Surlyk, F., 1972. Morphological adaptations and population structures of the Danish chalk brachiopods (Maastrichtian, Upper Cretaceous). Det Kongelige Danske Videnskabernes Selskab, Biologiske Skrifter 19, pp. 1-57

Şenalp, M., Gökçen, S. L., 1978. Sedimentological studies of the oil-saturated sandstones of the Haymana Region (SW Ankara). TJK Bülteni, 21/1, pp. 87- 94.

Şengör, A.M.C., Yılmaz, Y., 1981. Tethyan evolution of Turkey : A plate tectonic approach : Tectonophysics, 75, pp. 181 - 241.

Şengör, A., M., C., 1987. Cross faults and differential stretching in their hanging walls in regions of low- angle normal faulting: examples from western Turkey. In Continental extensional tectonics, Geological Society of London, Special Publication, 28, pp. 575–589.

Şengör, A. M. C., 1984. The Cimmeride orogenic system and the tectonics of Eurasia, Geol. Soc. America Spec. Paper 195.

Şengör, A.M.C., Yılmaz, Y., Ketin, I., 1982 Remnants of a pre-late Jurassic ocean in northern Turkey Fragments of Permian - Triassic Paleo - Tethys? Reply : Geol. Soc. America Bull., 93, pp. 932 - 936.

Takashima, R., Nishi, H., Yamanaka, T., Hayashi, K., Waseda, A., Obuse, A., Tomosugi, T., Deguchi, N., Mochizuki, S., 2010. High-resolution terrestrial carbon isotope and planktic foraminiferal records of the Upper Cenomanian to the Lower Campanian in the Northwest Pacific. Earth and Planetary Science Letters, Vol. 289, Issues 3-4, pp. 570-582.

- Thurrow, J., Brumsack, H. J., Rullkötter, J., and Meyers, P., 1992. The Cenomanian/Turonian Boundary Event in the Indian Ocean - A key to understand the global picture: *Geophysical Monograph*, v. 70, pp. 253–273.
- Toker, V., 1975. Haymana yöresinin (SW Ankara) planktonik foraminifera ve nannoplanktonlarla biyostratigrafik incelenmesi. PhD. Thesis, Ankara Üniversitesi Fen Fakültesi, pp. 1-57.
- Toker, V., 1977. Haymana ve Kavak formasyonlarındaki planktonik foraminifera ve nannoplanktonlar. TBTA VI. Bilim Kongresi, pp. 57-70.
- Toker, V., 1979. Haymana yöresi (GB Ankara) Üst Kretase planktonik foraminiferaları ve biyostratigrafi incelemesi. *TJK Bülteni*, 22, pp. 121-132.
- Toker, V., 1980. Haymana yöresi (GB Ankara) nannoplankton biyostratigrafisi. *TJK Bülteni*, 23/2, pp. 165-178.
- Toker, V., 1981. Haymana yöresi (GB Ankara) Tersiyer oluşuklarının planktonik foraminiferlerle biyostratigrafik incelemesi. *KTÜ Yer Bilimleri Dergisi*, Jeoloji 1, 2, pp. 115-126.
- Tüysüz, O., Melinte-Dobrinescu, M., C., Yılmaz, İ., Ö., Kırıcı, S., Svabenicka, L., Skupien, P., 2016. The Kapanboğazı formation: A key unit for understanding Late Cretaceous evolution of the Pontides, N Turkey. *Palaeogeography, Palaeoclimatology, Palaeocology*, pp. 17.
- Ünalın, G., Yüksel, V., Tekeli, T., Gönenc, O., Seyirt, Z., Hüseyin, S., 1976. Haymana-Polatlı yöresinin (Güneybatı Ankara) Üst Kretase-Alt Tersiyer stratigrafisi ve paleocoğrafik evrimi. *TJK Bülteni*, 19, pp. 159-176.

Van Hinsbergen, D. J. J., Maffione, M., Plunder, A., Kaymakçı, N., Ganerod, M., Hendriks, B., W., H., Corfu, F., Gürer, D., de Gelder, G., I., N., O., Peters, K., McPhee, P., J., Brouwer, F., M., Advokaat, E., L., Vissers, R., L., M., 2016. Tectonic evolution and paleogeography of the Kırşehir Block and the Central Anatolian Ophiolites, *Tectonics*, 35, pp. 983–1014, doi:10.1002/2015TC004018.

Vahidinia, M., Youssef, M., Ardestani, M., S., Sadeghi, A., Dochev, D., 2013. Integrated biostratigraphy and stage boundaries of the Abderaz Formation, east of the Kopeh-Dagh sedimentary basin, NE Iran. *Journal of African Earth Sciences* 90 · January 2013

Vahidinia, M., Youssef, M., Ardestani, M.S., Sadeghi, A. & Dochev, D. 2014. Integrated biostratigraphy and stage boundaries of the Abderaz Formation, east of the KopehDagh sedimentary basin, NE Iran. *Journal of African Earth Sciences*, 90, 87-104.

Van Houten, F., B., (1973). Origin of red beds: a review 1961–1972. *Annu Rev Earth Planet Sci* 1:39–61

Vaptzarova, Y. 1976. Zonation du Crétacésupérieur du typeCarpatique en Bulgarie du Nord-Ouest d'après les Fora-minifères planctoniques. –*Geologica Balc.*, 6, 3, 93-109.

Wang, C., Hu, X., Huang, Y., Wagreich, M., Scott, R., Hay, W., 2011. Cretaceous oceanic red beds as possible consequence of oceanic anoxic events. *Sedimentary Geology*, 235, pp. 27-37.

Wagreich, M., 1992. Correlation of Late Cretaceous calcareous nannofossil zones with ammonite zones and planktonic foraminifera: the Austrian Gosau sections. *Cretaceous Research.*, 13, pp.505-516.

Wagreich, M., Neuhuber, S., 2005. Stratigraphy and geochemistry of an Early Campanian deepening succession (Bibereck Formation, Gosau Group, Austria). - *Earth Science Frontiers*, 12, 123-131, Beijing.

Wagreich, M., Hu, X., Sageman, B., 2010: Causes of oxic-anoxic changes in Cretaceous marine environments and their implications for Earth systems—an introduction. *Sedimentary Geology* 235, 1-4, doi: 10.1016/j.sedgeo.2010.10.012.

Wagreich M, Hohenegger J, Neuhuber S. 2012. Nannofossil biostratigraphy, strontium and carbon isotope stratigraphy, cyclostratigraphy and an astronomically calibrated duration of the Late Campanian *Radotruncana calcarata* Zone. *Cretaceous Research* 38: pp. 80-96.

Wagreich, M., Dinares-Turell, J., Wolfgring, E., 2016. A reference section for the Santonian-Campanian boundary and sea-level fluctuations: The Postalm section, Austria, revisited [Abstract]. EGU General Assembly 2016, held 17-22 April, 2016 in Vienna Austria, p.1164.

Walaszczyk, I., Lees, J., A., Peryt, D. Cobban, W., A., Wood, C., J, 2012. Testing the congruence of the macrofossil vs microfossil record in the Turonian-Coniacian boundary succession of the Wagon Mound-Springer composite section (NE New Mexico, USA). *Acta Geol. Pol.* 62, 4, pp. 581-594.

Wei, Y., Chengshan, W., 2005. Correlation of Cretaceous oceanic red beds in Turkey, Caucasus and Himalaya. *Earth Science Frontiers*, 12(2): pp. 51-59 (in Chinese with English abstract).

Wilson, J., L., 1975. *Carbonate Facies in Geological History* Springer, Berlin–Heidelberg, New York, p. 471.

Wissing, F.N., Herrig, E., 1999. *Arbeitstechniken der Mikropaläontologie. Eine Einführung.* Ferdinand Enke Verlag, Stuttgart, pp. 1-191

Wolfgring E, Hohenegger J, Wagreich M. 2016a. Assessing pelagic palaeoenvironments using foraminiferal assemblages—a case study from the late Campanian *Radotruncana calcarata* Zone (Upper Cretaceous, Austrian Alps). *Palaeogeography, Palaeoclimatology, Palaeoecology*

Wolfgring, E., Wagreich, M., 2016b. A quantitative look on northwestern Tethyan foraminiferal assemblages, Campanian Nierental Formation, Austria. *PeerJ* 4:e1757; DOI 10.7717/peerj.1757

Wolfgring, E., Wagreich, M., Dinarès-Turell, J., Yilmaz, I.O., Böhm, K., 2017. Plankton biostratigraphy and magnetostratigraphy of the Santonian–Campanian boundary interval in the Mudurnu–Göynük Basin, northwestern Turkey, *Cretaceous Research*, doi: 10.1016/j.cretres.2017.07.006.

Wonders, A. A. H. 1980. Middle and Late Cretaceous planktonic foraminifera of the western Mediterranean area. *Utrecht Micropaleontological Bulletins* 24, 157 pp.

Yılmaz, İ., Ö., 2008. Cretaceous Pelagic Red Beds and Black Shales (Aptian-Santonian) NW Turkey: Global Oceanic Anoxic and Oxidic Events. *Turkish Journal of Earth Sciences*, Vol. 17, pp. 263-296.

Yılmaz, İ., Ö., Venneman, T., Altiner, D., Satır, M., 2004. Stable isotope evidence for meter-scale sea level changes in Lower Cretaceous Inner Platform and Pelagic Carbonate Successions of Turkey. *Geologica Carpathica*, 55, 1, pp. 19-36.

Yılmaz, İ., Ö., Altiner, D., Tekin, U., K., Tüysüz, O., Ocakoğlu, F., Açıkalın, S., 2010. Cenomanian-Turonian Oceanic Anoxic Event (OAE2) in the Sakarya Zone, northwestern Turkey: Sedimentological, cyclostratigraphic and geochemical records. *Cretaceous Research* 31, pp. 207-226.

Yılmaz, İ., Ö., Altiner, D., Tekin, U., K., Ocakoğlu, F., 2012. The first record of the “Mis-Barremian” Oceanic Anoxic Event and the Late Hauterivian platform drowning of the Bilecik platform, Sakarya Zone, western Turkey. *Cretaceous Research*, 38, pp. 16-39.

Yurtsever, T., Ş., Tekin, U., K., Demirel, İ., H., 2003. First evidence of the Cenomanian/Turonian boundary event (CTBE) in the Alakırcay Nappe of the Antalya Nappes, southwest Turkey. *Cretaceous Research* 24, pp. 41-53.



Yüksel, S., 1970, Etude geologique de la region d'Haymana (Turquie central e): These  
Fac. Sci. Univ. Nancy, Fransa.



## APPENDIX

### PLATE 1

Scale bar = 100  $\mu$ m

Figure 1: *Costellagerina pilula* BELFORD, sample no. NS 30, *G. elevata-D. asymetrica* concurrent range subzone, spiral view

Figure 2: *Costellagerina pilula* BELFORD, sample no. NS 30, *G. elevata-D. asymetrica* concurrent range subzone, spiral view

Figure 3: *Costellagerina pilula* BELFORD, and CIFELLI, sample no. NS 41, *G. elevata* zone, spiral view

Figure 4: *Costellagerina pilula* BELFORD, sample no. NS 41, *G. elevata* zone, spiral view

Figure 5: *Costellagerina bulbosa* S. W. PETTERS, EL-NAKHAL, and CIFELLI, sample no. NS 41, *G. elevata* zone, spiral view

Figure 6: *Costellagerina bulbosa* S. W. PETTERS, EL-NAKHAL, and CIFELLI, sample no. NS 44, *G. elevata* zone, spiral view

Figure 7: *Costellagerina bulbosa* S. W. PETTERS, EL-NAKHAL, and CIFELLI, sample no. NS 41, *G. elevata* zone, spiral view

Figure 8: *Costellagerina bulbosa* S. W. PETTERS, EL-NAKHAL, and CIFELLI, sample no. NS 41, *G. elevata* zone, spiral view

Figure 9: *Costellagerina bulbosa* S. W. PETTERS, EL-NAKHAL, and CIFELLI, sample no. NS 44, *G. elevata* zone, spiral view

Figure 10: *Costellagerina bulbosa* S. W. PETTERS, EL-NAKHAL, and CIFELLI, sample no. NS 44, *G. elevata* zone, spiral view

Figure 11: *Costellagerina bulbosa* S. W. PETTERS, EL-NAKHAL, and CIFELLI, sample no. NS 44, *G. elevata* zone, spiral view

Figure 12: *Costellagerina bulbosa* S. W. PETTERS, EL-NAKHAL, and CIFELLI, sample no. NS 46, *G. elevata* zone, spiral view

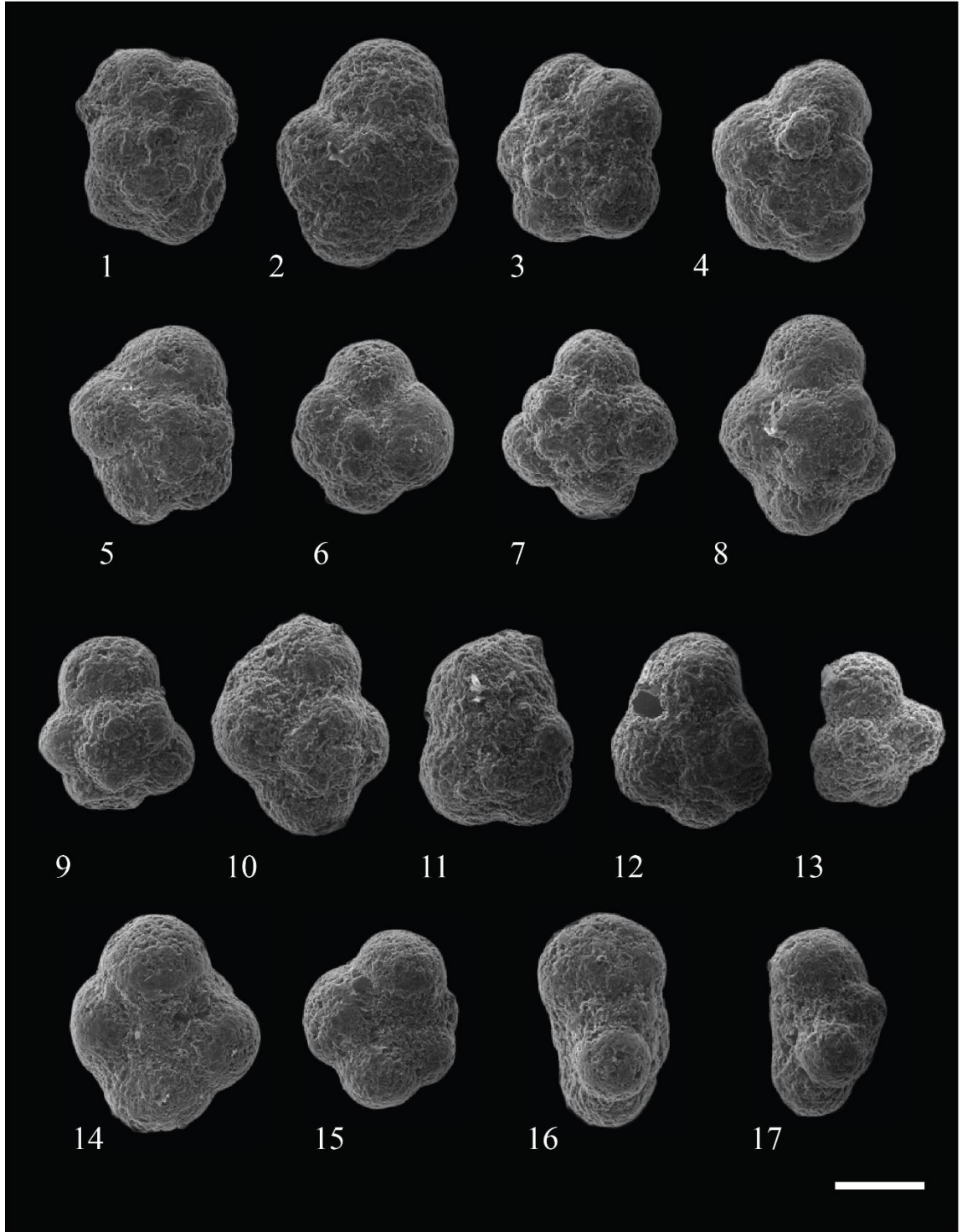
Figure 13: *Costellagerina bulbosa* S. W. PETTERS, EL-NAKHAL, and CIFELLI, sample no. NS 46, *G. elevata* zone, spiral view

Figure 14: *Costellagerina bulbosa* S. W. PETTERS, EL-NAKHAL, sample no. NS 40, *G. elevata* zone, umbilical view

Figure 15: *Costellagerina bulbosa* S. W. PETTERS, EL-NAKHAL, sample no. NS 41, *G. elevata* zone, umbilical view

Figure 16: *Costellagerina bulbosa* S. W. PETTERS, EL-NAKHAL, sample no. NS 40, *G. elevata* zone, lateral view

Figure 17: *Costellagerina bulbosa* S. W. PETTERS, EL-NAKHAL, sample no. NS 41, *G. elevata* zone, lateral view



## PLATE 2

Scale bar = 100  $\mu$ m

Figure 1: *Contusotruncana fornicata* PLUMMER, sample no. NS 40, *G. elevata* zone, spiral view

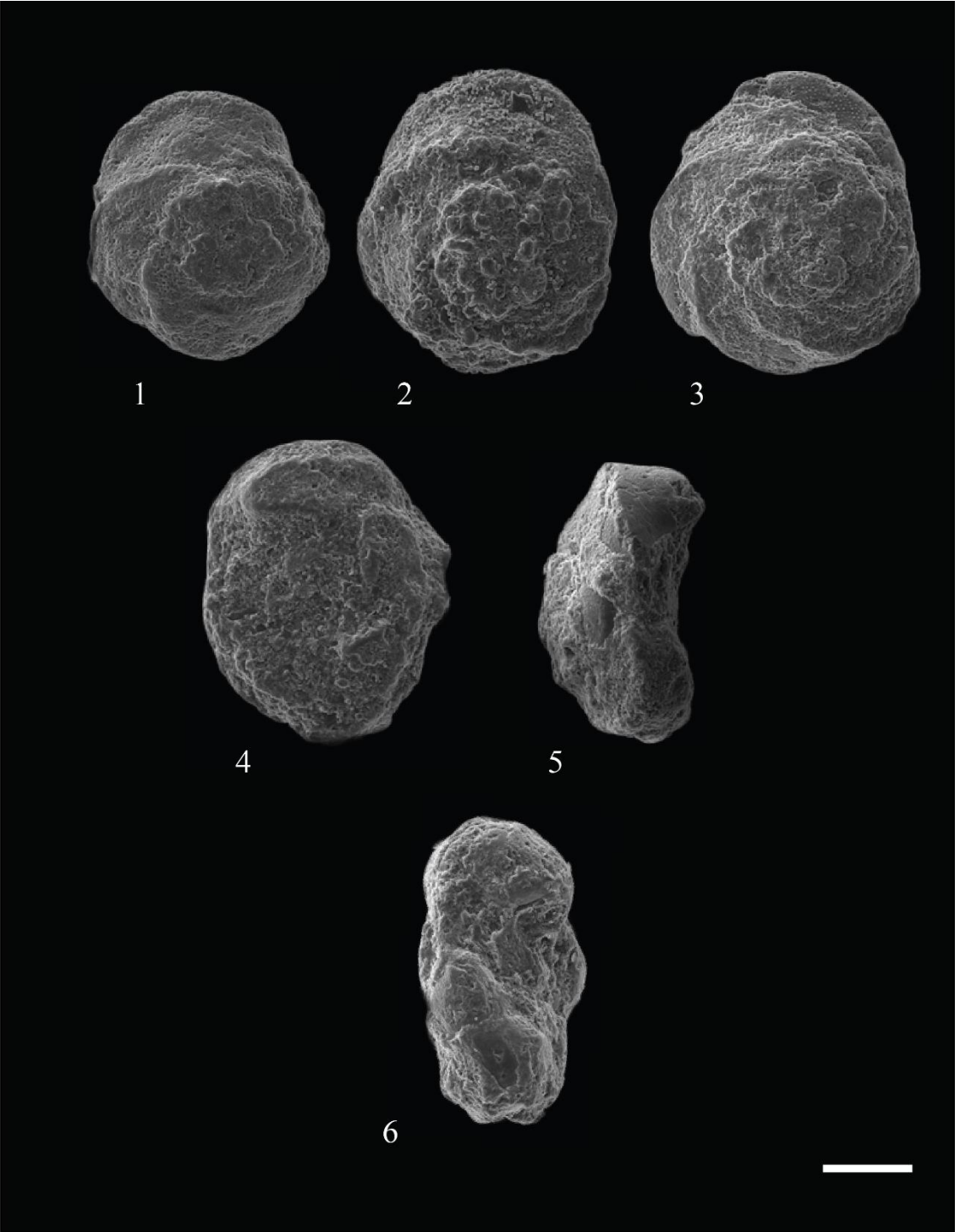
Figure 2: *Contusotruncana fornicata* PLUMMER, sample no. NS 55, *Globotruncanella* spp. zone, spiral view

Figure 3: *Contusotruncana fornicata* PLUMMER, sample no. NS 73, *G. aegyptiaca* zone, spiral view

Figure 4: *Contusotruncana fornicata* PLUMMER, sample no. NS 40, *G. elevata* zone, umbilical view

Figure 5: *Contusotruncana fornicata* PLUMMER, sample no. NS 53, *Globotruncanella* spp. zone, lateral view

Figure 6: *Contusotruncana* cf. *plummerae* GANDOLFI, sample no. NS 50, *G. ventricosa* zone, lateral view



### PLATE 3

Scale bar = 100  $\mu$ m

Figure 1: *Dicarinella algeriana* CARON, sample no. NS 3, *W. archaeocretacea* zone, spiral view

Figure 2: *Dicarinella algeriana* CARON, sample no. NS 10, *W. archaeocretacea* zone, lateral view

Figure 3: *Dicarinella takayanagii* HASEGAWA, sample no. NS 11, *W. archaeocretacea* zone, spiral view

Figure 4: *Dicarinella takayanagii* HASEGAWA, sample no. NS 11, *W. archaeocretacea* zone, spiral view

Figure 5: *Dicarinella takayanagii* HASEGAWA, sample no. NS 1, *D. algeriana* subzone, spiral view

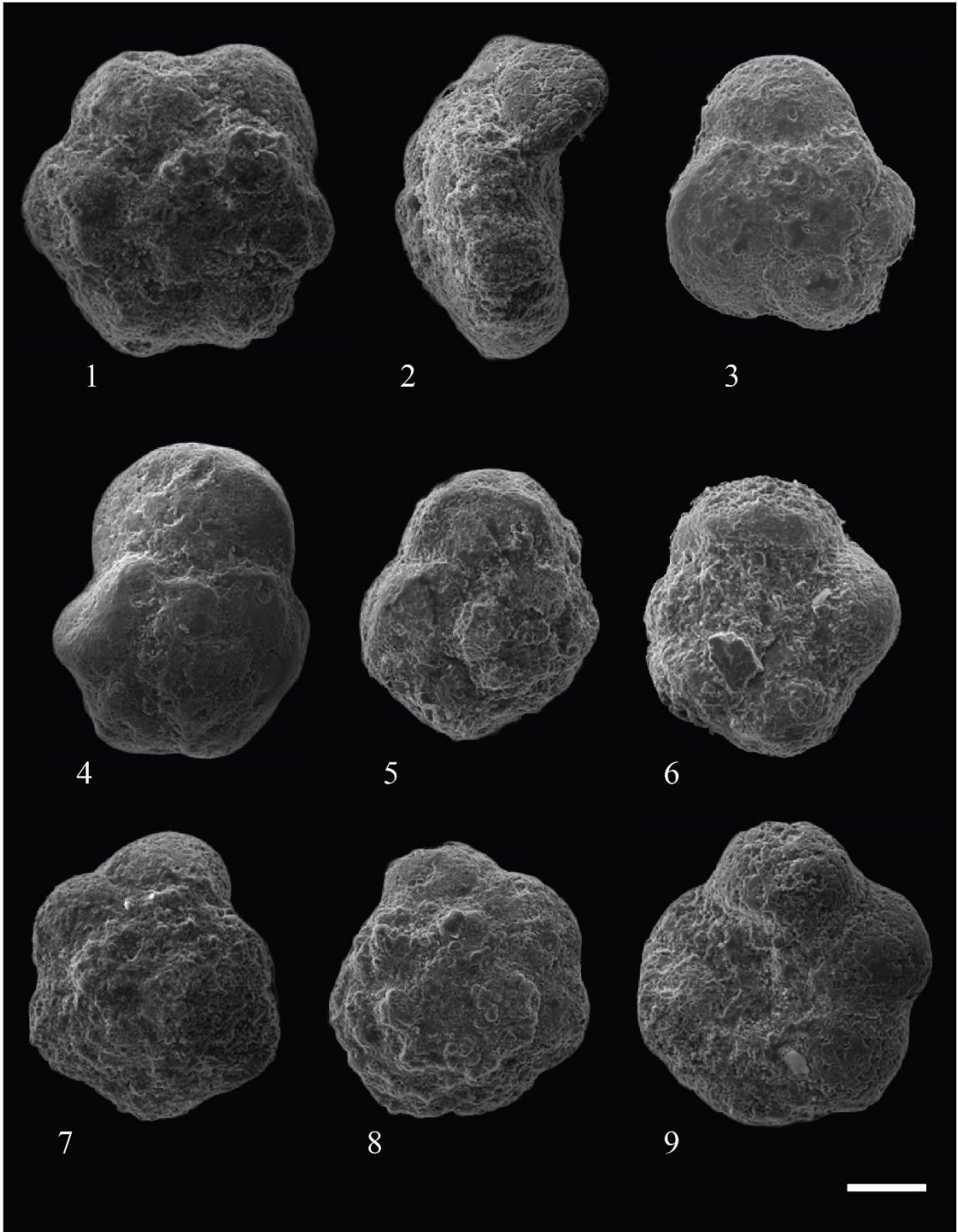
Figure 6: *Dicarinella takayanagii* HASEGAWA, sample no. NS 11, *W. archaeocretacea* zone, umbilical view

Figure 7: *Dicarinella imbricata* MORNOD, sample no. NS 17, *H. helvetica* zone, spiral view

Figure 8: *Dicarinella imbricata* MORNOD, sample no. NS 17, *H. helvetica* zone, spiral view

Figure 9: *Dicarinella imbricata* MORNOD, sample no. NS 17, *H. helvetica* zone, umbilical view





## PLATE 4

Scale bar = 100  $\mu$ m

Figure 1: *Dicarinella asymetrica* SIGAL, sample no. NS 28, *G. elevata*-*D. asymetrica* subzone, spiral view

Figure 2: *Dicarinella concavata* BROTZEN, sample no. NS 28, *G. elevata*-*D. asymetrica* subzone, spiral view

Figure 3: *Dicarinella canaliculata* REUSS, sample no. NS 3, *W. archaeocretacea* zone, spiral view

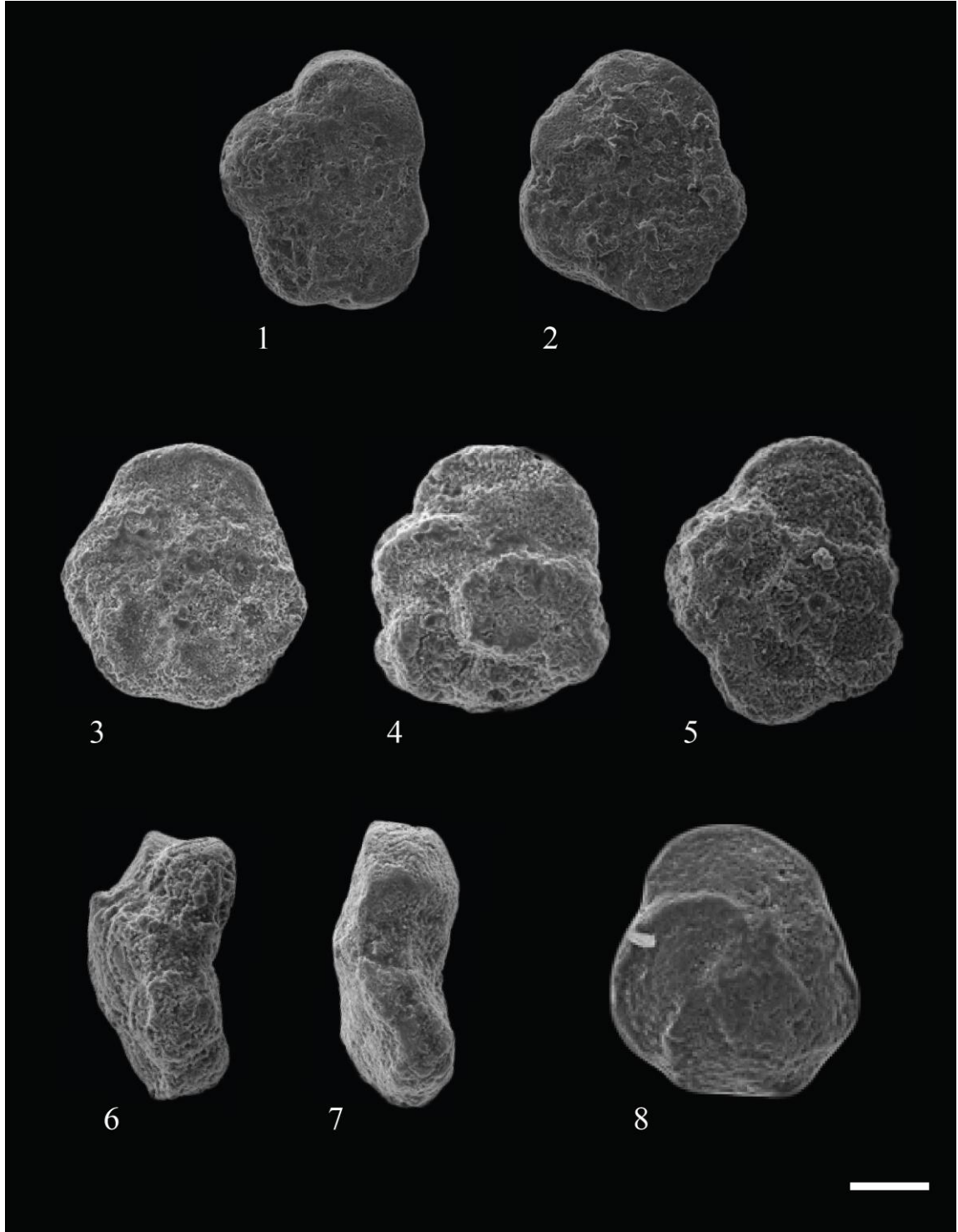
Figure 4: *Dicarinella canaliculata* REUSS, sample no. NS 10, *W. archaeocretacea* zone, spiral view

Figure 5: *Dicarinella canaliculata* REUSS, sample no. NS 3, *W. archaeocretacea* zone, spiral view

Figure 6: *Dicarinella canaliculata* REUSS, sample no. NS 3, *W. archaeocretacea* zone, lateral view

Figure 7: *Dicarinella canaliculata* REUSS, sample no. NS 3, *W. archaeocretacea* zone, lateral view

Figure 8: *Dicarinella hagni* SCHEIBNEROVA, sample no. NS 3, *W. archaeocretacea* zone, spiral view



## PLATE 5

Scale bar = 100  $\mu$ m

Figure 1: *Globotruncana orientalis* EL NAGGAR, sample no. NS 59, *Globotruncanella* spp. zone, spiral view

Figure 2: *Globotruncana orientalis* EL NAGGAR, sample no. NS 57, *Globotruncanella* spp. zone, lateral view

Figure 3: *Globotruncana orientalis* EL NAGGAR, sample no. NS 39, *G. elevata* zone, lateral view

Figure 4: *Globotruncana mariei* BANNER and BLOW, sample no. NS 39 *G. elevata* zone, spiral view

Figure 5: *Globotruncana mariei* BANNER and BLOW, sample no. NS 39, *G. elevata* zone, spiral view

Figure 6: *Globotruncana mariei* BANNER and BLOW, sample no. NS 41, *G. elevata* zone, umbilical view

Figure 7: *Globotruncana mariei* BANNER and BLOW, sample no. NS 50, *G. ventricosa* zone, spiral view

Figure 8: *Globotruncana mariei* BANNER and BLOW, sample no. NS 50, *G. ventricosa* zone, umbilical view

Figure 9: *Globotruncana ventricosa* WHITE, sample no. NS 62, *G. aegyptiaca* zone, spiral view

Figure 10: *Globotruncana ventricosa* WHITE, sample no. NS 62, *G. aegyptiaca* zone, spiral view

Figure 11: *Globotruncana ventricosa* WHITE, sample no. NS 53, *Globotruncanella* spp. zone, lateral view

Figure 12: *Globotruncana falsostuarti* SIGAL, sample no. NS 64, *G. aegyptiaca* zone, spiral view

Figure 13: *Globotruncana aegyptiaca* NAKKADY, sample no. NS 72, *G. aegyptiaca* zone, spiral view

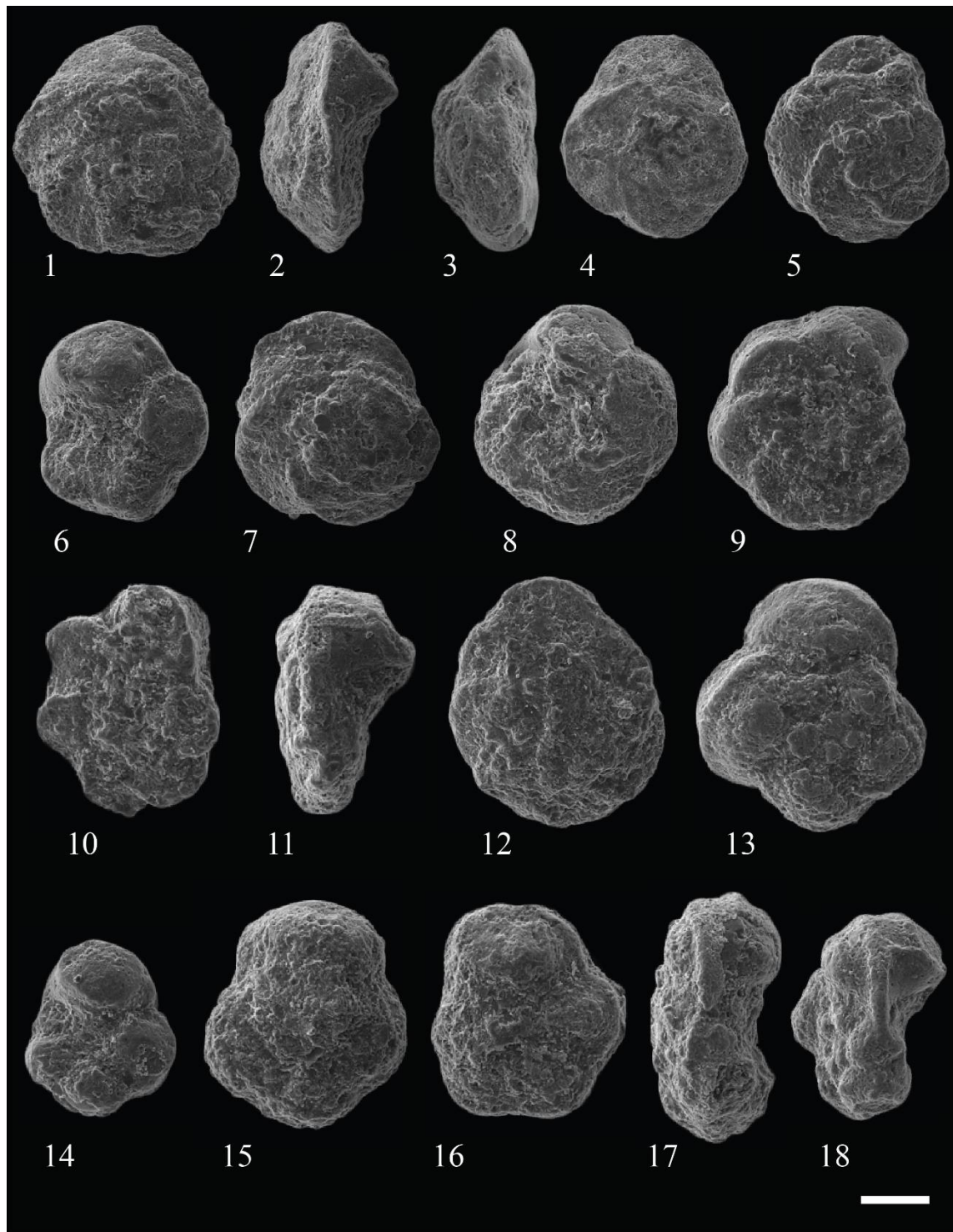
Figure 14: *Globotruncana aegyptiaca* NAKKADY, sample no. NS 70, *G. aegyptiaca* zone, umbilical view

Figure 15: *Globotruncana aegyptiaca* NAKKADY, sample no. NS 61, *G. aegyptiaca* zone, umbilical view

Figure 16: *Globotruncana aegyptiaca* NAKKADY, sample no. NS 61, *G. aegyptiaca* zone, umbilical view

Figure 17: *Globotruncana aegyptiaca* NAKKADY, sample no. NS 61, *G. aegyptiaca* zone, lateral view

Figure 18: *Globotruncana aegyptiaca* NAKKADY, sample no. NS 68, *G. aegyptiaca* zone, lateral view



## PLATE 6

Scale bar = 100  $\mu$ m

Figure 1: *Globotruncana linneiana* D'ORBIGNY, sample no. NS 61, *D. aegyptiaca* zone, spiral view

Figure 2: *Globotruncana linneiana* D'ORBIGNY, sample no. NS 74, *D. aegyptiaca* zone, spiral view

Figure 3: *Globotruncana linneiana* D'ORBIGNY, sample no. NS 31, *G. elevata*-*D. asymetrica* concurrent range subzone, umbilical view

Figure 4: *Globotruncana linneiana* D'ORBIGNY, sample no. NS 52, *Globotruncanella* spp. zone, umbilical view

Figure 5: *Globotruncana linneiana* D'ORBIGNY, sample no. NS 33, *G. elevata*-*D. asymetrica* concurrent range subzone, lateral view

Figure 6: *Globotruncana linneiana* D'ORBIGNY, sample no. NS 43, *G. elevata* zone, lateral view

Figure 7: *Globotruncana arca* CUSHMAN, sample no. NS 61, *G. aegyptiaca* zone, spiral view

Figure 8: *Globotruncana arca* CUSHMAN, sample no. NS 43, *G. elevata* zone, spiral view

Figure 9: *Globotruncana arca* CUSHMAN, sample no. NS 50, *G. ventricosa* zone, spiral view

Figure 10: *Globotruncana arca* CUSHMAN, sample no. NS 52, *Globotruncanella* spp. zone, spiral view

Figure 11: *Globotruncana arca* CUSHMAN, sample no. NS 56, *Globotruncanella* spp. zone, spiral view

Figure 12: *Globotruncana arca* CUSHMAN, sample no. NS 54, *Globotruncanella* spp. zone, spiral view

Figure 13: *Globotruncana arca* CUSHMAN, no. NS 54, *Globotruncanella* spp. zone, spiral view

Figure 14: *Globotruncana arca* CUSHMAN, sample no. NS 31, *G. elevata-D. asymetrica* concurrent range subzone, spiral view

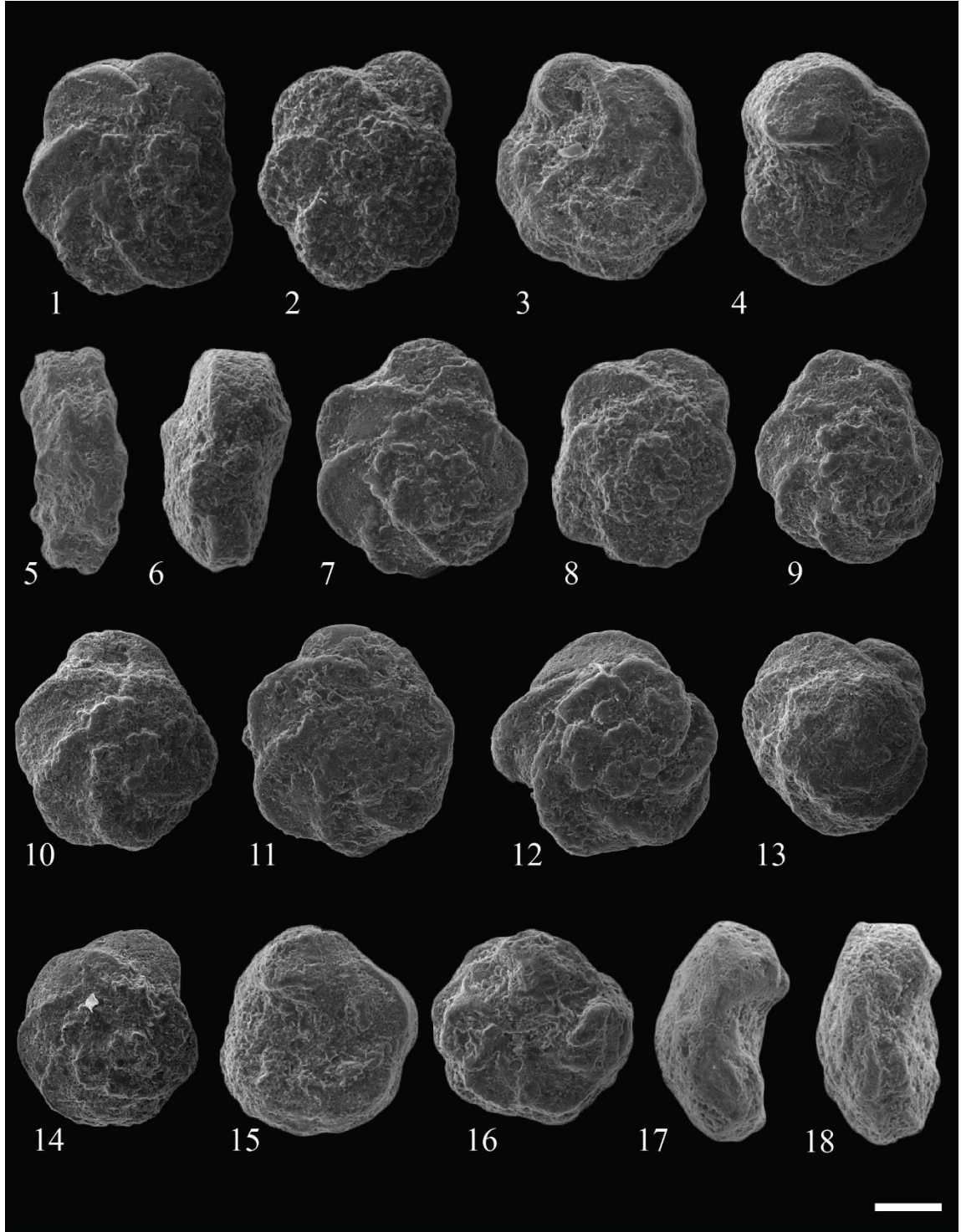
Figure 15: *Globotruncana arca* CUSHMAN, sample no. NS 51, *G. ventricosa* zone, umbilical view

Figure 16: *Globotruncana arca* CUSHMAN, sample no. NS 42, *G. elevata* zone, umbilical view

Figure 17: *Globotruncana arca* CUSHMAN, sample no. NS 39, *G. elevata-D. asymetrica* concurrent range subzone, lateral view

Figure 18: *Globotruncana arca* CUSHMAN, sample no. NS 39, *G. elevata-D. asymetrica* concurrent range subzone, lateral view





## PLATE 7

Scale bar = 100  $\mu$ m

Figure 1: *Globotruncana hilli* PESSAGNO, sample no. NS 68, *G. aegyptiaca* zone, spiral view

Figure 2: *Globotruncana hilli* PESSAGNO, sample no. NS 44, *G. elevata* zone, spiral view

Figure 3: *Globotruncana hilli* PESSAGNO, sample no. NS 49, *G. ventricosa* zone, spiral view

Figure 4: *Globotruncana hilli* PESSAGNO, sample no. NS 52, *Globotruncanella* spp. zone, spiral view

Figure 5: *Globotruncana hilli* PESSAGNO, sample no. NS 68, *G. aegyptiaca* zone, lateral view

Figure 6: *Globotruncana hilli* PESSAGNO, sample no. NS 55, *Globotruncanella* spp. zone, lateral view

Figure 7: *Globotruncana hilli* PESSAGNO, sample no. NS 36, *G. elevata-D. asymetrica* concurrent range subzone, lateral view

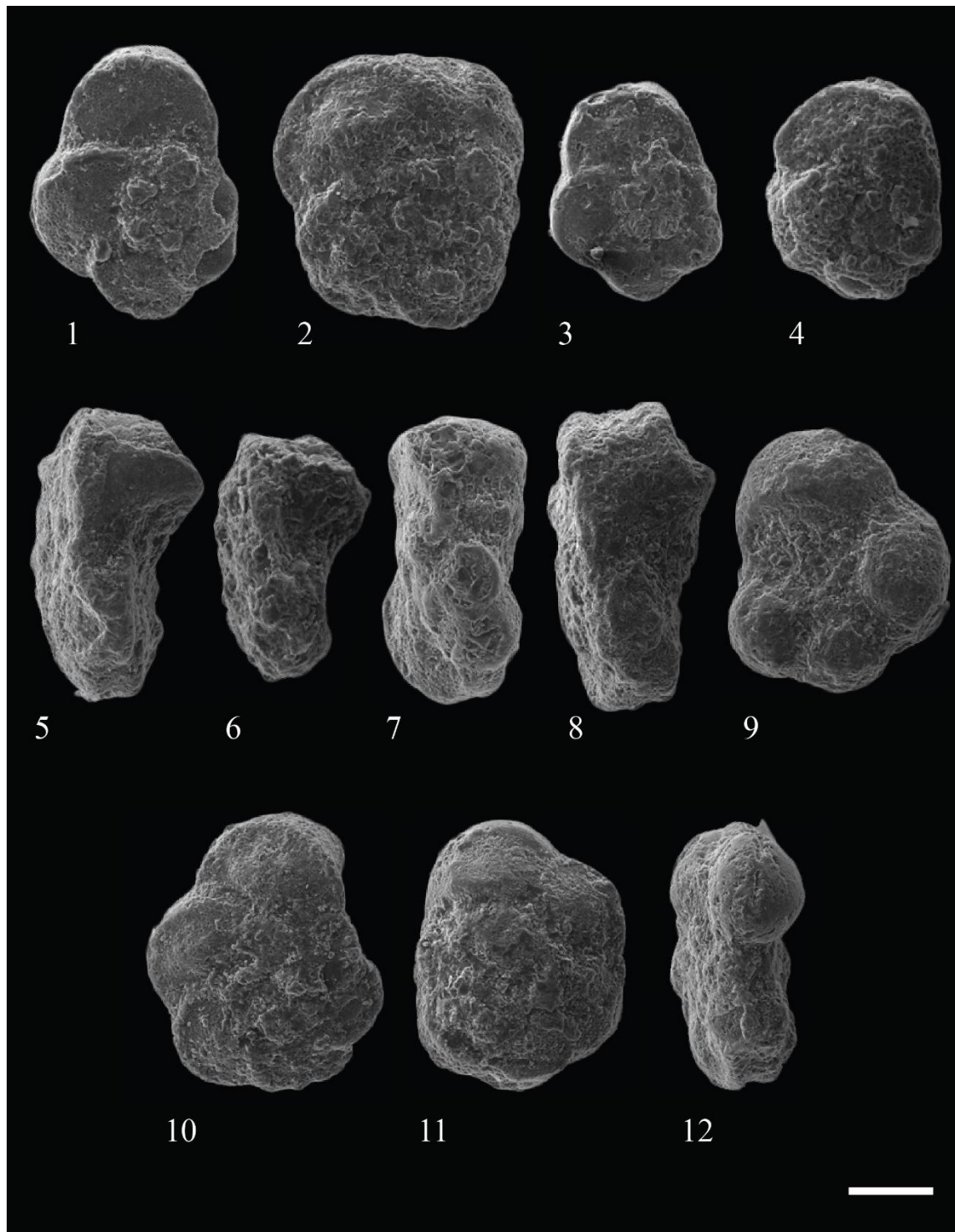
Figure 8: *Globotruncana hilli* PESSAGNO, sample no. NS 49, *G. ventricosa* zone, lateral view

Figure 9: *Globotruncana hilli* PESSAGNO, sample no. NS 47, *G. elevata* zone, umbilical view

Figure 10: *Globotruncana bulloides* VOGLER, sample no. NS 62, *D. asymetrica* zone, spiral view

Figure 11: *Globotruncana bulloides* VOGLER, sample no. NS 30, *G. elevata-D. asymetrica* concurrent range subzone, umbilical view

Figure 12: *Globotruncana bulloides* VOGLER, sample no. NS 57, *Globotruncanella* spp. zone, lateral view



## PLATE 8

Scale bar = 100  $\mu$ m

Figure 1: *Globotruncanita atlantica* CARON, sample no. NS 43, *G. elevata* zone, spiral view

Figure 2: *Globotruncanita atlantica* CARON, sample no. NS 53, *Globotruncanella* spp. zone, spiral view

Figure 3: *Globotruncanita stuartiformis* DALBIEZ, sample no. NS 52, *Globotruncanella* spp. zone, spiral view

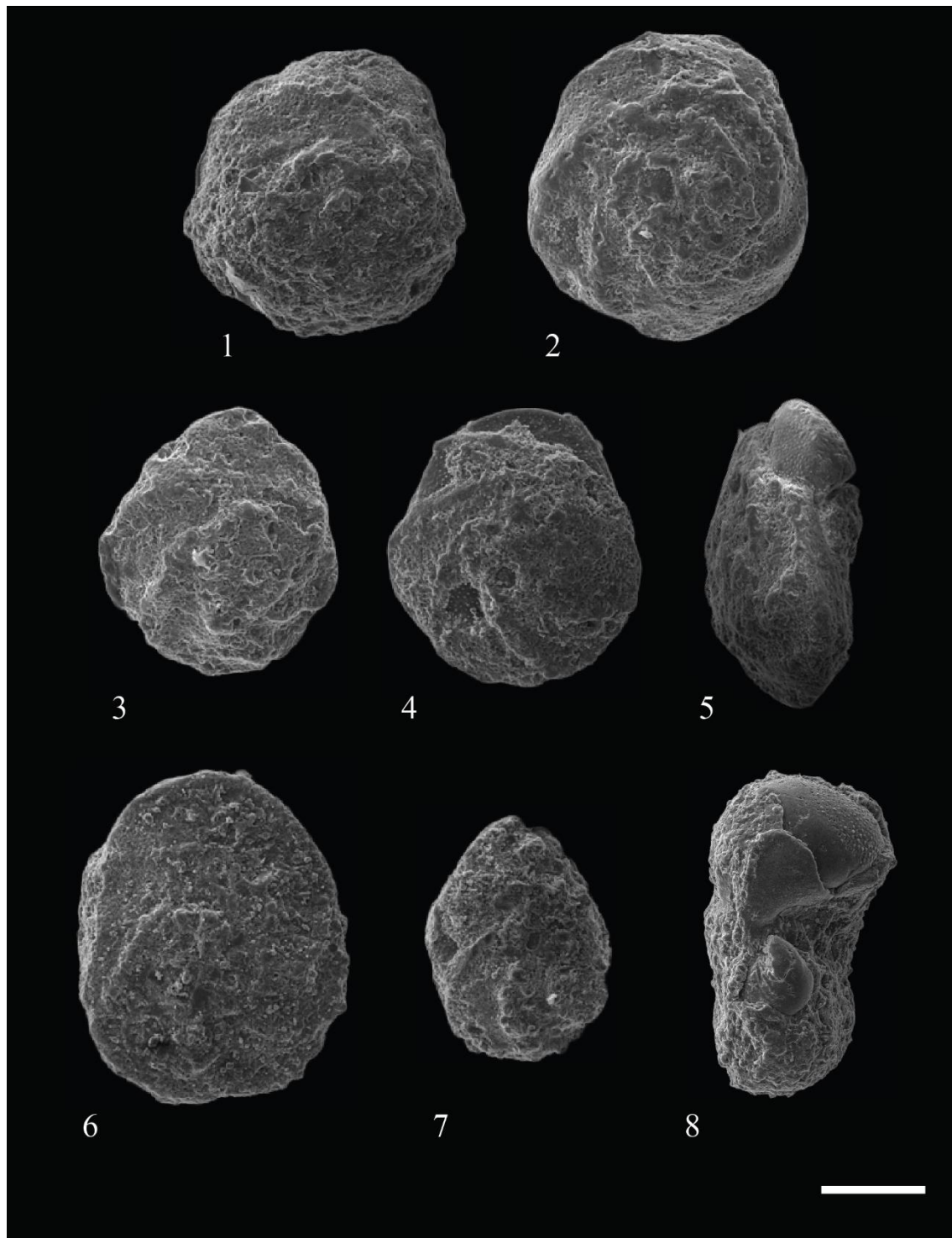
Figure 4: *Globotruncanita stuartiformis* DALBIEZ, sample no. NS 70, *G. aegyptiaca* zone, spiral view

Figure 5: *Globotruncanita stuartiformis* DALBIEZ, sample no. NS 48, *G. elevata* zone, lateral view

Figure 6: *Globotruncanita angulata* TILEV, sample no. NS 68, *G. aegyptiaca* zone, spiral view

Figure 7: *Globotruncanita pettersi* GANDOLFI, sample no. NS 64, *G. aegyptiaca* zone, spiral view

Figure 8: *Gansserina gansseri* BOLLI, sample no. NS 75, *G. gansseri* zone, lateral view



## PLATE 9

Scale bar = 100  $\mu$ m

Figure 1: *Helvetoglobotruncana helvetica* BOLLI, sample no. NS 14, *H. helvetica* zone, lateral view

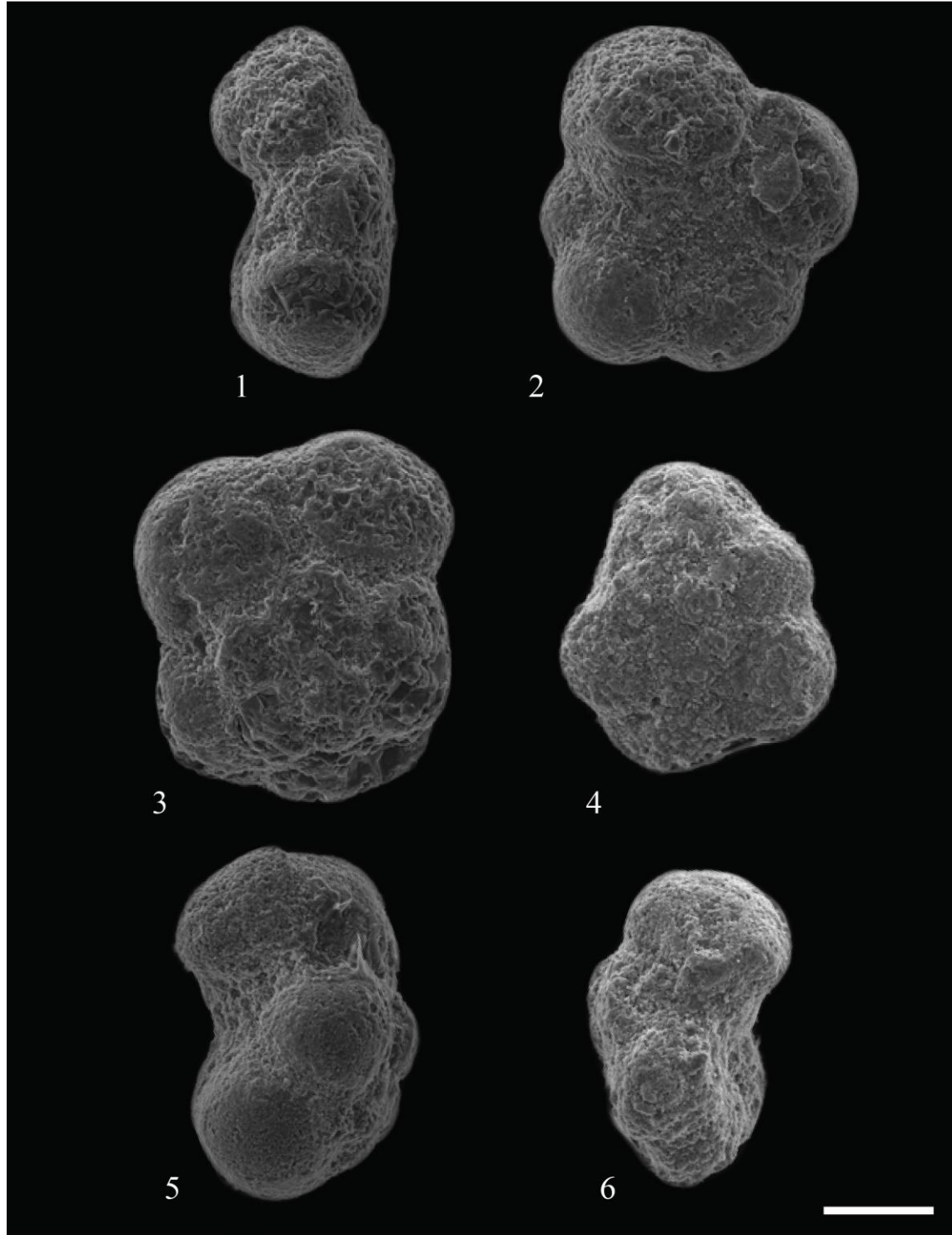
Figure 2: *Helvetoglobotruncana helvetica* BOLLI, sample no. NS 14, *H. helvetica* zone, umbilical view

Figure 3: *Whiteinella praehelvetica* TRUJILLO, sample no. NS 14, *H. helvetica* zone, spiral view

Figure 4: *Whiteinella praehelvetica* TRUJILLO, sample no. NS 14, *H. helvetica* zone, spiral view

Figure 5: *Whiteinella praehelvetica* TRUJILLO, sample no. NS 14, *H. helvetica* zone, lateral view

Figure 6: *Whiteinella praehelvetica* TRUJILLO, sample no. NS 14, *H. helvetica* zone, lateral view





## PLATE 10

Scale bar = 100  $\mu$ m

Figure 1: *Heterohelix planata* CUSHMAN, sample no. NS 57, *Globotruncanella* spp. zone, side view

Figure 2: *Heterohelix planata* CUSHMAN, sample no. NS 62, *G. aegyptiaca* zone, side view

Figure 3: *Heterohelix planata* CUSHMAN, sample no. NS 62, *G. aegyptiaca* zone, side view

Figure 4: *Heterohelix planata* CUSHMAN, sample no. NS 62, *G. aegyptiaca* zone, side view

Figure 5: *Heterohelix planata* CUSHMAN, sample no. NS 64, *G. aegyptiaca* zone, side view

Figure 6: *Heterohelix punctulata* CUSHMAN, sample no. NS 40, *G. elevata* zone, side view

Figure 7: *Heterohelix punctulata* CUSHMAN, sample no. NS 41, *G. elevata* zone, side view

Figure 8: *Heterohelix punctulata* CUSHMAN, sample no. NS 41, *G. elevata* zone, side view

Figure 9: *Heterohelix* sp. 1, sample no. NS 41, *G. elevata* zone, side view

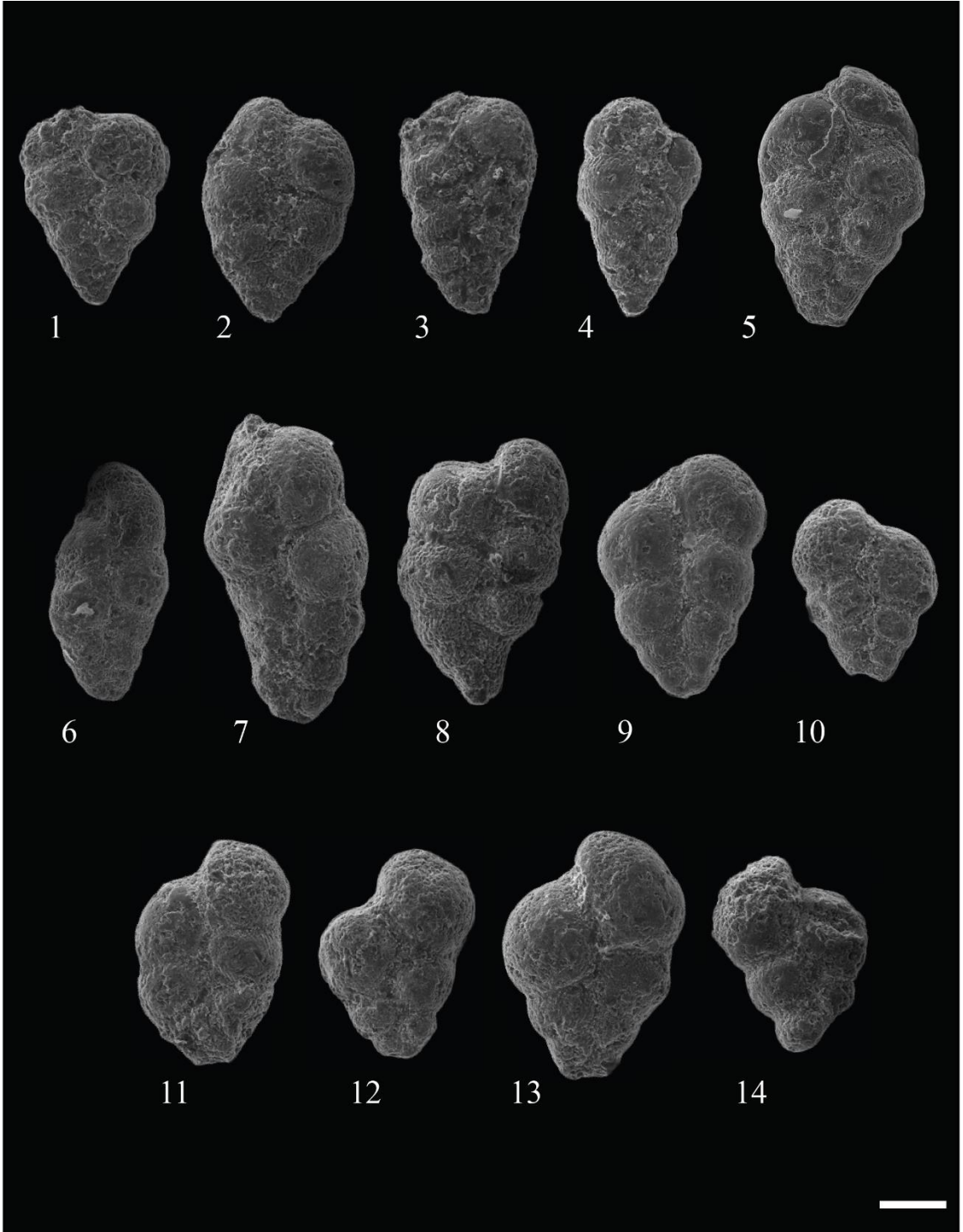
Figure 10: *Heterohelix* sp. 1, sample no. NS 43, *G. elevata* zone, side view

Figure 11: *Heterohelix* sp. 2, sample no. NS 47, *G. elevata* zone, side view

Figure 12: *Heterohelix* sp. 2, sample no. NS 41, *G. elevata* zone, side view

Figure 13: *Heterohelix* sp. 2, sample no. NS 43, *G. elevata* zone, side view

Figure 14: *Heterohelix* sp. 2, sample no. NS 53, *Globotruncanella* spp. zone, side view



## PLATE 11

Scale bar = 100  $\mu$ m

Figure 1: *Heterohelix globulosa* EHRENBERG, sample no. NS 61, *G. aegyptiaca* zone, side view

Figure 2: *Heterohelix globulosa* EHRENBERG, sample no. NS 62, *G. aegyptiaca* zone, side view

Figure 3: *Heterohelix globulosa* EHRENBERG, sample no. NS 75, *G. gansseri* zone, side view

Figure 4: *Heterohelix globulosa* EHRENBERG, sample no. NS 75, *G. gansseri* zone, side view

Figure 5: *Heterohelix globulosa* EHRENBERG, sample no. NS 75, *G. gansseri* zone, side view

Figure 6: *Heterohelix globulosa* EHRENBERG, sample no. NS 44, *G. elevata* zone, lateral view

Figure 7: *Pseudotextularia nuttalli* VOORWIJK, sample no. NS 36, *G. elevata-D. asymetrica* concurrent range subzone, side view

Figure 8: *Pseudotextularia nuttalli* VOORWIJK, sample no. NS 37, *G. elevata-D. asymetrica* concurrent range subzone, side view

Figure 9: *Pseudotextularia nuttalli* VOORWIJK, sample no. NS 31, *G. elevata-D. asymetrica* concurrent range subzone, lateral view

Figure 10: *Pseudotextularia nuttalli* VOORWIJK, sample no. NS 36, *G. elevata*-*D. asymetrica* concurrent range subzone, lateral view

Figure 11: *Pseudotextularia nuttalli* VOORWIJK, sample no. NS 41, *G. elevata* zone, lateral view



## PLATE 12

Scale bar = 100  $\mu$ m

Figure 1: *Laeviheterohelix turgida* NEDERBRAGT, sample no. NS 30, *G. elevata-D. asymetrica* concurrent range subzone, side view

Figure 2: *Laeviheterohelix turgida* NEDERBRAGT, sample no. NS 30, *G. elevata-D. asymetrica* concurrent range subzone, side view

Figure 3: *Laeviheterohelix turgida* NEDERBRAGT, sample no. NS 31, *G. elevata-D. asymetrica* concurrent range subzone, side view

Figure 4: *Laeviheterohelix turgida* NEDERBRAGT, sample no. NS 32, *G. elevata-D. asymetrica* concurrent range subzone, lateral view

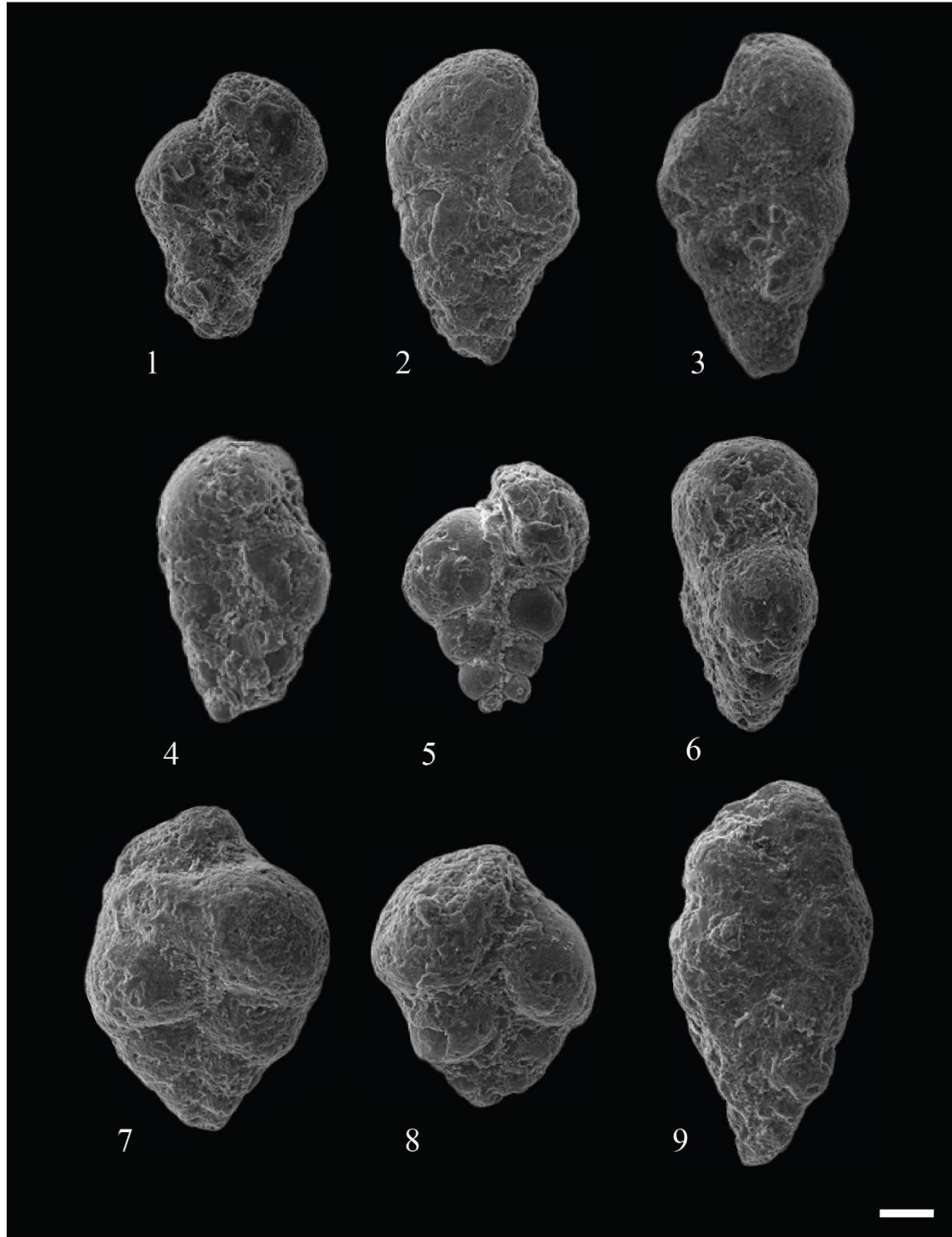
Figure 5: *Laeviheterohelix* sp. 1, sample no. NS 31, *G. elevata-D. asymetrica* concurrent range subzone, side view

Figure 6: *Laeviheterohelix* sp. 1, sample no. NS 31, *G. elevata-D. asymetrica* concurrent range subzone, side view

Figure 7: *Laeviheterohelix* sp. 1, sample no. NS 31, *G. elevata-D. asymetrica* concurrent range subzone, side view

Figure 8: *Laeviheterohelix* sp. 1, sample no. NS 32, *G. elevata-D. asymetrica* concurrent range subzone, side view

Figure 9: *Heterohelix* cf. *moremani*, sample no. NS 30, *G. elevata-D. asymetrica* concurrent range subzone, side view





## PLATE 13

Scale bar = 100  $\mu$ m

Figure 1: *Marginotruncana pseudolinneiana* PESSAGNO, sample no. NS 18, *H. helvetica* zone, spiral view

Figure 2: *Marginotruncana coronata* BOLLI, sample no. NS 36, *G. elevata-D. asymetrica* concurrent range subzone, spiral view

Figure 3: *Marginotruncana coronata* BOLLI, sample no. NS 18, *H. helvetica* zone, spiral view

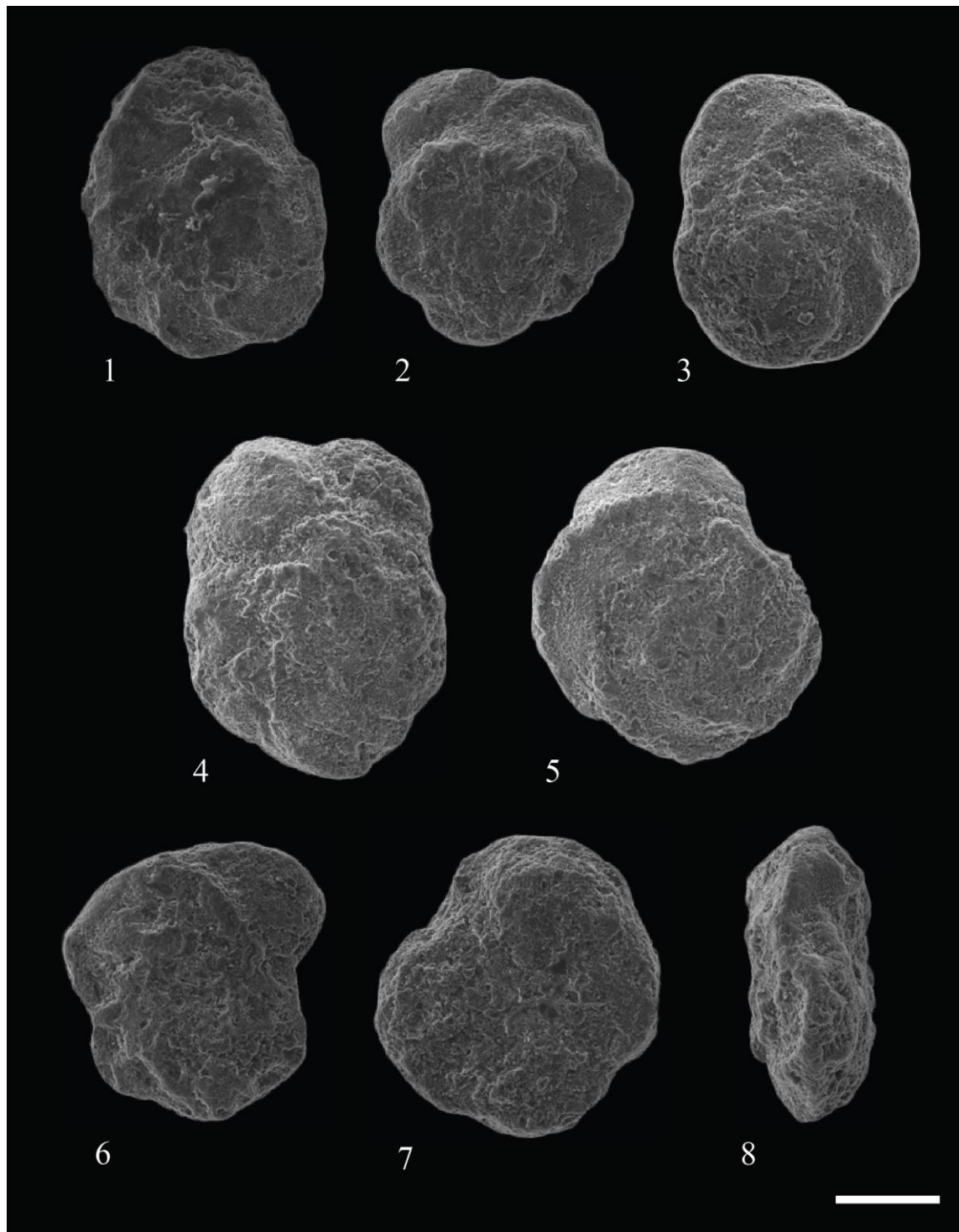
Figure 4: *Marginotruncana tarfayaensis* LEHMANN, sample no. NS 37, *G. elevata-D. asymetrica* concurrent range subzone, spiral view

Figure 5: *Marginotruncana sinuosa* PORTHAULT, sample no. NS 38, *G. elevata-D. asymetrica* concurrent range subzone, spiral view

Figure 6: *Marginotruncana paraconcavata* PORTHAULT, sample no. NS 28, *G. elevata-D. asymetrica* concurrent range subzone, spiral view

Figure 7: *Marginotruncana* cf. *paraconcavata* PORTHAULT, sample no. NS 28, *G. elevata-D. asymetrica* concurrent range subzone, umbilical view

Figure 8: *Marginotruncana paraconcavata* PORTHAULT, sample no. NS 28, *G. elevata-D. asymetrica* concurrent range subzone, lateral view



## PLATE 14

Scale bar = 100  $\mu$ m

Figure 1: *Muricohedbergella hoelzli* HAGN and ZEIL, sample no. NS 5, W. *archaeocretacea* zone, spiral view

Figure 2: *Muricohedbergella hoelzli* HAGN and ZEIL, sample no. NS 5, W. *archaeocretacea* zone, umbilical view

Figure 3: *Muricohedbergella hoelzli* HAGN and ZEIL, sample no. NS 5, W. *archaeocretacea* zone, spiral view

Figure 4: *Muricohedbergella hoelzli* HAGN and ZEIL, sample no. NS 5, W. *archaeocretacea* zone, lateral view

Figure 5: *Archaeoglobigerina cretacea* D'ORBIGNY, sample no. NS 70, *G. aegyptiaca* zone, lateral view

Figure 6: *Muricohedbergella planispira* TAPPAN, sample no. NS 13, W. *archaeocretacea* zone, spiral view

Figure 7: *Muricohedbergella planispira* TAPPAN, sample no. NS 10, W. *archaeocretacea* zone, spiral view

Figure 8: *Muricohedbergella planispira* TAPPAN, sample no. NS 10, W. *archaeocretacea* zone, spiral view

Figure 9: *Muricohedbergella planispira* TAPPAN, sample no. NS 35, *G. elevata-D. asymetrica* concurrent range subzone, spiral view

Figure 10: *Muricohedbergella planispira* TAPPAN, sample no. NS 36, *G. elevata-D. asymetrica* concurrent range subzone, lateral view

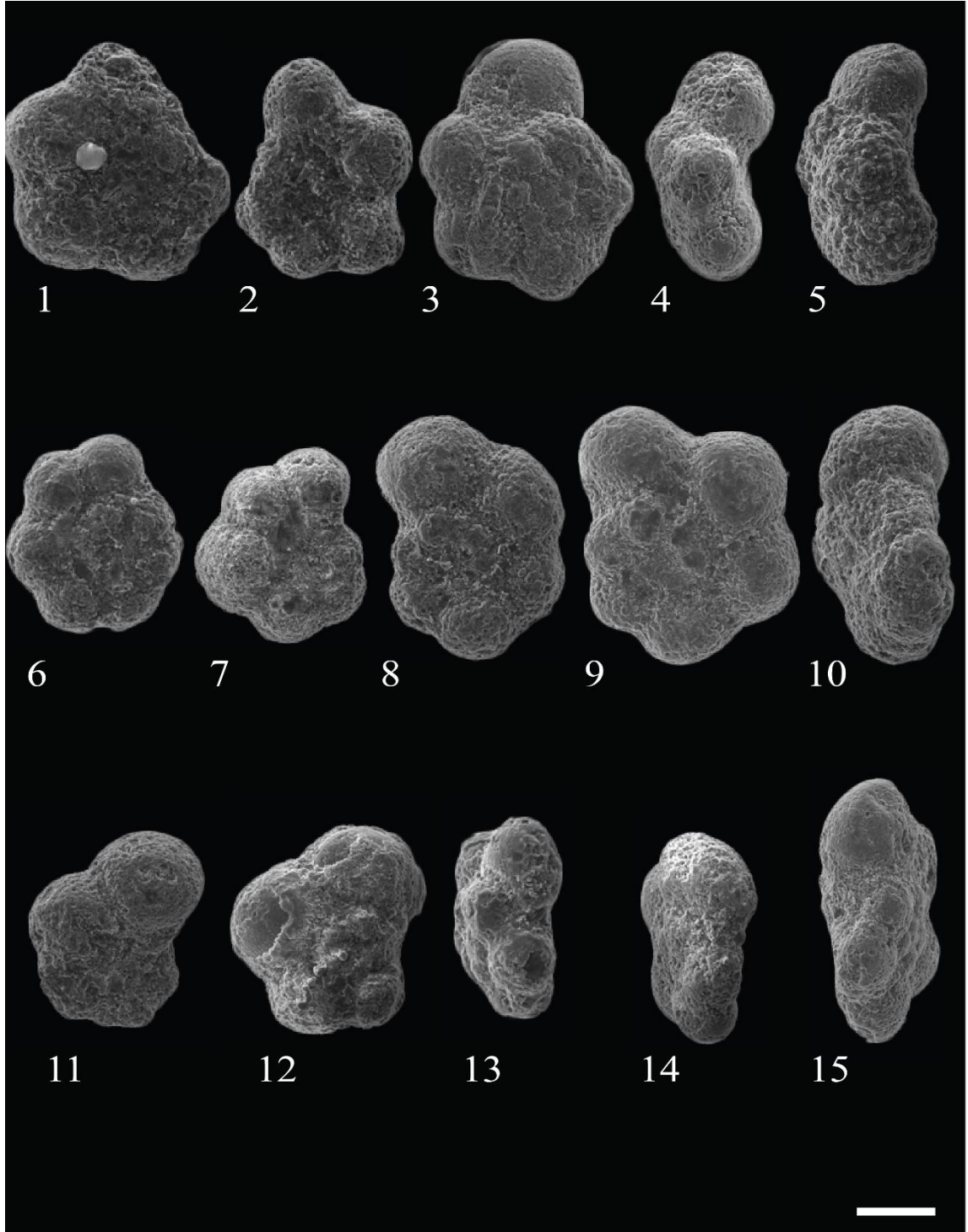
Figure 11: *Muricohedbergella holmdelensis* OLSSON, sample no. NS 28, *G. elevata-D. asymetrica* concurrent range subzone, spiral view

Figure 12: *Muricohedbergella holmdelensis* OLSSON, sample no. NS 28, *G. elevata-D. asymetrica* concurrent range subzone, spiral view

Figure 13: *Muricohedbergella holmdelensis* OLSSON, sample no. NS 50, *G. ventricosa* zone, lateral view

Figure 14: *Muricohedbergella holmdelensis* OLSSON, sample no. NS 36, *G. elevata-D. asymetrica* concurrent range subzone, lateral view

Figure 15: *Muricohedbergella holmdelensis* OLSSON, sample no. NS 53, *Globo truncanella* spp. zone, lateral view



## PLATE 15

Scale bar = 100  $\mu$ m

Figure 1: *Praeglobotruncana stephani* GANDOLFI, sample no. NS 5, *W. archaeocretacea* zone, spiral view

Figure 2: *Praeglobotruncana stephani* GANDOLFI, sample no. NS 3, *W. archaeocretacea* zone, spiral view

Figure 3: *Praeglobotruncana stephani* GANDOLFI, sample no. NS 5, *W. archaeocretacea* zone, spiral view

Figure 4: *Praeglobotruncana stephani* GANDOLFI, sample no. NS 3, *W. archaeocretacea* zone, spiral view

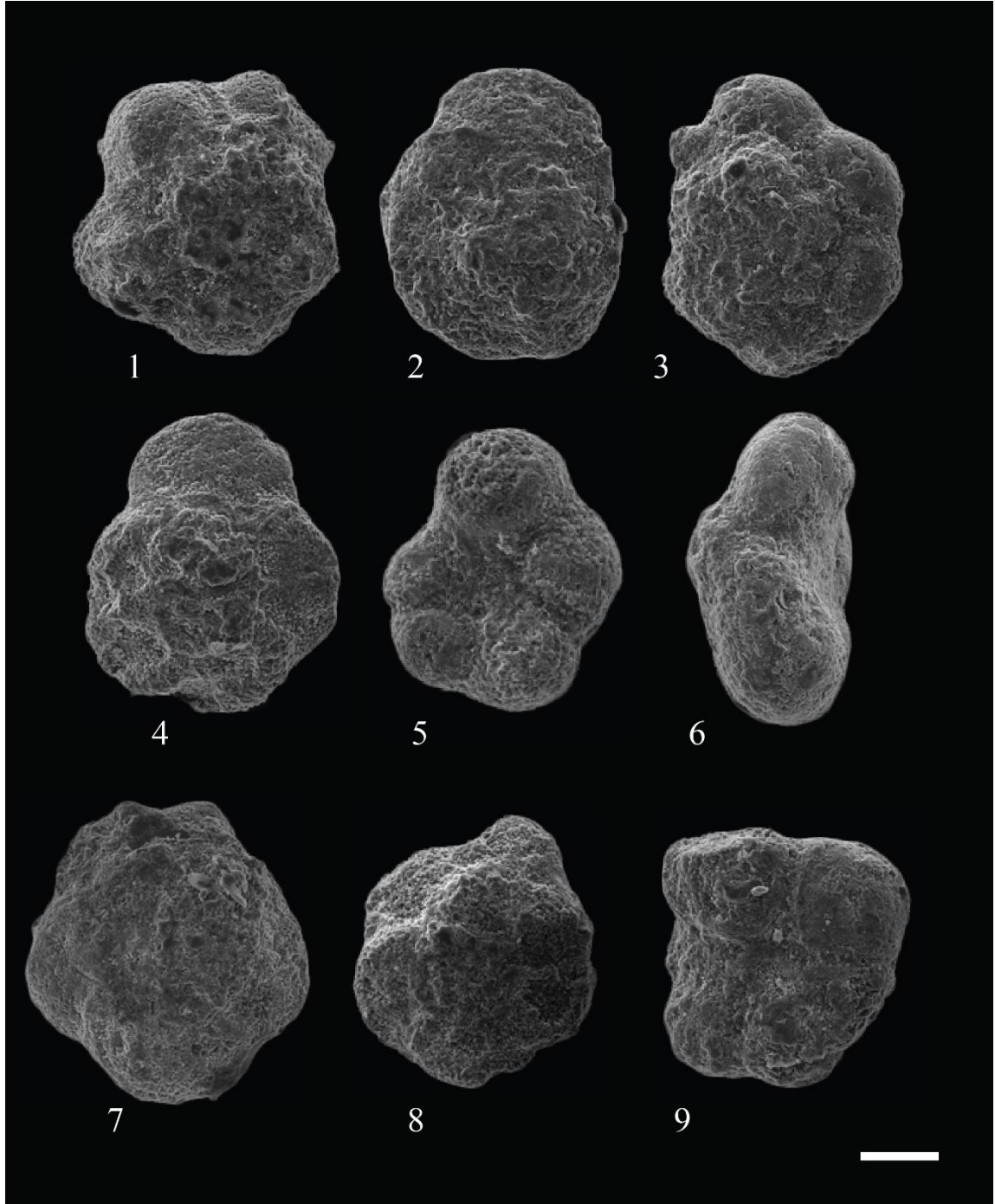
Figure 5: *Praeglobotruncana stephani* GANDOLFI, sample no. NS 10, *W. archaeocretacea* zone, umbilical view

Figure 6: *Praeglobotruncana stephani* GANDOLFI, sample no. NS 10, *W. archaeocretacea* zone, lateral view

Figure 7: *Praeglobotruncana gibba* KLAUS, sample no. NS 3, *W. archaeocretacea* zone, spiral view

Figure 8: *Praeglobotruncana gibba* KLAUS, sample no. NS 3, *W. archaeocretacea* zone, spiral view

Figure 9: *Praeglobotruncana gibba* KLAUS, sample no. NS 3, *W. archaeocretacea* zone, umbilical view



## PLATE 16

Scale bar = 100  $\mu$ m

Figure 1: *Rugoglobigerina rugosa* PLUMMER, sample no. NS 49, *G. ventricosa* zone, spiral view

Figure 2: *Rugoglobigerina rugosa* PLUMMER, sample no. NS 51, *G. ventricosa* zone, spiral view

Figure 3: *Rugoglobigerina rugosa* PLUMMER, sample no. NS 53, *Globotruncanella* spp. zone, spiral view

Figure 4: *Rugoglobigerina rugosa* PLUMMER, sample no. NS 53, *Globotruncanella* spp. zone, spiral view

Figure 5: *Rugoglobigerina rugosa* PLUMMER, sample no. NS 53, *Globotruncanella* spp. zone, spiral view

Figure 6: *Rugoglobigerina rugosa* PLUMMER, sample no. NS 53, *Globotruncanella* spp. zone, umbilical view

Figure 7: *Rugoglobigerina rugosa* PLUMMER, sample no. NS 62, *G. aegyptiaca* zone, spiral view

Figure 8: *Rugoglobigerina rugosa* PLUMMER, sample no. NS 68, *G. aegyptiaca* zone, umbilical view

Figure 9: *Rugoglobigerina rugosa* PLUMMER, sample no. NS 69, *G. aegyptiaca* zone, spiral view



Figure 10: *Rugoglobigerina rugosa* PLUMMER, sample no. NS 71, *G. aegyptiaca* zone, umbilical view

Figure 11: *Rugoglobigerina rugosa* PLUMMER, sample no. NS 71, *G. aegyptiaca* zone, spiral view

Figure 12: *Rugoglobigerina rugosa* PLUMMER, sample no. NS 71, *G. aegyptiaca* zone, umbilical view

Figure 13: *Rugoglobigerina rugosa* PLUMMER, sample no. NS 74, *G. aegyptiaca* zone, spiral view

Figure 14: *Rugoglobigerina rugosa* PLUMMER, sample no. NS 74, *G. aegyptiaca* zone, umbilical view

Figure 15: *Rugoglobigerina rugosa* PLUMMER, sample no. NS 74, *G. aegyptiaca* zone, umbilical view

Figure 16: *Rugoglobigerina macrocephala* BRONNIMANN, sample no. NS 74, *G. aegyptiaca* zone, spiral view

Figure 17: *Rugoglobigerina macrocephala* BRONNIMANN, sample no. NS 67, *G. aegyptiaca* zone, spiral view

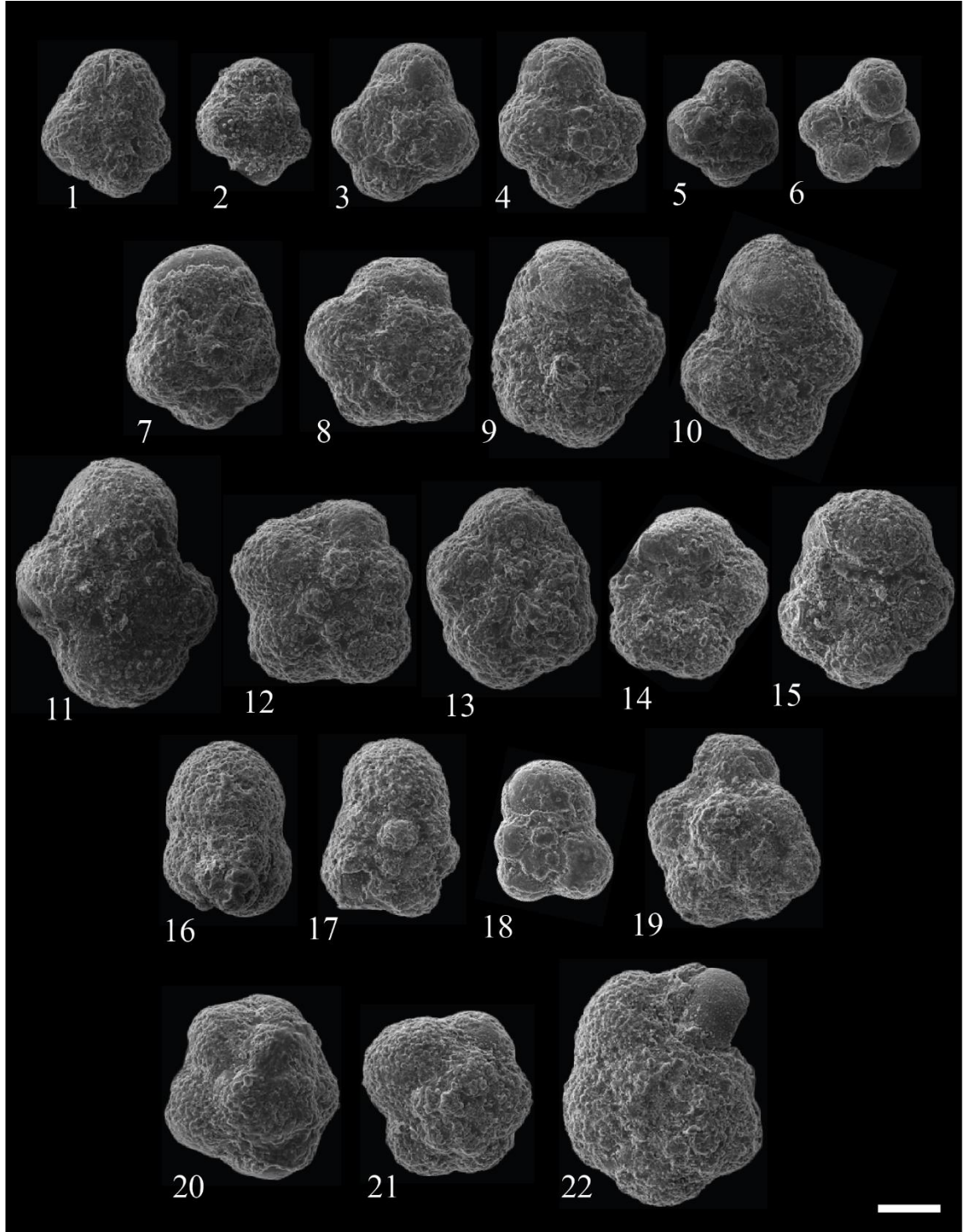
Figure 18: *Rugoglobigerina macrocephala* BRONNIMANN, sample no. NS 53, *Globotruncanella* spp. zone, umbilical view

Figure 19: *Rugoglobigerina pennyi* BRONNIMANN, sample no. NS 62, *G. aegyptiaca* zone, spiral view

Figure 20: *Rugoglobigerina milamensis* SMITH and PESSAGNO, sample no. NS 74, *G. aegyptiaca* zone, spiral view

Figure 21: *Rugoglobigerina milamensis* SMITH and PESSAGNO, sample no. NS 67, *G. aegyptiaca* zone, spiral view

Figure 22: *Rugoglobigerina hexacamerata* BRONNIMANN, sample no. NS 68, *G. aegyptiaca* zone, spiral view



## PLATE 17

Scale bar = 100  $\mu\text{m}$

Figure 1: *Sigalia deflaensis* SIGAL, sample no. NS 25, *G. elevata-D. asymetrica* concurrent range subzone, side view

Figure 2: *Sigalia deflaensis* SIGAL, sample no. NS 28, *G. elevata-D. asymetrica* concurrent range subzone, side view

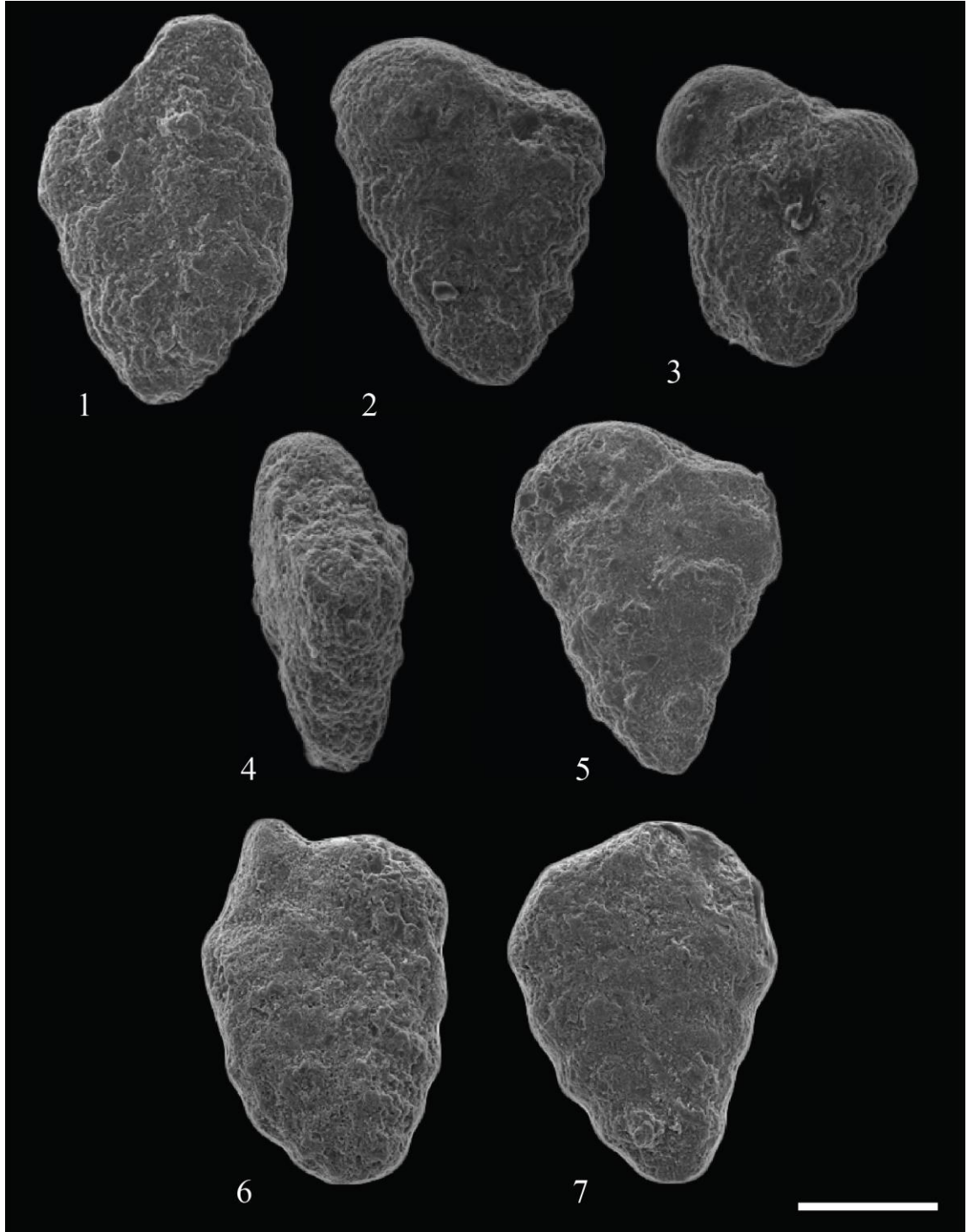
Figure 3: *Sigalia deflaensis* SIGAL, sample no. NS 30, *G. elevata-D. asymetrica* concurrent range subzone, side view

Figure 4: *Sigalia deflaensis* SIGAL, sample no. NS 28, *G. elevata-D. asymetrica* concurrent range subzone, lateral view

Figure 5: *Sigalia carpatica* SALAJ and SAMUEL, sample no. NS 36, *G. elevata-D. asymetrica* concurrent range subzone, side view

Figure 6: *Sigalia* sp., sample no. NS 37, *G. elevata-D. asymetrica* concurrent range subzone, side view

Figure 7: *Sigalia* sp., sample no. NS 37, *G. elevata-D. asymetrica* concurrent range subzone, side view



## PLATE 18

Scale bar = 100  $\mu$ m

Figure 1: *Ventilabrella browni* MARTIN, sample no. NS 40, *G. elevata* zone, side view

Figure 2: *Ventilabrella browni* MARTIN, sample no. NS 40, *G. elevata* zone, side view

Figure 3: *Ventilabrella browni* MARTIN, sample no. NS 47, *G. elevata* zone, side view

Figure 4: *Ventilabrella browni* MARTIN, sample no. NS 47, *G. elevata* zone, side view

Figure 5: *Ventilabrella eggeri* CUSHMAN, sample no. NS 40, *G. elevata* zone, side view

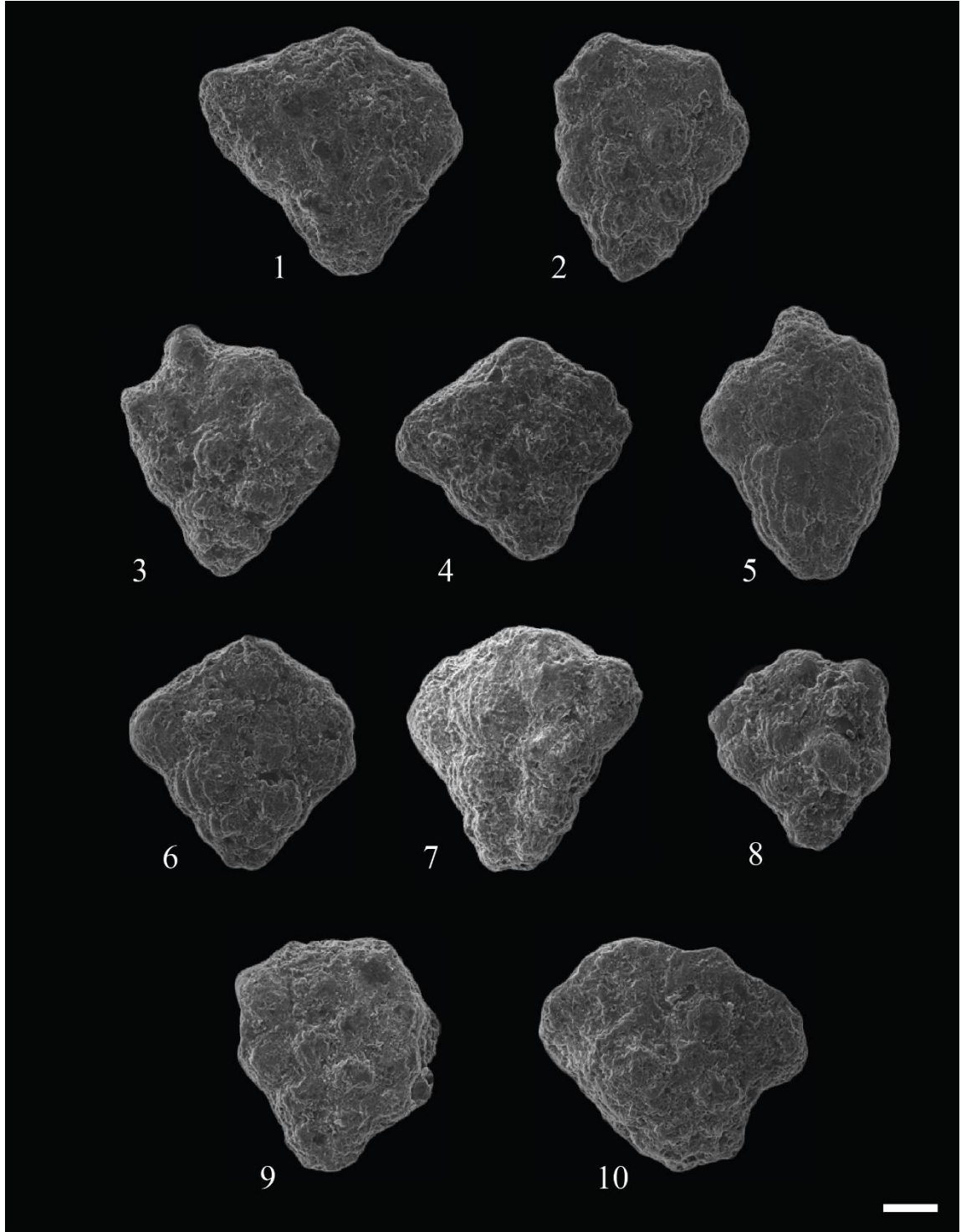
Figure 6: *Ventilabrella eggeri* CUSHMAN, sample no. NS 40, *G. elevata* zone, side view

Figure 7: *Ventilabrella eggeri* CUSHMAN, sample no. NS 42, *G. elevata* zone, side view

Figure 8: *Ventilabrella* sp. CUSHMAN, sample no. NS 53, *Globotruncanella* spp. zone, side view

Figure 9: *Ventilabrella* sp., sample no. NS 30, *G. elevata-D. asymetrica* concurrent range subzone, side view

Figure 10: *Ventilabrella* sp., sample no. NS 47, *G. elevata* zone, side view



## PLATE 19

Scale bar = 100  $\mu$ m

Figure 1: *Whiteinella baltica* DOUGLAS and RANKIN, sample no. NS 21, *D. asymetrica* zone, spiral view

Figure 2: *Whiteinella baltica* DOUGLAS and RANKIN, sample no. NS 37, *G. elevata-D. asymetrica* concurrent range subzone, spiral view

Figure 3: *Whiteinella baltica* DOUGLAS and RANKIN, sample no. NS 17, *H. helvetica* zone, spiral view

Figure 4: *Whiteinella baltica* DOUGLAS and RANKIN, sample no. NS 17, *H. helvetica* zone, spiral view

Figure 5: *Whiteinella baltica* DOUGLAS and RANKIN, sample no. NS 33, *G. elevata-D. asymetrica* concurrent range subzone, spiral view

Figure 6: *Whiteinella baltica* DOUGLAS and RANKIN, sample no. NS 9, *W. archaeocretacea* zone, spiral view

Figure 7: *Whiteinella baltica* DOUGLAS and RANKIN, sample no. NS 3, *W. archaeocretacea* zone, spiral view

Figure 8: *Whiteinella baltica* DOUGLAS and RANKIN, sample no. NS 44, *G. elevata* zone, spiral view

Figure 9: *Whiteinella baltica* DOUGLAS and RANKIN, sample no. NS 5, *W. archaeocretacea* zone, lateral view



Figure 10: *Whiteinella baltica* DOUGLAS and RANKIN, sample no. NS 13, *W. archaeocretacea* zone, lateral view

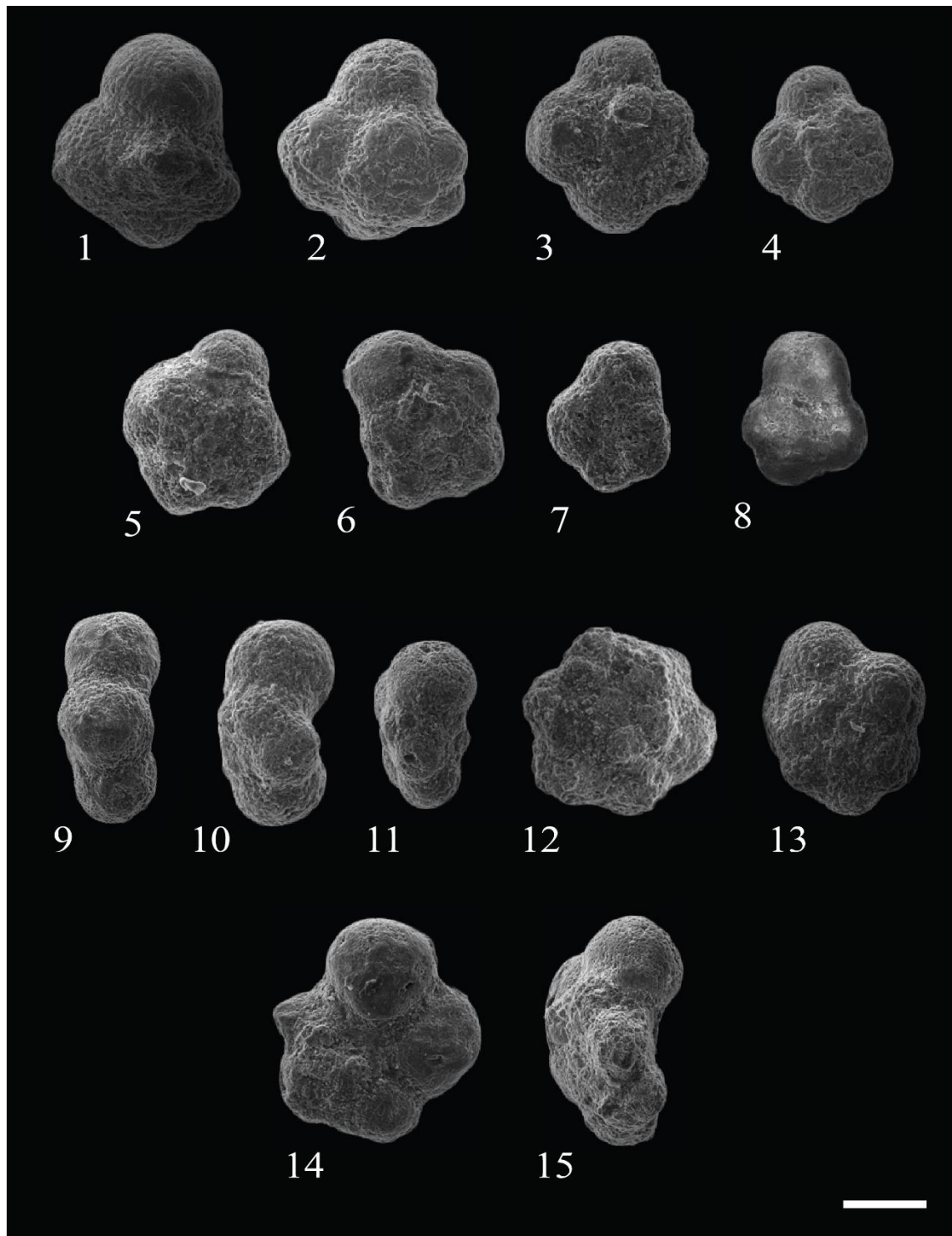
Figure 11: *Whiteinella baltica* DOUGLAS and RANKIN, sample no. NS 3, *W. archaeocretacea* zone lateral view

Figure 12: *Whiteinella brittonensis* TAPPAN, sample no. NS 18, *H. helvetica* zone, umbilical view

Figure 13: *Whiteinella brittonensis* TAPPAN, sample no. NS 14, *H. helvetica* zone, umbilical view

Figure 14: *Muricohedbergella delrioensis* CARSEY, sample no. NS 18, *H. helvetica* zone lateral view

Figure 15: *Muricohedbergella delrioensis* OLSSON, sample no. NS 14, *H. helvetica* zone spiral view



## PLATE 20

Scale bar = 100  $\mu\text{m}$

Figure 1: *Globotruncanella petaloidea* GANDOLFI, sample no. NS 52,  
*Globotruncanella* spp. zone, spiral view

Figure 2: *Globotruncanella petaloidea* GANDOLFI, sample no. NS 53,  
*Globotruncanella* spp. zone, umbilical view

Figure 3: *Globotruncanella petaloidea* GANDOLFI, sample no. NS 52,  
*Globotruncanella* spp. zone, lateral view

Figure 4: *Rugotruncana circumnodifer* FINLAY, NS 62, *G. aegyptiaca* zone, spiral view

Figure 5: *Rugotruncana circumnodifer* FINLAY, NS 66, *G. aegyptiaca* zone, spiral view

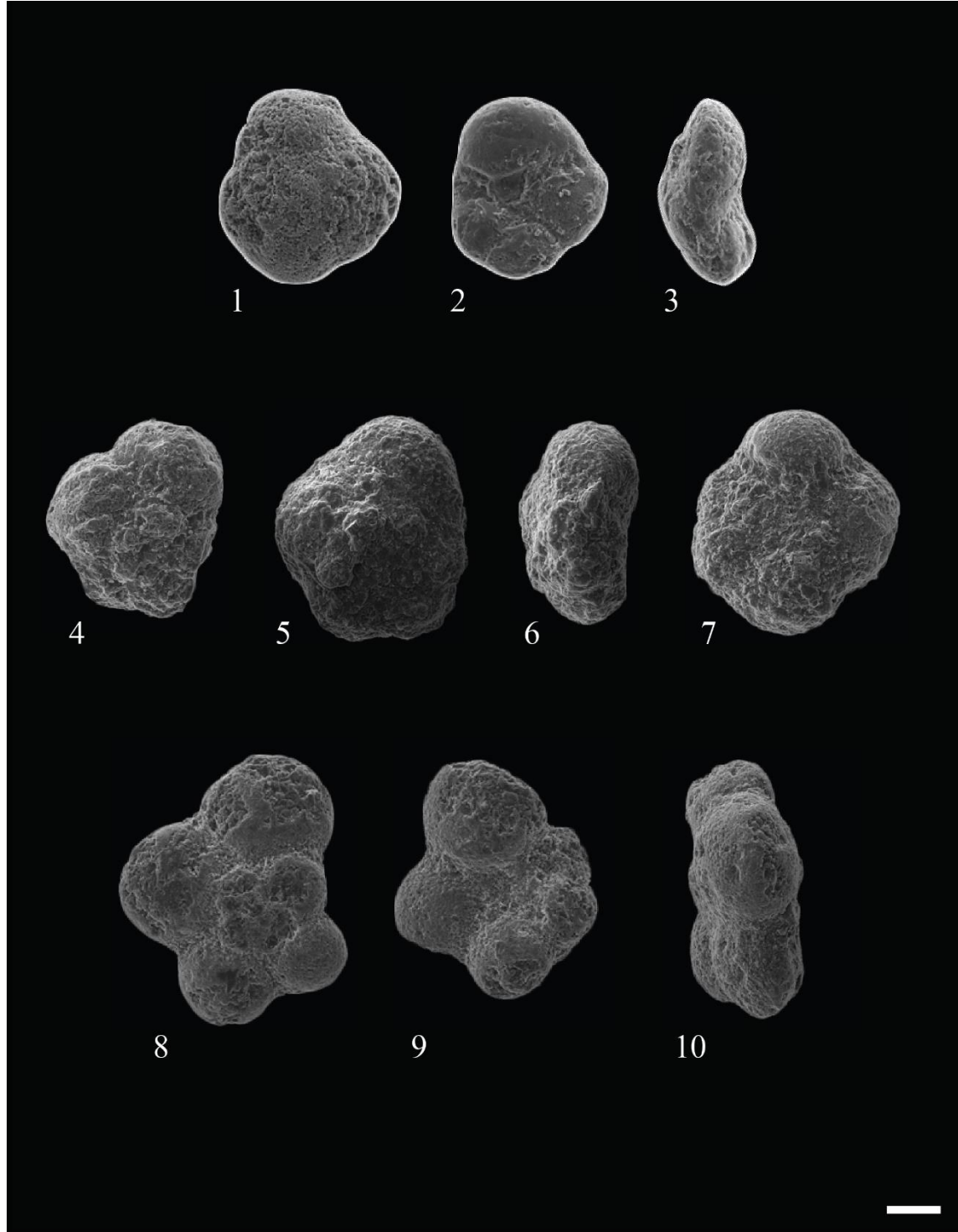
Figure 6: *Rugotruncana circumnodifer* FINLAY, NS 66, *G. aegyptiaca* zone, lateral  
view

Figure 7: *Rugotruncana circumnodifer* FINLAY, NS 67, *G. aegyptiaca* zone, umbilical  
view

Figure 8: *Muricohedbergella flandrini* PORTHAULT, sample no. NS 37, *G. elevata-D.*  
*asymetrica* concurrent range subzone, spiral view

Figure 9: *Muricohedbergella flandrini* PORTHAULT, sample no. NS 28, *G. elevata-D.*  
*asymetrica* concurrent range subzone, umbilical view

Figure 10: *Muricohedbergella flandrini* PORTHAULT, sample no. NS 36, *G. elevata-D.*  
*asymetrica* concurrent range subzone, lateral view



## PLATE 21

Scale bar = 100  $\mu\text{m}$

Figure 1: *Macroglobigerinelloides cf. bentonensis* MORROW, sample no. NS 10, *W. archaeocretacea* zone, lateral view

Figure 2: *Macroglobigerinelloides messinae* BRONNIMANN, sample no. NS 41, *G. elevata* zone, umbilical view

Figure 3: *Macroglobigerinelloides bollii* PESSAGNO, sample no. NS 38, *G. elevata-D. asymetrica* concurrent range subzone, umbilical view

Figure 4: *Macroglobigerinelloides bollii* PESSAGNO, sample no. NS 38, *G. elevata-D. asymetrica* concurrent range subzone, lateral view

Figure 5: *Macroglobigerinelloides bollii* PESSAGNO, sample no. NS 40, *G. elevata* zone, lateral view

Figure 6: *Macroglobigerinelloides bollii* PESSAGNO, sample no. NS 53, *Globotruncanella* spp. zone, umbilical view

Figure 7: *Macroglobigerinelloides bollii* PESSAGNO, sample no. NS 38, *G. elevata-D. asymetrica* concurrent range subzone, umbilical view

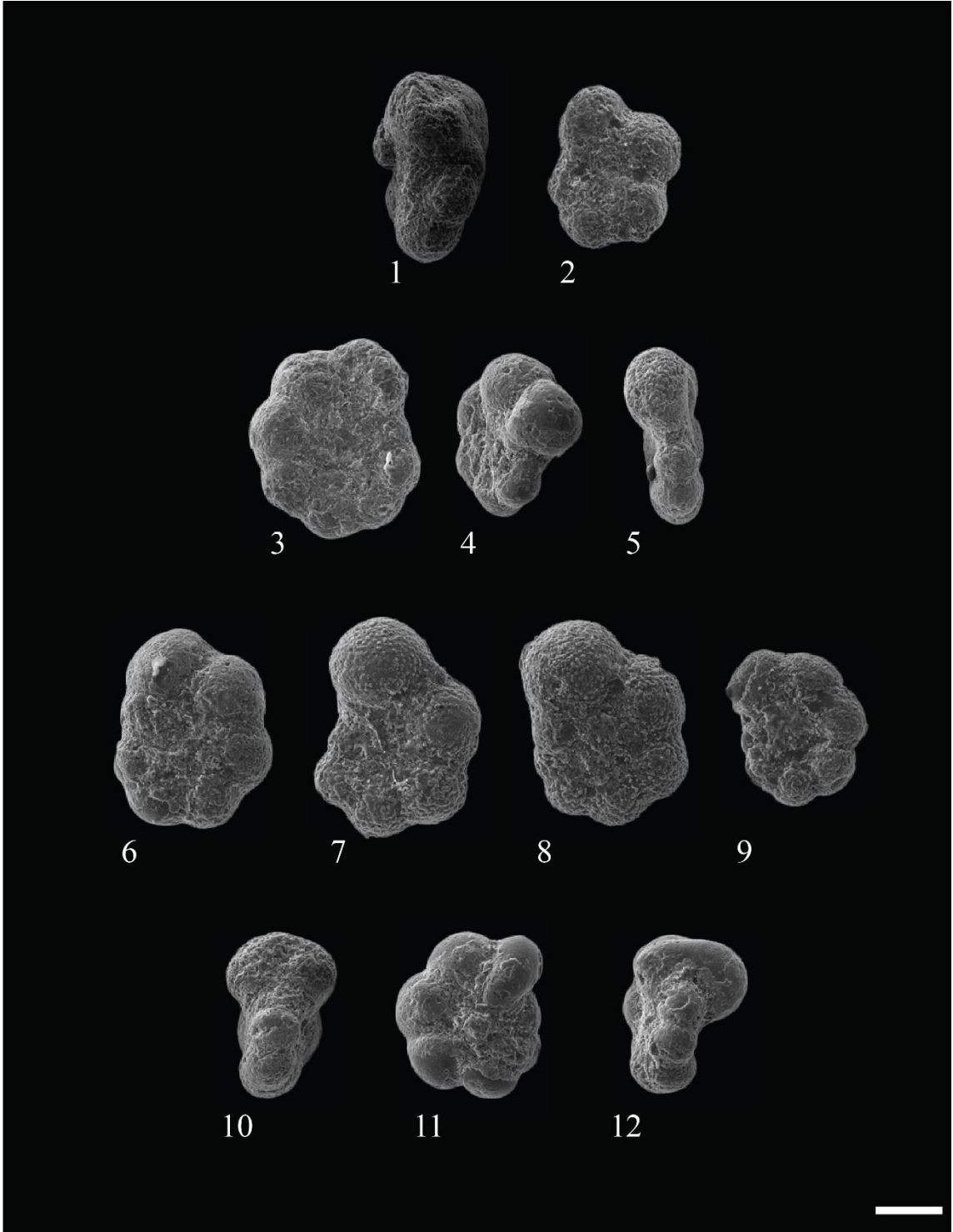
Figure 8: *Macroglobigerinelloides bollii* PESSAGNO, sample no. NS 62, *G. aegyptiaca* zone, umbilical view

Figure 9: *Macroglobigerinelloides bollii* PESSAGNO, sample no. NS 65, *G. aegyptiaca* zone, umbilical view

Figure 10: *Macroglobigerinelloides prairihillensis* PESSAGNO, sample no. NS 37, *G. elevata-D. asymetrica* concurrent range subzone, lateral view

Figure 11: *Macroglobigerinelloides prairihillensis* PESSAGNO, sample no. NS 49, *G. ventricosa* zone, umbilical view

Figure 12: *Macroglobigerinelloides prairihillensis* PESSAGNO, sample no. NS 49, *G. ventricosa* zone, lateral view



## PLATE 22

Figure 1: *Archaeoglobigerina blowi* PESSAGNO, sample no. NS 41, *G. elevata* zone, X150

Figure 2: *Muricohedbergella monmouthensis* TAPPAN, sample no. NS 66, *G. aegyptiaca* zone, X150

Figure 3: *Muricohedbergella planispira* TAPPAN, sample no. NS 8, *W. archaeocretacea* zone, X150

Figure 4: *Muricohedbergella planispira* TAPPAN, sample no. NS 1, *D. algeriana* subzone, X150

Figure 5: *Muricohedbergella flandrini* PORTHAULT, sample no. NS 29, *G. elevata-D. asymetrica* concurrent range subzone, X100

Figure 6: *Muricohedbergella flandrini* PORTHAULT, sample no. NS 26, *G. elevata-D. asymetrica* concurrent range subzone, X100

Figure 7: *Muricohedbergella flandrini* PORTHAULT, sample no. NS 26, *G. elevata-D. asymetrica* concurrent range subzone, X100

Figure 8: *Muricohedbergella delrioensis* CARSEY, sample no. NS 18, *H. helvetica* zone, X130

Figure 9: *Muricohedbergella delrioensis* CARSEY, sample no. NS 14, *H. helvetica* zone, X130

Figure 10: *Muricohedbergella delrioensis* CARSEY, sample no. NS 2, *D. algeriana* subzone zone, X150



Figure 11: *Muricohedbergella holmdelensis* OLSSON, sample no. NS 26, *G. elevata-D. asymetrica* concurrent range subzone, X130

Figure 12: *Muricohedbergella holmdelensis* OLSSON, sample no. NS 26, *G. elevata-D. asymetrica* concurrent range subzone, X130

Figure 13: *Rugoglobigerina rugosa* PLUMMER, sample no. NS 66, *G. aegyptiaca* zone, X100

Figure 14: *Rugoglobigerina pennyi* BRONNIMANN, sample no. NS 72, *G. aegyptiaca* zone, X100

Figure 15: *Macroglobigerinelloides bollii* PESSAGNO, sample no. NS 46, *G. elevata* zone, X100

Figure 16: *Macroglobigerinelloides bollii* PESSAGNO, sample no. NS 41, *G. elevata* zone, X130

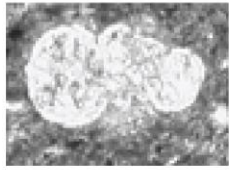
Figure 17: *Macroglobigerinelloides bollii* PESSAGNO, sample no. NS 24, *G. elevata-D. asymetrica* concurrent range subzone, X130

Figure 18: *Macroglobigerinelloides bollii* PESSAGNO, sample no. NS 23, *D. asymetrica* zone, X100

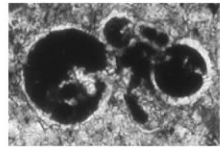
Figure 19: *Macroglobigerinelloides bollii* PESSAGNO, sample no. NS 22, *D. asymetrica* zone, X100

Figure 20: *Macroglobigerinelloides prairihillensis* PESSAGNO, sample no. NS 33, *G. elevata-D. asymetrica* concurrent range subzone, X150

Figure 21: *Macroglobigerinelloides prairihillensis* PESSAGNO, sample no. NS 24, *G. elevata-D. asymetrica* concurrent range subzone, X150



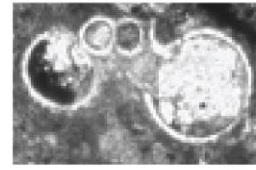
1



2



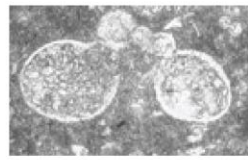
3



4



5



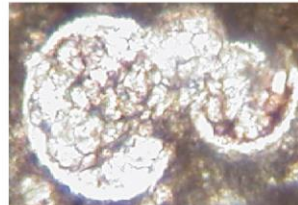
6



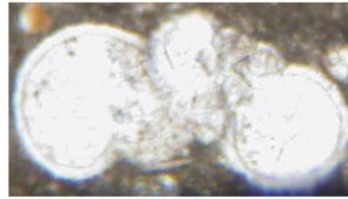
7



8



9



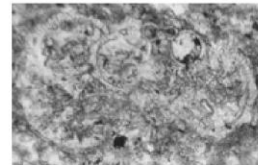
10



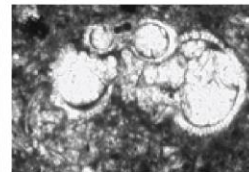
11



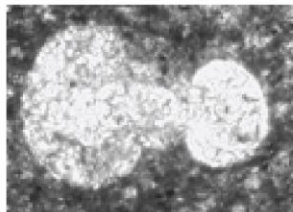
12



13



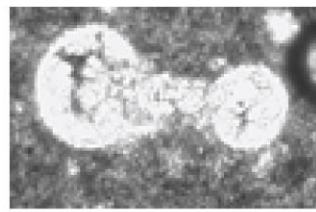
14



15



16



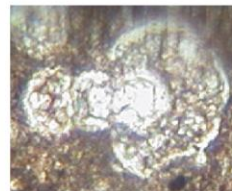
17



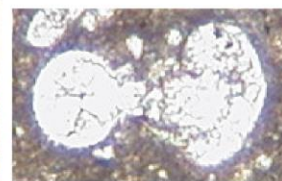
18



19



20



21

## PLATE 23

Figure 1: *Dicarinella algeriana* CARON, sample no. NS 3, *W. archaeocretacea* zone, X150

Figure 2: *Dicarinella algeriana* CARON, sample no. NS 3, *W. archaeocretacea* zone, X150

Figure 3: *Dicarinella algeriana* CARON, sample no. NS 3, *W. archaeocretacea* zone, X150

Figure 4: *Dicarinella algeriana* CARON, sample no. NS 1, *D. algeriana* subzone, X150

Figure 5: *Dicarinella canaliculata* ROSALINA, sample no. NS 14, *H. helvetica* zone, X90

Figure 6: *Dicarinella canaliculata* ROSALINA, sample no. NS 14, *H. helvetica* zone, X100

Figure 7: *Dicarinella canaliculata* ROSALINA, sample no. NS 18, *H. helvetica* zone, X100

Figure 8: *Dicarinella asymetrica* SIGAL, sample no. NS 20, *D. asymetrica* zone, X130

Figure 9: *Dicarinella asymetrica* SIGAL, sample no. NS 24, *G. elevata-D. asymetrica* concurrent range subzone, X130

Figure 10: *Dicarinella asymetrica* SIGAL, sample no. NS 33, *G. elevata-D. asymetrica* concurrent range subzone, X80

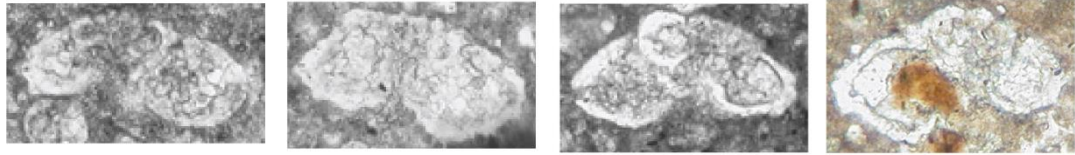
Figure 11: *Dicarinella concavata* BROTZEN, sample no. NS 20, *D. asymetrica* zone, X130

Figure 12: *Dicarinella concavata* BROTZEN, sample no. NS 24, *G. elevata-D. asymetrica* concurrent range subzone, X80

Figure 13: *Dicarinella concavata* BROTZEN, sample no. NS 33, *G. elevata-D. asymetrica* concurrent range subzone, X80

Figure 14: *Globotruncanita elevata* BROTZEN, sample no. NS 24, *G. elevata-D. asymetrica* concurrent range subzone, X80

Figure 15: *Globotruncanita elevata* BROTZEN, sample no. NS 24, *G. elevata-D. asymetrica* concurrent range subzone, X80

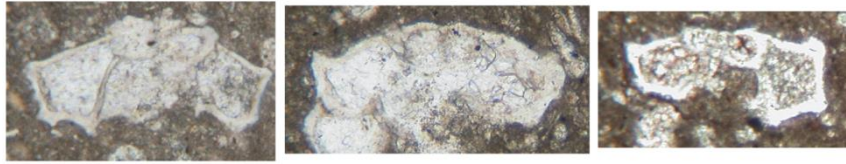


1

2

3

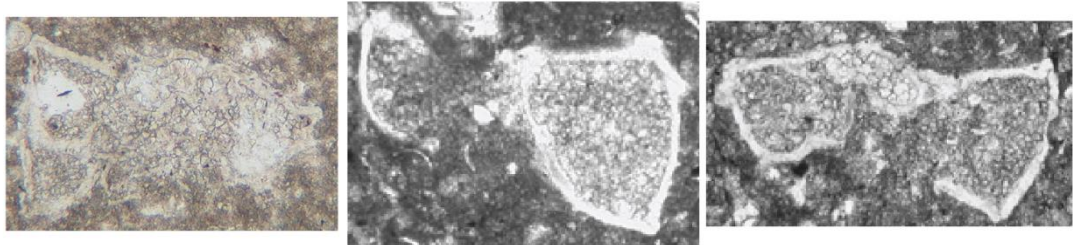
4



5

6

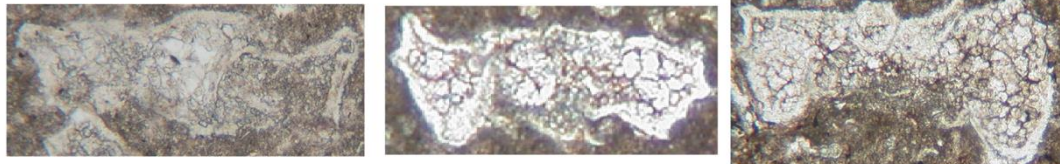
7



8

9

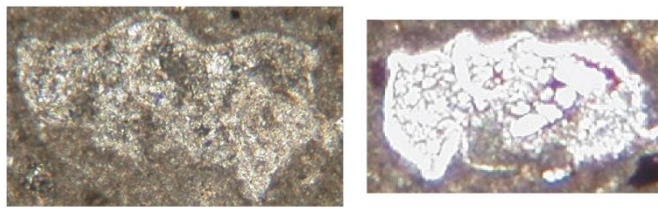
10



11

12

13



14

15

## PLATE 24

Figure 1: *Globotruncana bulloides* VOGLER, sample no. NS 62, *G. aegyptiaca* zone, X110

Figure 2: *Globotruncana bulloides* VOGLER, sample no. NS 62, *G. aegyptiaca* zone, X110

Figure 3: *Globotruncana bulloides* VOGLER, sample no. NS 62, *G. aegyptiaca* zone, X110

Figure 4: *Globotruncana hilli* PESSAGNO, sample no. NS 68, *G. aegyptiaca* zone, X130

Figure 5: *Globotruncana hilli* PESSAGNO, sample no. NS 68, *G. aegyptiaca* zone, X110

Figure 6: *Globotruncana arca* CUSHMAN, sample no. NS 39, *G. elevata* zone, X80

Figure 7: *Globotruncana arca* CUSHMAN, sample no. NS 39, *G. elevata* zone, X80

Figure 8: *Globotruncana arca* CUSHMAN, sample no. NS 61, *G. aegyptiaca* zone, X80

Figure 9: *Globotruncana arca* CUSHMAN, sample no. NS 61, *G. aegyptiaca* zone, X120

Figure 10: *Globotruncana lapparenti*, BROTZEN, sample no. NS 34, *G. elevata-D. asymetrica* concurrent range subzone, X80

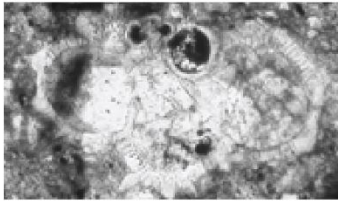
Figure 11: *Globotruncana cf. lapparenti*, BROTZEN, sample no. NS 32, *G. elevata-D. asymetrica* concurrent range subzone, X80

Figure 12: *Globotruncana lapparenti*, BROTZEN, sample no. NS 34, *G. elevata-D. asymetrica* concurrent range subzone, X110

Figure 13: *Globotruncanita insignis* GANDOLFI, sample no. NS 37, *G. elevata-D. asymetrica* concurrent range subzone, X150

Figure 14: *Globotruncanita insignis* GANDOLFI, sample no. NS 37, *G. elevata-D. asymetrica* concurrent range subzone, X150

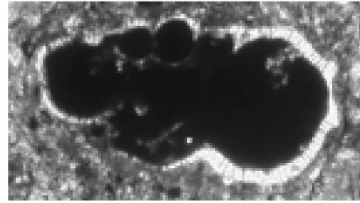
Figure 15: *Globotruncanita cf. ventricosa* WHITE, sample no. NS 37, *G. elevata-D. asymetrica* concurrent range subzone, X150



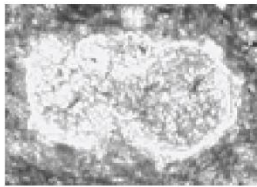
1



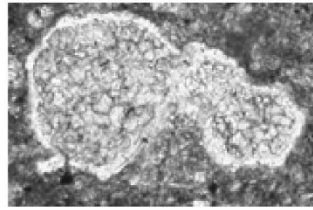
2



3



4



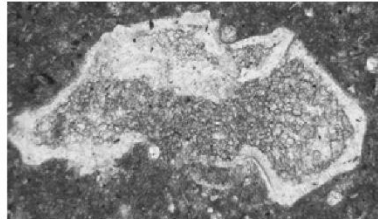
5



6



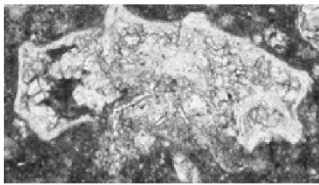
7



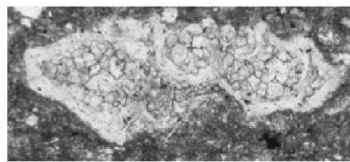
8



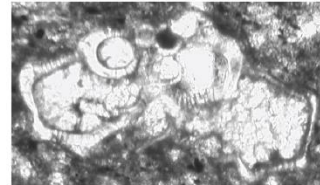
9



10



11



12



13



14



15



## PLATE 25

Figure 1: *Globotruncana linneiana* D'ORBIGNY, sample no. NS 72, *G. aegyptiaca* zone, X120

Figure 2: *Globotruncana linneiana* D'ORBIGNY, sample no. NS 70, *G. aegyptiaca* zone, X100

Figure 3: *Globotruncana linneiana* D'ORBIGNY, sample no. NS 43, *G. elevata* zone, X120

Figure 4: *Globotruncana linneiana* D'ORBIGNY, sample no. NS 41, *G. elevata* zone, X150

Figure 5: *Globotruncana linneiana* D'ORBIGNY, sample no. NS 41, *G. elevata* zone, X120

Figure 6: *Globotruncana linneiana* D'ORBIGNY, sample no. NS 32, *G. elevata-D. asymetrica* concurrent range subzone, X100

Figure 7: *Globotruncana linneiana* D'ORBIGNY, sample no. NS 29, *G. elevata-D. asymetrica* concurrent range subzone, X100

Figure 8: *Globotruncana linneiana* D'ORBIGNY, sample no. NS 26, *G. elevata-D. asymetrica* concurrent range subzone, X120

Figure 9: *Globotruncana linneiana* D'ORBIGNY, sample no. NS 26, *G. elevata-D. asymetrica* concurrent range subzone, X120

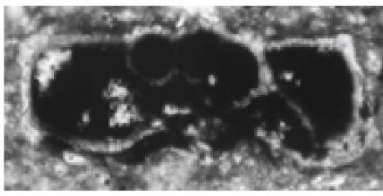
Figure 10: *Globotruncana linneiana* D'ORBIGNY, sample no. NS 26, *G. elevata-D. asymetrica* concurrent range subzone, X120

Figure 11: *Globotruncana linneiana* D'ORBIGNY, sample no. NS 24, *G. elevata-D. asymetrica* concurrent range subzone, X120

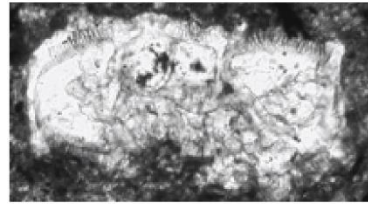
Figure 12: *Globotruncana linneiana* D'ORBIGNY, sample no. NS 24, *G. elevata-D. asymetrica* concurrent range subzone, X80

Figure 13: *Globotruncana linneiana* D'ORBIGNY, sample no. NS 24, *G. elevata-D. asymetrica* concurrent range subzone, X100

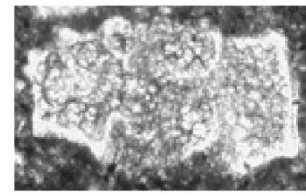
Figure 14: *Globotruncana linneiana* D'ORBIGNY, sample no. NS 23, *D. asymetrica* zone, X100



1



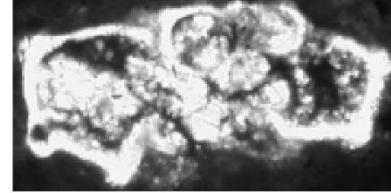
2



3



4



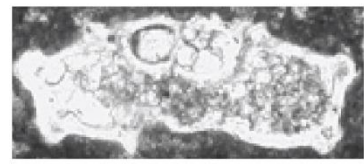
5



6



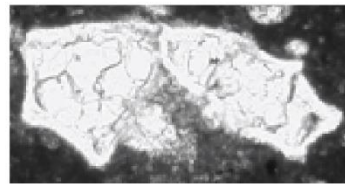
7



8



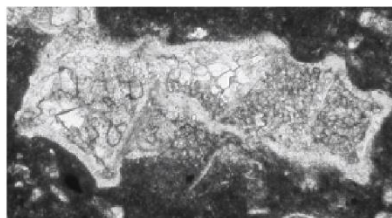
9



10



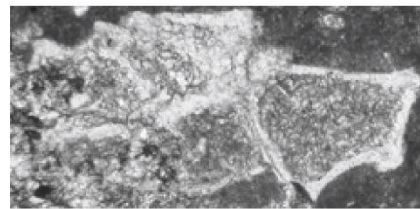
11



12



13



14

## PLATE 26

Figure 1: *Heterohelix globulosa* EHRENBERG, sample no. NS 71, *G. aegyptiaca* zone, X180

Figure 2: *Heterohelix globulosa* EHRENBERG, sample no. NS 66, *G. aegyptiaca* zone, X150

Figure 3: *Heterohelix globulosa* EHRENBERG, sample no. NS 55, *Globotruncanella* spp. zone, X250

Figure 4: *Heterohelix globulosa* EHRENBERG, sample no. NS 45, *G. elevata* zone, X150

Figure 5: *Heterohelix globulosa* EHRENBERG, sample no. NS 38, *G. elevata-D. asymetrica* concurrent range subzone, X150

Figure 6: *Heterohelix globulosa* EHRENBERG, sample no. NS 37, *G. elevata-D. asymetrica* concurrent range subzone, X150

Figure 7: *Heterohelix globulosa* EHRENBERG, sample no. NS 36, *G. elevata-D. asymetrica* concurrent range subzone, X180

Figure 8: *Heterohelix globulosa* EHRENBERG, sample no. NS 30, *G. elevata-D. asymetrica* concurrent range subzone, X250

Figure 9: *Heterohelix globulosa* EHRENBERG, sample no. NS 24, *G. elevata-D. asymetrica* concurrent range subzone, X200

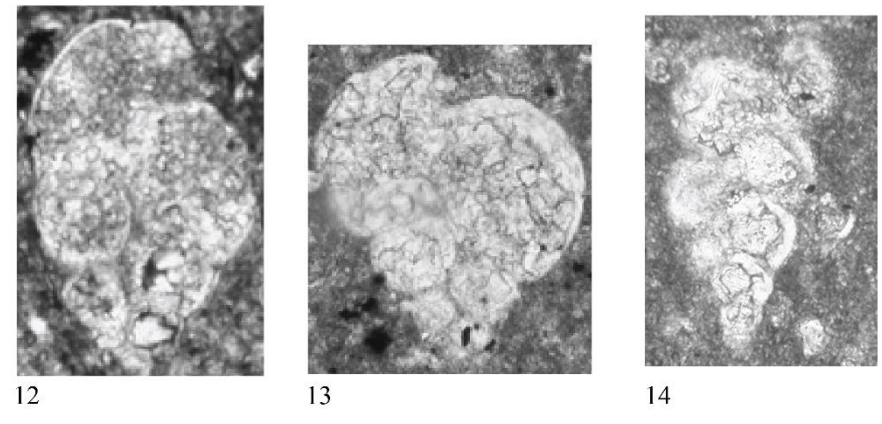
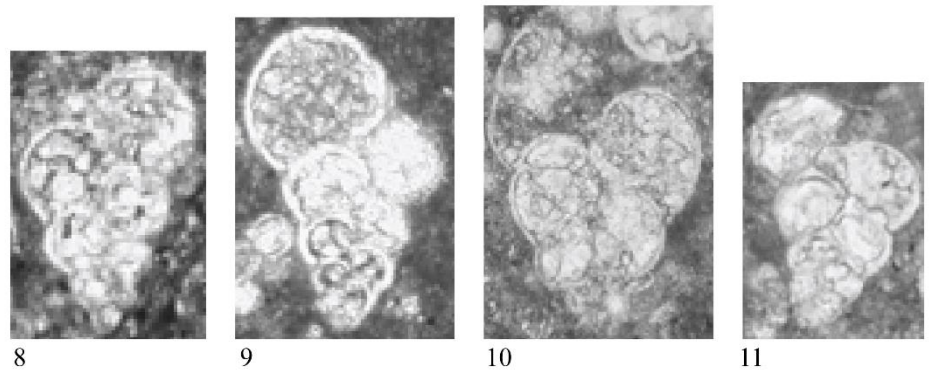
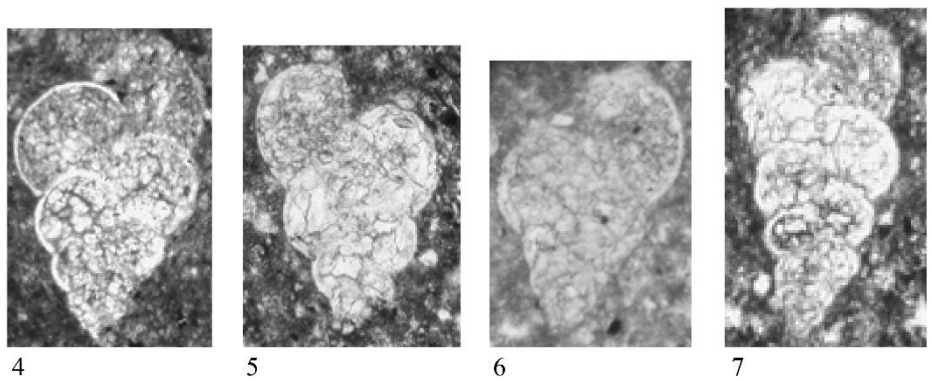
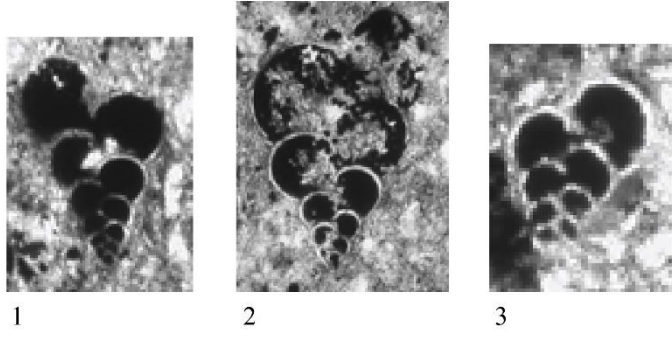
Figure 10: *Heterohelix globulosa* EHRENBERG, sample no. NS 22, *G. asymetrica* zone, X180

Figure 11: *Heterohelix globulosa* EHRENBERG, sample no. NS 25, *G. elevata-D. asymerica* concurrent range subzone, X180

Figure 12: *Laeviheterohelix turgida* NEDERBRAGT, sample no. NS 45, *G. elevata* zone, X150

Figure 13: *Laeviheterohelix* sp. 1, sample no. NS 38, *G. elevata-D. asymerica* concurrent range subzone, X150

Figure 14: *Heterohelix moremani* CUSHMAN, sample no. NS 23, *D. asymerica* zone, X150



## PLATE 27

Figure 1: *Marginotruncana pseudolinneiana* PESSAGNO, sample no. NS 14, *H. helvetica* zone, X110

Figure 2: *Marginotruncana pseudolinneiana* PESSAGNO, sample no. NS 18, *H. helvetica* zone, X100

Figure 3: *Marginotruncana pseudolinneiana* PESSAGNO, sample no. NS 20, *D. asymetrica* zone, X100

Figure 4: *Marginotruncana coronata* BOLLI, sample no. NS 14, *H. helvetica* zone, X110

Figure 5: *Marginotruncana renzi* GANDOLFI, sample no. NS 14, *H. helvetica* zone, X100

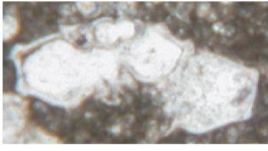
Figure 6: *Marginotruncana coronata* BOLLI, sample no. NS 14, *H. helvetica* zone, X100

Figure 7: *Marginotruncana marginata* REUSS, sample no. NS 14, *H. helvetica* zone, X150

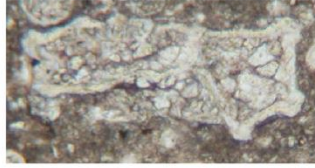
Figure 8: *Marginotruncana marginata* REUSS, sample no. NS 14, *H. helvetica* zone, X150

Figure 9: *Marginotruncana marginata* REUSS, sample no. NS 18, *H. helvetica* zone, X110

Figure 10: *Marginotruncana sigali* REICHEL, sample no. NS 24, *G. elevata-D. asymetrica* concurrent range subzone, X90



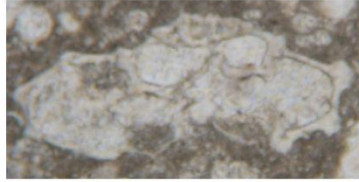
1



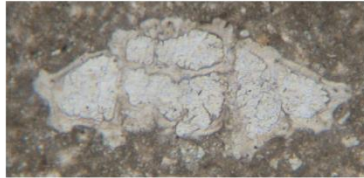
2



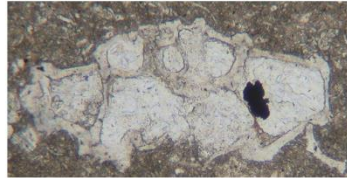
3



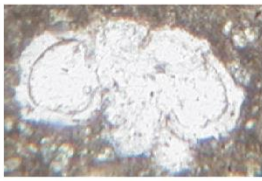
4



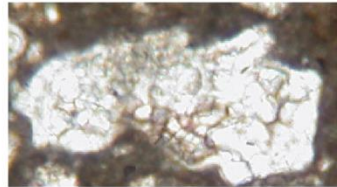
5



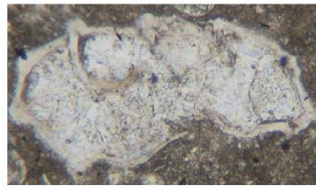
6



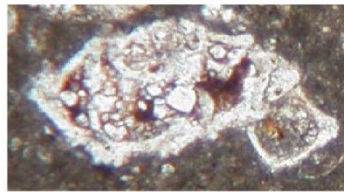
7



8



9



10



## PLATE 28

Figure 1: *Rotalipora deeckeii* FRANKE sample no. NS 1, *D. algeriana* subzone, X80

Figure 2: *Rotalipora deeckeii* FRANKE sample no. NS 1, *D. algeriana* subzone, X70

Figure 3: *Rotalipora cushmani* RENZ, sample no. NS 1, *D. algeriana* subzone, X90

Figure 4: *Rotalipora cushmani* RENZ, sample no. NS 2, *D. algeriana* subzone, X80

Figure 5: *Praeglobotruncana gibba* KLAUS, sample no. NS 2, *D. algeriana* subzone, X110

Figure 6: *Praeglobotruncana gibba* KLAUS, sample no. NS 1, *D. algeriana* subzone, X100

Figure 7: *Praeglobotruncana gibba* KLAUS, sample no. NS 1, *D. algeriana* subzone, X120

Figure 8: *Praeglobotruncana gibba* KLAUS, sample no. NS 2, *D. algeriana* subzone, X110

Figure 9: *Praeglobotruncana gibba* KLAUS, sample no. NS 2, *D. algeriana* subzone, X120

Figure 10: *Praeglobotruncana stephani* GANDOLFI, sample no. NS 1, *D. algeriana* subzone, X120

Figure 11: *Praeglobotruncana stephani* GANDOLFI, sample no. NS 1, *D. algeriana* subzone, X110

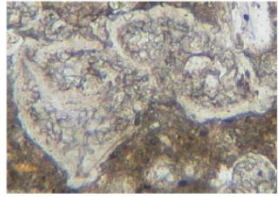
Figure 12: *Praeglobotruncana stephani* GANDOLFI, sample no. NS 1, *D. algeriana* subzone, X120

Figure 13: *Praeglobotruncana stephani* GANDOLFI, sample no. NS 2, *D. algeriana* subzone, X110

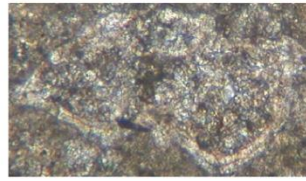
Figure 14: *Praeglobotruncana stephani* GANDOLFI, sample no. NS 2, *D. algeriana* subzone, X120

Figure 15: *Praeglobotruncana stephani* GANDOLFI, sample no. NS 18, *H. helvetica* zone, X110

Figure 16: *Schakoina cenomana* SCHAKO, sample no. NS 33, *G. elevata-D. asymetrica* concurrent range subzone, X100



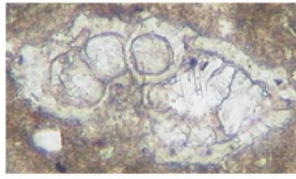
1



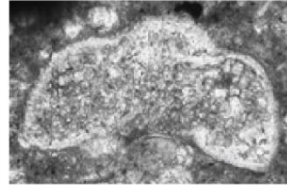
2



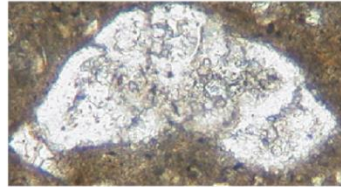
3



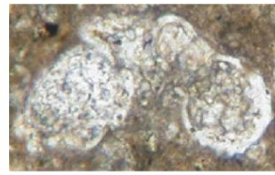
4



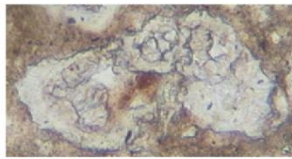
5



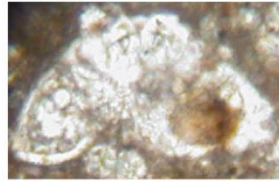
6



7



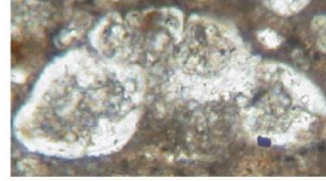
8



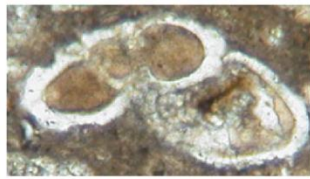
9



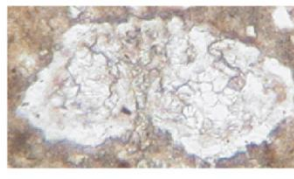
10



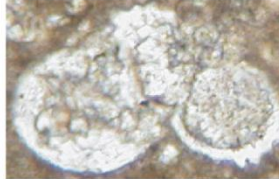
11



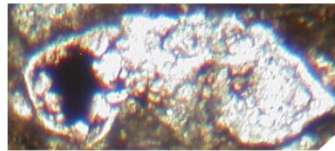
12



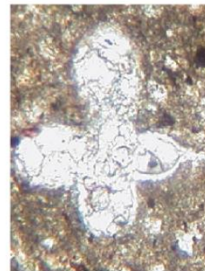
13



14



15



16

## PLATE 29

Figure 1: *Whiteinella baltica* DOUGLAS AND RANKIN, sample no. NS 14, *H. helvetica* zone, X100

Figure 2: *Whiteinella baltica* DOUGLAS AND RANKIN, sample no. NS 14, *H. helvetica* zone, X100

Figure 3: *Whiteinella aprica* LOEBLICH AND TAPPAN, sample no. NS 14, *H. helvetica* zone, X120

Figure 4: *Whiteinella archaeocretacea* PESSAGNO, sample no. NS 14, *H. helvetica* zone, X120

Figure 5: *Whiteinella archaeocretacea* PESSAGNO, sample no. NS 14, *H. helvetica* zone, X120

Figure 6: *Whiteinella paradubia* SIGAL, sample no. NS 14, *H. helvetica* zone, X100

Figure 7: *Whiteinella paradubia* SIGAL, sample no. NS 14, *H. helvetica* zone, X100

Figure 8: *Whiteinella paradubia* SIGAL, sample no. NS 17, *H. helvetica* zone, X100

Figure 9: *Helvetoglobotruncana helvetica* BOLLI, sample no. NS 14, *H. helvetica* zone, X130

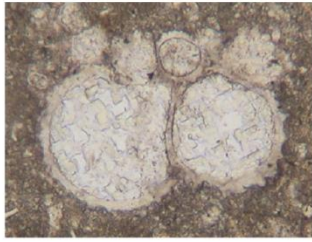
Figure 10: *Helvetoglobotruncana helvetica* BOLLI, sample no. NS 14, *H. helvetica* zone, X130

Figure 11: *Helvetoglobotruncana helvetica* BOLLI, sample no. NS 14, *H. helvetica* zone, X130

Figure 12: *Helvetoglobotruncana helvetica* BOLLI, sample no. NS 14, *H. helvetica* zone, X130

Figure 13: *Whiteinella praehelvetica* TRUJILLO, sample no. NS 14, *H. helvetica* zone, X100

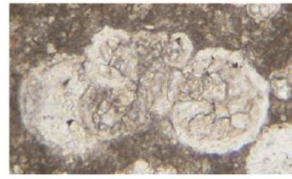
Figure 14: *Whiteinella praehelvetica* TRUJILLO, sample no. NS 14, *H. helvetica* zone, X100



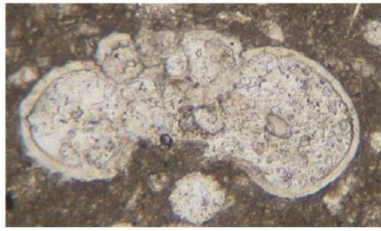
1



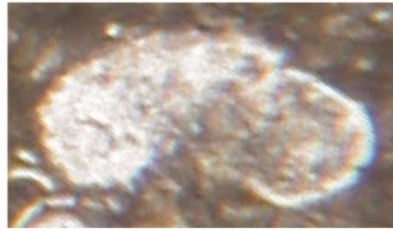
2



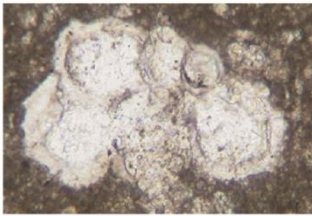
3



4



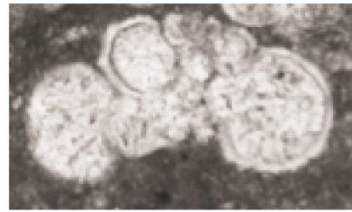
5



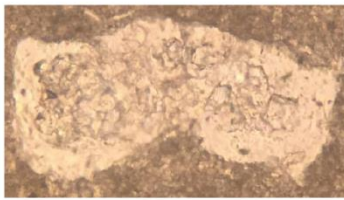
6



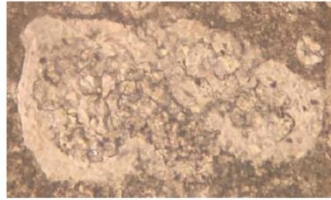
7



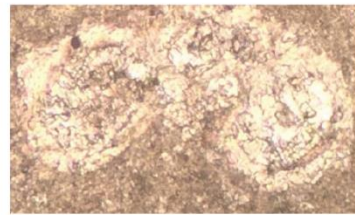
8



9



10



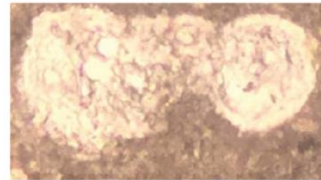
11



12



13



14